Robustness Analysis and Controller Synthesis for Bilateral Teleoperation Systems via IQCs

İlhan Polat

Robustness Analysis and Controller Synthesis for Bilateral Teleoperation Systems via IQCs

Proefschrift

ter verkrijging van de graad van doctor
aan de Technische Universiteit Eindhoven,
op gezag van de Rector Magnificus prof. dr. ir. C.J. van Duijn,
voorzitter van het College voor Promoties,
in het openbaar te verdedigen op donderdag ## xxxxx 2013 om ##:## uur
door İlhan Polat,
ingenieur werktuigbouwkunde,
geboren te Gaziantep, TURKIJE.

Dit proefschrift is goedgekeurd door de promotor:
Prof.dr. ir. Maarten Steinbuch

Samenstelling promotiecommissie:

Rector Magnificus	voorzitter
Prof.dr. Maarten Steinbuch	Technische Universiteit Eindhoven
Prof.dr. Siep Weiland	Technische Universiteit Eindhoven
Prof.dr. Vincent Hayward	Universitè Pierre et Marie Curie
Prof.dr. Claudio Melchiorri	Università di Bologna
Prof.dr. Stefano Stramigioli	Technische Universiteit Twente
Prof.dr. Henk Nijmeijer	Technische Universiteit Eindhoven
Prof.dr. Maurice Heemels	Technische Universiteit Eindhoven

Typeset with LuaTEX. Printed by some company

Table Of Contents

Introduction

The success of the technological advances often can be associated with an unprecedented convenience that they bring in. At the heart of this convenience lies the ability to relax the limitations of the human body to a certain extent. From this point of view, it is not a surprise that the three most prominent technological wonders of the last century, namely the *Television*, the *Telephone* and the *Radio* (which was originally called "radiotelegraphy"), bears the same Greek prefix *tele-* which corresponds to "*at a distance*" in our context. This shows that there is something of extreme importance about our drive to extend our capabilities beyond the constraints that our bodies impose.

It is quite remarkable, in retrospect, that these "gadgets" did not perish but rather kept on evolving since, initially, they were far from perfect. Quite to the contrary, they were hardly operational. Even the commercialized version of the early TVs had a narrow bandwidth and minimum image quality. Similarly radio and telephone was barely transmitting sensible information as far as the signal-to-noise ratio is concerned. Nevertheless, they have provided the ways of communication which were unimaginable before their time. Therefore the added value dominated the shortcomings and even though they were quite imperfect, we kept using them. The important lesson to be learned is that a technology should not be judged by its imperfections, but rather should be weighed by its contribution in this context and the convenience that is either immediately brought in by using it, or its foreseen potential by the "early adopters".

The success is also related to the fact that these technologies mainly relied on the human brain itself at their early stages. For example, the human brain did most of the noise filtering and data recovery by just guessing the missing pieces and identifying patterns from the signal brought by the respective medium. Today, with our smart mobile phones and 3D LED TVs, we can assume that the computational load, or whatever it's equivalence in terms of attention span capacity, on the human brain is drastically reduced. In other words, it is true that we are still identifying patterns and utilizing the relevant parts of our brain to make sense of a TV broadcast[1]. However, we do not need to use a higher level of concentration to reconstruct the words that we hear or to identify the image on the display thanks to the high quality output. We cannot exaggerate the importance of the human brain and its immersion power.

We are on the same track and leaving essentially the same footprints with the technological developments involving our touch sense. Though various science fiction items already used such ideas extensively, the real technology tends to follow

---

[1]Pun intended.
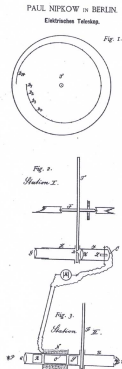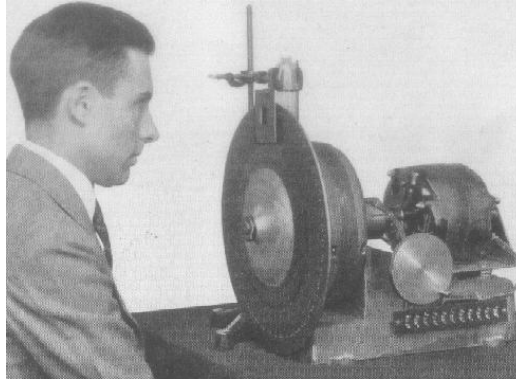
(a)   (b)

Figure 1.1: Some historical details from the early mechanical television era: (a) Nipkow disc from Paul Gottlieb Nipkow's patent application, (b) Watching Television in 1928; the rotating perforated disc has 50 holes spirally placed, and rotates 18 times a second. Images are from [74, 111] respectively.

from quite a distance. Considering the importance of our sense of touch in any given situation, the added value of extending our perception in this modality needs no motivation. Take the most familiar, the vibrating mobile phone in the silent mode in our pocket. This is a very important example since every individual learns what that vibration might mean, either an SMS or a call, depending on the vibrational pattern. This means that the sense of touch can be used to convey messages that are not immediately related to physical act of touching. More importantly we can process those messages for inference which forms the basis of the so-called "haptics" and haptic technology.

The type of information from the cell-phone example is said to be received via the haptic channel (or the collaborative use of tactile and proprioceptive modalities). At this point we have to emphasize that, we use the term "sense of touch" rather vaguely as a shortcut and we leave it to the experts of the field to define the sophisticated mechanisms (pertaining to the somatosensory system) that we utilize when we manipulate objects, say with our bare hands.

Since our skin and muscles form one of most sophisticated and complex sensory systems, the somatosensory system, the brain can easily interpret the slightest changes and this extra signal processing power gives us a chance to hack into this system by providing artificial inputs via haptic displays. Still, it is rather conspicuous that it is impossible to achieve a total immersion with today's technology. The essential complication is twofold: the high sensitivity of the very same sensory system makes it difficult to fake or mimic a natural phenomenon by artificial means and on the other hand we do not have a well-defined mapping from the to-be-created sensation to the required excitation signals. Moreover, even if we have

such mappings available, the related hardware must execute the computed haptic signal profiles perfectly which is generally not the case and a trade-off strategy should be constructed. In other words, we need a clear approximation metric to be able to compare two different touch technologies to judge whether one is better than the other. Unfortunately, this metric and thus the strategy is also absent.

Then, we could simply ask *Why bother?*

1.1   The Objectives

We first give a summary about the current concepts of the involved technology (as we foresee from a narrow "today's" perspective). Later on, we define our microscopic focus of this thesis within this vast generality. This would provide additional insights to what follows in the later sections.

Touch related applications are diverse. The diversity is not only in terms of the sensation they are related to (texture, shape etc.) but also how they encode the information and transmit via various modalities (e.g. vibrational patterns in mobile electronics, variable resistance to motion in game consoles and steering wheels etc.). There is no particular reason to limit ourselves with the daily needs or even luxurious demands regarding our touch sense as mobile phones taught us that a vibration in our pocket means a contact request from someone which is hardly ever related to the touch sense. It should be pretty awkward to experience if someone actually would come and shake our pockets to draw our attention (unless it is socially accepted). Therefore, we have devised a way to translate one particular message into another by simply teaching ourselves and getting used to it. Thus, it does not seem improbable that other types of physical measurements in terms temperature, light intensity etc., converted into pressure or tactile patterns in time domain.

Hence, it is our belief that the crux of this technology is establishing a interpretable protocol between our brain and the machine but not exactly reflecting the particular state of some distant or virtual physical medium. This would be the main argument of this thesis when we distinguish our approach with its comparable counterparts. For this reason, we have identified the nuances in Appendix B to narrow down our focus further by defining different types of touch related concepts.

Bilateral Teleoperation

Bilateral teleoperation, simply, is teleoperation equipped with force feedback to the human operator with the hope to increase the realism by recreating the force vectors of the distant medium at the local environment. The majority of the bilateral teleoperation research is devoted to kinesthetic feedback. In particular, the human interacts with the local device by moving a constrained handle to explore the environment or using a stylus-like stick. Hence, the experience is mostly based on the success of imitating a physical tool. Therefore, the tactile cues are of secondary nature. The challenge, of course, is to increase the performance level to a tactile

display level while still maintaining the tool usage capability. The particular MIS tasks that are performed with a scalpel are one of the hot topics of research effort. It requires not only kinesthetic feedback, though a major accomplishment by itself, but tactile feedback too, for understanding the nature of the texture or the stiffness of the tissue. Similarly, teleoperated peg-in-hole type of tasks are also a major area of investigation; e.g., ground-satellite robotic mission directives or underwater construction tasks would benefit much from such possibilities to reduce the operational cost, duration, and success rate.

There are many interesting challenges when it comes to this recreation process. For example, in a microassembly task, the experienced forces are substantially different from what we feel during daily tasks. Gravity is our main source of reference when interpreting a distant location. However, gravity becomes almost negligible in the micro domain, as adhesive forces such as Van der Waals, electrostatic and surface tension forces dominate — the most common example is that the the parts that are picked up in microdomain tend to stick to the tweezers. Similarly in a space- or underwater- operation, there might be different forces that are not directly visible/interpretable by vision alone, say underwater currents or relative forcing between free bodies in space etc.

If we manage to create a believable level of force feedback sensation in these otherwise inaccessible domains, there are a few very important quasi-philosophical and also task-dependent questions that need to be answered. A few of these questions are:

- Should the device reflect the unfamiliar forces to the human operator for the sake of realism which are utterly counter-intuitive and even worse appear to be happening at random?

- Is there any correlation between increased realism and increased comfort? In case of a difficult task, what good does the realism bring in by replicating the difficult task at a distant location in the local environment?

- Do we need to reflect the human motion to the remote location perfectly since this can be considered as a waste of resources? In other words, we neglect the fact that a robot can perform certain tasks much more precisely than a human operator. Is there any downsampling/upsampling protocol to vary the motion precision depending on the receiver?

- If we decide to filter the irrelevant force information (e.g., mental/muscular fatigue, tremor on the operator side and measurement noise, nonlinear effects on the remote device side), how should we know what to transmit and what to filter out?

- Do we use the full capacity of our *internal data bus* to transfer touch information, or put differently, is there any space left to encode other quantities on top of the touch sense?

- Can we assume that all users more or less reach to the same understanding given a kinesthetic cue sequence?

These are interesting questions and answering them in a rigorous fashion is very challenging. The reason for enumerating a few of them here is that the problem is much more involved than what we can achieve within the scope of this thesis. In other words, we cannot, despite the recurring claims found in the literature, answer these questions within the scope of control theory/robotics alone. Instead we will focus on a framework that would help to set up such teleoperation devices such that experts in the involved fields can use these devices to answer those items above.

1.1.1   *Structure and Objectives of this Thesis*

To restrict the scope of this thesis further, we exclusively stay in bilateral teleoperation concept as we have defined it previously (via the classification given in Appendix B) and focus on the control theoretical aspects of the teleoperation for a stable interaction with sufficient performance levels. The reason of such a terminological classification is to precisely draw the boundaries of what will follow in the later chapters. Such a restriction is necessary to keep the discussion of the involved approaches/methodologies mutually exclusive which are often presented in a rather intertwined fashion in the literature.

In Chapter 2, we first give an opinionated version of the literature to point out to the underlying connections between seemingly different methodologies and also provide an arguably simpler explanation of the well-known *wave variables* formalism. By doing so, we classify such methods in the corresponding mainstream control theory methods and demonstrate that they are indeed outdated in the light of the recent advances. Moreover, we argue that the by-now-standard assumption of *passivity* property on the human and environment is not experimentally validated. We also claim that the success of passivity-based methods are due to the conservatism of these tests and not due to the validity of the assumption.

In a similar fashion, in Chapter 3, we enumerate the available performance objectives by which we should design bilateral teleoperation systems proposed in the literature. Then we argue why these objectives might not be valid candidates for the problem at hand.

In Chapter 4, we also show both theoretically and numerically that the frequency domain methods (and a limited number of nonlinear methods) found in the literature can be combined under one framework via *Integral Quadratic Constraints* (IQCs). With these results, we demonstrate that the proposed approach of this thesis does not bring in additional complications or conservatism. In fact, via numerical case studies, we show that the results are precisely the same with those of the techniques available in the literature. Therefore, there is no fundamental reason to use a specialized terminology of the networks and microwave systems which in turn alienates mainstream control theory experts. We also remark that uncertainty modeling is a key aspect in obtaining better controllers for bilateral teleoperation. To highlight

the reasons why we promote this framework, we also give examples of different combinations of uncertainties for which classical tools that are employed in the teleoperation literature are not suitable but already available in the robust control literature for almost two decades.

After establishing this link with the methods in the literature, we turn to the controller synthesis problem in Chapter 5. We formulate the problem as a generalized plant and work out the scarce details that are found in the literature to obtain a better model- based control synthesis algorithm using static and dynamic IQCs. For the interested reader, we also explicitly identify what the implementation-related bottlenecks are. Then, in Chapter 6, we utilize this framework to design controllers for an experimental setup.

In Chapter 7, we provide some concluding remarks and for the reader's convenience, in Appendix A, we recap the basics of the network theory.

Let us turn to our initial question "*Why Bother?*". We do because there is no need to obtain the ultimate, perfect touch sensation for the human in order to interpret the signals correctly. It is the same principle with LED TVs. Nowhere on the screen, a color different than red, green, or blue is emitted. However, we tend to approximate the combined output of the closely positioned RGB LED triplets to the closest color since the distance between the emitters are negligible for the viewer and we achieve the color perception. Therefore, realism is not our primary objective. However, before we can even enter the discussion of what leads to a satisfactory sense of touch, we need to make sure that the teleoperation devices, i.e., our tools that we actually try to understand the sense of touch with, are stable and exhibit consistent performance such that experts from neuroscience, psychophysiology, and other related scientific fields can join and assess different ways of protocolling with the human brain in this modality. Otherwise their conclusions would be contaminated by the device properties. We can even speculate that this is often the case, though no proof will be presented here.

Thus the precise goal of this thesis is first to show the state-of-art control problems in the literature regarding the bilateral teleoperation with a critical evaluation of the claims often found in various studies. Then, we consider the stability properties and control problem of bilateral teleoperation without fully understanding the underlying problem. Unlike many sources in the literature, we openly discuss the reasons behind the lack of understanding and clearly point out the vague performance objectives reported in the literature. The method adopted here and the application to an experimental setup constitute yet another stab at problem from a pure engineering/applied mathematics point-of-view. It is more general than the existing literature in the sense that the uncertainties and perturbations can be handled more systematically while defining performance objectives. However, this is not enough to argue that we have actually set up a beneficial and widely applicable framework that leads to a stable and high-performance bilateral teleoperation systems.

A Brief and Opinionated Literature Survey

Teleoperation systems are structurally simple, two connected robotic manipulators, but equally challenging systems. This is especially true from a system theoretical point of view. As an example, if we just focus on the local and the remote devices that would be used for manipulation, we see that they are, whether linear or nonlinear, motion-control systems with well-studied properties. Hence, one can view the open-loop teleoperation, i.e., standalone devices without any communication in between, as a system with a block diagonal structure in which each input to this block effects only one of the devices. However, unlike the typical motion-control systems, these two disjoint systems must be stabilized simultaneously by the same controller[1], that is performing sufficiently well in order to "fool" the user such that the user feels a force feedback as if s/he is actually operating at the remote medium. With this structure, the outputs of either of these subsystems become exogenous inputs of the other and these are regulated by the to-be-designed controller. Therefore, it is this controller that makes a teleoperation system perform adequately or, as in many cases, drive to instability.

For example, in the case of the so-called *free-air motion*, i.e., the remote device is free to roam in the remote site, the human force input to the local device and/or the position of the local device should[2] be tracked by the remote device. In the case of a hard-contact of the remote device with the environment, however, these inputs should be counteracted if the force vector points into the obstacle. Hence, the force signal is simultaneously tracked for mimicking the user motion and is defied in case of a resisting force at the remote site. As if this is not challenging enough, when the user suddenly decides to release the local device, this resistance should die out as soon as possible, preventing a kickback. To sample the artificial nature of such a behavior, consider a user who leans to a wall located at position x_0 and beyond, applying a horizontal force and then retreating after some time. It is not expected that the wall continues to push the user even after the user has the position $x < x_0$. Such behavior would not only be unrealistic but also misleading as it can be confused with a sticky surface as far as the immersion is concerned. There are many other scenarios that would further complicate the requirements but, in short, the user and the environment properties are time-varying and make it difficult to

---

[1]We need to emphasize that the delayed/undelayed local control loops can be seen as the entries of a structured central controller. Thus, there is no reason to distinguish local control methods at this point.

[2]Or better, that's what we believe today.

design a straightforward control law such that these and many other details are handled properly, and more importantly, simultaneously.

With this short motivation, we can safely claim that looking at the overall system as a typical motion control system is not sufficient in terms of complexity (though necessary). In general, motion tracking specifications constitute a subset of the general performance requirements of bilateral teleoperation systems.

The inception of the bilateral teleoperation technology is often attributed to the work of Raymond Goertz in Argonne National Laboratories, [55] (in [9], it is traced back to Nikola Tesla and, in [178], even some 16th century tools are accepted as precursors of the contemporary teleoperation). The main motivation of Goertz' work (similarly later in Europe by Vertut [190]) was handling and manipulating nuclear material. Thus the very first teleoperators were purely mechanical to cope with hostile environment conditions. Though not much happened in terms of commercial product realizations, the concept of telemanipulation kept its appeal and a large body of research was reported until the 1980s. In that decade, with the help of the ever-increasing computational power and the popularity of Virtual Reality (VR), teleoperation technology received more attention for a possible use in the space-, underwater-, and medical-related tasks. Together with the advances in control theory and network theory (e.g. [50, 132]), a more systematic control methodology has been adopted. Especially, stability analysis results that can be related to design guidelines (physical parameter bounds, bandwidth limitations etc.) were utilized and limits of performance were explored. A particular phenomenon, namely the destabilizing effect of the delays in the teleoperation, lead the experts of the field to delve more into the systematic analysis tools and qualitative aspects of teleoperation. Especially, the use of the concepts such as, "passivity", "scattering transformations", and "wave variables" has become the standard methods of analysis and synthesis (see, e.g., [3, 59, 137]). Arguably, this point is where bilateral teleoperation branched off from the general control theory and became a specialized area of research, specifically dealing with a particular problem that is still a matter of unresolved debate, as we touch upon later in this chapter.

We start to summarize the advances from this point as this thesis is precisely built on top these systematic analysis and synthesis results gathered in the last two decades. However, the reader is referred to [17, 79], and [178] for a more detailed overview including other practical aspects of teleoperation analysis and the hardware developments with a more historical perspective which will be omitted here.

As we keep on narrowing down our focus to the control theoretical parts of this challenging problem, we have to note that many parts of the bilateral teleoperation problem can be scrutinized under different frameworks. Hence, there is no shortage of techniques for which the bilateral teleoperation problem is an ideal test case. In this plethora of methods, for example, the variation of human and environment properties give naturally rise to a robust or an adaptive control approach, the hard-contact problem can be analyzed by viewing it as switched control systems, jump control systems or constrained linear systems etc. Thanks to these advances,
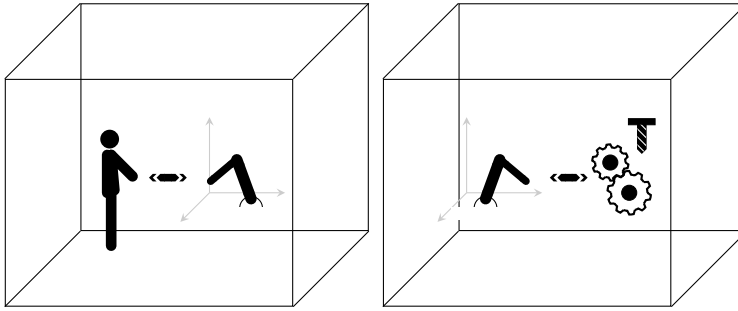
Figure 2.1: General Teleoperation System

as we elaborate, the main unsolved problem is not a methodological one but a motivational one. In other words we are lacking not the solution methods but rather a fundamental understanding of the problem in terms of what the requirements are and what a good device is if compared to another. Let us sample a few important and successful approaches reported so far together with their shortcomings if any.

We emphasize that the literature covered here is far from comprehensive and deliberately shaped with pragmatic intentions. Hence a large body of research is left out. This is certainly not due to their lack of thoroughness or else, but simply due to the irrelevance for the purpose of this chapter. In general, the methods that are left out either don't define a performance objective or only focus on the particular detail about bilateral teleoperation instead of the human perception. The reasoning behind this choice should be more apparent after Chapter 3.

2.1   MODELING OF BILATERAL TELEOPERATION SYSTEMS

The dominating modeling paradigm of bilateral teleoperation systems is the two-port network approach. Consider the following quote from 1989:

> The modeling approach is to transform the teleoperation system model into an electrical circuit and simulate it using SPICE, the electronic circuit simulation program developed at UC Berkeley. ([59])

As seen from Hannaford's motivation, the computer-based simulation tools are used extensively since then. Arguably, this is one of the main reasons why network and electrical circuit based modeling dominated the teleoperation literature. Reinforced with the circuit simulation tools, experts of the field started to construct analogies that go beyond a mere mechanical-electrical system analogy. Consequently, the most prominent concept borrowed from these analogies is the two-port network view of bilateral teleoperation systems. The reader is referred to Appendix A for a short recap of network theory. Today, the quoted convenience also applies to almost all physical systems, i.e., one can simulate arbitrary models

via many computational packages. Yet, it's a de facto standard to use the circuit modeling while the teleoperation devices are mostly mechanical. Hence, it's not clear whether the benefit of such an artificial step still exists. Once the system is represented by a mathematical model, as it is demonstrated in the later sections, the mechanical/electrical analogy is, roughly, an equivalence based on the resulting model and works in the "from electrical to mechanical" direction too. Therefore, the circuit based modeling approach is merely a convention rather than a requirement.

2.1.1 *Two-port Modeling of Teleoperation Systems*

In the teleoperation context, if one uses the "load-source" analogy for the manipulated environment and the human, then the system models all the bilateral interaction between the load and the source ports (as in Figure 2.2a). This modeling view is quite powerful since the components are described via their input/output (or external) properties, i.e., across variable/through variable relations (e.g. force/velocity, voltage/current etc.). Also, the non/linearity properties of the components are not relevant at the outset if we are only interested in energy exchange, which is the basis of the so-called Time-Domain Passivity Methods [60] which we also mention later in this chapter. Thus, the user, the control system, the environment, the remote and local devices and the communication delays are seen as 1- and 2-ports exchanging energy in time. Since the external behavior of the ports can be characterized completely by the power variables associated with the terminals, e.g., voltage drop across the terminals and current flowing through them, it is indeed very convenient to model these components with electrical ports as interacting "black boxes" (See Figure 2.2a).

Remark 2.1. *We should emphasize here that, in this context, the energy exchange is used as a gauge of a potentially unstable behavior. The motivation relies on the fact that in order to classify a system as an unstable one, the system should exhibit unstable behavior at its port(s) and to exhibit such behavior additional energy is needed. Hence if all the components are incapable of contributing energy in the loop, finite energy excitations will eventually decay and the system would reach its steady state after a transient response[3]. As one can directly identify, this is simply the rough sketch of the celebrated passivity theorem. Based on this argument, there is a recurring theme in the literature that a teleoperation system should be passive in order to have a stable interconnection. This is due to the hypothesis that end terminations are also passive. However, in a few studies, this is mistakenly taken as a sufficient and necessary condition for stability and hence creates quite some confusion for the non-experts of the field. Passivity is not an essential feature of the teleoperation systems but only a convenient shortcut for deriving interconnection stability conditions. We should iterate that stability is the top-priority objective and does not require passivity by any means even if we do guarantee stability by rendering the sub-components passive.*

---

[3]For the sake of brevity, marginal stability or limit cycles also require extra energy for the sustain.
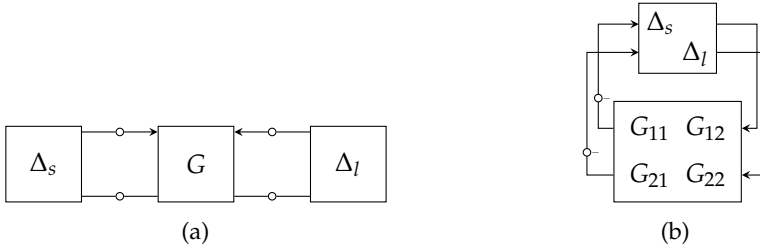
Figure 2.2: Two representations of a 2-port network. Here Δ_s and Δ_l represents the source and the load immitances respectively. In the teleoperation context, they are the human operator and the explored environment.

Clearly, thanks to this modeling method, we don't even need to know exactly what Δ_l, Δ_s blocks are, except their class (e.g. linear/nonlinear, time invariant/time varying etc.) to analyze the interconnection via G and its port behavior. Thus, the problem of modeling of the human arm or of the uncertain environment is circumvented. However, with the same reasoning, the passivity property does not distinguish particular systems as long as they are passive. That is to say, some of the crucial information is lost about these specific ports; we discard any impedance or admittance relations shared by the port variables.

Energy based modeling is also the natural basis of bond-graphs. Bond-graphs, much like port representations, are graphical tools to model the dynamical systems via energy balancing between subcomponents (See [53] for an introduction). In other words, the bond-graphs are built on top of the notion of bonds representing the instant energy or power exchange between nodes via edges drawn between them. Therefore, bond-graphs already present a powerful framework for the abstraction of the bilateral interaction between the local and the remote site. For a classical use of bond-graphs in impedance control, the reader is referred to Hogan's trilogy ([76–78]). There are also many studies with application focus, e.g., [104] using hydraulic systems for bilateral teleoperation, among many others.

2.1.2 *Assumptions on the Local and Remote "Ports"*

As mentioned above, network theory offers a great opportunity for modeling teleoperation systems, or better, avoiding a refined modeling. Still, to invoke the stability analysis and synthesis results of network theory, there is a need to distinguish Δ_s, Δ_l further in the universum of 1-ports. Otherwise, with no additional assumptions there is not much we can conclude from such an interconnection since they can be any arbitrary model with arbitrary behavior set as long as they respect the port condition. This is obviously a crude approximation of the real physical interaction that teleoperation systems exhibit.

In the teleoperation and haptics literature, it is customary to assume the load and the source terminations as "passive" mathematical operators (see Appendix A).

Starting with this hypothesis, the stability problem can be converted to a typical energy dissipation problem. Hence the view of the designer is tuned to look out for the energy sources and interaction between two distant media. This approach treats the human and the environment as passive 1-port circuit elements together with additional voltage and/or current sources modeling the intentional force input to the system. The controller(s) act as the energy regulator preventing excess energy generation to avoid a possible instability even in the cases where extra energy does not endanger stability or in fact needed by the user to accomplish certain task or stabilize the system.

Additionally, as summarized in Appendix A and in Chapter 4, one can use the network theory based conditions to assess the stability and performance conditions thanks to this hypothesis.

This brings us to the discussion of the justification of the assumption as it is generally not given in full generality in the literature. Is it indeed calid to assume that the human can be modeled as a passive system? If one scans through the literature about the passivity of human operators, it is the Hogan's paper [75] that is almost universally cited. The striking detail is, however, that Hogan never claims that the human hand/arm is a passive system. Instead he clearly shows that under very specific conditions, human behavior is indistinguishable from that of a passive system:

> Thus, despite the fact that the limb is actively controlled by neuro-muscular feedback, its apparent stiffness is equivalent to that of a completely passive system. In the light of Colgate's recent proof [3][4] that an apparently passive impedance is the necessary and sufficient condition for a stable actively-controlled system to remain stable on contact with an arbitrary passive environment, this experimental result strongly suggests that neural feedback in the human arm is carefully tuned to preserve stability under the widest possible set of conditions.

Moreover, the task reported in the paper that is given to human operators and analyzed afterwards, can be considered as a biased one because the success of the test is related to the passive behavior of the human. The task is, roughly speaking, holding a handle which is perturbed by random disturbances and trying to keep the handle still at a predefined position on the 2D plane. Hence, the task is simply to mimic a passive system. Had it been the case that measurements on the human arm would exhibit a non-symmetric stiffness matrix in the arm model, it would simply be a failure of the test subject (regardless of the physical limitations of the human arm in general). Note that this is a plausible situation for rehabilitation tasks. The other possibility would then be that the test subject was unable to keep up with the changes, or using the control theory jargon, the bandwidth of the subject

---

[4]Reference [27] of this thesis. However exactness of stability characterization for two LTI passive complex uncertainty blocks was already well-known in SSV theory (e.g., [142]) and also in the classical network theory works at the time of writing. Therefore it is a misattribution.

was lower than the required agility to perform the test adequately. The well-known phenomenon due to such human input is the "pilot induced oscillations" in which the pilot of an aircraft, while trying to stabilize the aircraft, via overcorrecting inputs, destabilizes the system due to many distinct reasons (the phase lag of the pilot, response time of the aircraft etc.). We refer to the interesting report [124] for a more detailed exposition. Also, if for some reason, the task at hand is to prevent the system to reach a steady state at a certain position and the perturbations are applied accordingly i.e., to create a virtual negative potential, the results obtained from the experiments would most probably differ from that of [134]. Thus, it's emphasized here that the passivity of the human is closely linked to the requirements of the tasks.

Remark 2.2. *A particular detail should be clarified about the measurements taken in [75]. It is stated that:*

> *While normal human subjects held the handle of the manipulandum at a stable position in the workspace, small perturbations were applied. Measurements of the human's restoring force were made after the system had returned to steady state following the perturbation but before the onset of voluntary intervention by the subjects.*

Therefore, it is emphasized that only the involuntary response is taken into account during the measurements in order to capture the natural properties of the human arm before the human correction intervenes. In fact, due to this crucial distinction the results such as [40] don't disprove Hogan's results since the voluntary input is included in the model.

We believe that it is unaviodable to introduce some concepts from the muscle physiology in order to put Hogan's argument into some mechanical engineering perspective. It is simply impossible for us to give a detailed analysis, however, mentioning the involved process via some mechanical analogies in order to relate the results of Hogan and Mussa-Ivaldi ([134]) seems feasible. This would emphasize the reason why we think that the common inference from their experiments in the literature is not inline with the conclusions of these studies. We refer the reader to the physiology literature e.g., [54, 80, 129, 139, 181, 198] and references therein for a full treatment. Hence, we will only give a rough picture about the apparent behavior. Nevertheless the point that we want to emphasize is, fortunately, not related to the inner workings of the human muscles.

The skeletal muscle activation takes place via a process described by the *sliding filaments model* (Figure 2.4). The muscles consist of muscle fibers and muscle fibers are made up of *myofibrils*. The myofibrils involve different types of thin and thick filaments, mainly of the type *actin*, *myosin* and *titin* filaments. The myosin filaments involve extensions that can bind to the thin actin filaments. The relative motion of these filaments are produced due to these extensions via ATP hydrolysis. Moreover, these extensions stay connected or disconnected to actin filament unless more ATP is utilized. Hence, the muscle needs extra energy to relax which is the reason behind
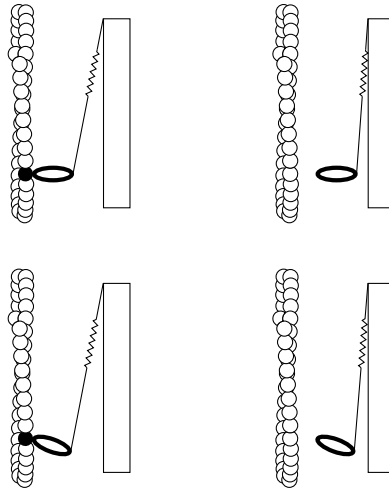
Figure 2.3: Muscle activation mechanism (adapted from [54])

"*rigor mortis*" and some types of the muscle spasms when this additional energy source can not be provided or ATP can not bind to the actin filament for some reason. Moreover, binding or detachment of these extensions is also regulated by the Ca^{++}, Mg^{++} concentration in the muscle cell and controlled, eventually, by motor neurons using yet another chemical trigger.

Therefore, the individual muscle activation at the basic level is analogous to a clock escapement mechanism [66] i.e. each time the lever arm pulls back a thread of the gear and the cycle repeats. The resulting relative motion is very much like a graphite coming out of a mechanical pencil when pressed from the eraser cap. Obviously, muscle behavior is not rachet-like but smooth. This is because each of these mechanism operate independently. Thus, at each time instant, different myosin extensions can be found at different phases of the cycle very much like a helical gear pair that are always in contact at one point. Using this analogy, ATP molecules are used to open and to close the pencil clutch made up of myosin extensions and actin filament is pushed forwards. Moreover, titin filaments can be thought of as the connecting rod of the pencil from the cap to the clutch which is mostly responsible for the passive elasticity of the muscles.

In summary, the muscles have varying non/backdrivable configurations. More-over, we can lock our muscles in place e.g., we can try to keep our arm at one position during drilling etc. to increase the precision. Then, the arm becomes a stiff object with inherent stiffness of the connection rod (titin), pencil clutch (myosin actin), muscle tendons and various other involved processes resisting to the applied strain.

Coming back to our original discussion, the stiffness of the arm that has been the subject of the experiments mentioned above is, again invoking the analogy, based on the closed clutch response of the arm. In other words, what is measured is a
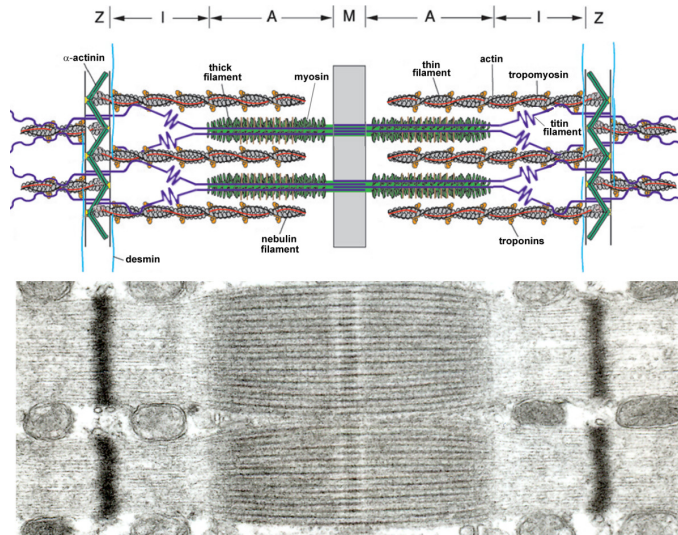
Figure 2.4: The simplified illustration of the sliding filaments model for a single sarcomere. (Source: [140])

cumulative spring-like behavior of the arm that is actively controlled to be kept at a certain configuration. This is related to the "human's restoring force" given in Remark 2.2.

Having a spring-like property naturally implies that the arm is passive. But the problem with this argument, as far as we understand, is that there is no reason to assume that the human arm model involves a symmetric positive definite stiffness matrix at each time instant for an arbitrary trajectory. In fact, as shown clearly in [134], the major eigenvector of the stiffness matrix varies both in terms of direction and magnitude. Therefore, it might be possible to extract energy from the human arm with some particular pathological trajectory. Just in the case of a frozen time analysis of a time-varying operator does not imply stability, the conclusion is only valid for postural analysis at a fixed configuration of the human arm but not for an arm trajectory.

Therefore, it is our belief that the assumption of human arm being a passive system is incorrect for most teleoperation tasks.

Since it is customary in the literature to include the passivity hypothesis, let us invoke it here too for the sake of the argument. The question of how, then, a human can possibly move anything while remaining passive is one that makes the whole story even more complicated. The voluntary input of the human is taken as an exogenous and state independent input to the system. Hence, the human cognitive input is an additional but independent force source acting on the handle together with the passive human arm immitance as depicted in Figure 2.5. In other words, the contribution of the exogenous force and the arm dynamics are assumed
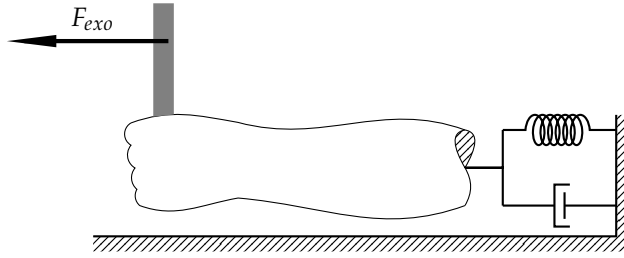
Figure 2.5: A pictorial representation of the state independent human force input. By state dependence, we mean that the vector F_{exo} is completely decoupled from the arm characteristics and can be taken as a genuine exogenous input.

to remain mutually exclusive.

The reader would spot that this is not in line with Hogan's remark since the activation state in the muscles should be altered in order to apply some force. In other words, we need to alter the stiffness matrix of the arm to be able to move but, to the best of our knowledge, this is not given in any teleoperation study. In other words, the answer to the question of whether the human's restoring force would exhibit the same properties during the force exertion phase is not known to us. It has been also shown that the applied force is also related to the muscle tension-length properties [81] which we have not considered in our analogy.

Therefore, we have to further separate the human force into two parts, namely, the active neuromuscular feedback force that keeps the human arm passive and the voluntary and cognitive force input applied to the system. How this is usually performed is not clear in the literature. To the best of our knowledge, this issue is considered (but still briefly) only in [93, Sec. II.B] and references therein.

This ambiguity becomes much more important since the control oriented focus of this thesis necessitates that we concentrate on worst cases rather than the experiments performed within the cognitive range of human operators. In other words, we are interested in the cases where things go wrong due to various reasons, such as sampling disturbances, measurement noises, directionality etc. Therefore it cannot be a satisfactory argument if stability depends on the user's neuromuscular feedback or, simply, the user's stabilization capabilities. In order to use the bilateral teleoperation devices in real-life, stability should be addressed regardless of the set of prescribed human actions. Hogan's findings are not sufficient for supporting the passivity assumption often found in the literature.

In summary, the passivity of the human and the environment (or the virtual environment in haptics/virtual reality applications), is only plausible in certain cases; then it should be verified regardless, in order to assume that the corresponding mathematical models are passive. Still, analysis and synthesis methods that invoke this assumption lead to many real-world implementations with varying degrees of realism. An obvious follow-up question is "how can then the reported

analysis and synthesis results based on this passivity assumption lead to successful implementations which would imply the validity of the assumption?". We need to focus on the "successful" part in order to answer this question. If we again scan through the literature these successful implementations are only successful under strict assumptions about the user behavior together with any combination of the following device properties

- The controller stabilizes the loop via excessive apparent damping hence either or both free air or hard contact realism is lost.

- The bandwidth of the force and position tracking are exceedingly small.

- The remote and local devices exhibit position drifts over time.

- The performance of the device is time-varying and not uniform.

We argue that the success of these methods is due to the conservatism of the analysis/synthesis tools and does not validate the passivity hypotheses on the respective models. Many frequency-domain methods, which assume LTI terminations at both ends of the teleoperation network, are reported to achieve stable bilateral interaction in real setups. While impressive, this shouldn't have been possible had the tests not been exceedingly conservative since the real setups involve sudden contacts i.e. they are essentially time-varying systems. We recall the well-known fact that the behavior set of the time-varying systems are significantly richer than LTI systems. Once again, we remind the reader that the proper metrics to gauge the success of teleoperation systems are not known and we use the typical error-norm based control design rationale.

A compact version of the argument above is given by Yokokohji and Yoshikawa in [200]:

> Passivity of the system can be a sufficient condition of stability only when the system interacts passive environments. In the case of master-slave systems, if we could assume that the operator and the environment are passive systems, then the sufficient condition of stability is that the master-slave system itself must be passive. Strictly speaking, however, the operator is not passive because he/she has muscles as the power source. Colgate et al. [21][5] mentioned that even if the system has an active term, the system stability is guaranteed unless the active term is in some way state dependent. Obviously, the operator is passive when $\tau_{op} = 0$. Therefore, we will give the following assumption about τ_{op}: "*The operators input τ_{op} independent to the state of the master-slave system. In other words, the operator does not generate τ_{op} that will cause the system to be unstable.*" Dudragne et al. [3][6] gave a similar assumption in order to use

---

[5]Reference [27] of this thesis.
[6]Reference [38] of this thesis.

the concept of passivity for stability distinction. The above assumption seems tricky in a sense, but it is necessary to ensure the system stability by the passivity.

Finally, a supplementary remark is also given by Buerger and Hogan in [15]:

> When passivity is used as a stability objective, the only assumption made about the environment is that it, too, is passive. This is likely sufficient to guarantee coupled stability with humans (though, to date, it has not been conclusively proven that human limbs are passive; see [29][7] for an argument for treating them as such). However, given the properties of human arms described above, passivity is unnecessarily restrictive. Our experience has shown that some controllers that are known to be nonpassive are adequately stable in clinical rehabilitation tasks [26][8].

We should mention here that Hogan's paper together with other identification experiments are extremely important for many fields and needs no motivation. The discussion above only points out that the frequently reported inference that follows from his results is not in line with the results.

The idea of modeling the teleoperation as a two-port network seems to have multiple origins and we have no reference to point out a common source. However, in general, the popularity of two-ports can be attributed to [3, 59, 137, 157, 200].

2.1.3 *Uncertain Models of Bilateral Teleoperation for Robustness Tests*

Another possibility of modeling the human arm and its cognitive input is to define a reference position signal "filtered" by the human arm impedance[9] e.g., [93, 114]. Various studies pointed out that the identification experiments suggest a mass-spring-damper system pattern is evident in the frequency response data of the human arm recorded under various task performance similar to the one given in [75]. The general method is to instruct the human to perform a specific task and then perturb the hardware with certain predesigned disturbance signals such that the output can be evaluated to obtain a mathematical model. In the literature, the model structure is often set a priori to be a second order transfer function and the parameters are optimized to minimize the mismatch between the experimental and predicted response. It is also well-known that the human can change the inherent impedance of the arm during the task execution (see, e.g., [186]). Therefore, the studies are performed in the ranges where it is safe to assume that the human arm characteristics are constant or constant up to negligible changes.

---

[7]Reference [75] of this thesis.

[8]Reference [16] of this thesis.

[9]The term *impedance* is used in a more general sense than its common usage to denote LTI transfer functions such that no distinction is made between linear and nonlinear or time-invariant and time-varying operators.
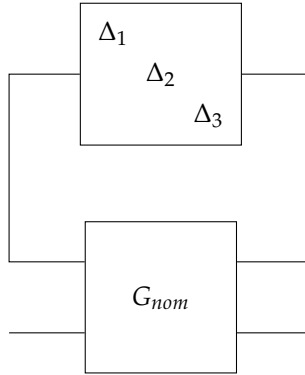
Figure 2.6: Uncertain model representation by taking out the uncertainty blocks

The modeling is straightforward via uncertain mass-spring-damper system differential equation manipulations. Suppose the human arm admits the second order model

$$M(\Delta_1)\ddot{x} + B(\Delta_2)\dot{x} + K(\Delta_3)x = F_h - F_m$$

where F_h, F_m denote the human force and the force feedback inputs, respectively. Then choosing a multiplicative or additive uncertainty structure and via basic linear fractional transformations, the signal relations are converted to the interconnection shown in Figure 2.6. The arrows are deliberately left out as it is up to the designer to get different immitance models.

Many studies have appeared in the literature regarding such modeling and the majority of these assume a mechanical model of order from two to five. Note that this is an assumption made a priori and only applies to the specific task performed by the human in the experiment from which the frequency response data is collected. The commonly utilized models, unfortunately most given for the fixed postural arm configuration can be found in [4, 15, 29, 49, 82, 93, 103, 110, 115, 180, 185]. Obtaining these measurements are time-consuming and difficult to parameterize. For this reason, although the results along this direction are scarce, they are, as in the passivity case, very valuable.

The disadvantage of such parametrization of the human arm is contrasted with the passivity approach methods invoking the argument of the time-varying nature of the arm parameters. It is often rightfully argued that the uncertainty ranges in which the stiffness and damping (and partially inertial) coefficients change, are too large to be considered in the structured singular value based robustness tools. Moreover, many auxiliary effects such as the visual feedback, cognitive lag of the brain etc. are not considered in the identification experiments; in the passivity approach all of these are lumped into a single port condition. Obviously, the main difficulty is to get a model (out of hypothetical insights, identification experiments etc.) which is not required in the passivity approach.

The papers [114, 154] offer interesting alternatives for human modeling as they attempt to incorporate many of the aforementioned effects, but the results are prospective and yet to be utilized.

2.2 Analysis

The stability analysis is one of the major problems in designing stable yet high-performance teleoperation systems. It's often not feasible to manually tune some local controllers and make test subjects use it in order to verify the design specifications. Moreover, by relying only on the experiments, one can miss an important destabilizing scenario if the field experiments do not cover that particular case. Hence, an a priori certificate of stability is much sought after. The stability analysis can also give some guidelines about the parameter selection in the hardware design phase and can lead to minimized design iterations. Therefore, having a realistic stability test is essential in building these systems.

Similar to the modeling section, the analysis in the literature extensively relies on network theory based results. In fact this is where the network theory stands out as a complete tool for analysis and synthesis of bilateral teleoperation systems via the hypothesis that human and the environment models are passive.

The common terminology for stability is somewhat different than that of the contemporary control theory as *nominal stability* is used for the stability properties of isolated two disjoint media; when the interaction is set up between these two media the closed- loop stability problem is called *coupled stability*. To the best of our knowledge, this terminology is introduced in [27] hence we refer to this paper (or Colgate's thesis [26]) for more details.

It's also worth mentioning that the passivity and stability is used often interchangeably and also usually referred to the classical texts [20, 65, 131] for the precise definitions. Hence, there is a little guesswork required to classify the stability definitions given in the literature in order to locate which version is meant. The important distinguishing point is that marginal stability is often accepted in the definition of stability results since it arises frequently in lossless (hence passive) models where energy conservation is assumed. However, the analysis results that rely on such assumptions do not guarantee asymptotic interconnection stability, but only lead to certain passivity properties of the interconnection (see [95, Thm. 6.1] and [112, Sec. V] for the discussion on strict passivity).

As given in Section 2.1, the passivity property is crucial to many studies in the literature. The direct physical interpretation of the abstract concepts gives even more appeal to such energy book-keeping methods. Another advantage of passivity methods is that the nonlinear counterparts of the results are also available in the literature and relatively easy to utilize. However, this convenience misses out many relevant details that are specific to teleoperation systems and result with too general conditions. Let us recall a general version of the passivity theorem:

Theorem 2.3. *The negative feedback connection of two passive systems is passive. The neg-*

Figure 2.7: A transparent two-port network with passive terminations. The actuation of the railcar is taken as a state-independent input to the system. (Source: Fred Dean Jr., [Flickr:Fred Dean Jnr])

ative feedback connection of a passive system with a strictly passive system is asymptotically stable.

Note that, this result is valid for both nonlinear and linear systems. Invoking the theorem twice on the teleoperation system allows us to conclude that, under the passivity assumption of the human and the environment, if the two-port is passive then the interconnection is passive. Moreover, if any of the involved operators is strictly passive the teleoperation system is asymptotically stable.

The passivity theorem is in general not necessary for stability but only sufficient. Because there do exist stable interconnections that involves nonpassive subsystems. In particular, the conservatism brought in by passivity assumption is arbitrarily high (especially in the nonlinear case). Facetious as it may seem, the test also takes into account the port terminations shown in Figure 2.7 for a table-top joystick. We have to emphasize that the three-carriage railcar with two cabs, is a valid, almost perfectly transparent two-port network with passive end terminations. Hence, a regular passivity-based stability test includes those end terminations for a simple hand-held device. In other words, if we only consider the passivity property of the involved subcomponents and do not distinguish further, there is no possible way to distinguish a table-top teleoperation system from a train since both are passive. It's that conservative.

The major disadvantage of the passivity methods is that the procedure is focused almost only on the energy exchange. The performance specifications are very difficult to formulate and also difficult to integrate into the analysis and synthesis steps using only the inner product structure. As an example, the signals that are not port variables such as position errors, nonlinear effects etc., that are functions of these signals, can't be utilized easily in the performance specifications. Same difficulty arises in the normed space structures though much more can be achieved. Similarly,

peak-to-peak gain minimization methods are not mature enough to handle any practical system without excessive conservatism.

Another disadvantage is that the power- or the energy-based analysis, due to the inner-product structure, can not distinguish the individual signals. Consider the ideal case where the human and the local device is pushing each other and cancelling each other's contribution. In this case the external or observable energy exchange based on the port variables is zero (negligible) which can not be distinguished from the case of not touching at all (a small motion on the device).

When the network, human, and the environment models are assumed to be Linear Time Invariant (LTI), the frequency domain methods allow us the analyze the teleoperation systems for stability and performance. The most common stabiliy analysis tool for such models is the Llewellyn's stability criteria (also often called absolute stability theorem or unconditional stability theorem). For linear networks, the following definitions seem to be used quite widely (modified from [20]):

Definition 2.4 (Potential Instability). *A two-port network is said to be potentially unstable if there exist two passive one-port immitances that, when terminated at the ports, produce a persisting natural frequency.*

Definition 2.5 (Absolute Stability at $i\omega_0$). *A two-port network is said to be absolutely stable if it is not potentially unstable.*

2.2.1 *Llewellyn Stability Criteria*

The well known conditions for stability of a two-port network, formulated in [13, 116, 162], are recalled in Appendix A. As shown in [162], the conditions stated in Theorem A.7 are invariant under immitance substitution. This result forms the basis for almost all passivity-based frequency domain bilateral teleoperation stability analysis approaches in the literature. We also derive this theorem from an IQC perspective and show that it is actually the passivity counterpart of the of the D-scalings in the μ-tools. This has also been derived in a scaled teleoperation context in [153] using only Structured Singular Value (SSV) arguments.

Thanks to the frequency domain formulation, it is possible to rewrite the condition (A.12) as a fraction and see the problematic regions in which the fraction gets close to or crosses to the instability, together with one of the conditions given in (A.11).

2.2.2 *µ-analysis*

As given in Section 2.1.3, stability in the face of uncertainties can also be analyzed in the generalized plant framework of robust control. After rewriting the signal relations, the teleoperation system can be written as an uncertain interconnection as shown in Figure 2.9. In this setting, G is the model of the nominal bilateral teleoperation system and Δ is a block diagonal collection of uncertainties, such as the human, the environment, delays, etc. Stability tests are based on structural
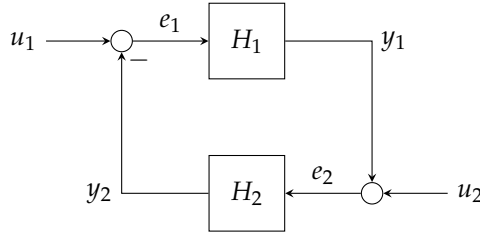
Figure 2.8: Negative feedback interconnection
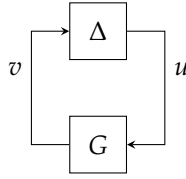
Figure 2.9: Uncertain Interconnection

hypotheses on the diagonal blocks of the operator Δ such as gain bounds or passivity. These properties should allow us to develop numerically verifiable conditions for the system G that guarantee interconnection stability. This is intuitive because we have no access to the actual Δ and we can only describe its components by means of indirect properties.

If the interconnection subsystems are represented in the scattering parameters, the μ test is precisely equivalent to the test of Llewellyn's theorem and often called as Rollett's stability parameter. This is due to the well-known equivalence between the small-gain and passivity theorem [36]. We have to note that the equivalence is stated in terms of the stability characterization. Otherwise, the small-gain theorem requires a normed space structure whereas passivity theorem requires an inner product space structure, hence the applicability is relatively limited. This is also related to the fact that we need to work with power variables exclusively in the passivity framework and this is not always convenient if the performance specifications are related to other variables.

In the literature, this analysis method often follows the scattering transformations such that, the passivity assumption avoids the explicit modeling and then small-gain theorem is utilized mainly to handle the delay problem via with the involved norm bounded operators. A refinement can be found in [153] where the authors utilize a direct μ-analysis to reduce the conservatism, however rather remarkably, it's not picked up by other studies and the analysis is mainly limited to small-gain conditions even in the linear systems.

We could have also directly chosen to utilize the uncertain modeling of the human and the environment and utilize μ-analysis for the teleoperation system had the specific models been available.

2.2.3 *Modeling the Communication Delay*
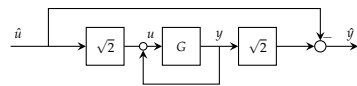
Over the past two decades, it has been confirmed in various studies that, if present, communication delays are a major source of instability (reports date back to 60's, e.g., [177] and the references in [3]). Even when the delay duration t is known and constant, the delay operator can be shown to be nonpassive since e^{-st} is not positive real. Hence, when combined with the passivity framework, it violates the assumptions on the uncertain operators.

At end of the 80's and early 90's, two prominent studies ([3, 137]) proposed to handle the delay robustness problem using scattering transformations. This notion is best explained, in our humble opinion, by loop transformations since the original articles refer to microwave and transmission line theories which use quite specialized terminology. One can also find a slightly different system theoretical view of these transformations in [28]. If we restrict the discussion to LTI operators[10], the key concept of the scattering transformation or the wave variables methods is to map the closed right half plane to the closed unit disk via a special case of bijective Möbius (or linear fractional or bilinear) transformation:

$$W : \mathbb{C}_+ \cup \mathbb{C}_0 \mapsto \{z \in \mathbb{C} \mid |z| \leq 1\} , \ W(z) = \frac{z-1}{z+1} \tag{2.1}$$

One can directly verify that $1 \mapsto 0, \infty \mapsto 1$ and $0 \mapsto -1$ under W. Pictorially, the mapping is given in Figure 2.10 using a Smith chart which is located at the origin. Hence, positive real transfer matrices become norm bounded by 1 such that we can analyze the interconnection using the small-gain theorem.

Let us demonstrate a few properties of this transformation. First, this mapping can be shown with a block diagram. Assume that G is a proper positive real LTI SISO system and let the input/output relation be given by $y = Gu$. Then, with a standard manipulation, we obtain a feedback interconnection that leads to the mapping

$$W(G(s)) = \frac{G(s)-1}{G(s)+1} = -1 + \frac{2G(s)}{G(s)+1} \implies$$

(2.2)

Simply following the signal paths, we also see that the input/output relation becomes

$$\tilde{y} := W(G(s))\tilde{u}.$$

where

$$\begin{pmatrix} \tilde{y} \\ \tilde{u} \end{pmatrix} = \sqrt{2} \begin{pmatrix} -1 & 1 \\ 1 & 1 \end{pmatrix} \begin{pmatrix} u \\ y \end{pmatrix} \tag{2.3}$$

Note that, physical realization of this transformation requires a simple feedforward and a feedback control action to which typically referred with *"Wave encoding"*.

---

[10]In the nonlinear case, it's a *completion of square* argument to switch from the inner product structure to a norm structure provided that the signal space is suitable for such operation.
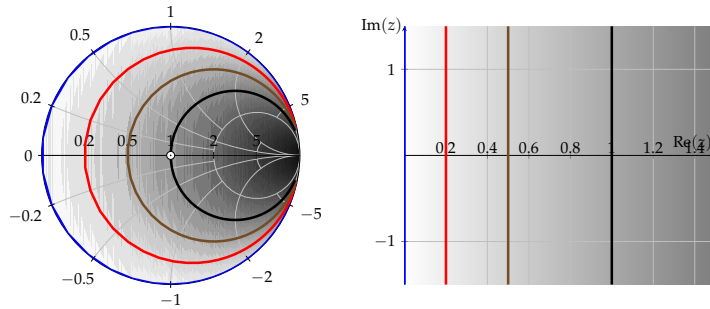
Figure 2.10: Mapping the closed right half plane onto the unit disc.

Often these variables are normalized with $\sqrt{2}$ at the outset. The seperation of $\sqrt{2}$ blocks is a matter of convention and provides symmetry in the block diagrams. Also we have,

$$(W \circ W)(G) = \frac{-1}{G},$$
$$(W \circ W \circ W)(G) = \frac{-1}{W(G)},$$
$$(W \circ W \circ W \circ W)(G) = G$$

which shows the effect of the $90°$ clock-wise rotations of the Riemann sphere about the axis parallel to the imaginary axis (W is an element of Möbius group with $\circ$ operation). This stereographic projection idea is also the main idea behind the derivation of the stability parameter of Edwards and Sinsky ([41]).

Obviously once this transformation is introduced, there is a need for the "inverse" of W on the operator that is seen by the operator G such that the loop equations remain unchanged, that is to say we have to introduce another transformation that undoes W. The simplest way to obtain a mapping $\hat{W}$ is to follow the block diagram backwards as shown in Figure 2.11. A block diagram reduction step(or rotating three more times as shown above) shows that

$$\hat{W}(z) = -\frac{z+1}{z-1} = -\frac{1}{W(z)}$$

which is nothing but the inverse of the relation (2.3). The negative sign usually does not show up in the formulations in the literature because the passive interconnections require a sign change in the loop to indicate the "from" and "to" ports. A more detailed derivation is given in [28]. Also note that a positive real transfer matrix, when negated, has its Nyquist curve confined to the close left half plane (anti-positive real) which is equivalent to a $180°$ rotation or application of W to the closed left half
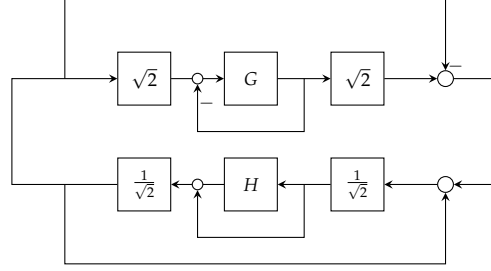
Figure 2.11: Scattering transformation and its inverse.

plane twice. Thus, some care is needed for the book-keeping of the negative signs and seemingly the best practice is to absorb the negative sign into H at the outset and work with $-H$ afterwards. This makes the required forward and backward transformations in the loop identical. One can see that there are many variants of this mapping, especially in wave variables context, e.g., $\frac{z-b}{z+b}$ but for simplicity we take $b = 1$ as it doesn't play any role in our presentation of the method.

Under the mapping W, the Nyquist curve of e^{-sT} (the unit circle) is mapped onto the imaginary axis, and hence unbounded, i.e.

$$\frac{e^{-i\omega T} - 1}{e^{-i\omega T} + 1} = i \tan \frac{\omega T}{2}$$

One can also obtain a similar qualitative result by seeing the unit circle $\mathbb{T}$ as the image of the imaginary axis under W:

$$W(\mathbb{T}) = (W \circ W)(i\widetilde{\omega}T) = \frac{1}{i\widetilde{\omega}T}$$

We don't need to track the points individually as we are only interested in the domain and its image under these transformations.

Therefore when we connect a passive operator to a small-gain operator, neither small-gain nor passivity theorem can be applied directly since each operator is not in the class of the other operator. In other words, delay uncertainty does not satisfy the norm constraint $\|W(e^{-i\omega t})\|_\infty \leq 1$ to invoke the small-gain theorem in the transformed coordinates. Had it been the case that the uncertainty was bounded by one, then it would have been possible to conclude stability directly in the passivity theorem anyhow. Thus, these transformations are not directly beneficial for analysis, however, following the cue from the previous mapping results, studies [3] and [137] made it possible to design controllers that renders the passive subsystem a norm bounded one and hence allowing delay robustness to be inspected via small-gain theorem. The resulting loop is stable regardless of delay period, hence they belong to the class of methods often distinguished as "delay-independent" methods. According to the literature, these are the most common methods applied in the face of delay uncertainty.

Delay is Small-Gain

Another possibility is to utilize the simple fact that the delay operator is gain-bounded and obtain the generalized plant by pulling out the uncertainty out of the loop. Obviously, this would be a very crude characterization of the unit circle since a unit disk is used as the uncertainty instead. However, as we show later, wave variables/scattering transformations directly use this conservative formulation to model the delay in the stabilization of the loop.

A similar approach is reported in [115] using μ-synthesis. By exploiting the low frequency property of the operator $e^{-sT} - 1$ and covering with a dynamic filter, the conservatism is reduced. But the authors have omitted the uncertainty of the human and the environment. Therefore, their analysis is only valid for nominal teleoperation systems. Though, this can be extended to more general cases, we have to note that, they don't consider the human as "some impedance+state-independent force input" but as an finite-energy force input signal filtered through the human characteristics. Technically, this amounts to the common disturbance input-filtering often used in the H_∞ design problems.

2.3   Synthesis

Complementary to the analysis section, we cover a few popular controller structures among many others except the art of control engineering; manual PID tuning.

2.3.1   *Two-, Three-, and Four-Channel Control Architectures*

In the teleoperation literature, the control laws are categorized in terms of how many measurement signals are sent over to the opposite medium during the teleoperation for control. The actual controller synthesis method is often not considered in this classification. Hence the naming "n-channel control". The naming scheme can be better visualized as shown in Figure 2.12.

Position-Postion and Position-Force Controllers

The most basic control architecture among all is probably the PERR (position error) control in which the position of both the local and the remote site devices are collected by the controller and control commands are applied to both devices to minimize the position difference regardless of which device is falling behind in terms of tracking.

Assume that the local and the remote device are at rest at position $x = 0$ in the respective world coordinates. Also assume that the user moves the local device to position $x = 10 \, \text{cm}$. What the control algorithm should do is to measure the position difference and force each device accordingly to minimize the error. Hence, the control law is of the form

$$\begin{pmatrix} F_l \\ F_r \end{pmatrix} = \begin{pmatrix} -1 \\ 1 \end{pmatrix} K_p(s) \begin{pmatrix} 1 & -1 \end{pmatrix} \begin{pmatrix} x_l \\ x_r \end{pmatrix}.$$

where F_r, F_l denote the control action at the local and the remote sites. $K_p(s)$ can be a constant or a SISO dynamical system or any other esoteric control law. One can perform the same with velocity signals (to comply with the passivity analysis) if available in noise-free measurements. Otherwise, a position drift is unaviodable even with integral action.

Typically, this control architecture would give a sluggish performance since there is no preference or priority in correcting the error signal on each side. Therefore, while the remote site is pulled forward to track the local device, simultaneously, the local device is pushed back with the same force. This results in a feel similar to extending a damper, only in this case, it softens up according to the position error instead of the travel velocity.

Another widely used control architecture is the so-called Position-Force Controller. In this method the first channel in the PERR control structure is replaced with the remote site force input. Hence, the local site device tracks the remote site encountered force while the remote site device tracks the position of the local site device which can be represented by the following description

$$\begin{pmatrix} F_l \\ F_r \end{pmatrix} = \begin{pmatrix} K_f(s)F_{env} \\ K(s)(x_l - x_r) \end{pmatrix}.$$

Clearly, the side-effect of PERR type control is avoided since the position and force errors are tracked independently in two seperate channels. But this brings in another tuning problem: If the position control gain dominates, the force tracking behaves aggresively in the hard contact case due to the overuse of control action to drive the remote device into the obstacle and generally results with a kickback of the local device. Conversely, a domination of the force gain results in chattering of the remote device on the obstacle due to the discontinuous nature of the force reference signal if the user touches the handle just softly enough to sustain an oscillation. Therefore, not only the gains of the individual channels are hard to tune, but also the relative magnitudes of the gains makes the tuning more tedious.

Force-Force+PERR

To increase the bandwidth and to reduce the side-effects of the aforementioned methods, a feedforward controller is added to the position-force control architecture.

$$\begin{pmatrix} F_l \\ F_r \end{pmatrix} = \begin{pmatrix} K_{f1}(s)F_{env} \\ K(s)(x_l - x_r) + K_{f2}(s)F_{hum} \end{pmatrix}.$$

Hence, this scheme is called a three-channel controller. This has been introduced in [63] and also analyzed in [135].

Lawrence Control Architecture

In [112], a general control scheme was proposed (later extended by [43, 61]). In this architecture, also the remaining channel of remote position is sent over to the
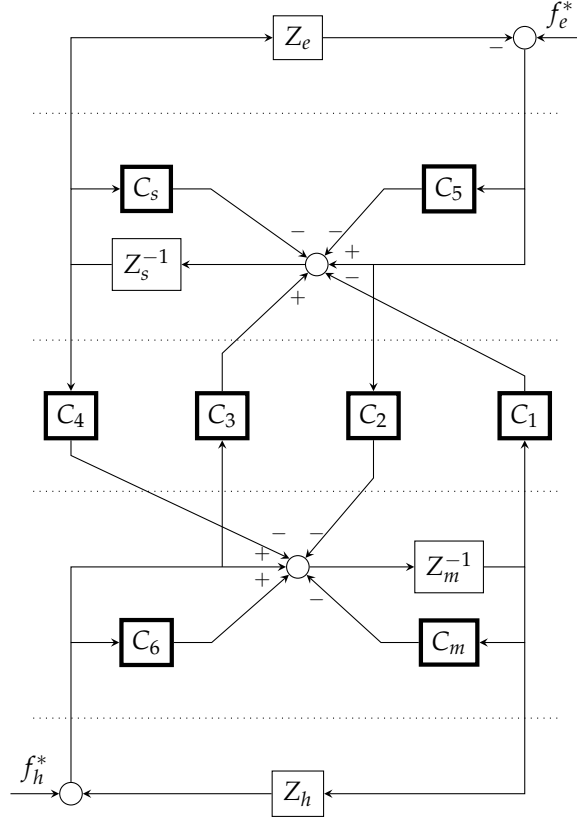
Figure 2.12: Extended Lawrence Architecture, adapted from [63]. Starred signals are the exogenous force inputs by the human/environment

local site, completing the number of measurement channels to four. The individual controller blocks and the resulting overall block diagram is shown in Figure 2.12.

Instead of a such classification, one can directly start with a MIMO control structure while keeping the control problem formulation fixed. For this purpose, let $Y_1 \subseteq \mathbb{R}^{f_1} \times \mathbb{R}^{f_2}$ denote the force measurement space, $Y_2 \subseteq \mathbb{R}^{p_1} \times \mathbb{R}^{p_2}$ denote the position measurement space harvested from arbitrary number of sensors and consider the control mapping $K : Y_1 \times Y_2 \to \mathbb{R}^{m_1} \times \mathbb{R}^{m_2}$ from the measurements to the local and remote control actions via

$$\begin{pmatrix} F_l \\ F_r \end{pmatrix} = K \begin{pmatrix} x_l \\ x_r \\ F_{hum} \\ F_{env} \end{pmatrix} := \begin{bmatrix} -C_m & C_4 & C_5 & -C_2 \\ C_1 & C_s & C_3 & -C_6 \end{bmatrix} \begin{pmatrix} x_l \\ x_r \\ F_{hum} \\ F_{env} \end{pmatrix} \quad (2.4)$$

where m_1, m_2 denote the actuation inputs with overactuated robotic manipulators in

mind. The grayed entries are the control subcomponents that work on the variables sent over the network. If we recap the architectures above with this notation, they can be represented as

$$K_{PERR} = \begin{bmatrix} -k & k & 0 & 0 \\ k & -k & 0 & 0 \end{bmatrix} \begin{pmatrix} x_l \\ x_r \\ F_{hum} \\ F_{env} \end{pmatrix},$$

$$K_{PF} = \begin{bmatrix} 0 & 0 & 0 & k_f \\ k & -k & 0 & 0 \end{bmatrix} \begin{pmatrix} x_l \\ x_r \\ F_{hum} \\ F_{env} \end{pmatrix},$$

$$K_{3\text{-channel}} = \begin{bmatrix} 0 & 0 & 0 & k_{f1} \\ k & -k & 0 & k_{f2} \end{bmatrix} \begin{pmatrix} x_l \\ x_r \\ F_{hum} \\ F_{env} \end{pmatrix}$$

respectively. Each k_i represents some constant or dynamic controller. Obviously, one can generate many more architectures by populating different entries and the zero blocks.

In [64] (see also [158] for a specialized treatment), the perfect transparency conditions are given for the undelayed case as the following; If $C_1, \cdots, C_6$ are not functions of Z_h and Z_e, transparency is achieved if and only if the transparency-optimized control law

- $C_1 = Z_{cs}$

- $C_2 = 1 + C_6$

- $C_3 = 1 + C_5$

- $C_4 = -Z_{cm}$

where $Z_{cs} := Z_e + C_m, Z_{cm} := Z_h + C_s$ hold for nonzero C_2, C_3.

2.3.2   *Wave Variable-Scattering Transformation Control for delays*

We have discussed the transformation from a passive interconnection to small-gain interconnection via the Möbius transformation W. However we have assumed that the interconnection did not involve any communication delays. When the delays are introduced in the loop as depicted in Figure 2.13, the transformations actually shift the stability problem from one domain to another. In other words, the transformations make the delay operators unbounded-gain as we have showed previously. Therefore, interconnection of passive and small-gain operators avoids to be handled by neither small-gain nor passivity theorems. Hence, we are left with
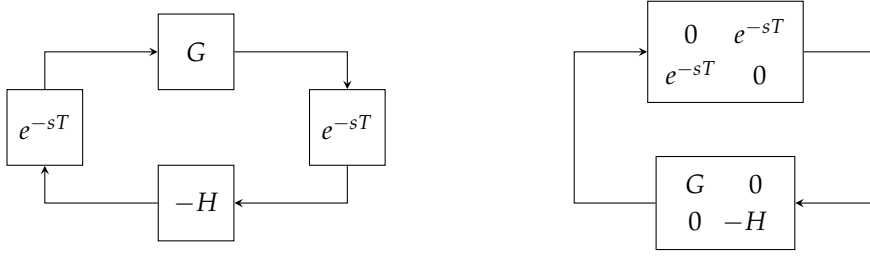
Figure 2.13: A delayed interconnection in the input/output setting and block diagram as a two block interconnection.

the only option to modify the system. This technique has dominated the literature thanks to [3, 137, 138].

Suppose we are given strictly passive LTI systems G, H interconnected as shown in Figure 2.13 on the left with communication delays. We, then, rewrite the interconnection as a two block interconnection as shown on the right for which we will use the shorthand $P - \Delta$ interconnection (delay block being the Δ). Now if the system P was strictly small-gain i.e. $\|P\|_\infty < 1$, thanks to the small-gain theorem, we would have directly conclude with stability since $\|\Delta\|_\infty = 1$, i.e.,

$$\begin{bmatrix} 0 & e^{i\omega T} \\ e^{i\omega T} & 0 \end{bmatrix} \begin{bmatrix} 0 & e^{-i\omega T} \\ e^{-i\omega T} & 0 \end{bmatrix} = I \quad \forall \omega, T$$

This fact also justifies why this methodology works regardless of the delays involved. However, P is strictly passive and thus not necessarily a unity gain-bounded operator. But we have showed how to transform such operators into norm bounded ones. This is actually the key point of the wave variable transformations. We simply use the mapping $W(P)$ and obtain

$$W(P) = (P - I)(P + 1)^{-1} = \begin{bmatrix} G - I & 0 \\ 0 & -H - I \end{bmatrix} \begin{bmatrix} G + I & 0 \\ 0 & -H + I \end{bmatrix}^{-1} \quad (2.5)$$

$$= \begin{bmatrix} W(G) & \\ & W(-H) \end{bmatrix} \quad (2.6)$$

This constitutes as a simple justification of the common "left" and "right" scattering transformation of the port terminations, leaving the delay operators in the "hybrid" structure untouched in the two port network terminology. Note that, we have only applied the mapping W to P and there is no inverse mapping to "undo" this in the loop. Technically speaking, this is not precisely a complete loop transformation since we have applied W to system P but not to the delay block Δ. Thus, the additional feedback and feedforward branches together with the $\sqrt{2}$ gains shown in (2.2) constitutes a genuine controller. In other words, the transformation block diagram is precisely achieved by the use of a feedforward/feedback control law,

which can be represented by Equation (2.4). The explicit derivation of the wave
variable controller entries, in terms of a MIMO controller, is given in [24]. One can
also verify that the control law given in [3] can be obtained via this formulation.

It is this very reason that the motivation often found in the literature is slightly
misleading. Because, we did not and also could not do any modification on the
delays. Quite the contrary, we have modified our system such that we can use the
small-gain theorem to conclude stability in the face of Δ. Therefore, we refrain from
seeing this method as a passification of the communication channel. It is certainly
possible to reflect the transformation on Δ and invoke an impedance matching
argument but we think that this only complicates the presentation. Because it's
the change in the control action that stabilizes the loop, and not the change in the
characteristics of the delay operator or making the communication line a lossless LC
line. We have to emphasize that this transformation does not guarantee stability if
the original P is not strictly passive. However if any other plant $\hat{P}$ from an arbitrary
class of systems X can be brought into a unity norm-bounded form with some other
transformation/control law. Then we can infer another set of physical interpretations
as we would have X-ified the communication channel. Thus, if we replace X with
"passive" the class of systems become the passive system class and we declare that
we have passified the communication channel. However, the communication line
stays untouched in both cases, though the control action on the system would be
different. Therefore, it is, in our opinion, better to state the changes done on the
system instead in terms of control laws.

Clearly, we have introduced the same conservatism by treating Δ as a gain-
bounded operator that μ-analysis approaches also utilize. Moreover, we have di-
rectly transformed the strictly passive operator to a small-gain operator. In case of a
passivity excess, i.e., the mapped operator is confined only in a subregion of the
unit disk, we, yet again, introduce further conservatism by using encapsulating the
smaller disk with the unit disk, for which one can shift the disk to the origin and
use the scaled small-gain theorem to reduce the conservatism. We should note also
that, this method works for any norm-bounded linear/nonlinear Δ operator as long
as the passivity structure is preserved and certainly not limited to delays (as in the
passivity case, it's that conservative).

Furthermore, if one shuffles the loop equations and bring Δ to a block diagonal
form while the system in turn admits an anti-diagonal structure, it's possible to
formulate a μ-synthesis problem. By doing so we can recover the setup of [115].
Then, we can easily see that a wave variable control law above is in the subset of
all stabilizing controllers set (due to the particular zero blocks in the controller
structure). Thus, in terms of the conservatism involved, μ-synthesis with constant
D-scalings ($D = I$) covers the wave variables controller design implicitly.

It has been noted the these control algorithms are prone to position drifts due
to the velocity communication and different alternatives have been proposed to
tackle this mismatch e.g., [23, 199]. Also there are generalizations of the scattering
transformations available in the literature, e.g., [72] to exploit the degree of freedom
on the mapping W using different rotation-scaling combinations for the unitary
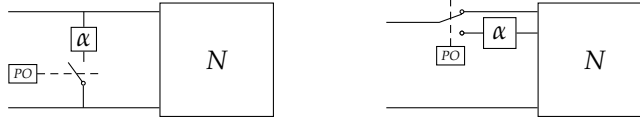
Figure 2.14: Passivity Controller (PC) implemetations.

transformation matrix and also [183] for multidimensional systems. Delay problems are also addressed in this context e.g., [22, 133, 136, 188] and references therein.

2.3.3 *Time-Domain Passivity Control*

In [60], the passivity approach is formulated in the time domain and the energy exchange is literally monitored and regulated. An initial version of this idea can also be found in [199]. The basic idea is to see whether at any port energy is generated, using a "passivity observer" (PO): for an N-port network the observed total energy is given by

$$E_{obsv}(n) = \sum_{k=0}^{n} \Delta T_k (F(k)^T V(k))$$

where ΔT_k is the sampling period at each step with nonuniform sampling in mind. If $E_{obsv}(n)$ is greater than or equal to zero then the energy is dissipated by the network, conversely if it is negative at some k, then the network has generated energy equal to the amount of $-E_{obsv}(n)$. Note that this is a cumulative term and it is not implied that the energy is generated in the last step analogous to the integral-action control. Also, it has been shown that observing the energy flow only at the open-ports is sufficient to monitor the total "net" energy flow which is analogous to the observability concept in the linear control theory.

The "Passivity Control" (PC) is implemented on top of this observer architecture as a virtual dissipative element. It relies on the passivity observer and if the energy generation is detected a dissipative element is introduced. The practical implementation is very similar to a safety relay circuit, i.e., it's only active when some relay switch is triggered. Depending on the causality (following the our analogy, as a current sensing or a voltage sensing relay), the PC can be implemented in series or parallel to the port.

This concept is then generalized to two-ports in [165, 166]; also results regarding the delay problem in the Time Domain Passivity Control context can be found in [164]. Since the essential architecture is a PI controller, it also suffers from the same problems that integral-action controllers suffer such as, wind-up and integrator reset etc. Some of these problems are addressed in [99].

2.3.4   *Others*

We have shown that most of the proposed methods in the literature use passivity or small-gain theorems and the involved mathematical operators are often indistinguishable from any other physical setup that is not a teleoperation system. It's our belief that, without any further refinements, all the above methods can be shown to be, essentially, equivalent stability characterizations as far as practical implications are concerned.

There are other approaches such as Energy Bounding Algorithm (EBA), [97, 175], sliding mode control, [18, 144], reset control, [191], model predictive control [10, 176] and many more which we will omit here. These studies also involve model-based control techniques with varying degree of dependence on the model.

The proposed methods often avoid the discussion on how to tune the PID controllers for the local, remote, and the communication line. It's as if those details are easy to handle and the attention is shifted to the n-channel architecture. We have no evidence supporting this in the control design papers. Alternatively, very conservative upper and lower bounds are given on the parameters of individual controllers and, therefore, the underlying control architecture is extremely simple since otherwise the proposed methods suffer from exceeding complexity in the derivations. This is yet another reason for why we have chosen the IQC framework for robustness analysis and model-based control path in the first place.

It's our humble opinion, however, that a "one-size-fits-for-all" design toward operator- and task-aware control laws without dedicated modeling and/or classification, seems very unlikely to produce a generally applicable results with high-performance guarantees. Nevertheless, robust control at least addresses the conservatism reduction in a systematic way, if there is no other way to model the teleoperation systems. Moreover, Linear Parameter Varying controllers are to the best of our knowledge, not yet pursued to the extent the theory allows for.

We cannot claim that we have surveyed the literature in this brief and biased survey in a comprehensive manner. The omission, as we have mentioned before, is a pragmatic choice. Though a body of research is left out (in particular most of the nonlinear methods), the covered part also constitutes a significant volume and in the next chapter they are detailed further. However, we have to note that, most nonlinear methods are the counterparts of the linear passivity theorem methods given here and they do not introduce a different look on the modeling and analysis problem per se. Thus, the motivation holds for some of those nonlinear cases.

Moreover, the number of studies reported in the literature is rapidly increasing and quite difficult to follow even under the guidance of at least two survey papers published recently [79, 145]. We have to point out that there is still no consensus on the simplest conventions and the results are often very challenging to differentiate. Hence, there is a great need to have authoritative and comprehensive sources since the survey papers above don't go into details. As a closing remark, we would like refer to the outstanding survey of [100] which provides also a comprehensive outlook to the teleoperation literature in a relatively detailed fashion up to 2006. It should

give the reader a good idea how involved and, as a subjective note, unnecessarily complicated the bilateral teleoperation literature is.

Performance Objectives

Bilateral teleoperation problem is probably one of the most difficult problems in the control field due to its subjective nature involving the human comfort and liking. However, to put it bluntly, the experts are not helping either. In other words, most of the "good performance" motivations come out of modeling first-principles but not out of the user experience. Some literature argue that since most of the tools we utilize are (almost-)lossless, say, a screwdriver or even a simple stick, it's natural to seek for a passive bilateral teleoperation system (though if we insist on this analogy, a lossless system should be sought after) that ideally behaves like a rigid transmission mechanism. In the work of Daniel and McAree [32], it has been strongly recommended that one should focus completely on the underlying physics and in fact the authors boldly established an essential limit to what can be achieved by bilateral teleoperation:

> Although our motivation comes from the problem of building teleop-
> erators to perform tasks of this sort, there is much here that we feel is
> common to all teleoperation. The performance of every force-reflecting
> system is ultimately governed by dynamic interactions between the
> master, the slave, the human operator, and the environment. For some
> applications different effects may dominate; e.g., transmission delays
> limit what can be achieved in space applications of telerobotics ([...]).
> But one can never achieve better performance than that determined by
> rudimentary physics. For this reason, we call the limits of performance
> examined here *fundamental limits of performance*. ([32])

This statement summarizes perfectly what the contemporary bilateral teleoperation literature promotes. The reason why we strongly disagree with this statement should be evident at the end of this chapter and later in Chapter 6. Still, to provide a contextual introduction to the discussion, we first remind that the underlying physics does not only consist of two distant robots interacting with their corresponding surroundings. The actual physiscs involve the human liking and that gives us freedom to display whatever is considered to be "cool, nice, crisp, real, helpful" by the human operator. It doesn't matter if we are off by 10 N or some other reflected quantity is not in accordance with the actual measurement; as long as the human operator is happy with the result in terms of immersion and touch sensation, we are done. There is nothing fundamental in terms of technological limits of performance and there is nothing wrong with approximating (or even altering) the reality to

achieve the required technology. In fact in our opinion, this is an instance of the common academic practice; obfuscation by purism.

In order to justify such fundamental limitations, we have two missing ingredients in [32]; the required precise tools that do not bring in any lossy simplifications and the exact mechanism described completely by the actual physics. Unfortunately, their analysis rely completely on LTI root loci tools and human preference is openly skipped. Therefore their results can at best be the fundamental limitations of what the literature claims the bilateral teleoperation is to be.

In general, there is no established consensus on what makes a teleoperation system "good". Quite the contrary, this question is openly and unambiguously avoided in some well-acknowledged articles. Instead some possibilities are proposed and rigorously pursued to the end without actually validating if these possibilities reflect our intention. Therefore, the conclusions that these studies arrive at are the implications of their initial hypotheses. However, the studies that follow these publications do not take this crucial detail into account and proceed as if these performance objectives are indeed the ultimate goals. We have to claim that the motivation of most of the studies given in the literature erroneously put emphasis on performance objectives that are at best suggestions and often questionable.

On the other hand, there is a different school that focuses only on stability of the teleoperation system in the face of human, environment, communication line, quantization and many more uncertainty/perturbation sources. Especially some nonlinear control studies do not even bother to define performance criteria. This view simply regards the human/environment as perturbations for our precious robotic systems and neglects the "*reason d'etre*" of the very problem that is under consideration. In our opinion, operator perception is the indispensable performance objective and can not be overlooked. But it is also very difficult to quantify. More importantly, it is beyond the scope and expertise of control theory (though with certain overlap) to find the relevant objectives. Other experts of the related fields need to contribute from a technological point of view in contrast with a pure physiological point of view and, in fact, should guide the control theorists and practitioners towards the relevant issues. This lack of performance specifications is the main reason why we have left out a considerable body of research out in our literature survey.

We strongly believe that the contemporary bilateral teleoperation control results, including this thesis, cannot and thus should not claim a comprehensive understanding of a good and useful bilateral teleoperation system. Because we just don't know, yet.

3.1   Types of Performance

In terms of the quality of the force-feedback, there are a few leading choices of methodological performance definitions. The widely accepted so-called "transparency" stems from the ideal case of lossless, undistorted exact replica of the

remote side physics at the local site. Hence the ultimate goal is selected to be faithfully representing the remote site motion and allowing the user intervene just as good as s/he is operating directly at the remote site. Let us provide some background how transparency is often provided and/or motivated. We choose to follow [73] for no particular reason other than the manuscript being the introduction/survey chapter of a recent collection of *Advances in Telerobotics* (but alternatively [38, 59, 200] and many others can be followed too); first we again recognize the motivation for modeling via *n*-ports

> For the analysis and control synthesis the modeling of the bilateral teleoperation system as interconnection of two-ports, [...], is convenient.

Then, the intuitive definition of transparency is provided. We draw the attention to the transition from the informal description to the technical formulation of transparency.

> Transparency of the telerobotic system is the major goal in bilateral control architecture design.
>
> **Definition** (Transparency). *The telerobotic system is transparent if the human operator feels as if directly interacting with the (remote) task [10]*[1]
>
> Formally, transparency is achieved if the transmitted and the environment impedances match [11][2] as also indicated above
>
> $$Z_t = Z_e$$
>
> or alternatively if HSI (master) and teleoperator (slave) movements are equal and the force displayed to the human operator is exactly the reaction force from the environment [12][3]
>
> $$x_h = x_e \text{ and } f_h = f_e$$
>
> Transparency in this sense is in practice not achievable as the device dynamics comprising inertia and friction cannot completely cancelled by control. Communication effects, especially time delay, severely degrade the achievable transparency. The development of quantitative measures is part of the transparency analysis...

This transition is practically in all documents which treat transparency as the major goal in the literature. In particular human *feel* suddenly disappears from the picture and only the physics between the tips of robotic devices are considered. We have no source in the literature that avoids or at least mentions this interesting omission. Let us first give a detailed discussion of transparency to be able to clarify what is exactly omitted since there are a few layers of omission in such arguments.

---

[1]Reference [158] of this thesis.
[2]Reference [112] of this thesis.
[3]Reference [200] of this thesis.

3.1.1 *Transparency*

Typically, we classify materials as opaque or transparent based on how good we can see through an item made up of that particular material. If we simply replace the act of seeing the other side with touching the remote location, the less distorted a system transmits the remote motion to the local site, the more transparent the system is. Hence the term *transparency*. This is defined in [112, 200] independently. In fact, the notion of transparency is of three ideal response definitions in [200]. Resuming the notation from Chapter 2, a perfect or ideal transparent 2-port network admits the hybrid matrix

$$\begin{pmatrix} v_{hum} \\ f_{hum} \end{pmatrix} = \begin{pmatrix} 0 & I \\ -I & 0 \end{pmatrix} \begin{pmatrix} f_{env} \\ v_{env} \end{pmatrix}$$

If we wish to translate this into a control theoretical performance objective, we have essentially two options. First option is minimizing the difference between the measured force/velocity signals of the actual system and the force/velocity signals of the hypothetical perfectly transparent system would have exhibited in that particular configuration. Second option is to make our system behave like an ideal transparent system as much as possible.

Let N denote the overall controlled teleoperation system model with the controller K, i.e. $N(K)$. Then we can define a performance index

$$\min_K \left| \left| \begin{pmatrix} f_{hum} - F_r \\ f_{env} - F_l \\ x_{loc} - x_{rem} \\ \vdots \end{pmatrix} \right| \right|$$

for all the admissible signals of time in some suitable normed space that we wish to consider. Alternatively, using a suitable system norm the problem becomes

$$\min_K \left| N(K) - \begin{pmatrix} 0 & I \\ -I & 0 \end{pmatrix} \right|.$$

Notice that selection of the suitable norm is far from trivial and we might even need an amalgam of different norms to bound both the energy and the maximum value of the error signals. However, this choice is understandably limited to the tools that we have for analysis and synthesis. This choice of enforcing an ideal teleoperation is obviously intuitive and agrees with the underlying physics if only we remove the human perception out of the loop. Thus, one could only argue that the global minimizer of these optimization problems would lead to the best teleoperation system unless we include the operator's opinion. However, there are two additional implicit assumptions made here. On one hand, it is assumed that there is a partial ordering, in other words, if K_1 has the cost c_1 and K_2 has the cost c_2 with $c_1 < c_2$ then this implies that K_1 is better than K_2 which is not necessarily true, or better,

it might hold only for some particular K's. In general no such ordering can be expected from this performance index. Moreover, it's not easy to search for such K. As we have observed in the literature, almost every transparency optimized control method selects the full performance first hence assuming the global minimizer and then tries to stabilize the system in the face of those performance specifications. Obviously after adding dampers or other dissipative elements the system is no longer a transparent teleoperation system and moreover we don't have a way to measure how much we are off from the initial perfectly transparent system since we only know what is ideal.

On the other hand, we do not have a metric for how much we need to get close to the ideal matrix. Let us first quote three very important questions posed by Lawrence in his well-known paper [112];

> In practice, perfectly transparent teleoperation will not be possible. So it makes sense to ask the following questions:
>
> - What degree of transparency is necessary to accomplish a given set of teleoperation tasks?
> - What degree of transparency is possible?
> - What are suitable teleoperator architectures and control laws for achieving necessary or optimal transparency?
>
> We focus on the second two questions in this paper. Instead of evaluating the performance of a specific teleoperation architecture, as in [2], we seek to understand the fundamental limits of performance and design trade-offs of bilateral teleoperation in general, without the constraints of a preconceived architecture. ([112])

Lawrence then invokes the passivity assumption of the end terminations and hence the passivity theorem is utilized to arrive at structural properties of the controller K. Evidently, this allows for the back-substitution of the controller entries and solution for the ideal case. Then the resulting controller is denoted with "*Transparency Optimized Controller*". In control jargon, this amounts to a cross-coupling control action where the bilateral dynamical differences are canceled out and then SISO control channels are tuned to maximum performance bound to the stability constraints.

Even if we accept it to be the distinguishing performance criterion, we have to emphasize that we have not touched the most important question, that is the first of the three, rather we hope to achieve the required transparency levels just enough to fool the user. After two decades, this point is simply discarded and many studies in the literature somewhat treats the conclusions of Lawrence in a different context than what has been given by Lawrence. As is for the case for Hogan's paper on passivity, Lawrence never claims that this is a definite performance measure. Instead he clearly shows the implications that follow from such assumptions.

Finally, there are interesting studies inline with our claims about irrelevance of the remote media recreation in bilateral teleoperation problem. For example,

[12, 96, 193] and a few other studies report that there is a saturation effect on how much realism that can be projected to the user. In other words, there is an inherent bandwidth limitation for the realism increase such that beyond a certain band of frequency, the transparency does not increase significantly, possibly unless backed up by tactile feedback. Even further, in the case of shared control applications, it might happen that transparency is not needed at all.

3.1.2   *Z-width*

In [30], the performance of a haptic device is related to the dynamic range of impedances (hence the name Z) that the device can display to the user. In this context we have two extremes; on one hand we have purely the local device impedance for the free-air motion and on the other hand we have the maximally stiff local device for the rigid and immobile obstacle collision. Let Z_f, Z_c denote these two distinct cases. Then the more pronounced the difference between these impedances, the more capable the teleoperation system can reflect various impedances inbetween. Thus, we implicitly assume that the rigid contact case and the free-air case are the extreme points of the uncertainty set and testing for these two cases are sufficient to conclude that any impedance on the path from Z_f to Z_c is a valid impedance that can be displayed by the device. This in turn implies that there is an ordering in the uncertainty set from "big" to "small" etc. and moreover the destabilizing uncertainty is at the boundary of the set such that these two extreme cases can vouch for stability over the whole possible environments. We are not convinced that this should be the case for all possible environment scenarios. A particular subset of second-order mass-spring-damper models of environments can be shown to be compatible with this claim if passivity theorem is used. However, when combined with other uncertain blocks in the loop we do not see how the argument follows. Note that it is well-known in the robust control literature that a destabilizing uncertainty need not to be living on the boundary of the uncertainty set. Therefore, either by gridding the uncertainty set and testing the stability conditions on a large number of points or by a specific relaxation on the constraints conditions should be translated to finitely many (and computationally tractable) number of points stability is guaranteed over the whole uncertainty set.

Similar to what Lawrence has given, the authors also include a clear statement of purpose:

> This paper will not address the psychophysics of what makes a virtual wall "feel good" except to say that one important factor seems to be dynamic range. An excellent article on this topic has recently been written by Rosenberg and Adelstein [11][4]. We will present instead some of our findings, both theoretical and experimental, concerning achievable dynamic range. In short, we will address the question of how to

---

[4]Reference [163] of this thesis.

build a haptic interface capable of exhibiting a wide range of mechanical impedances while preserving a robust stability property. ([30])

Under these assumptions, via defining a functional to measure the distance between Z_f and Z_c, we can assess the performance of different bilateral teleoperation devices. In [25], this so-called Z-width is defined as

$$Z_{\text{width}} = \int_{\omega_0}^{\omega_1} \Big| \log |Z_c(i\omega)| - \log |Z_f(i\omega)| \Big| d\omega \tag{3.1}$$

or alternatively, a simulation/experiment-based method can be utilized as in [192].

Note that (3.1) does not appear in the original paper [30] but proposed in [25, 145] though we can see neither the reasoning behind this expression nor how it constitutes a comparative quantity. In both [25, 30] no additional information is provided except some general rules of thumb about device damping and other related issues.

It should be noted that the differences at each frequency are lumped into one scalar number and moreover, the impedance gain curves can cross each other (see [25]) and might lead to an overly optimistic result. Similarly, resonance peaks and zeros of the involved impedances can be smeared out if we solely rely on this functional.

Since Z_f and Z_c are functions of the environment impedance, these curves can be obtained for one particular environment at a time. This also holds for the derivation of [112]. In [25], the difference is evaluated for more than one environment and then averaged out i.e. let $Z_{act}(Z_e)$ be the impedance displayed to the user in order to render Z_e on the local site. Then, for a particular controller, average Z-error to each candidate Z_e is given by

$$Z_{avgerr} = \frac{1}{n} \sum_{j=1}^{n} \left[\frac{1}{\omega_{1j} - \omega_{0j}} \int_{\omega_0}^{\omega_1} \Big| \log |(Z_{act}(Z_{ej}))(i\omega)| - \log |Z_{ej}(i\omega)| \Big| d\omega. \right] \tag{3.2}$$

This cost function is denoted by "*Transparency Error*" or "*Fidelity*". We refer to [192] for a more detailed discussion.

3.1.3 *Fidelity*

In [19], a variant of a transparency error is proposed to assess the performance. In this context, the emphasis is on the variation of the environment impedance and the resulting effect on the displayed impedance. Also the motivation is focused on the surgical procedures via bilateral teleoperation. If, for example, the remote device slides over some tissue that involves a tumor or any other irregularity that would be felt had the same motion performed directly by the surgeon, the better the nuances transmitted, the higher the fidelity. This performance objective, in a sense, emphasizes the high frequency content of the information (closer to tactile bandwidth). It has been noted that the Just Noticeable Difference (JND) of [14,25] %

for distinguishing relative compliance of similar surfaces goes under 1 % for rapid compliance variation detection while, say, scanning a surface [37]. Similar to the definitions given for transparency, the change of the displayed impedance $Z_{disp}(Z_e)$ with respect to the change in the environment Z_e can obtained via a straightforward calculation.

Consider again the system interconnection as depicted in Figure 2.2b. Given the scalar complex LTI uncertainty block Δ and the LTI plant $G \in \mathcal{RH}_\infty^{2\times 2}$. The upper LFT interconnection of $\Delta_e - G$ is given by,

$$P = G_{11} + G_{12}\Delta_e(1 - G_{22}\Delta_e)^{-1}G_{21}$$

Here P denotes the impedance seen by the operator, G denotes the teleoperation system and Δ_e being the environment impedance. Now, under the well-posedness assumption, define the derivative operation with respect to change in Δ_e

$$\frac{d}{d\Delta_e}P = G_{12}(1 - G_{22}\Delta_e)^{-2}G_{21}$$

then, though not pursued in [19] and left as a complication, this can, in turn, be rewritten as an LFT again;

$$\begin{pmatrix} q_1 \\ q_2 \\ z \end{pmatrix} = \begin{pmatrix} G_{22} & & \\ & G_{22} & \\ & & G_{12} \end{pmatrix} \begin{pmatrix} 1 & 0 & 1 \\ 1 & 1 & 1 \\ 1 & 1 & 1 \end{pmatrix} \begin{pmatrix} 1 & & \\ & 1 & \\ & & G_{21} \end{pmatrix} \begin{pmatrix} p_1 \\ p_2 \\ w \end{pmatrix}$$

and

$$\begin{pmatrix} p_1 \\ p_2 \end{pmatrix} = \begin{pmatrix} \Delta_e & 0 \\ 0 & \Delta_e \end{pmatrix} \begin{pmatrix} q_1 \\ q_2 \end{pmatrix}.$$

one can simply read off the interconnection from the block diagram below:
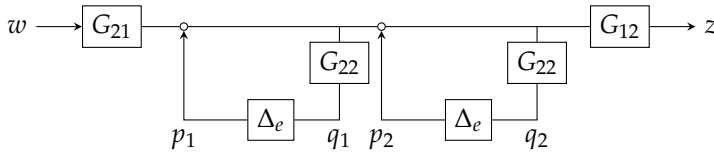
Note that the matrix case follows a similar but more involved step via computing the Fréchet derivative. Moreover one can recognize the familiar plant-uncertainty representation clearer without any complication.

Consequently, the authors define a transparency-like performance objective using a rather subtle choice of system 2-norms.

Definition (System 2-norm). *Let H be a stable strictly proper LTI system with transfer matrix H(s). Then*

$$\|H\|_2^2 := \int_{-\infty}^{\infty} \text{tr}(H^*(i\omega)H(i\omega))d\omega$$

The measure of fidelity is defined as the norm

$$\left\| W_s \frac{dP}{d\Delta_e} \bigg|_{\Delta_{enom}} \right\|_2$$

where W_s is a typically low-pass type weighting function to emphasize the frequency band of interest. Therefore the synthesis problem is to find the optimizer, controller K to the problem

$$\sup_{\substack{\text{Stability} \\ \text{Other Constraints}}} \inf_{\Delta_{ei} \in \mathbf{\Delta_e}} \left\| W_s \frac{dP}{d\Delta} \bigg|_{\Delta_{ei}} \right\|_2$$

where Δ_{ei} are the worst case environments that are of interest.

There are a few interpretations of this norm in the literature, mainly, the determin-istic "area under the Bode Plot" interpretation i.e. energy of the impulse response for scalar case, and the stochastic "steady-state white-noise-input response". We are under the impression that the authors argue in the line of the former interpretation with a similar reasoning given in the Z-width discussion via an area computation.

Designing a robust controller while minimizing the $\mathcal{H}_2$ norm of an uncertain system in the face of a predefined uncertainty set i.e. "Robust $\mathcal{H}_2$ Synthesis" problem has already recevied a lot of attention and the results can be found in the literature, e.g., [39]. Hence, the problem definition in [19] is in fact tractable. However, it's not clear to us why we choose the system 2-norm for the performance cost. Additionally, the infimum needs to be computed in the face of a set of infinitely many points hence an appropriate relaxation is required. This point is also not given though a gridding approach seems to be utilized in the numerical optimization procedure described in the paper.

It is also not clear in which case we should utilize this performance objective. The initial difficulty is that all the involved operators are LTI hence there is no time variation involved. The test reads as; *we select an arbitrary element in the predefined uncertainty set, say Δ_e, and evaluate the derivative at Δ_e. Hence, in some ϵ- neighborhood of $\Delta_e \in \mathbf{\Delta_e}$ we can see the change in P*. Thus, if the environment is slightly off from our nominal guess, this tells us how much fidelity measure would change. But the environment is still assumed to be LTI.

Note that, this does not imply that time-variations are taken into account. Suppose a particular admissible trajectory $\hat{\Delta}_e(t)$ in time is given such that $\hat{\Delta}_e(t_1) = \Delta_e$ i.e. its time-frozen LTI copy coincides with the particular nominal environment model Δ_e and at some time instant t_2, it coincides with another LTI model $\mathring{\Delta}_e$ that is within some ϵ-neighborhood of Δ_e. Even if we achieve very good fidelity properties evaluated at each Δ_e and a sequence of LTI model elements each being in the small neighborhood of the other, this does not guarantee that we would have good fidelity for the trajectory $\hat{\Delta}_e$. Actually, it might be more desirable to have low fidelity since drastic changes in the performance with respect to LTI uncertainties might confuse the user.

Same misconception is visible also in the transparency formulations in the literature. Evaluating the LTI expressions in nominal environments e.g., $Z_e = 0, \infty$ does not imply that the transitions are covered.

3.2   CLOSING REMARKS AND DISCUSSION

There are a few other performance criteria reported in the literature. Consider the definition of the impedance seen by the operator P above. In [83, 92], this term is divided into two individual terms, denoted by "reproducibility" and "operationality". The idea is similar to a sensitivity/complementary sensitivity function definitions.

In [200], also an ideal response is also partitioned into two parts and denoted by "index of maneuverability" and, in essence, is similar to what is given above, hence omitted.

We refer to the survey papers [79, 145] for a general treatment and [100, 155] and references therein for a more detailed overview about many variations in the literature.

In summary, there are no general perfomance criteria that can lead to a dedicated control design procedure. The aforementioned performance objectives always start from the direct manipulation case and assume a distance between the interacting bodies. Then the implications of such hypotheses are pursued and some results are obtained. It might very well happen that all or none of those conclusions are correct. Put better, these studies always try to remedy the distortion caused by the split of two interacting bodies i.e. teleoperation. Thus, the goal becomes too ambitious at the outset. Similar to the delay phenomenon, there is not much we can do about the distortion within the laws of physics. In fact, even the slightest delay can destabilize the system which is again an indicator of the fragility of the problem formulation. Thus, we can speculate that by doing so, we create a stability problem that we should not have had in the first place. Moreover, as we have mentioned in the introduction, the problem is exclusively about human perception and is not related to the reconstruction of the remote scene. As long as we can "fool" the user for the sake of efficiency and operational comfort, we are done.

Because we fail to provide an alternative performance criterion, we are forced to use a particular analogy from the audio technology, to express more clearly what we intend to emphasize.

When it comes to the faithful reconstruction of the recorded audio, contemporary high-end sound systems offer great fidelity, hence the name hi-fi systems[5]. There has been such a great success that now listeners and component manufacturers are striving for a full audio immersion i.e. listening to a recording that feels like actually sitting in the concert hall or venue. However, very similar to the transparency discussion in bilateral teleoperation, there is a fundamental obstacle in rendering a live performance sound with the recorded version of it. Following quote is from [6]:

---

[5]The term was coined way before the systems become truly hi-fi if compared to today's systems

> "What on earth can be the readily identifiable difference", I wrote in 1995, "between the sound of a loudspeaker producing the live sound of an electric guitar and that same loudspeaker reproducing the recorded sound of an electric guitar?" I went on to conjecture that the act of recording inevitably diminishes the dynamic range of the real thing. The in-band phase shift from the inevitable cascade of high-pass filters that the signal encounters on its passage from recording microphone to playback loudspeakers smears the transients that, live, the listener perceives in all their spiky glory. And as a high-pass filter is never encountered with live acoustic music, that's where the essential difference must lie, I concluded, quoting Kalman Rubinson (...) that "Something in Nature abhors a capacitor."

> But two more recent experiences suggest that there must be more to the difference than the presence of unnatural high-pass filters. (...)

The author goes on to list the involved hardware, the signal chain, and other relevant details about the mic set-up at both events. In the first event, a performer plays a piece through the listed hardware and is simultaneously recorded by the author. Then the recorded version of the performance is played back to the same audience from the same hardware. In the second event, a nontrivial analog/ digital hybrid device, which supposedly replicates a grand piano via sophisticated mechanisms, used to generate the sound. In both events, it has been noted that though the reproduction quality was quite impressive for the audience, a certain liveness was missing.

> So these days, I'm starting to feel that it is something that is never captured by recordings at all that ultimately defines the difference between live and recorded sound. (...)[the described systems] succeeded in every sonic parameter but one: the intensity of the original sound. Intensity, defined as the sound power per unit area of the radiating surface, is the reason why, even if you could equalize a note played on a flute to have the same spectrum as the note played on a piano at the same sound pressure level, it will still sound different.

> Ultimately, therefore, it is perhaps best to just accept that live music and recorded music are two different phenomena. (...) Eisenberg's thesis[6] is that any attempt to capture the sound of an original event is doomed to failure, and that stripping a concert from its cultural context by recording only the audio bestows a sterility on the result from which it cannot escape. The recording engineer may be able to pin the butterfly to the disc, but it sure doesn't fly any more.(...)

> In Eisenberg's words, "In the great majority of cases, there is no original musical event that a record records or reproduces. Instead, each playing

---

[6]See [42]

of a given record is an instance of something timeless. The original musical event never occurred; it exists, if it exists anywhere, outside history."

Obviously, these are all subjective opinions rather than rigorous scientific propositions though the first anecdote can be considered as a user experience study. However, we have to remind that the audio technology is tremendously advanced if compared to haptics and teleoperation. In fact, the comparison is not fair in the sense that bilateral teleoperation is not a true technology yet but rather in its infancy. Still, after decades of improvements, the sound systems are not capable of producing a live sound, real enough to make the listener immerse into, though come impressively close. Not to mention that audio technology is even a unilateral process. Nevertheless, the performance objective studies that we have enumerated a few above claim to compete at the level of hi-fi systems which is simply too ambitious. The reader should also keep in mind that the sound technology is unilateral and there is no interaction with the loudspeaker though still lacking the sufficient realism.

Coming back to our discussion, in the light of our analogy, we think that the bilateral teleoperation literature is focused on finding the system that can deliver the "live sound" rather than a high quality "playback". This holistic search is certainly relevant to the field but it cannot serve as the justification for being a driver of technological advances reported in the literature. Task-dependence is already emphasized in many studies as an item of importance and a too general performance criterion would be very unlikely to serve as a general guideline. Though, we acknowledge the motivation behind the holistic approach and a truly transparent device might be the ideal, we also believe that the timing and the feasibility of this approach needs to be modified. The immediate engineering problems such as the communication delays and other contemporary technological problems are the strong indicators of the fact that such a goal cannot be tackled prematurely. We cannot overemphasize the key issue; even the undelayed case remains unresolved let alone (time-varying or constant) delayed case.

Again from our analogy, it took decades for the hi-fi systems to reach to the current level to claim that a search for the live sound is justified. The sound reconstruction task is divided into components such as amplifiers, pre-amplifiers, direct digital-to-analog converters etc. for the signal conditioning and similarly the sound regeneration is also divided into active-passive loudspeakers with having dedicated single or multiple tweeters, sub-woofers etc. Only then the community is convinced that the hardware is not the problem[7]. Similarly, TVs and other futuristic vision technologies are following the same trend for the ultimate vision quality. However, if compared with these, bilateral teleoperation definitions are nothing but academic stability problem exercises. Moreover, as we show in the next chapter, these problems are, whether linear or nonlinear, no different than the mainstream

---

[7]We also have to state that there is an additional compulsive habit of overemphasizing the component quality such as the transmission cables etc. Hence, we can observe a trend among hi-fi enthusiasts of picking up artifacts that are impossible to be audible or simply do not exist.

control problems in disguise. Therefore, we can not yet argue about a dedicated stability and a performance problem for bilateral teleoperation.

This is the reason why we have chosen a significantly advanced methodology, again from mainstream control theory, and applied to the bilateral teleoperation problem. This does not imply that we have offered a valid alternative, in fact, quite to the contrary, our goal is to make it obvious that the studies so far can be subsumed into a general and widely used methodology and there is no benefit of the current specialization of the field. However, we have also shown that if the problem is in fact a special case of a general control problem there is no need to use the outdated versions of the techniques proposed in the control literature while important advances are reported in the literature in the past two decades over the plain small-gain/passivity theorem-based results.

A search over the number of studies in the literature published in the 2000's to date with "bilateral teleoperation" and "delay" as keywords gives hundreds of results. Yet we have no clear understanding of why these devices are unstable. We can pinpoint different effects depending on whether we look at it from an energy exchange/passivity point of view or from sensitivity function-based analysis. But this does not help us to prioritize certain design aspects of a high-performance system and unfortunately we have to assume a few questionable hypotheses along the way. It's very difficult to follow the train-of-thought often given in the literature as we first define the ultimate performance of a teleoperation system then we openly accept the fact that this is not achievable, however, we, in turn, do not modify our performance criteria and then completely neglect the issue. Finally we convert the problem into a stability of some interconnected devices with a great uncertainty associated with them and then, in the majority of the cases inject damping to the hardware which deteriorates not only the relative performance but usability of the device as a whole. Specific to the problem at hand, having a stable but poor-performing bilateral teleoperation has less functionality than that of a unilateral teleoperation as the added-value of robotic manipulators are wasted with the inclusion of damping.

After using the audio analogy extensively, let us finish the alternative suggestions with the same analogy. As we have briefly mentioned the hi-fi loudspeakers involve different dedicated components for different frequency bands such as tweeters for high-frequency band, sub/woofers for the low frequency bands and occasionally mid-range speakers etc. with individual drivers. Even though different components are utilized, the resulting harmony of these components leads to a very satisfactory listening experience if compared to generic single driver loudspeakers. Now, obviously somatosensory system already involves such sensors which are reported to be responsible for different frequency bands (see Appendix B). Hence, this already gives us a direct cue for separating the motion into different categories in terms of the frequency/amplitude content. We do not have a working methodology yet however we would like to include our reasoning here for comparison.

There has been quite a number of studies published on combining the tactile feedback with kinesthetic feedback such as [89, 98, 109, 128, 141] among many

others and references therein. In many of these reports it has been clearly shown that combining these modalities lead to substantial increase in human perception about the unstructured environment. Not only the motion but also temperature can be transmitted via the tactile thermal actuators. Hence, different overloading of the vibrational patterns can also be obtained. We have to underline that the studies mentioned above do not necessarily promote our reasoning for the control design but rather superimposing tactile and kinesthetic perception simultaneously. However, there is no apparent obstacle to use the same hardware for cooperative kinesthetic profiling.

Therefore, from a control design perspective this gives rise to a completely different type of performance objective that has no relation with the immediate transparency requirements. In other words, the performance of the device is now comprised of the individual excitation of the required human receptors. And this is inline with what we have touched in the introduction of this thesis. To the critical reader this might look like we are shifting the difficulties of the control design to the hardware design since the required devices are indeed nontrivial. We would argue that it is not the case. The required hardware already exists but used in a different context. We have performed preliminary signal processing studies and there is no significant result that can be reported here. Nevertheless, to finalize this discussion, we can speculate about the links to a plausible solution along these lines.

The immediate possibilities are to separate either the amplitude or the frequency content of the force signal for playback. In the frequency case, instead of a "*physics*" matching goal, we instead encode the force signal to be similar to an audio signal. Then, the bilateral teleoperation system goal is to playback the measured force pattern with different components simultaneously. This has been pursued for pre-recorded signals in [106] within the concept of "Event-based" haptics. The authors do not use measured signals but material contact signals from a contact-bank or look-up table but an increase of perception quality is noted. If we can achieve this separation, we have the option to separate the bandwidth of different components and hence making the performance specifications much more relaxed if compared to "one device/all frequencies" strategy. Moreover, the high frequency contact information can be shifted to the "tweeter" of the device and this makes the low frequency force playback much easier. The low-bandwidth transmission is already well-studied and within reach of the current technology. Hence, a standalone high frequency action can be added on top of the perception which would otherwise lead to a deteriorated performance if pursued with the same device. A hard contact can still be displayed with a relatively compliant "sub/woofer" and an agile stiff tweeter. Note that we are good at capturing the relative changes but not very good at perceiving the low end of the spectrum (see Section 3.1.3). Moreover, a stiff wall can possibly be rendered up to the perception threshold via it's Fourier components in other words, a hard contact perception might be achieved with a combination of mid-high frequency vibrations contingent upon the task requirements. The force signal can be transmitted and decomposed into frequency band at the local site or directly decomposed and sent over different channels with different line. This might

even encapsulate the Model-mediation-like fast/slow bus discrimination without the need of recreating a proxy virtual environment update (See e.g. [130]). Moreover, this solution already embodies an inherent robustness to packet losses and similar artifacts as we have no obligation to match the physics any more. We conjecture that this would not jeopardize the stability but will make the sensation only deteriorate as we would expect from a noisy telephone conversation. As a bonus property, transmitting only the low-frequency device motion, the high-frequency content of the human input is filtered without any additional phase lag which can be beneficial for avoiding hand tremor of the surgeon etc.

It can be argued whether this would lead to a faithful representation of the remote location and we can directly see that the answer is no. However, we are trying to remove precisely that requirement and put a device-dependent varying degree of realism instead of working for stability and neglecting performance.

Without any further evidence, there is not much we can extrapolate hence we will leave this discussion to future work. Our main focus is on incorporating wavelet decomposition in particular with respect to Haar bases for encoding/decoding the contact signals. In what follows we will instead use a typical force error/position error minimization based control design and show that at least we can achieve good robustness properties for a large class of uncertainties due to human/environment dynamics with relatively high performance.

Analysis

This chapter is based mainly on our publication [151] which is partially presented at [148–150]. We introduce the IQC analysis framework to unify frequency based analysis results while preserving the exactness of the conditions or if any without introducing extra conservatism . Via numerical case studies, we show that the results are precisely the same with those of the techniques available in the literature. There-fore, we prove that there is no fundamental reason to use a specialized terminology and set of techniques out of the mainstream robust control theory.

4.1 Quadratic Forms for Stability Analysis

In the sequel, instead of 2-port networks, we rather consider system interconnections as depicted in Figure 4.1a. In this setting, G is the model of the nominal bilateral teleoperation system and Δ is a block diagonal collection of uncertainties, such as the human, the environment, delays, etc. Stability tests are based on structural hypotheses on the diagonal blocks of the operator Δ such as gain bounds or passivity. These properties should allow us to develop numerically verifiable conditions for the system G that guarantee interconnection stability. This is intuitive because we have no access to the actual Δ and we can only describe its components by means of indirect properties. Over the past three decades many classical stability results have been unified and generalized in this direction by utilizing quadratic forms (see [125] and [85, 167, 169]).

For the sake of completeness, we present the general methodology by sampling a few important special cases. To begin with, consider the following reformulation

(a)   (b)

Figure 4.1: The general interconnection (a) and the assumed interconnection for passive systems (b). In general, the power variables require a sign change relative to the "from" and "to" ports in order to indicate the travel direction which translates to a negative sign in the block diagrams.

of the conditions of the small-gain theorem:

$$
\begin{array}{l}
\|\Delta\|_\infty \leq 1 \\
\|G\|_\infty < 1
\end{array}
\iff
\begin{array}{l}
\begin{pmatrix} \Delta(i\omega) \\ 1 \end{pmatrix}^* \begin{pmatrix} -1 & 0 \\ 0 & 1 \end{pmatrix} \begin{pmatrix} \Delta(i\omega) \\ 1 \end{pmatrix} \geq 0 \\
\begin{pmatrix} 1 \\ G(i\omega) \end{pmatrix}^* \begin{pmatrix} -1 & 0 \\ 0 & 1 \end{pmatrix} \begin{pmatrix} 1 \\ G(i\omega) \end{pmatrix} < 0
\end{array}
\tag{4.1}
$$

for all $\omega \in \mathbb{R}_e$. The middle 2×2 matrix on the right-hand side is called the "*multiplier*" (typically denoted by Π). It has been observed that the appearance of the same multiplier on both inequalities is far from a mere coincidence. In fact, it led to the following stability test: Assume that $G, \Delta \in \mathcal{RH}_\infty^{\bullet \times \bullet}$. Then, the $G - \Delta$ interconnection in Figure 4.1a is well posed and stable if there exists a Hermitian matrix Π such that

$$
\begin{pmatrix} \Delta(i\omega) \\ I \end{pmatrix}^* \Pi \begin{pmatrix} \Delta(i\omega) \\ I \end{pmatrix} \succeq 0, \quad \begin{pmatrix} I \\ G(i\omega) \end{pmatrix}^* \Pi \begin{pmatrix} I \\ G(i\omega) \end{pmatrix} \prec 0
\tag{4.2}
$$

hold for all $\omega \in \mathbb{R}_e$; one only requires the mild technical hypothesis that the left-upper/right-lower block of Π is negative/positive semi-definite. Thus, the intuition that we touched upon above is mathematically formalized by (4.2). Indeed, one can see that the former condition constrains the family of uncertainties, while the latter provides the related condition imposed on the plant for interconnection stability, both expressed in terms of the multiplier Π. In particular, we recover the passivity theorem in a similar fashion, if using the constant symmetric matrix $\Pi = \begin{pmatrix} 0 & I \\ I & 0 \end{pmatrix}$ as the multiplier under negative feedback. See [167] for a lucid "topological seperation" argument. Various other classical stability tests fall under this particular scenario based on the so-called static (frequency-independent) multipliers which, therefore, presents a significantly unified methodology.

If Δ admits a diagonal structure (as in Figure 2.2a), it is well known that the small-gain theorem and passivity theorem are conservative. A natural generalization toward a tighter analysis test is using a frequency-dependent Π matrix, which can be interpreted as adding dynamics to the multiplier. Two prominent examples of interest are the celebrated upper bound computations for μ or κ_m in robust control theory and, as we will show later, Llewellyn's stability conditions. As a shortcoming, these results are only valid for LTI operators but the real power and flexibility of these multiplier methods come from their generalizations to classes of nonlinear/time-varying operators via the IQC framework that appeared in [125].

An IQC for the input and output signals of Δ is expressed as

$$
\int_{-\infty}^{\infty} \begin{pmatrix} \widehat{\Delta(v)}(i\omega) \\ \hat{v}(i\omega) \end{pmatrix}^* \Pi(i\omega) \begin{pmatrix} \widehat{\Delta(v)}(i\omega) \\ \hat{v}(i\omega) \end{pmatrix} d\omega \succeq 0.
\tag{4.3}
$$

A bounded operator $\Delta : \mathcal{L}_2^m \to \mathcal{L}_2^n$ is said to satisfy the constraint defined by $\Pi(i\omega)$ if (4.3) holds for all $v \in \mathcal{L}_2^m$. The following sufficient stability condition for the interconnection in Figure 4.1a forms the basis for the IQC framework.

Theorem 4.1 ([125]). *Let $G \in \mathcal{RH}_{\infty}^{m \times n}$ be given and let $\Delta : \mathcal{L}_2^m \to \mathcal{L}_2^n$ be a bounded causal operator. Suppose that*

1. *for every $\tau \in [0, 1]$, the interconnection of G and $\tau \Delta$ is well posed;*

2. *for every $\tau \in [0, 1]$, $\tau \Delta$ satisfies the IQC defined by $\Pi(i\omega)$ which is bounded as a function of $\omega \in \mathbb{R}$;*

3. *there exists some $\epsilon > 0$ such that*

$$\begin{pmatrix} I \\ G(i\omega) \end{pmatrix}^* \Pi(i\omega) \begin{pmatrix} I \\ G(i\omega) \end{pmatrix} \preceq -\epsilon I \text{ for all } \omega \in \mathbb{R}. \tag{4.4}$$

Then the $G - \Delta$ interconnection in Figure 4.1a is stable.

We include a few remarks about this result:

Remark 4.2. *Note that both properties 1 and 2 in Theorem 4.1 have to hold for $\tau \Delta$ if τ moves from $\tau = 0$ (for which stability is obvious) to the target value $\tau = 1$ (for which stability is desired). But, the reason for using a scalar τ is to scale the uncertainty size, therefore it does not have to be a multiplication operation, e.g., in the delay uncertainty cases, scaling the uncertainty τe^{-sT} is incorrect for the application of IQC theorem. Instead, the result can still be used if one considers $e^{-s\tau T}$ for $\tau \in [0, 1]$, as we will derive a multiplier class later in this chapter. In summary, the homotopy argument can be customized and by no means limited to $\tau \Delta$.*

Let the multiplier $\Pi(i\omega)$ partitioned as

$$\Pi = \begin{pmatrix} \Pi_1 & \Pi_2 \\ \Pi_2^* & \Pi_3 \end{pmatrix} \tag{4.5}$$

In our examples the left-upper $m \times m$ block is negative semi-definite for all $\omega \in \mathbb{R}_e$ which guarantees concavity. In other words, convex combinations of two particular uncertainty element Δ_1, Δ_2 that satisfies the IQC, also satisfy the IQC since

$$\begin{pmatrix} \tau \Delta_1 + (1 - \tau) \Delta_2 \\ I \end{pmatrix}^* \begin{pmatrix} - & \cdot \\ \cdot & \cdot \end{pmatrix} \begin{pmatrix} \tau \Delta_1 + (1 - \tau) \Delta_2 \\ I \end{pmatrix}$$

is a concave function. Furthermore, we assume that the right-lower $m \times m$ block of $\Pi(i\omega)$ positive semidefinite for all $\omega \in \mathbb{R}_e$. Then

$$\begin{pmatrix} 0 \\ I \end{pmatrix}^* \begin{pmatrix} \cdot & \cdot \\ \cdot & + \end{pmatrix} \begin{pmatrix} 0 \\ I \end{pmatrix} \succeq 0$$

i.e. $0 \in \Delta$. Hence, given a Δ that satisfies the IQC with $\Pi_1 \succeq 0, \Pi_3 \preceq 0$, select $\Delta_1 = 0, \Delta_2 = \Delta$, for every $\tau \in [0, 1]$, $\tau \Delta$ satisfies the IQC. The reason why we are so interested in zero is the fact that when $\Delta = 0$, it corresponds to the (unperturbed) nominal system and, as is for the IQC theorem, many stability results rely on tracking the stability property while

traveling on the nominal system→fully uncertain system path, e.g., root loci, Nyquist test, boundary crossing theorem, μ-analysis etc.

It is then easy to see that (4.2) implies property 2 in Theorem 4.1; hence one only needs to verify (4.2) for the original uncertainty Δ.

Remark 4.3. *Often $\Pi(i\omega)$ is a continuous function of $\omega \in \mathbb{R}_e$. Then property 3 is equivalent to*

$$\begin{pmatrix} I \\ G(i\omega) \end{pmatrix}^* \Pi(i\omega) \begin{pmatrix} I \\ G(i\omega) \end{pmatrix} \prec 0 \ \text{for all} \ \omega \in \mathbb{R}_e. \tag{4.6}$$

If Δ is LTI then (4.3) holds for all $v \in \mathcal{L}_2^m$ if and only if

$$\begin{pmatrix} \Delta(i\omega) \\ I \end{pmatrix}^* \Pi(i\omega) \begin{pmatrix} \Delta(i\omega) \\ I \end{pmatrix} \succeq 0 \ \text{for all} \ \omega \in \mathbb{R}. \tag{4.7}$$

The IQC reduces to a frequency-domain inequality (FDI). This provides the link to our introductory discussion.

Suppose that Δ is LTI and $\Pi(i\omega)$ is a continuous function of $\omega \in \mathbb{R}_e$ and assume that (4.2) holds for both inequalities for all ω. Then, using the relations, $w = \Delta v, v = Gw$ for all $u, y \in \mathcal{L}_2$, we obtain the following contradiction

$$0 \preceq v^* \begin{pmatrix} \Delta \\ I \end{pmatrix}^* \Pi \begin{pmatrix} \Delta \\ I \end{pmatrix} v \tag{4.8}$$

$$= \begin{pmatrix} w \\ v \end{pmatrix}^* \Pi \begin{pmatrix} w \\ v \end{pmatrix} \tag{4.9}$$

$$= w^* \begin{pmatrix} I \\ G \end{pmatrix}^* \Pi \begin{pmatrix} I \\ G \end{pmatrix} w \tag{4.10}$$

$$\prec 0, \tag{4.11}$$

hence

$$\text{im} \begin{pmatrix} I \\ G \end{pmatrix} \cap \text{im} \begin{pmatrix} \Delta \\ I \end{pmatrix} = \{0\}, \ \forall \omega \in \mathbb{R}_e.$$

Using this we can conclude that

$$\det \begin{pmatrix} I & \Delta \\ G & I \end{pmatrix} \neq 0 \ \forall \omega \in \mathbb{R}_e$$

and, with an application of Schur complement formula, we have (4.6) and (4.7) implying

$$\det(I - G(i\omega)\Delta(i\omega)) \neq 0 \ \text{for all} \ \omega \in \mathbb{R}_e, \tag{4.12}$$

which is the precise condition that forms the basis of SSV theory [142]. This gives some intuition for the validity of the IQC theorem and relates to μ in SSV theory.

Remark 4.4. *In combination with the previous remarks, properties 2 and 3 imply* $\det(I - \tau G(\infty)\Delta(\infty)) \neq 0$ *for* $\tau \in [0,1]$ *which is nothing but property 1. Two conclusions can be drawn: On one hand, under these circumstances property 1 is redundant in Theorem 4.1. On the other hand, if 1 and 2 have been verified, it suffices to check* (4.6) *only for finite* $\omega \in \mathbb{R}$ *in order to infer stability with the IQC theorem.*

If we have an IQC constraint that is satisfied for all $\Delta \in \mathbf{\Delta}$ with some particular uncertainty set $\mathbf{\Delta}$, checking robust stability boils down to the verification of the corresponding FDI (4.4) or (4.6). Instead of validating these in a frequency-by-frequency fashion, one can make use of the Kalman - Yakubovich - Popov (KYP) Lemma (see [160] and below) in order to convert the FDI into a genuine linear matrix inequality (LMI) by using state space representations. For the finite frequency intervals, one can further use the Generalized KYP Lemma ([84]) to limit the analysis to some physically relevant frequency band.

4.2   Basic IQC Multiplier Classes

In the previous section, we have shown how classical frequency domain techniques can be embedded into the IQC formulation. In this section, we focus on the types of existing multipliers for different uncertainty classes. Although they frequently appear in the robust control literature, we include them for completeness.

4.2.1   *Parametrized Passivity*

Another well-known version of the passivity theorem, which we will denote as theorem of parameterized passivity (see e.g. [36, Thm. VI.5.10]), allows to consider cases in which the "non-passivity" of some block is compensated by an excess of passivity in other blocks without endangering stability. This can even be utilized to determine the lowest tolerable level of passivity of the uncertainties for which a given interconnection remains stable. For output strictly passive uncertainties, stability can be characterized as in the next result, which is a direct consequence of the general IQC theorem.

Corollary 4.5. *The interconnection of* $G_p, \Delta \in \mathcal{RH}_\infty^{\bullet \times \bullet}$ *as in Figure 4.1b is stable if there exist a* $p \geq 0$ *such that*

$$\begin{pmatrix} \Delta(i\omega) \\ I \end{pmatrix}^* \begin{pmatrix} -pI & I \\ I & 0 \end{pmatrix} \begin{pmatrix} \Delta(i\omega) \\ I \end{pmatrix} \succeq 0 \tag{4.13}$$

$$\begin{pmatrix} I \\ -G_p(i\omega) \end{pmatrix}^* \begin{pmatrix} -pI & I \\ I & 0 \end{pmatrix} \begin{pmatrix} I \\ -G_p(i\omega) \end{pmatrix} \prec 0 \tag{4.14}$$

hold for all $\omega \in \mathbb{R}_e$.
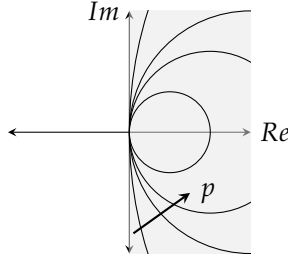
Figure 4.2: As p increases, the admissible region for the Nyquist curves of Δ shrinks to smaller disks in the right half plane.

Remark 4.6. *Note that* (4.13) *and* (4.14) *are nothing but*

$$\Delta(i\omega) + \Delta^*(i\omega) \succeq p\Delta^*(i\omega)\Delta(i\omega), \tag{4.15}$$
$$G_p(i\omega) + G_p^*(i\omega) \succ -pI. \tag{4.16}$$

The case $p = 0$ recovers the classical passivity theorem. Moreover, the larger the value of $p > 0$, the smaller is the set of uncertainties described by (4.15), as illustrated in Figure 4.2 for different values of p. In fact, this result is used in Colgate's condition thanks to the damping term b and closely related to the impedance bounds of Bounded Impedance Absolute Stability [58] using "impedance circles". Input strictly passive uncertainties follow after shifting the uncertainty such that zero is in the uncertainty set with identical arguments.

4.2.2   *Dynamic LTI Uncertainties*

Often system identification experiments lead to system representations that match the physical system within some tolerance levels. There can be also other sources of such frequency dependent mismatch and they are usually captured by frequency dependent weights. The usual practice is to define a nominal system that always "pass through middle point of the error bound" at each frequency and the rest is defined either multiplicatively that is in the form of $G_{nom}(I + W\Delta)$ or additively that is $G_{nom} + W\Delta$ which can be converted from one form to another.

For the sake of simplicity, let us assume that Δ, G_{nom} are SISO LTI systems. Since the magnitude of the uncertainty is scaled by the weight W and in turn the weight can be absorbed by the plant, without loss of generality, we can assume that $\|\Delta\|_\infty \leq 1$ i.e.

$$1 \geq \Delta(i\omega)^*\Delta(i\omega) \quad \forall \omega \in \mathbb{R}_e$$

Obviously, this inequality remains true if we multiply both sides with a positive scalar that is

$$\lambda \geq \lambda\Delta(i\omega)^*\Delta(i\omega) \quad \forall \omega \in \mathbb{R}_e, \lambda > 0$$

We can also represent this inequality as follows,

$$\begin{pmatrix} \Delta(i\omega) \\ 1 \end{pmatrix} \begin{pmatrix} -\lambda & 0 \\ 0 & \lambda \end{pmatrix} \begin{pmatrix} \Delta(i\omega) \\ 1 \end{pmatrix} \geq 0, \quad \forall \omega \in \mathbb{R}_e \lambda > 0$$

Note that, validity of this step relies on the commutative property of $\Delta\lambda = \lambda\Delta$. Hence, we have parametrized all the unity norm bounded uncertainty constraints. For some historical reason, this type of norm-bound multipliers is referred to as D scalings. In particular we have obtained the family of constant(static) D scalings. One can see that, we might use a different λ at each freqency and the inequality still holds true.

$$\begin{pmatrix} \Delta(i\omega) \\ 1 \end{pmatrix} \begin{pmatrix} -\lambda(i\omega) & 0 \\ 0 & \lambda(i\omega) \end{pmatrix} \begin{pmatrix} \Delta(i\omega) \\ 1 \end{pmatrix} \geq 0, \lambda(i\omega) > 0 \quad \forall \omega \in \mathbb{R}_e$$

Note again that this result relies on the commutativity property

$$\Delta(i\omega)\lambda(i\omega) = \lambda(i\omega)\Delta(i\omega).$$

This type of multipliers are the celebrated Dynamic D-scalings that are made famous by the μ-synthesis tool DK-iteration. Also, one can get a rough picture of the fast plant size growth in the DK-iteration process in the classical μ-synthesis. Since the approximation quality is increased via higher order terms as we try to reconstruct a function of ω from its finitely many discrete points, the approximate function involving the higher order terms absorbed by the plant at the D-analysis step for another K-synthesis step.

Now assume that $\Delta \in \mathcal{RH}_\infty^{n \times m}$. We can follow the same idea,

$$I \succeq \Delta(i\omega)^*\Delta(i\omega) \quad \forall \omega \in \mathbb{R}_e.$$

However, introducing a positive definite matrix λ necessitates a particular structure since we have lost the commutativity property i.e. $\Delta(i\omega)\lambda(i\omega) \neq \lambda(i\omega)\Delta(i\omega)$ in general[1]. The commutativity can be restored if we assume a diagonal structure, since $\Delta(i\omega)(\lambda_0(i\omega)I) = (\lambda_0(i\omega)I)\Delta(i\omega)$ where $\lambda_0 : \mathbb{R} \mapsto \mathbb{R}_+$. Thus, along the same lines with the SISO case, the constraints take the form

$$\begin{pmatrix} \Delta(i\omega) \\ I \end{pmatrix} \begin{pmatrix} -\lambda_0(i\omega)I & 0 \\ 0 & \lambda_0(i\omega)I \end{pmatrix} \begin{pmatrix} \Delta(i\omega) \\ I \end{pmatrix} \succeq 0, \lambda_0(i\omega) > 0 \quad \forall \omega \in \mathbb{R}_e$$

Clearly, one can repeat the same machinery for the repeated SISO Δ blocks to obtain "full-block" D-scalings.

As we have mentioned in the previous chapter and also will demonstrate again in this chapter, this particular multiplier type is the difference between small-gain

---

[1]To the best of our knowledge, for an arbitrary matrix A there is no systematic way to parameterize all matrices that satisfy $AB = BA$ and allow for a convenient description.

theorem and μ-analysis, and a similar argument holds for passivity theorem and Llewellyn's criteria.

Furthermore, although it's conservative, we have to emphasize that constant scalings are often employed for the analysis of norm-bounded static or time-varying nonlinearities where the Fourier transform of Δ does not make sense.

4.2.3   *Real Parametric Uncertainties*

In many applications, the uncertainties also originate from the lack of the precision on the actual values of the parameters in the system model. This applies in particular to the models used in bilateral teleoperation. Parameters such as the stiffness and the damping of the environment or the human arm are the simplest examples of this kind. After re-scaling and shifting, the real parametric uncertainties are assumed to take values in the interval $[-r, r]$ centered around the nominal value zero.

LTI uncertain parameters

The well-known DG multiplier family ([46, 127]) is used to assess robustness against unknown but constant parameters. In fact, for all bounded functions $D : \mathbb{R} \mapsto (0, \infty)$ and $G : \mathbb{R} \mapsto i\mathbb{R}$ one has

$$\begin{pmatrix} \delta \\ 1 \end{pmatrix}^* \begin{pmatrix} -D(\omega) & G(\omega) \\ G^*(\omega) & r^2 D(\omega) \end{pmatrix} \begin{pmatrix} \delta \\ 1 \end{pmatrix} \geq 0$$

for all $\delta \in [-r, r]$, just because it reads as

$$-D(\omega)|\delta|^2 + r^2 D(\omega) + (G(\omega)^* + G(\omega))\delta \geq 0$$

this holds since $|\delta|^2 \leq r^2$, $D(\omega) > 0$ and $G(\omega) + G(\omega)^* = 0$. Hence, the realness property $\delta = \delta^*$ is exploited via G scalings for all the elements in the uncertainty set which otherwise are only constrained to be norm bounded by r. Similar to the dynamic LTI uncertainties, we enlarge the set of multipliers by adding dynamics.

As a remark on such multipliers, we give a simple example on how to modify the plant/multiplier if the parameter interval is not centered around zero which apply to all real parametric uncertainties given in this subsection. We assume that the parameter lives in the interval $[a, b]$ with/out some physical units with $ab > 0$.

- The first step is always to check whether zero is in the interval. If not, by dummy feedforward/feedback in the loop one can always set the interval such that zero is included. In other words, the parameter interval $[a, b]$ can be rewritten as $\frac{a+b}{2} + [\frac{a-b}{2}, \frac{b-a}{2}]$. Then, including the constant feedthrough term as a feedback loop in the plant we obtain $[-r, r]$ interval with $r = \frac{b-a}{2}$.

- Alternatively, we can modify the multiplier using

$$\delta \in [a, b] \iff \left| \delta - \frac{b+a}{2} \right|^2 \leq \left(\frac{b-a}{2} \right)^2 \iff -\delta^2 + (b+a)\delta - ab \geq 0$$

and hence,

$$\begin{pmatrix} \delta \\ 1 \end{pmatrix}^* \begin{pmatrix} -D(\omega) & \frac{b+a}{2}D(\omega) + G(\omega) \\ \frac{b+a}{2}D(\omega) + G^*(\omega) & abD(\omega) \end{pmatrix} \begin{pmatrix} \delta \\ 1 \end{pmatrix} \geq 0.$$

Time-varying parameters with arbitrary rate of variation

In this case we employ constant multipliers; the time-varying parameter $\delta : [0, \infty) \mapsto [-r, r]$ satisfies the quadratic constraint

$$\begin{pmatrix} \delta(t) \\ 1 \end{pmatrix}^* \begin{pmatrix} -D & iG \\ -iG & r^2D \end{pmatrix} \begin{pmatrix} \delta(t) \\ 1 \end{pmatrix} \geq 0$$

for all $D > 0$, $G \in \mathbb{R}$ and for all $t \geq 0$. This implies the validity of (4.3) for the multiplication operator which maps $v \in \mathcal{L}_2^n$ into $w \in \mathcal{L}_2^n$ with $w(t) = \delta(t)v(t)$.

Time-varying parameters with bounded rate of variation

If there is a known bound on the rate-of-variation (ROV) of the time-varying parameter, it is conservative to use constant DG scalings. To characterize slowly-varying real parametric uncertainties, we use the so-called "swapping lemma" ([67, 87, 102], cf. [143]) which allows to take the ROV bound explicitly into account. For the sake of completeness, we include a scalar version of this well known result from adaptive control.

Lemma 4.7 (Swapping Lemma). *Consider the bounded and differentiable function δ : $[0, \infty) \to \mathbb{R}$ whose derivative is bounded as $|\dot{\delta}(t)| \leq d$ for all $t \geq 0$. Moreover, let $T(s) = C(sI - A)^{-1}B + D$ be a transfer function with a stable state-space realization and define*

$$T_c(s) := C(sI - A)^{-1}, \quad T_b(s) := (sI - A)^{-1}B.$$

If viewing T, T_c, T_b and δ (by point-wise multiplication) as operators $\mathcal{L}_2 \to \mathcal{L}_2$, one has $\delta T = T\delta + T_c \dot{\delta} T_b$ and thus

$$\underbrace{\begin{pmatrix} T & T_c \\ 0 & I \end{pmatrix}}_{T_{\text{left}}} \underbrace{\begin{pmatrix} \delta \\ \dot{\delta}T_b \end{pmatrix}}_{\Delta_s} = \underbrace{\begin{pmatrix} \delta & 0 \\ 0 & \dot{\delta}I \end{pmatrix}}_{\Delta_x} \underbrace{\begin{pmatrix} T \\ T_b \end{pmatrix}}_{T_{\text{right}}}$$

where x, s stand for "eXtended" and "Stacked" respectively.

We now claim that

$$\Pi(i\omega) = (\star)^* M_s \begin{pmatrix} T_{\text{left}}(i\omega) & 0 \\ 0 & T_{\text{right}}(i\omega) \end{pmatrix}$$

with

$$M_s = \begin{pmatrix} -D_a & 0 & iG_a & 0 \\ 0 & -D_b & 0 & iG_b \\ -iG_a & 0 & r^2 D_a & 0 \\ 0 & -iG_b & 0 & d^2 D_b \end{pmatrix}$$

for $T^* D_a T > 0$, $D_b > 0$ and G_a, $G_b \in \mathbb{R}$ is a valid IQC multiplier for the uncertainty Δ_s. In fact, one easily verifies

$$\begin{pmatrix} \Delta_x(t) \\ I \end{pmatrix}^T M_s \begin{pmatrix} \Delta_x(t) \\ I \end{pmatrix} \succeq 0 \text{ for all } t \geq 0$$

in the time domain. If we choose any $v \in \mathcal{L}_2$ and define $w = \begin{pmatrix} \Delta_x \\ I \end{pmatrix} T_{right} v$, we hence infer $\int_0^\infty w(t)^T M_s w(t)\, dt \geq 0$. On the other hand, due to Lemma 4.7, we also have

$$w = \begin{pmatrix} T_{\text{left}} \Delta_s \\ T_{\text{right}} \end{pmatrix} v = \begin{pmatrix} T_{\text{left}} & 0 \\ 0 & T_{\text{right}} \end{pmatrix} \begin{pmatrix} \delta \\ \dot{\delta} T_b \\ 1 \end{pmatrix}$$

which proves the claim. Thus, after augmenting the corresponding channel with zero columns so as to make the plant compatible with Δ_s, the robustness test can be performed.

4.2.4 *Delay Uncertainty*

The delay robustness problem has been studied extensively and the dominating approach is the use of scattering transformations/wave variable techniques, among other methods ([3, 5, 7, 44, 79, 113, 115, 119, 137, 138, 144, 199]). We refer to the survey article [79] for a detailed exposition of these methods. A great deal of research has been devoted to delay robustness tests in robust control that are applicable to a wide class of teleoperation systems. We also refer to [161] for a general treatment of the subject (e.g. based on Lyapunov-Krasovskii functionals as utilized by [34, 35]) and to IQC based results as e.g. in [48, 88, 91, 174] (In [33], it has been reported that the results of [91] is utilized however the conditions and the derivations are omitted).

Here, we consider constant but uncertain delays and the maximum delay duration is bounded from above by $\bar{\tau} > 0$ seconds. We emphasize that it requires only a simple modification of the multiplier in order to arrive at robustness tests for different types of delays as reported in the literature.

If using the uncertainty $\Delta(s) = e^{-s\tau}$ in the configuration of Figure 4.1a, the nominal value $\tau = 0$ leads to $\Delta(s) = 1$ and not to zero as desired. This is resolved by utilizing the shifted uncertainty $\tilde{\Delta}(s) = e^{-s\tau} - 1$ and correspondingly modifying the system to $\tilde{G}$ (by unity feedback around G) as in Figure 4.3a and without modifying the interconnection (cf. [115]).

The uncertainty is then characterized by using two properties of $\tilde{\Delta}$: For all ω, τ, the complex number $z = e^{-i\omega\tau} - 1$ is located on the unit circle centered at $(-1, 0)$
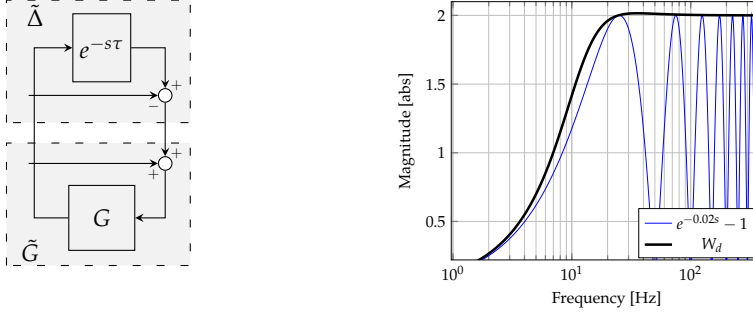
Figure 4.3: (a) Rewriting the interconnection such that $\tau = 0$ implies $\tilde{\Delta} = 0$. (b) Frequency domain covering of the shifted delay operator.

in the complex plane. Since condition $|z + 1| = 1$ translates into $z^*z + z^* + z = 0$, we infer for all bounded $\Omega : \mathbb{R} \to \mathbb{R}$ that

$$\begin{pmatrix} \tilde{\Delta}(i\omega) \\ 1 \end{pmatrix}^* \begin{pmatrix} \Omega(\omega) & \Omega(\omega) \\ \Omega(\omega) & 0 \end{pmatrix} \begin{pmatrix} \tilde{\Delta}(i\omega) \\ 1 \end{pmatrix} = 0 \;\; \forall \omega \in \mathbb{R} \tag{4.17}$$

for any delay time $\tau \in \mathbb{R}$. Furthermore, we need to take the low frequency property of the magnitude of the frequency response into account. This is typically captured by a frequency dependent weight. If we define,

$$W_d(s) = 2 \frac{(s + \frac{4}{\pi\bar{\tau}})(s + \frac{\beta}{\bar{\tau}})}{(s - \frac{\pi}{2\bar{\tau}}e^{i\theta})(s - \frac{\pi}{2\bar{\tau}}e^{-i\theta})}$$

with $\theta = \left(\frac{\pi}{2}\right)^2$ and some small $\beta > 0$, then W_d covers the delay uncertainty in the sense that $|\tilde{\Delta}(i\omega)| \leq |W(i\omega)|$ for all $\omega \in \mathbb{R}$ and for all $\tau \in [0, \bar{\tau}]$. An example of magnitude covering is shown in Figure 4.3b.

This property, in turn, translates into $(\tilde{\Delta})^*\tilde{\Delta} \leq (W_d)^*W_d$ for all $\omega \in \mathbb{R}$. Then we can utilize the classical D-scalings to obtain the following constraint with a dynamic multiplier:

$$(\star)^* \begin{pmatrix} -\mathcal{D}(\omega) & 0 \\ 0 & W_d(i\omega)^*\mathcal{D}(\omega)W_d(i\omega) \end{pmatrix} \begin{pmatrix} \tilde{\Delta}(i\omega) \\ 1 \end{pmatrix} \geq 0 \tag{4.18}$$

for all bounded $\mathcal{D} : \mathbb{R} \to (0, \infty)$. Then the overall multiplier family results from a conic combination of (4.17) and (4.18):

$$(\star)^* \begin{pmatrix} -\mathcal{D} + \Omega & \Omega \\ \Omega & W_d^*\mathcal{D}W_d \end{pmatrix} \begin{pmatrix} \tilde{\Delta} \\ 1 \end{pmatrix} \geq 0 \;\; \forall \omega \in \mathbb{R}_e$$

4.3   EQUIVALENT IQC BASED STABILITY TESTS FOR COMMON STABILITY ANALYSIS APPROACHES

4.3.1   *Llewellyn's Stability Criteria*

As shown in [162], the conditions stated in Theorem A.7 are invariant under immittance substitution. Hence, we assume that the network and the terminations are represented with an input/output mapping as depicted in Figure 4.1b.

The stability conditions of Theorem A.7 can be reproduced via the IQC theorem as follows. If Δ_l and Δ_s are passive and stable LTI systems, they satisfy

$$\Delta_l + \Delta_l^* \geq 0 \ \text{ and } \ \Delta_s + \Delta_s^* \geq 0$$

for all $\omega \in \mathbb{R}_e$. If we choose arbitrary $\lambda_1(\omega) > 0$ and $\lambda_2(\omega) > 0$, it is clear that the inequalities $\lambda_2(\Delta_l + \Delta_l^*) \geq 0$ and $\lambda_1(\Delta_s + \Delta_s^*) \geq 0$ persist to hold, which can, in turn, be combined into

$$
\begin{pmatrix} \Delta_s & 0 \\ 0 & \Delta_l \\ 1 & 0 \\ 0 & 1 \end{pmatrix}^*
\left(\begin{array}{cc|cc} 0 & 0 & \lambda_1 & 0 \\ 0 & 0 & 0 & \lambda_2 \\ \hline \lambda_1 & 0 & 0 & 0 \\ 0 & \lambda_2 & 0 & 0 \end{array} \right)
\begin{pmatrix} \Delta_s & 0 \\ 0 & \Delta_l \\ 1 & 0 \\ 0 & 1 \end{pmatrix} \succeq 0.
$$

After division by $\lambda_2(\omega)$ and with $\lambda(\omega) = \frac{\lambda_1(\omega)}{\lambda_2(\omega)}$ we obtain

$$
\begin{pmatrix} \Delta_s & 0 \\ 0 & \Delta_l \\ 1 & 0 \\ 0 & 1 \end{pmatrix}^*
\left(\begin{array}{cc|cc} 0 & 0 & \lambda & 0 \\ 0 & 0 & 0 & 1 \\ \hline \lambda & 0 & 0 & 0 \\ 0 & 1 & 0 & 0 \end{array} \right)
\begin{pmatrix} \Delta_s & 0 \\ 0 & \Delta_l \\ 1 & 0 \\ 0 & 1 \end{pmatrix} \succeq 0. \tag{4.19}
$$

In this fashion we have constructed a whole family of multipliers, parameterized by $\lambda(\omega) > 0$, such that the quadratic constraint (4.19) holds for all passive $\Delta_l, \Delta_s \in \mathcal{RH}_\infty$. Stability of the $N - \Delta$ interconnection is then guaranteed if one can find a positive $\lambda(\omega)$ for which the frequency domain inequality

$$
\begin{pmatrix} 1 & 0 \\ 0 & 1 \\ -N_{11} & -N_{12} \\ -N_{21} & -N_{22} \end{pmatrix}^*
\left(\begin{array}{cc|cc} 0 & 0 & \lambda & 0 \\ 0 & 0 & 0 & 1 \\ \hline \lambda & 0 & 0 & 0 \\ 0 & 1 & 0 & 0 \end{array} \right)
\begin{pmatrix} 1 & 0 \\ 0 & 1 \\ -N_{11} & -N_{12} \\ -N_{21} & -N_{22} \end{pmatrix} \prec 0 \tag{4.20}
$$

is also satisfied at each frequency $\omega \in \mathbb{R}_e$ (Negation of N results from the application of the IQC theorem to the negative feedback interconnection Figure 4.1b). The resulting condition is equivalent to checking whether, at each frequency, there exists a $\lambda > 0$ such that

$$
H = \begin{bmatrix} -2\lambda R_{11} & -\lambda N_{12} - N_{21}^* \\ -\lambda N_{12}^* - N_{21} & -2R_{22} \end{bmatrix} \prec 0
$$

holds. This leads us to the relation with the classical results. Indeed, the 2×2 matrix H is negative definite if and only if

$$R_{11} > 0 \quad \text{or} \quad R_{22} > 0$$

and

$$\det H = \left(-R_{12}^2 - X_{12}^2 \right) \lambda^2 - R_{21}^2 - X_{21}^2 + \left(4R_{11}R_{22} - 2R_{12}R_{21} + 2X_{12}X_{21} \right) \lambda > 0.$$

Since the leading and constant coefficient of the involved polynomial are negative, the apex of the corresponding parabola should stay above the λ-axis. Using the apex coordinates of a concave parabola one can show that this is equivalent to (A.12). Symmetry of the resulting conditions with respect to the indices is shown by simply switching the roles of λ_1 and λ_2 in our derivation.

Remark 4.8. *In the previous FDI condition (4.20) and if assuming $\lambda = 1$ over all frequencies, we also recover the Raisbeck's conditions [156]. A comparison of Raisbeck's and Llewellyn's criteria indicates that the use of frequency dependent multipliers demonstrates the possibility of a substantial decrease of conservatism in stability analysis. In fact, the difference between Llewellyn's conditions and of Raisbeck's is the use of dynamic multipliers instead of static ones.*

Remark 4.9. *One should also note that Llewellyn's original conditions are both sufficient and necessary and, hence, involve no conservatism. Exactness is due to the vast generality of the uncertainties, since one just assumes that the human and the environment are represented by passive LTI operators. The Nyquist curves of the corresponding positive real functions are only constrained to be lying in the closed right half plane. In reality, however, one is rather interested in operators whose Nyquist curves are confined to a sub-region of the closed right-half plane (or even other bounded sets elsewhere in the complex plane). Covering the relevant region of interest in the complex plane with the full closed right-half plane for describing the involved uncertainty provides a clear account of the conservatism of the stability tests in teleoperation systems. Thus, if one wishes to reduce conservatism, additional structural information about the operators should be included in order to further constrain the uncertainty set (e.g. [21, 58, 62, 195]). It will be illustrated in Section 4.4 how this can be achieved by using conic combinations of different multipliers which express refined properties of the involved operators.*

4.3.2   *Unconditional Stability Analysis of 3-port Networks*

For the analysis of 3-port networks, there exists no obvious unconditional stability result other than terminating one of the ports with a known environment model and then performing an analysis on the resulting 2-port network (see e.g. [94] and references therein). Still, we can obtain the exact conditions for a 3-port case in a straightforward fashion along the above described lines without port termination. However, as expected, the test derived in this section is more conservative than

those of port termination based methods since the additional information about the model with which the port is terminated renders the uncertainty set significantly smaller.

If compared to the previous section, the only modification is to take a system representation $N \in \mathcal{RH}_\infty^{3 \times 3}$ and three passive uncertainty blocks living in $\mathcal{RH}_\infty$ which are collected as

$$\Delta(i\omega) = \mathrm{diag}\left(\Delta_1(i\omega), \Delta_2(i\omega), \Delta_3(i\omega)\right) \tag{4.21}$$

in order to model the three port terminations. With

$$\Lambda(i\omega) = \mathrm{diag}\left(\lambda_1(\omega), \lambda_2(\omega), \lambda_3(\omega)\right) \succ 0 \tag{4.22}$$

we obtain the following quadratic constraint

$$\begin{pmatrix} \Delta \\ I \end{pmatrix}^* \begin{pmatrix} 0 & \Lambda \\ \Lambda & 0 \end{pmatrix} \begin{pmatrix} \Delta \\ I \end{pmatrix} \succeq 0$$

which reflects passivity of the three sub-blocks. The corresponding FDI for guaranteeing stability reads as

$$\begin{pmatrix} I \\ -N \end{pmatrix}^* \begin{pmatrix} 0 & \Lambda \\ \Lambda & 0 \end{pmatrix} \begin{pmatrix} I \\ -N \end{pmatrix} \prec 0. \tag{4.23}$$

Theorem 4.10 (Llewellyn's 3-port Criteria). *A network, represented by its 3×3 transfer function $N \in \mathcal{RH}_\infty^{3 \times 3}$ and interconnected to the stable, passive and block diagonal Δ as given in (4.21) is stable if and only if there exists a structured Λ with (4.22) such that (4.23) holds for all $\omega \in \mathbb{R}_e$.*

Exact conditions for unconditional stability could be obtained from (4.23) by symbolic computations. However, getting formulas similar to those in (A.11), (A.12) would lead to quite cumbersome expressions (see e.g. [94, 107, 184]). Moreover, variants of expressing negative definiteness would result in different formulations of the stability conditions in terms of scalar inequalities. In the IQC formulation this is completely avoided while it is still possible to easily verify the resulting conditions numerically.

4.3.3 *Rollett's Stability Condition*

With almost identical arguments as for Llewellyn's test, one derives the following quadratic constraints for positive λ and for stable LTI systems $\tilde{\Delta}_l$ and $\tilde{\Delta}_s$ whose gains are bounded by one:

$$\begin{pmatrix} \tilde{\Delta}_s & 0 \\ 0 & \tilde{\Delta}_l \\ 1 & 0 \\ 0 & 1 \end{pmatrix}^* \left(\begin{array}{cc|cc} -\lambda & 0 & & \\ 0 & -1 & & \\ \hline & & \lambda & 0 \\ & & 0 & 1 \end{array} \right) \begin{pmatrix} \tilde{\Delta}_s & 0 \\ 0 & \tilde{\Delta}_l \\ 1 & 0 \\ 0 & 1 \end{pmatrix} \succeq 0.$$

Interconnection stability is then assured if one can find a positive frequency dependent λ for which the FDI

$$\begin{pmatrix} 1 & 0 \\ 0 & 1 \\ S_{11} & S_{12} \\ S_{21} & S_{22} \end{pmatrix}^* \left(\begin{array}{cc|cc} -\lambda & 0 & & \\ 0 & -1 & & \\ \hline & & \lambda & 0 \\ & & 0 & 1 \end{array} \right) \begin{pmatrix} 1 & 0 \\ 0 & 1 \\ S_{11} & S_{12} \\ S_{21} & S_{22} \end{pmatrix} \prec 0 \qquad (4.24)$$

or, equivalently,

$$H = \begin{bmatrix} |S_{21}|^2 + \lambda(|S_{11}|^2 - 1) & S_{22}S_{21}^* + \lambda S_{12}S_{11}^* \\ S_{22}^*S_{21} + \lambda S_{12}^*S_{11} & |S_{22}|^2 - 1 + \lambda |S_{12}|^2 \end{bmatrix} \prec 0$$

hold for all $\omega \in \mathbb{R}_e$. Then, it is elementary to express $H \prec 0$ by $\det(H) > 0$ and by negativity of the diagonal entries of H for all $\omega \in \mathbb{R}_e$. Positivity of the determinant of H means

$$(1 - |S_{22}|^2 - |S_{11}|^2 + |\nabla|^2)\lambda - |S_{12}|^2 \lambda^2 - |S_{21}|^2 > 0.$$

If this is expressed as $f(\lambda) = -a\lambda^2 + b\lambda - c > 0$ with $a, c > 0$, we require the apex coordinates $\left(\frac{b}{2a}, \frac{b^2 - 4ac}{4a} \right)$ both to be positive. Since $a > 0$, we have

$$(1 + |\nabla|^2 - |S_{22}|^2 - |S_{11}|^2)^2 > 4 |S_{12}S_{21}|^2 \qquad (4.25)$$

due to $b^2 > 4ac$. Moreover, negativity of the diagonal terms is expressed as

$$\lambda(1 - |S_{11}|^2) > |S_{21}|^2 \quad \text{or} \quad 1 - |S_{22}|^2 > \lambda |S_{12}|^2. \qquad (4.26)$$

To make the connection to the classical auxiliary conditions, observe that evaluating $f(\lambda)$ at $\lambda_0 = \sqrt{\frac{c}{a}} = \frac{|S_{21}|}{|S_{12}|}$ would lead to the condition $b > 0$ since $f(\lambda_0) = b\sqrt{\frac{c}{a}} - 2c > 0$. Hence (4.26) becomes

$$1 - |S_{11}|^2 > |S_{12}S_{21}| \quad \text{or} \quad 1 - |S_{22}|^2 > |S_{12}S_{21}|. \qquad (4.27)$$

In the literature, the quantity λ_0 is called the "maximum stable power gain". Finally, after explicitly including the condition $b > 0$, one can take the square root of (4.25) and obtain

$$1 + |\nabla|^2 - |S_{22}|^2 - |S_{11}|^2 > 2 |S_{12}S_{21}|,$$

which is precisely Rollett's first condition.

There has been quite some discussion in various studies (e.g. [41, 118, 147, 197]) whether testing both conditions in (4.27) is really required, while it rolls out from our FDI arguments that one of these auxiliary inequalities is sufficient. In fact, (4.24) renders this discussion obsolete since we deal with a single matrix inequality to be
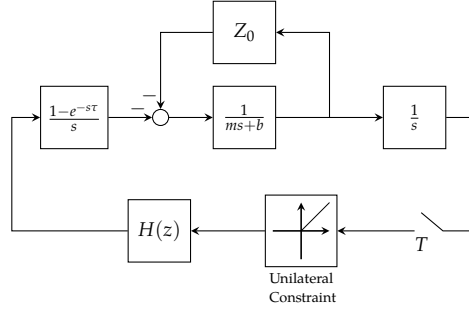
Figure 4.4: The teleoperation setup from [29]

tested at each frequency. This test is equivalent to the one based on the Edwards-Sinsky stability parameter μ ([41]) in the sense that only one condition needs to be verified. Alternatively, one can perform a symbolic computation of the largest eigenvalue of H and search for a positive λ that renders that quantity strictly negative. Recently, the μ parameter has been used in the context of teleoperation in [58] and their results can also be recovered by using multipliers similar to the ones given in the next section.

4.3.4 *Colgate's Minimum Damping Condition*

In this section, the analysis problem from [28, 31] is investigated by IQCs. In this example, the master device is modeled as $\frac{1}{ms+b}$ and is combined with a passive operator impedance $Z_0(s)$ as shown in Figure 4.4. We limit the analysis to the situation without the unilateral constraint. The overall operator and master device transfer function reads as $\Delta(s) = \frac{1}{ms+b+Z_0(s)}$. Since $Z_0(s)$ is passive and b is positive, the Nyquist curve of $\Delta^{-1}(s)$ is confined to the half-plane $\{z \in \mathbb{C} : \text{Re}\{z\} \geq b\}$ and $\Delta^{-1}(s)$ is strictly input passive with parameter b. In [31], the problem is converted to the small gain theorem with a geometric reasoning. In our setting, passivity is expressed as

$$\begin{pmatrix} 1 \\ \Delta(i\omega)^{-1} \end{pmatrix}^* \begin{pmatrix} -2b & 1 \\ 1 & 0 \end{pmatrix} \begin{pmatrix} 1 \\ \Delta(i\omega)^{-1} \end{pmatrix} \geq 0$$

which is clearly equivalent to

$$\begin{pmatrix} \Delta(i\omega) \\ 1 \end{pmatrix}^* \begin{pmatrix} -2b & 1 \\ 1 & 0 \end{pmatrix} \begin{pmatrix} \Delta(i\omega) \\ 1 \end{pmatrix} \geq 0$$

for all $\omega \in \mathbb{R}_e$. The FDI guaranteeing stability then reads as

$$\begin{pmatrix} 1 \\ -G_d(i\omega) \end{pmatrix}^* \begin{pmatrix} -2b & 1 \\ 1 & 0 \end{pmatrix} \begin{pmatrix} 1 \\ -G_d(i\omega) \end{pmatrix} < 0$$

for all $\omega \in \mathbb{R}_e$. Using the closed form formula in [31],

$$G_d(i\omega) = \frac{T}{2} \frac{e^{i\omega T} - 1}{1 - \cos(\omega T)} H(e^{i\omega T}),$$

this directly leads to Colgate's original condition:

$$-2b - G_d^*(i\omega) - G_d(i\omega) < 0$$

$$\Longleftrightarrow b > \frac{T}{2} \frac{1}{1 - \cos(\omega T)} \operatorname{Re}\left\{(1 - e^{-i\omega T})H(e^{i\omega T})\right\}.$$

The employed multiplier can be transformed into the one for the small-gain theorem along the following lines:

$$0 \le 2b \begin{pmatrix} \Delta(i\omega) \\ 1 \end{pmatrix}^* \begin{pmatrix} -2b & 1 \\ 1 & 0 \end{pmatrix} \begin{pmatrix} \Delta(i\omega) \\ 1 \end{pmatrix}$$

$$= \begin{pmatrix} \Delta(i\omega) \\ 1 \end{pmatrix}^* \left[\begin{pmatrix} 2b & -1 \\ 0 & 1 \end{pmatrix}^T \begin{pmatrix} -1 & 0 \\ 0 & 1 \end{pmatrix} \begin{pmatrix} 2b & -1 \\ 0 & 1 \end{pmatrix} \right] \begin{pmatrix} \Delta(i\omega) \\ 1 \end{pmatrix}$$

$$= \begin{pmatrix} 2b\Delta(i\omega) - 1 \\ 1 \end{pmatrix}^* \begin{pmatrix} -1 & 0 \\ 0 & 1 \end{pmatrix} \begin{pmatrix} 2b\Delta(i\omega) - 1 \\ 1 \end{pmatrix} \Longleftrightarrow |2b\Delta(i\omega) - 1| \le 1.$$

This links our arguments to those appearing in [28, 31] and reveals that the direct application of tools from robust control allows to circumvent any transformation to scattering parameters (or, in other words, the application of a loop transformation) for obtaining the stability conditions. In fact, the congruence transformation

$$\left(\frac{1}{\sqrt{2b}} \begin{pmatrix} 1 & -b \\ 1 & b \end{pmatrix} \right)^T \begin{pmatrix} -1 & 0 \\ 0 & 1 \end{pmatrix} \left(\frac{1}{\sqrt{2b}} \begin{pmatrix} 1 & -b \\ 1 & b \end{pmatrix} \right) = \begin{pmatrix} 0 & 1 \\ 1 & 0 \end{pmatrix}$$

with the scattering transformation matrix turns the small-gain multiplier into the one for passivity. This observation allows to easily show the equivalence of the small gain and passivity theorems through scattering transformations ([3]) and wave variable methods ([137, 138]).

4.3.5 *Regions in the Complex Plane*

Using a similar mechanism to what is given above, one can also characterize other domains in the complex plane different than the whole right half plane as long as it can be represented (or covered with) with a quadratic constraint. Thus, once a multiplier family is set, it's a matter of evaluating the respective FDI for the system at hand. For example, recently in [86], a vertical strip-like domain for one of the LTI uncertainties is assumed i.e. $-a \le \Delta_l + \Delta_l^* \le b$ for all $\omega \in \mathbb{R}_e$ with $a, b > 0$ and stability conditions are derived similar to those of Llewellyn's test along the lines of

[41]. In terms of quadratic constraints, a direct verification of the constraints below

$$\begin{pmatrix} \Delta(i\omega) \\ 1 \end{pmatrix}^* \begin{pmatrix} 0 & 1 \\ 1 & a \end{pmatrix} \begin{pmatrix} \Delta(i\omega) \\ 1 \end{pmatrix} \geq 0 \text{ and } \begin{pmatrix} \Delta(i\omega) \\ 1 \end{pmatrix}^* \begin{pmatrix} 0 & -1 \\ -1 & b \end{pmatrix} \begin{pmatrix} \Delta(i\omega) \\ 1 \end{pmatrix} \geq 0$$

show that these constraints characterize the domain

$$\{z \in \mathbb{C} : -a \leq \text{Re}\{z\} \leq b \text{ for } a, b > 0\}.$$

Hence, via introducing dynamic multipliers and scaling the overall multiplier with the corresponding λ of Δ_s, the stability condition is equivalent to, for each $\omega \in \mathbb{R}_e$ the existence of $\lambda_1(\omega), \lambda_2(\omega) > 0$ such that

$$\begin{pmatrix} 1 & 0 \\ 0 & 1 \\ -N_{11} & -N_{12} \\ -N_{21} & -N_{22} \end{pmatrix}^* \left(\begin{array}{cc|cc} 0 & 0 & 1 & 0 \\ 0 & 0 & 0 & \lambda_1 - \lambda_2 \\ \hline 1 & 0 & 0 & 0 \\ 0 & \lambda_1 - \lambda_2 & 0 & \lambda_1 a + \lambda_2 b \end{array} \right) \begin{pmatrix} 1 & 0 \\ 0 & 1 \\ -N_{11} & -N_{12} \\ -N_{21} & -N_{22} \end{pmatrix} \prec 0 \quad (4.28)$$

holds. By carrying out the multiplication, we obtain

$$\begin{pmatrix} -2R_{11} + (\lambda_1 a + \lambda_2 b) |N_{21}|^2 & -N_{12} - (\lambda_1 - \lambda_2)N_{21}^* + (\lambda_1 a + \lambda_2 b)N_{21}^* N_{22} \\ \star & -2(\lambda_1 - \lambda_2)R_{22} + (\lambda_1 a + \lambda_2 b) |N_{22}|^2 \end{pmatrix} \prec 0.$$

If compared to the results of [86], terms involving the bound b don't vanish. In fact, the authors prove the test for a half-plane defined as $\{z \in \mathbb{C} \mid \text{Re}\{z\} \geq a\}$ instead of a strip and the necessity direction of the proof is omitted. Hence, the upper bound on the real part of the uncertainty is not taken into account. Thus, their result is similar to the condition given in Corollary 4.5. In fact it becomes more visible if we separate the terms in (4.28) as the following:

$$(\star)^* \left(\begin{array}{cc|cc} 0 & 0 & 1 & 0 \\ 0 & 0 & 0 & \lambda_3 \\ \hline 1 & 0 & 0 & 0 \\ 0 & \lambda_3 & 0 & \lambda_3 a \end{array} \right) \begin{pmatrix} I \\ -N \end{pmatrix} \prec -(a+b)\lambda_2 \begin{pmatrix} N_{21}^* \\ N_{22}^* \end{pmatrix} \begin{pmatrix} N_{21} & N_{22} \end{pmatrix},$$

where we impose $\lambda_3 := \lambda_1 - \lambda_2 > 0$ for all frequencies since for each positive λ_3 we can find a λ_1 such that the inequality is satisfied. One can show that the left hand side is precisely the authors condition. Also the right hand side is a negative semidefinite perturbation that pushes the left hand side more into negative definiteness. Notice that this condition, as the authors also remark, shows that b term can be arbitrarily large. It is a matter of choosing λ_2 sufficiently small to render the inequalities feasible. In fact having $b \to \infty$ implies $\lambda_2 \to 0$. Hence rendering the second constraint above useless. The reason for the absence of b terms in [86] is due to the incorrect formulation of Llewellyn's stability theorem with nonstrict inequalities. Obviously it is not a major obstacle however as seen here it leads to wrong inferences about asymptotical stability.

In summary, having an upper bound on the real part of the impedance is not a structurally important modeling issue. Though in case of an unstructured uncertainty the conditions are indeed sufficient and necessary, we also see that our modeling approach is still conservative and including the *b* bound doesn't bring in any specialization in terms of the conditions. In other words, it doesn't matter if *b* is very small or very large. Thus, it does not offer any improvement.

Remark 4.11. *In [86], the results above are presented as novel stability conditions, but essentially, they are the reformulations of the general passivity theorem that can be found elsewhere. This formulation is also equivalent to [58] which also uses the Möbius transformation arguments given by [41]*[2] *up to scattering transformations which once again in turn equivalent to the formulation given above. Alternatively, [72] gives another reformulation using QSR-dissipativity which is the case of having static multipliers in our examples, which in turn another manifestation of [95, Thm. 6.2] for non-LTI end terminations.*

This is just another instance of our main argument; had the problem been formulated as a straightforward robustness test, it would have been relatively easy to see the connection with the classical results. However, since the problem formulation is given in a network theory context, any stability result that is not present in network theory is claimed to be original which is regrettably incorrect. The teleoperation literature should be synced with the systems theory literature to avoid doubling the efforts. This also applies to IQCs that if there exists a better tool out there which surpasses the convenience and generality of IQC framework then use of IQCs should be avoided. The point we wish to make is that none of the methods are essential in the solution of the bilateral teleoperation problem and thus there is no reason to insist on a certain way of looking at the problem.

Note that, we can take not just rectangles or circles but any arbitrary path connected region as long as we can describe the constraints with quadratic forms. Therefore the methodology is significantly general than merely dealing with active/passive uncertainty modeling. As a trivial example, we can cover/overbound the uncertainty region with an ellipsoid which in turn leads to a quite substantial improvement over the passivity case since then the constraint type will not be a positive realness test and yet the uncertainty set would be significantly smaller. Hence more potential for improvement. Another example is given above in the delay multiplier construction. We can also combine inequality/equality constraints to further restrict the robustness test in order to reduce conservatism.

Moreover, as is the case for the previous examples, one can impose the constraints above and possibly more on both the human and the environment uncertainties, without invoking the passivity theorem explicitly, in a few steps instead of deriving standalone conditions for each individual case with rather cumbersome manipulations.

---

[2]In fact, [41, 118] further include an argument and a correction about often cited but erroneous version of absolute stability theorem as we have clarified in IQC version above. For some reason, the nonstrict version given in [65], which is not accurate, is persistently being cited even when Llewelyn's original paper is cited.

4.3.6   *Exactness of Robustness Tests*

As mentioned before, IQC-based stability criteria are typically only sufficient. Still the classical conditions as discussed above turn out to be also necessary. Necessity of these criteria can as well be seen to be a specialization of celebrated exactness results in structured singular-value theory. In fact, IQC tests for structured LTI uncertainties with two or three full diagonal blocks as derived above are known to be always exact. This implies, in particular, that the 3-port counterpart of Llewellyn's conditions is indeed a necessary and sufficient test for stability. It's not feasible for us to provide a full treatment of all possible cases in which IQC-based robustness tests are known to be exact. Nevertheless, for a detailed discussion related to LTI uncertainties we refer to [46, 142, 170].

We would like to emphasize that these beautiful exactness properties come at the price of some limitations of the classical framework. For instance, Llewellyn's conditions are not sufficient for stability any more if we only assume that the uncertainties are passive but not necessarily LTI. On the other hand, if allowing for arbitrary causal and passive uncertainties, stability is still guaranteed if we can find a frequency-independent $\lambda > 0$ which renders the FDI (4.20) satisfied, and this property can be easily verified numerically.

4.4   NUMERICAL CASE STUDIES

In this section, we show how frequently encountered analysis problems can be solved under the IQC formulation with ease. We utilize the multipliers as given above for robustness tests applied to a simple teleoperation system taken from [194, 195]. Our main emphasis is on showing how one can reproduce the numerical results of such frequency domain techniques and how it is possible to substantially widen the range of allowed uncertainties in the IQC framework for which no classical analytical stability tests exist. This serves as an illustration for the possibility to improve analysis and, more importantly in future work, optimization-based controller synthesis results if better human/environment models become available.

4.4.1   *Algorithmic Verification*

We have discussed some classical stability tests that reduce to explicit scalar inequalities which can be verified in a frequency-by-frequency fashion. In contrast, the equivalent re-formulations in terms of IQCs open the way to verifying these conditions numerically, by applying algorithms from the by now well-established area of semi-definite programming [14]. For example, checking at each frequency the existence of some diagonal $\Lambda \succ 0$ which satisfies (4.23) boils down to an efficiently tractable LMI problem in the three diagonal entries of Λ, which can be readily implemented in software environments such as [117]. We also show how it is even possible to avoid any frequency-gridding and to reduce the tests to finite-dimensional semi-definite programming problems that can be solved in one shot.

This section serves to illustrate this procedure for Rollett's stability condition, which requires to determine a frequency-dependent bounded and strictly positive λ satisfying the FDI (4.24). Without loss of generality, it suffices to search for proper and rational functions λ that have no poles and are positive on the extended imaginary axis. Due to the well-established spectral factorization theorem (e.g. [47]), we can express any such function as $\psi^* \psi$ with some stable transfer function ψ (without zeros in the closed right half-plane). For some fixed pole $a < 0$ let us choose the basis vectors

$$\Phi_n(s) = \begin{pmatrix} 1 & \frac{1}{s-a} & \frac{1}{(s-a)^2} & \cdots & \frac{1}{(s-a)^{n-1}} \end{pmatrix}^T$$

for $n = \mathbb{N}$. By a well-known fact from approximation theory ([146]), the function ψ can be approximated to an arbitrary degree by $L^T \Phi_n$ for some suitable $L \in \mathbb{R}^n$ uniformly on the imaginary axis, if only n is taken sufficiently large. More precisely, $\inf_{L \in \mathbb{R}^n} \|\psi - L^T \Phi_n\|_\infty$ converges to zero for $n \to \infty$. In summary, any proper rational λ with $\lambda(i\omega) > 0$ for $\omega \in \mathbb{R}_e$ can be approximated arbitrarily closely by $\Phi_n^* L L^T \Phi_n$ or, in turn, by $\Phi_n^* D \Phi_n$ with $D = D^T \in \mathbb{R}^{n \times n}$.

This discussion justifies why one can parameterize the multiplier (middle term) in (4.24) as

$$\Psi_n^* \underbrace{\left(\begin{array}{cc|cc} -D & 0 & & \\ 0 & -1 & & \\ \hline & & D & 0 \\ & & 0 & 1 \end{array} \right)}_{M} \underbrace{\left(\begin{array}{cc|cc} \Phi_n & & & \\ & 1 & & \\ \hline & & \Phi_n & \\ & & & 1 \end{array} \right)}_{\Psi_n}$$

in terms of a frequency-dependent outer factor Ψ_n and a diagonally structured real symmetric matrix M in the middle. Let us denote the set of all these matrices M by $\mathcal{M}$ (dropping the dependence on n). For checking Rollet's condition we then need to verify the existence of $M \in \mathcal{M}$ such that the FDIs

$$\Phi_n^* D \Phi_n > 0 \ \text{ and } \ \begin{pmatrix} I \\ S \end{pmatrix}^* \Psi_n^* M \Psi_n \begin{pmatrix} I \\ S \end{pmatrix} \prec 0$$

are satisfied. We include the classical result ([160]) that allows us to convert these frequency domain inequalities into LMIs:

Theorem 4.12. *[KYP Lemma] Let $G = \left[\begin{array}{c|c} A & B \\ \hline C & D \end{array} \right]$ and suppose that A has no eigenvalues on the imaginary axis. For a real matrix $P = P^T$, the following two statements are equivalent:*

1. *The following FDI holds:*

$$G(i\omega)^* P G(i\omega) \succ 0 \ \forall \omega \in \mathbb{R}_e. \tag{4.29}$$

2. *There exists a symmetric matrix X with*

$$\begin{pmatrix} I & 0 \\ A & B \\ \hline C & D \end{pmatrix}^T \left(\begin{array}{cc|c} 0 & X & 0 \\ X & 0 & 0 \\ \hline 0 & 0 & P \end{array} \right) \begin{pmatrix} I & 0 \\ A & B \\ \hline C & D \end{pmatrix} \succ 0. \tag{4.30}$$

Now choose the minimal state space realizations

$$\Phi_n = \left[\begin{array}{c|c} A_\Phi & B_\Phi \\ \hline C_\Phi & D_\Phi \end{array}\right] \text{ and } \Psi_n \begin{pmatrix} I \\ S \end{pmatrix} = \left[\begin{array}{c|c} \mathcal{A} & \mathcal{B} \\ \hline \mathcal{C} & \mathcal{D} \end{array}\right].$$

This allows to apply the KYP Lemma in order to equivalently convert $\lambda > 0$ and (4.24) into the feasibility of the LMIs

$$\begin{pmatrix} I & 0 \\ A_\Phi & B_\Phi \\ C_\Phi & D_\Phi \end{pmatrix}^T \begin{pmatrix} 0 & Z & 0 \\ Z & 0 & 0 \\ 0 & 0 & D \end{pmatrix} \begin{pmatrix} I & 0 \\ A_\Phi & B_\Phi \\ C_\Phi & D_\Phi \end{pmatrix} \succ 0 \qquad (4.31)$$

and

$$\begin{pmatrix} I & 0 \\ \mathcal{A} & \mathcal{B} \\ \mathcal{C} & \mathcal{D} \end{pmatrix}^T \begin{pmatrix} 0 & \mathcal{X} & 0 \\ \mathcal{X} & 0 & 0 \\ 0 & 0 & M \end{pmatrix} \begin{pmatrix} I & 0 \\ \mathcal{A} & \mathcal{B} \\ \mathcal{C} & \mathcal{D} \end{pmatrix} \prec 0. \qquad (4.32)$$

More precisely, if one can computationally verify the existence of $X, Z, M \in \mathcal{M}$ and $D = D^T$ which satisfy (4.31) and (4.32), we have verified Rollet's condition. Conversely, if Rollet's condition holds, then these LMIs are guaranteed to have solutions if n is chosen sufficiently large.

Let us emphasize again that the very same procedure applies to considerable more complex interconnections and structured uncertainties Δ. In fact, for many interesting classes of uncertainties one can systematically construct multiplier families (see e.g. [125]) which are known to admit a description of the form $\Pi = \Psi^* M \Psi$, $M \in \mathcal{M}$ with a stable outer factor transfer matrix Ψ and with some set of structured symmetric matrices $\mathcal{M}$ that can itself be described as the feasible set of an LMI. Checking stability of the $G - \Delta$ interconnection in Figure 4.1a then requires to verify the validity of the FDI

$$\begin{pmatrix} I \\ G \end{pmatrix}^* \Psi^* M \Psi \begin{pmatrix} I \\ G \end{pmatrix} \prec 0.$$

Literally along the same lines as described above this is translated into a semi-definite program with Theorem 4.12.

Remark 4.13. *In our numerical examples the basis length n is chosen large enough that the performance level does not significantly change by further increasing n. As shown below, the required length n for adequate accuracy in the multipler approximation is (regardless of the conservatism of the test) often quite small in practice.*

In what follows, we will continue to utilize the shorthand notation of state-space realizations in a similar manner, i.e., $\mathcal{A}, \mathcal{B}, \mathcal{C}, \mathcal{D}$ for the combined outer factors by replacing S with the respective plant, and $A_\Phi, B_\Phi, C_\Phi, D_\Phi$ for the basis vector.

(a) Unconditional Stability (b) Uncertain stiff environment
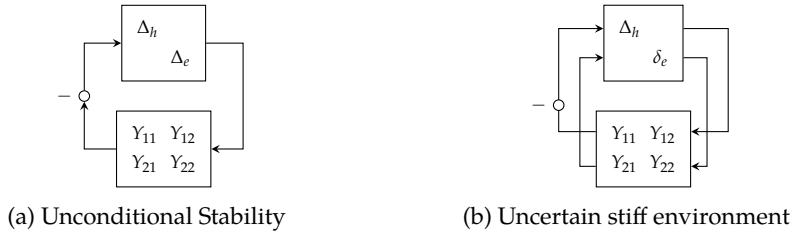
Figure 4.5: System interconnections for Section 4.4.3 and Section 4.4.4.

4.4.2 *System Model*

In [194], a simple teleoperation system described with the following equations is considered:

$$F_h + \tau_m = M_m \ddot{x}_m + B_m \dot{x}_m$$
$$\tau_s - F_e = M_s \ddot{x}_s + B_s \dot{x}_s.$$

Here M_m, M_s are the masses, B_m, B_s are the damping coefficients, τ_m, τ_s are the device motor torques, and x_m, x_s are the position coordinates of the local and the remote devices respectively. F_h, F_e denote the human and the environment forces. The human and the environment are assumed to be LTI passive operators and are denoted by Δ_h, Δ_e which substitute Δ_s, Δ_l as employed in the more general network-related context in the earlier sections.

Additionally, a particular PD type of a position-force controller scheme, denoted by **P-F**, is used:

$$\tau_s = K_p(\mu x_m - x_s) - K_v \dot{x}_s, \quad \tau_m = -K_f F_e.$$

The overall teleoperation system is then described, with $Y_m(s) = (M_m s + B_m)^{-1}$ and $Y_s(s) = \frac{\mu K_p}{M_s s^2 + (B_s + K_v)s + K_p}$, in terms of the following admittance matrix:

$$Y = \begin{pmatrix} Y_m & -K_f Y_m \\ -Y_m Y_s & \frac{M_m s^2 + B_m s + \mu K_f K_p}{(M_s s^2 + (B_s + K_v)s + K_p)} Y_m \end{pmatrix}. \tag{4.33}$$

As shown in [194], the system's performance is related to the transparency of the teleoperator, which is characterized by the maximal attainable product μK_f while maintaining stability (see also [32]). We will evaluate our results with respect to this performance measure. For all computations, we have used [45, 117, 187] with MATLAB 7.12.0 on a computer with a 2.4 GHz processor and with 4 GB RAM memory running Win 7-64 Bit OS. The system parameters are $M_m = 0.64, M_s = 0.61, B_m = 0.64, B_s = 11, K_v = 87.8, K_p = 4000$.

4.4.3 *Case 1 : Unconditional Stability Analysis via IQCs*

We start with applying Llewellyn's test based on (4.20) to the system given above. In a first computation, we choose a frequency grid of 2000 logarithmically spaced points in $[0,10\,000]$ rad/s and solve, at each grid point, a feasibility problem in $\lambda > 0$. This is incorporated into a bisection algorithm that searches for the maximum value of μK_f for which feasibility at each grid-point can be guaranteed. Due to gridding, this method typically gives an upper bound rather than the exact value on the guaranteed performance level, just because there is a chance to miss critical frequencies. Nevertheless, we obtained the exact value ≈ 0.137 as in [194]. The inner search for λ requires 8.52 s, while the overall computation takes about 117 s; note that the latter heavily depends on the initial bisection interval and on the desired accuracy.

In a second computation, we follow the path as described in Section 4.4.1. The resulting FDI is

$$\left(\Psi \begin{pmatrix} I \\ -Y \end{pmatrix} \right)^{*} M \left(\Psi \begin{pmatrix} I \\ -Y \end{pmatrix} \right) \prec 0 \tag{4.34}$$

where

$$\Psi = \left(\begin{array}{cc|cc} \Phi & 0 & 0 & 0 \\ 0 & 1 & 0 & 0 \\ \hline 0 & 0 & \Phi & 0 \\ 0 & 0 & 0 & 1 \end{array} \right), \quad M = \left(\begin{array}{cc|cc} 0 & 0 & M_1 & 0 \\ 0 & 0 & 0 & 1 \\ \hline M_1 & 0 & 0 & 0 \\ 0 & 1 & 0 & 0 \end{array} \right) \tag{4.35}$$

with some unstructured real symmetric matrix M_1.

Corollary 4.14. *The $Y - \Delta$ interconnection depicted in Figure 4.5a is stable for all passive blocks Δ_h and Δ_e if there exist symmetric matrices $\mathcal{X}, Z, M_1$ such that*

$$\begin{pmatrix} I & 0 \\ \mathcal{A} & \mathcal{B} \\ \mathcal{C} & \mathcal{D} \end{pmatrix}^{T} \begin{pmatrix} 0 & \mathcal{X} & 0 \\ \mathcal{X} & 0 & 0 \\ 0 & 0 & M \end{pmatrix} \begin{pmatrix} I & 0 \\ \mathcal{A} & \mathcal{B} \\ \mathcal{C} & \mathcal{D} \end{pmatrix} \prec 0$$

$$\begin{pmatrix} I & 0 \\ A_\Phi & B_\Phi \\ C_\Phi & D_\Phi \end{pmatrix}^{T} \begin{pmatrix} 0 & Z & 0 \\ Z & 0 & 0 \\ 0 & 0 & M_1 \end{pmatrix} \begin{pmatrix} I & 0 \\ A_\Phi & B_\Phi \\ C_\Phi & D_\Phi \end{pmatrix} \succ 0.$$

We applied Corollary 4.14 with a basis of length $n = 8$ and with the pole $a = -7$. In this way we computed again the maximal value $\mu K_f \approx 0.137$ for which stability can be guaranteed in about 36 s.

Remark 4.15. *Since Y is strictly proper, (4.34) cannot be satisfied at $\omega = \infty$ because its left-hand side vanishes. However, the interconnection is certainly well-posed such that the FDI only needs to be verified for all finite frequencies (Remark 4.4). Therefore, the gridding approach can be applied directly. In the alternative path without gridding, we can circumvent this trouble by replacing Y with $Y + \epsilon I$, with $\epsilon = 10^{-5}$ in our case. Let us stress that this perturbation (also in the cases presented below) is only required in those channels that are related to passive uncertainties.*

4.4.4 *Case 2: Stability with Uncertain Stiff Environments*

We characterize the admissible environments as pure springs modeled by $Z_e = \frac{k}{s}$ with an uncertain constant stiffness coefficient $k \in [0, \bar{k}] \, \mathrm{N/m}$. After merging $-\frac{k}{s}$ with the system (and slightly perturbing the pole of the integrator to render the nominal system stable) we are left with the uncertainty structure $\Delta = \mathrm{diag}(\Delta_h, \delta_e)$ where the human uncertainty is assumed to be passive LTI and δ_e is an uncertain real scalar parameter in the interval $[0, 1]$. Using a modified *DG*-scaling for the shifted parameter range, we can easily adapt the multiplier and obtain, next to $\lambda > 0$ and $d > 0$, the following FDI for interconnection stability:

$$
\begin{pmatrix} 1 & 0 \\ 0 & 1 \\ -Y_{11} & -Y_{12} \\ Y_{21} & Y_{22} \end{pmatrix}^{*} \left(\begin{array}{cc|cc} 0 & 0 & \lambda & 0 \\ 0 & -d & 0 & \frac{d}{2}+ig \\ \hline \lambda & 0 & 0 & 0 \\ 0 & \frac{d}{2}-ig & 0 & 0 \end{array} \right) \begin{pmatrix} 1 & 0 \\ 0 & 1 \\ -Y_{11} & -Y_{12} \\ Y_{21} & Y_{22} \end{pmatrix} \prec 0. \qquad (4.36)
$$

With the frequency grid as in the previous case we obtained too optimistic results (after comparing the values with those computed below), which suggests the need to refine the grid. With additional 1500 points in the interval $[10^{-6}, 100] \frac{\mathrm{rad}}{\mathrm{s}}$, we obtained the exact value of $(\mu K_f)_{\max} \approx 0.215$ for $\bar{k} = 1000 \frac{\mathrm{N}}{\mathrm{m}}$ in 127.7 s. We infer that the grid resolution, whether logarithmic or linear, plays a crucial role for the computations.

   This reveals that, especially for systems that have high bandwidth and complex dynamics, it is instrumental to choose a sufficiently fine frequency grid in stability analysis. This is the very reason for the alternative path of computations (via multiplier parametrization and LMIs in state-space) as proposed above. In this particular example, the resulting condition boils down to two simple LMIs to be verified numerically. After normalizing the environment uncertainty by scaling, we just need to verify feasibility of the LMIs in the next result.

Corollary 4.16. *The $Y - \Delta$ interconnection in Figure 4.5b is stable for all passive LTI Δ_h and LTI real parametric uncertainty $\delta_e \in [0, 1]$ if there exist symmetric matrices $\mathcal{X}, Z_2, D_2$ and a skew symmetric matrix G_2 such that*

$$
\begin{pmatrix} I & 0 \\ \mathcal{A} & \mathcal{B} \\ \mathcal{C} & \mathcal{D} \end{pmatrix}^{T} \begin{pmatrix} 0 & \mathcal{X} & 0 \\ \mathcal{X} & 0 & 0 \\ 0 & 0 & M \end{pmatrix} \begin{pmatrix} I & 0 \\ \mathcal{A} & \mathcal{B} \\ \mathcal{C} & \mathcal{D} \end{pmatrix} \prec 0,
$$

$$
\begin{pmatrix} I & 0 \\ A_\Phi & B_\Phi \\ C_\Phi & D_\Phi \end{pmatrix}^{T} \begin{pmatrix} 0 & Z_2 & 0 \\ Z_2 & 0 & 0 \\ 0 & 0 & D_2 \end{pmatrix} \begin{pmatrix} I & 0 \\ A_\Phi & B_\Phi \\ C_\Phi & D_\Phi \end{pmatrix} \succ 0
$$
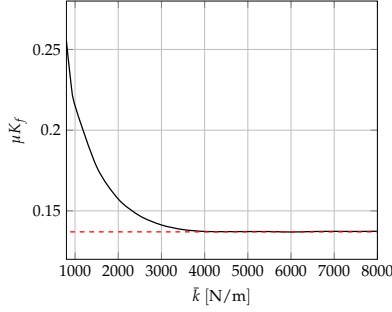
Figure 4.6: Performance loss for increasing environment stiffness uncertainty. The dashed line shows the value for unconditional stability from Section 4.4.3.

hold, where

$$M = \begin{pmatrix} 0 & 0 & 1 & 0 \\ 0 & -D_2 & 0 & \frac{1}{2}D_2 + G_2 \\ 1 & 0 & 0 & 0 \\ 0 & \frac{1}{2}D_2 - G_2 & 0 & 0 \end{pmatrix}, \Psi = \begin{pmatrix} 1 & 0 & 0 & 0 \\ 0 & \Phi_2 & 0 & 0 \\ 0 & 0 & 1 & 0 \\ 0 & 0 & 0 & \Phi_2 \end{pmatrix}.$$

For this example we have used the basis Φ_2 with length 12 and selected the pole $a = -16$. Bisection over μK_f took 29.3 s and the resulting maximum admissible value is found to be 0.215 for a sample value of $\bar{k} = 1000$. Values higher than 0.215 would render the nominal system unstable, which means that we obtain the best possible result. The performance curve for different values of $\bar{k}$ is given in Figure 4.6.

4.4.5 *Case 3: Robustness against Delays*

We reconsider the plant given in (4.33) and modify it in order to relate the results to the undelayed cases given above. We assume that there exist communication delays present in the forward and backward path and, without loss of generality, we choose both maximally allowed delay durations to be equal for simplicity. We thus consider

$$Y = \begin{pmatrix} Y_m & -K_f Y_m e^{-s\tau} \\ -Y_m Y_s \mu K_p e^{-s\tau} & \frac{M_m s^2 + B_m s + \mu K_f K_p e^{-2s\tau}}{(M_s s^2 + (B_s + K_v)s + K_p)(M_m s + B_m)} \end{pmatrix}$$

where $\tau \in [0, \bar{\tau}]$. By pulling out the delay uncertainties from Y, the nominal plant Y_d is given by

$$Y_d = \begin{pmatrix} Y_m & 0 & -Y_m & 0 \\ 0 & sY_s & 0 & -K_p Y_s \\ 0 & K_f & 0 & 0 \\ \mu Y_m & 0 & -\mu Y_m & 0 \end{pmatrix}$$

and is interconnected to the structured uncertainty block

$$\Delta = \text{diag}\left(\Delta_h, \Delta_e, e^{-s\tau}, e^{-s\tau}\right).$$

In accordance with Section 4.2.4, a unity feedback is applied and two delay weights are included in the plant.

Corollary 4.17. *The $Y_d - \Delta$ interconnection is stable for all passive LTI Δ_h, Δ_e and LTI delay uncertainties if there exist symmetric matrices $\mathcal{X}$, M_1, M_2, D_3, D_4, R_3, R_4 and Z_i for $i = 1, \dots, 4$ such that*

$$\begin{pmatrix} I & 0 \\ \mathcal{A} & \mathcal{B} \\ \mathcal{C} & \mathcal{D} \end{pmatrix}^T \begin{pmatrix} 0 & \mathcal{X} & 0 \\ \mathcal{X} & 0 & 0 \\ 0 & 0 & P \end{pmatrix} \begin{pmatrix} I & 0 \\ \mathcal{A} & \mathcal{B} \\ \mathcal{C} & \mathcal{D} \end{pmatrix} \prec 0$$

and

$$\begin{pmatrix} I & 0 \\ A_\Phi^i & B_\Phi^i \\ C_\Phi^i & D_\Phi^i \end{pmatrix}^T \begin{pmatrix} 0 & Z_i & 0 \\ Z_i & 0 & 0 \\ 0 & 0 & Y_i \end{pmatrix} \begin{pmatrix} I & 0 \\ A_\Phi^i & B_\Phi^i \\ C_\Phi^i & D_\Phi^i \end{pmatrix} \succ 0$$

hold where $Y_1 = M_1$, $Y_2 = M_2$, $Y_3 = D_3$, $Y_4 = D_4$,

$$P = \begin{pmatrix} P_{11} & P_{12} \\ P_{12}^T & P_{22} \end{pmatrix}, \begin{cases} P_{11} = \text{diag}\left(0, 0, -D_3, R_3, -D_4, R_4\right), \\ P_{12} = \text{diag}\left(M_1, M_2, 0, R_3, 0, R_4\right), \\ P_{22} = \text{diag}\left(0, 0, D_3, 0, D_4, 0\right) \end{cases}$$

and

$$\Psi = \begin{pmatrix} \Phi_1 & & & & & & & & & & & \\ & \Phi_2 & & & & & & & & & & \\ & & \Phi_3 & & & & & & & & & \\ & & \Phi_5 & & & & & & & & & \\ & & & \Phi_4 & & & & & & & & \\ & & & \Phi_6 & & & & & & & & \\ \hline & & & & \Phi_1 & & & & & & & \\ & & & & & \Phi_2 & & & & & & \\ & & & & & & \Phi_3 W_d & & & & & \\ & & & & & & \Phi_5 & & & & & \\ & & & & & & & \Phi_4 W_d & & & & \\ & & & & & & & \Phi_6 & & & & \end{pmatrix}.$$

This test has been applied for various maximum delay durations $\bar{\tau} \in [0.01, 0.1]$s with 0.005s increments and the results are shown in Figure 4.7. At each $\bar{\tau}$ point, the bisection algorithm took on average 577.4s (varying in $[435, 1040]$s). The basis lengths and the pole locations are selected as $n_i = 3, 3, 3, 3, 5, 5$ and $a_i = -16, -17, -19, -8, -13, -14$ respectively. The pole locations are selected away from the system's poles but arbitrary otherwise.

4.4.6 *Additional Remarks*

In concluding this section, we would like to address the issue of conservatism in our numerical examples. The first two cases involve none at all for sufficiently long basis functions as confirmed numerically.

If considering only passive LTI uncertainties in standard problems, there is no room for further algorithmic improvements since the resulting tests are guaranteed to be exact. On the other hand, there is a huge potential in searching for refined uncertainty characterizations in order to reduce conservatism. We have illustrated that there is no need to confine the analysis to passive uncertainties as long as they can be associated with some integral quadratic constraint, possibly through some physical experiments (see e.g. [15] for a parametric uncertainty case which can be improved directly using the multipliers given above). Thus, once IQCs are known for individual uncertainty blocks, it has been also demonstrated how to computationally verify robust stability against their combined influence on the interconnection with ease.

On the other hand, this might not be the case for the test in Corollary 4.17. To quantify the potential conservatism, we use extreme values for the stiff environment and the delay uncertainty and determine the maximum achievable values of μK_f for which the transfer function seen by the human is still strictly passive. Environments that are modeled as pure stiffnesses are considered to be "worst cases" since their Nyquist curves are located at the boundary of the closed right half plane and since their low frequency contribution, unlike pure mass models, is significant. As shown in Figure 4.8, the performance decreases for increasing levels of $\bar{\tau}$ and $\bar{k}$, but the trade-off curve does not change significantly beyond the value $\bar{k} = 100\,000\,\text{N/m}$. We have also overlayed the results of Figure 4.7. If it is indeed true that a pure stiffness environment is the worst case, then the difference between the two lowest curves in Figure 4.8 can be attributed to the conservatism of the test in Corollary 4.17. Thus, we can conclude that the conservatism is not very large; this is of particular significance for delay-independent robust stability tests which would result in values in the range of $\mu K_f \approx 10^{-5}$.

Let us briefly compare with results obtained for time-varying environments. This makes a particularly interesting case since, in practice, a remote device might explore environments with varying characteristics. We have analyzed the non-delayed system where the environment is a pure spring with a stiffness coefficient $k(t) \in [0, 1000]\text{N/m}$ and different bounds on the rate-of-variation as shown in Figure 4.9. Classical absolute stability tests can only handle arbitrary fast variations which leads to small values of performance of $\approx 2 \cdot 10^{-5}$. The inclusion of information about the ROV (as possible through the class of multipliers discussed above) substantially reduces the conservatism as is visible in the plot.

In the literature, one often encounters PID-based controller architectures which make it possible to analyze the effect of variations in the controller gains onto the performance of the teleoperation system. In our set-up, we can attribute the increase of performance to the increase of μK_f due to the simplicity of the system structure. If
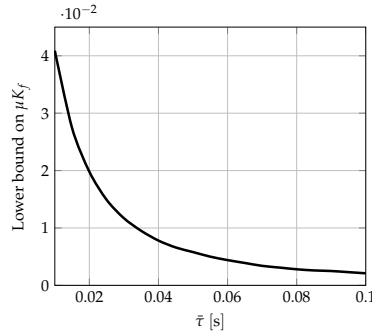
Figure 4.7: Performance loss for increasing maximal delay duration.
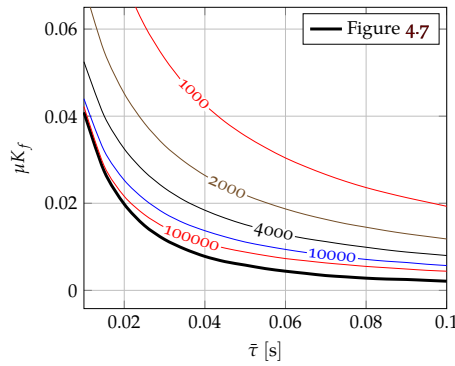
Figure 4.8: Robust performance for different stiff environment cases in the face of increasing delay uncertainty duration.

moving towards more complicated controller architectures, such clear relations are not expected to be valid any more. This precludes obtaining graphical or analytical stability and performance tests with robustness guarantees. As we show in Chapter 5, IQC framework allows the incorporation of a performance channel and to develop robust performance analysis tests, very much along the same lines as discussed for stability in this chapter. Such formulations of the performance problems make it convenient to compare different PID controllers.

In conjunction with robust performance analysis, we can further utilize robust controller synthesis methods with dynamic IQCs using the results of [56, 57, 171, 172, 189]. In [171], a general class of robust synthesis problems has been identified which can be handled by convex optimization techniques. The well-known μ-synthesis algorithm, based on the so-called D/K-iteration, has been extended to general dynamic IQCs in [189] for problems that do not admit a convex formulation. In addition to robustness analysis for existing PID controller, this opens the way for model based controller synthesis.
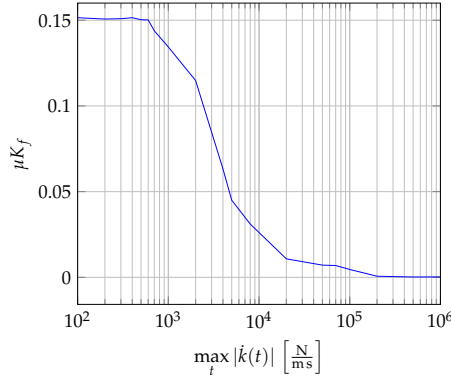
Figure 4.9: The performance loss with respect to the increase in ROV bound of the time-varying uncertain parameter $k(t) \in [0, 1000]\mathrm{N/m}$.

4.5   Discussion

In this chapter, we have investigated the analysis problem from a Integral Quadratic Constraints (IQCs) perspective. The content is mainly based on [151]. We include a particular reasoning for the use of these recent tools provided by the robust control theory. These points have often come up during the author's discussions held with experts, colleagues and practitioners.

First and foremost argument is on the comparison with other passivity-based techniques. As we sampled a few cases in this chapter, IQC tests are far more general than passivity-based analysis results since passivity is a system property and therefore, only specific to a class of systems. IQCs are system property qualifiers by which the designer obtains a robustness test. Thus, if the designer decides to perform a robustness test against passive uncertainties then a particular IQC is selected and the stability test follows from that constraint. Furthermore, via IQCs it is possible to combine different properties of the same class of systems. Suppose we have a class of uncertainties that are both passive and small-gain, then it's not clear how to combine small-gain theorem and passivity theorem exclusively to remove the resulting conservatism had we had used only one of these stability results since each neglects the other system property.

The equivalence we have presented is a consequence of the so-called Main Loop Theorem which is originally formulated for μ-analysis but tailored for our context (see [203, Thm. 11.7]):

Theorem 4.18. *Let N be an LTI network interconnected to a human model Δ_1 from the class of passive LTI operators and to the environment Δ_2 from some class of models. For our convenience, let us also use M to denote the 1-port immitance operator seen by Δ_1 (or perceived by the human). Then the following two statements are equivalent:*

i) The interconnection of N with both arbitrary uncertainties Δ_1 and Δ_2 from their respective classes is stable.

ii) The $M - \Delta_1$ interconnection is stable for all Δ_1 and Δ_2, if M is strictly passive for all Δ_2 in the respective class.

In other words, passivity-based techniques focus on verifying condition ii) by implicitly fixing to one class of uncertainties (here passivity) and then test whether the system seen by that uncertainty is also strictly in that class, while our IQC approach is based on checking i).

This formulation also allows us to exemplify the point that we strongly underline in this chapter: Assertion ii) resists to be utilized in a convenient way if we are aware of an extra property that also characterizes Δ_1 such as the small-gain and passive LTI operator example we have given above. The main difficulty is that in many cases it is unknown how to translate this information into a test for M that needs to be verified for all admissible Δ_2. However, the IQC formulation based on (i) does not exhibit this complication, which is one of its powerful features as demonstrated with the delay robustness example.

Synthesis

As we have shown in the previous chapters, the bilateral teleoperation problem can be carried over to a more general framework of IQCs. By doing so not only the existing results are preserved, but also substantial generalization options are obtained. Moreover, the shortcomings of the classical results and the underlying relations are clearly seen.

Hence, we can proceed with the controller design problem and obtain controllers using the results for IQC synthesis literature. Since the results here can be considered as established, we adopt a "running example" type of style instead of repeating already available results in the literature with theorems and proofs enumerated one after another.

5.1 Robust Controller Design using IQCs

LMI-based control synthesis methods are in general nonconvex and even the existence of a possible convexification step is not known. The μ-synthesis and Lyapunov-based synthesis methods are the two main venues of obtaining conditions for the design of a robust controller.

Clearly, the situation is not much different for IQC synthesis which is closely related to μ- tools. As we have shown in chapter 4, the dynamic multipliers are of the most importance when it comes to reducing the conservatism involved in the frequency-domain stability analysis techniques. However including dynamics to the multipliers makes the problem harder for the robust control synthesis problem. Since there is no known convex robust control design method known, we resort back to a nonconvex multiplier/controller iteration as is the case with the classical μ-tools with the so-called *DK*-iteration. However, it has been recently shown that, a large class of robust control design problems are convex depending on the uncertainty contribution on certain entries of the plant data, [171].

5.1.1 *Notation and Definitions*

We start with state-space descriptions of systems in the following form

$$\begin{pmatrix} \dot{x} \\ z \\ y \end{pmatrix} = \underbrace{\begin{pmatrix} A & B_w & B_u \\ C_z & D_{wz} & D_{uz} \\ C_y & D_{wy} & D_{uy} \end{pmatrix}}_{G} \begin{pmatrix} x \\ w \\ u \end{pmatrix} \tag{5.1}$$

Here, w denotes the generalized disturbance signals (perturbations, reference signals etc.), z denotes the controlled output signals that is selected as the objectives of the control design (minimization of error norms, control actions etc.) y signals are the measurements and u are the controller inputs. Typically, the second row is called the *performance channel* and the last row is, similarly, the *control channel*. The integers n, n_u, n_w, m_z, m_y denote the number of states, control inputs, disturbance inputs, control outputs, and measurements respectively. For the performance characterization, we also use a quadratic form

$$\int_0^\infty \begin{pmatrix} w(t) \\ z(t) \end{pmatrix}^T P_p \begin{pmatrix} w(t) \\ z(t) \end{pmatrix} dt \le -\epsilon \|w\|^2. \tag{5.2}$$

As a typical example, the robust $\mathcal{L}_2$ gain from w to z can be rewritten as such by using

$$P_p = \begin{pmatrix} -\gamma^2 I_{n_w} & 0 \\ 0 & I_{m_z} \end{pmatrix}$$

We will also be referring to the state-space representation of a controller K via

$$\begin{pmatrix} \dot{x}_K \\ u \end{pmatrix} = \begin{pmatrix} A_K & B_K \\ C_K & D_K \end{pmatrix} \begin{pmatrix} x_K \\ y \end{pmatrix} \tag{5.3}$$

with n_K being the number of states of the controller. The common assumption of $D_{uy} = 0$ is also adopted here. This causes no loss of generality as long as the interconnection of G-K interconnection is well-posed i.e. $(I - D_{uy}D_K)$ is nonsingular. Then, the closed loop plant $(G \star K)(s)$ state-space matrices are obtained as

$$\left[\begin{array}{c|c} \mathcal{A} & \mathcal{B} \\ \hline \mathcal{C} & \mathcal{D} \end{array} \right] = \left[\begin{array}{cc|c} A + B_u D_K C_y & B_u C_K & B_w + B_u D_K D_{wy} \\ B_K C_y & A_K & B_K D_{wy} \\ \hline C_z + D_{uz} D_K C_y & D_{uz} C_K & D_{wz} + D_{uz} D_K D_{wy} \end{array} \right] \tag{5.4}$$

$$= \left[\begin{array}{cc|c} A & 0 & B_w \\ 0 & 0 & 0 \\ \hline C_z & 0 & D_{wz} \end{array} \right] + \left[\begin{array}{cc} 0 & B_u \\ I & 0 \\ \hline 0 & D_{uz} \end{array} \right] \left[\begin{array}{cc} A_K & B_K \\ C_K & D_K \end{array} \right] \left[\begin{array}{cc|c} 0 & I & 0 \\ C_y & 0 & D_{wy} \end{array} \right]. \tag{5.5}$$

Here two-letter subscripts, $\cdot_{ab}$ denote the term that represents the contribution from input a to output b which hopefully gives some relief to the reader since the manipulations quickly get ugly.

Definition 5.1 (Generalized Plant). *The plant G is said to be a generalized plant if there exists at least one controller K such that the interconnection of G and K is stable. Equivalently, G is a generalized plant if (A, B_u) is stabilizable and (A, C_y) is detectable.*

5.1.2 *Solving Analysis LMIs for Controller Matrices*

Once we have the generalized plant description we can design a controller that achieves closed loop stability and a performance level characterized by P_p. Before

we state the nominal controller synthesis conditions, we provide a "trick", the so-called Linearization Lemma which can be found in [173]. It is also important to follow the rationale behind the arguments given in [172] for general quadratic performance synthesis.

Lemma 5.2. *Assume we are given with a quadratic form in which A, S are constant matrices and $B(v)$, $Q(v)$ and $R(v) \succeq 0$ are matrix functions of some decision variables denoted by v such that*

$$\begin{pmatrix} A \\ B(v) \end{pmatrix}^T \begin{pmatrix} Q(v) & S \\ S^T & R(v) \end{pmatrix} \begin{pmatrix} A \\ B(v) \end{pmatrix} \prec 0 \tag{5.6}$$

should be verified. Also assume that there exists a decomposition such that

$$R(v) = T(U(v))^{-1}T^T$$

where $U(v) \succ 0$ is affine in v then (5.6) can be converted to the LMI problem

$$\begin{pmatrix} A^T Q(v) A + A^T S B(v) + B^T(v) S^T A & B^T(v) T \\ T^T B(v) & -U(v) \end{pmatrix} \prec 0 \tag{5.7}$$

Proof. Applying Schur Complement formula with respect to the lower right block of the LMI and simply carrying out the block multiplication in the quadratic inequality shows the equivalence. □

Note that, even if $R(v) = R$ i.e. some constant matrix, this step is needed for resolving the quadratic dependence of $B(v)$.

Following our analysis results from the previous chapter, we have seen that for a stable closed loop system $G \star K$ to have a performance level of P_p the condition

$$\begin{pmatrix} I & 0 \\ \mathcal{A} & \mathcal{B} \\ \hline 0 & I \\ \mathcal{C} & \mathcal{D} \end{pmatrix}^T \left(\begin{array}{cc|c} 0 & \mathcal{X} & 0 \\ \mathcal{X} & 0 & 0 \\ \hline 0 & 0 & P_p \end{array} \right) \begin{pmatrix} I & 0 \\ \mathcal{A} & \mathcal{B} \\ \hline 0 & I \\ \mathcal{C} & \mathcal{D} \end{pmatrix} \prec 0$$

should hold for some symmetric matrix $\mathcal{X}$. However, in the absence of the knowledge of a stabilizing controller we encounter an immediate problem. If we assume the controller matrices in calligraphic closed loop matrices as unknowns then they multiply the unknown matrix $\mathcal{X}$ variables and hence destroying the affine dependence on the unknowns, rendering the constraint as a Bilinear Matrix Inequality (BMI). Also in the analysis case the stability was assumed at the outset however here the positivity constraint, $\mathcal{X} \succ 0$ should be included to guarantee closed loop stability. Thus, the synthesis problem is more involved. The resolution of this problem appeared mainly in [122, 172] (also in a strict $\mathcal{H}_\infty$ context, [51, 52] with an two-step procedure of elimination of the controller parameters and obtaining some of the LMI variables and then resolving the LMIs for controller parameters).

The essential trick is to manifacture a new set of derived variables from the original variables such that the problem is not altered but conditions become LMIs again. For this purpose, suppose we partition the matrices

$$\mathcal{X} = \begin{pmatrix} X & U \\ U^T & \bullet \end{pmatrix}, \mathcal{X}^{-1} = \begin{pmatrix} Y & V \\ V^T & \bullet \end{pmatrix},$$

where $\bullet$ denotes the entries that we are not interested in. Also using the relations $\mathcal{X}\mathcal{X}^{-1} = I$, we have

$$\mathcal{Y} = \begin{pmatrix} Y & I \\ V^T & 0 \end{pmatrix}, \mathcal{Z} = \begin{pmatrix} I & 0 \\ X & U \end{pmatrix}.$$

Then by a congruence transformation the analysis LMI

$$\begin{pmatrix} \mathcal{Y} & 0 \\ 0 & I \end{pmatrix}^T \begin{pmatrix} I & 0 \\ \mathcal{A} & \mathcal{B} \\ 0 & I \\ \mathcal{C} & \mathcal{D} \end{pmatrix}^T \left(\begin{array}{cc|c} 0 & \mathcal{X} & 0 \\ \mathcal{X} & 0 & 0 \\ \hline 0 & 0 & P_p \end{array} \right) \begin{pmatrix} I & 0 \\ \mathcal{A} & \mathcal{B} \\ 0 & I \\ \mathcal{C} & \mathcal{D} \end{pmatrix} \begin{pmatrix} \mathcal{Y} & 0 \\ 0 & I \end{pmatrix} \prec 0$$

becomes

$$\begin{pmatrix} I & 0 \\ \mathbf{A} & \mathbf{B} \\ 0 & I \\ \mathbf{C} & \mathbf{D} \end{pmatrix}^T \left(\begin{array}{cc|c} 0 & I & 0 \\ I & 0 & 0 \\ \hline 0 & 0 & P_p \end{array} \right) \begin{pmatrix} I & 0 \\ \mathbf{A} & \mathbf{B} \\ 0 & I \\ \mathbf{C} & \mathbf{D} \end{pmatrix} \prec 0 \tag{5.8}$$

where boldface variables are defined as

$$\left(\begin{array}{c|c} \mathbf{A} & \mathbf{B} \\ \hline \mathbf{C} & \mathbf{D} \end{array} \right) := \left(\begin{array}{cc|c} AY + B_u M & A + B_u N C_y & B_w + B_u N D_{wy} \\ K & AX + LC_y & XB_w + LD_{wy} \\ \hline C_z Y + D_{uz} M & C_z + D_{uz} N C_y & D_{zw} + D_{uz} N D_{wy} \end{array} \right)$$

together with

$$\begin{pmatrix} K & L \\ M & N \end{pmatrix} := \begin{pmatrix} U & XB_u \\ 0 & I \end{pmatrix} \begin{pmatrix} A_K & B_K \\ C_K & D_K \end{pmatrix} \begin{pmatrix} V^T & 0 \\ C_y Y & I \end{pmatrix} + \begin{pmatrix} XAY & 0 \\ 0 & 0 \end{pmatrix} \tag{5.9}$$

It is indeed not that easy to follow the inner workings of this transformation however after a tedious multiplication exercise it can be seen that the aforementioned bijective transformation does the job. Thus, boldface variables are now functions of X, Y, K, L, M, N matrices and moreover the constraint is once again an LMI (after the application of Lemma 5.2). For stability characterization we also need $\mathcal{X} \succ 0$ and using the same transformation $\mathcal{Y}^T \mathcal{X} \mathcal{Y} \succ 0$, we obtain

$$\mathbf{X} := \begin{pmatrix} X & I \\ I & Y \end{pmatrix} \succ 0.$$

Therefore, instead of BMIs we have obtained LMI conditions all involving boldface variables entering affinely. This set of variables are typically denoted by $v =$

$\{X, Y, K, L, M, N\}$. Unfortunately, $K(s)$ and K creates a naming clash however we will not resolve this to comply with the literature, instead we'll rely on the reader for the distinction and try to state whichever is meant in case of an ambiguity.

With all this preparation, we arrive at the nominal synthesis problem :

Theorem 5.3. *The nominal synthesis problem is solvable if there exists a feasible set of variables v such that*

$$\mathbf{X} \succ 0, \begin{pmatrix} I & 0 \\ \mathbf{A} & \mathbf{B} \\ 0 & I \\ \mathbf{C} & \mathbf{D} \end{pmatrix}^T \left(\begin{array}{cc|c} 0 & I & 0 \\ I & 0 & 0 \\ 0 & 0 & P_p \end{array} \right) \begin{pmatrix} I & 0 \\ \mathbf{A} & \mathbf{B} \\ 0 & I \\ \mathbf{C} & \mathbf{D} \end{pmatrix} \prec 0 \tag{5.10}$$

hold. Once a feasible solution is found by the aid of Lemma 5.2, the controller can be obtained by first by finding arbitrary invertible U and V matrices by solving $I - XY = UV^T$ and then back substituting the variables into (5.9)

In summary, we have obtained a nominally stabilizing and P_p-performance level guaranteeing controller. Next, we include uncertainty channels to our plant G and add a robustness constraint in our design. Unfortunately, this breaks down our "LMIzation" step and there is no known method to obtain LMI solutions from the BMI constraints given below.

5.1.3 *Adding Uncertainty Channels*

We renew our plant representation by the following relations

$$\begin{pmatrix} \dot{x} \\ q \\ z \\ y \end{pmatrix} = \underbrace{\begin{pmatrix} A & B_p & B_w & B_u \\ C_q & D_{pq} & D_{wq} & D_{uq} \\ C_z & D_{pz} & D_{wz} & D_{uz} \\ C_y & D_{py} & D_{wy} & 0 \end{pmatrix}}_{G} \begin{pmatrix} x \\ p \\ w \\ u \end{pmatrix} \tag{5.11}$$

and $p = \Delta q$. The positive integers n_p, m_q are the uncertainty operator row/column numbers respectively. Also this extra channel is often called the "uncertainty channel". Once again we start off with the robustness/performance analysis LMI. For that we also need to connect our stabilizing controller. The new closed loop matrices are obtained as

$$\left[\begin{array}{c|cc} \mathcal{A} & \mathcal{B}_p & \mathcal{B}_w \\ \hline \mathcal{C}_q & \mathcal{D}_{pq} & \mathcal{D}_{wq} \\ \mathcal{C}_q & \mathcal{D}_{pz} & \mathcal{D}_{wz} \end{array} \right] = \left[\begin{array}{cc|cc} A & 0 & B_p & B_w \\ 0 & 0 & 0 & 0 \\ \hline C_q & 0 & D_{pq} & D_{wq} \\ C_z & 0 & D_{pz} & D_{wz} \end{array} \right] +$$

$$\left[\begin{array}{cc} 0 & B_u \\ I & 0 \\ \hline 0 & D_{uq} \\ 0 & D_{uz} \end{array} \right] \left[\begin{array}{cc} A_K & B_K \\ C_K & D_K \end{array} \right] \left[\begin{array}{cc|cc} 0 & I & 0 & 0 \\ C_y & 0 & D_{py} & D_{wy} \end{array} \right]. \tag{5.12}$$

Suppose a block diagonal collection of uncertainty operator set $\mathbf{\Delta}$ characterized by a family of constant multipliers $\mathbf{P}$ is known. Moreover, assume that the $\Delta \star (G \star K)$ is well-posed for all $\Delta \in \mathbf{\Delta}$. For notational convenience we also introduce the partitions

$$P = \begin{pmatrix} Q & S \\ S^T & R \end{pmatrix}, \quad P_p = \begin{pmatrix} Q_p & S_p \\ S_p^T & R_p \end{pmatrix}$$

Again, as given in Chapter 4, the closed loop system is robustly stable for all $\Delta \in \mathbf{\Delta}$ and achieves performance characterized by the multiplier P_p if there exist a $P \in \mathbf{P}$ and a symmetric matrix $\mathcal{X}$ such that

$$\begin{pmatrix} I & 0 & 0 \\ \mathcal{A} & \mathcal{B}_p & \mathcal{B}_w \\ 0 & I & 0 \\ \mathcal{C}_q & \mathcal{D}_{pq} & \mathcal{D}_{wq} \\ 0 & 0 & I \\ \mathcal{C}_z & \mathcal{D}_{pz} & \mathcal{D}_{wz} \end{pmatrix}^T \left(\begin{array}{cc|cc|cc} 0 & \mathcal{X} & & & & \\ \mathcal{X} & 0 & & & & \\ \hline & & Q & S & & \\ & & S^T & R & & \\ \hline & & & & Q_p & S_p \\ & & & & S_p^T & R_p \end{array} \right) \begin{pmatrix} I & 0 & 0 \\ \mathcal{A} & \mathcal{B}_p & \mathcal{B}_w \\ 0 & I & 0 \\ \mathcal{C}_q & \mathcal{D}_{pq} & \mathcal{D}_{wq} \\ 0 & 0 & I \\ \mathcal{C}_z & \mathcal{D}_{pz} & \mathcal{D}_{wz} \end{pmatrix} \prec 0$$

(5.13)

For the controller synthesis case, unfortunately previous transformation does not resolve the additional bilinear terms and in fact it is not even known if such a transformation is possible or not. We can either try to solve BMIs directly with nonconvex optimization techniques or we can use another nonconvex solution which is known as the multiplier-controller iteration.

Notice that if we have the stabilizing controller then the outer factors are constant matrices and we have an LMI problem. Conversely, if we have a feasible multiplier such that the inequality is satisfied then it's a matter of applying the aforementioned transformation and linearizing lemma to obtain a controller. Hence, we can perform an iteration by either fixing the multiplier or the controller.

5.1.4   *The Multiplier-Controller Iteration with Static Multipliers*

If we start with a uncertain generalized plant representation, we have neither the controller nor the robustness multipliers. Moreover, we don't have a method to search for both simultaneously. Thus, we first consider the nominal control design problem and obtain a nominally stabilizing controller as given above. It can also be shown that, the closed loop, with the well-posedness assumption and a simple continuity argument, has some, possibly very limited, robustness properties against the uncertainty set we would like to consider. In other words, there is no reason for the controller to be robustly stabilizing against the full uncertainty region that we originally modeled since we did not enforce it by any constraint.

Remark 5.4. *Repeating what we have touched upon in Remark 4.2, this is briefly the rationale behind the common assumption of star-shaped uncertainty region, i.e., $[0, 1]\mathbf{\Delta} \in \mathbf{\Delta}$. However, it is important to note that, the scaling needs not to be a simple scalar $r \in [0, 1]$ such that the uncertainty is scaled with $r\Delta$. This point is often implicitly assumed and rarely*

mentioned. Thus, the notation $r\Delta$ should be taken conceptually. As an example, the delay uncertainty cannot be scaled with $re^{-s\tau}$ for any $r \in [0,1]$ since it would scale the unit-circle. In fact what we want to scale is the τ variable as $e^{-sr\tau}$ such that when $r = 0$ we have $e^0 = 1$ i.e. a non-delayed line and for $r = 1$ we have $e^{-s\tau}$ i.e. full duration of the maximum allowed delay. Similarly, saturation and dead-zone nonlinearities are examples of such nontrivial scaling cases. Hence, the star-shapedness in this context becomes a parametrization of the size of the uncertainty from the nominal case to the full-sized uncertainty. Nevertheless most uncertainty types are amenable to scaling with r-multiplication hence there is no need to invent yet another notation for an already complicated procedure. Therefore, every uncertainty needs to be scaled in a customized way but for notational convenience we will still use $r\Delta$ to denote the scaled uncertainty size.

Summarizing our current situation, we have obtained a nominally stabilizing controller and we have parameterized a custom scaling method for each of our uncertainty subblocks. Now we would like to search for the maximum achievable r via analysis. Hence, we can search over the maximum r such that the scaled closed loop is robustly stable for all $\Delta \in r\Delta$.

Formally we have the following two theorems that constitutes the initialization and also the two steps of the iteration: We assume that the uncertain LTI plant

$$G : \mathcal{L}_{2e}^{n_p+n_w+n_u} \to \mathcal{L}_{2e}^{m_q+m_z+m_y},$$

is a generalized plant i.e. there exists an LTI controller

$$K : \mathcal{L}_{2e}^{m_y} \to \mathcal{L}_{2e}^{n_u},$$

such that the nominal closed loop plant $G_{nom} \star K \in \mathcal{RH}_{\infty}^{m_z \times n_w}$ where

$$G_{nom}(s) = 0_{n_p \times m_q} \star G = \begin{pmatrix} 0_{(m_z+m_y) \times m_q} & I_{m_z+m_y} \end{pmatrix} G(s) \begin{pmatrix} 0_{n_p \times (n_w+n_u)} \\ I_{n_w+n_u} \end{pmatrix}.$$

Theorem 5.5 (Analysis Step). *The interconnection of an LTI uncertain plant $G(s)$ given by (5.12) with a nominally stabilizing controller K given by (5.3), depicted in Figure 5.1 and admits the realization given in (5.12) is robustly stable in the face of all $\Delta \in r\Delta$ and achieves the performance level characterized by P_p if there exist a symmetric matrix $\mathcal{X}$ and $P \in \mathbf{P}$ such that (5.13) hold.*

One can simply perform a line search for the largest possible $r \in [0,1]$ such that the conditions are numerically verified and P_p is optimized. Then the resulting multiplier P is fixed and we switch to the controller design step.

Theorem 5.6 (Synthesis Step). *Assume an uncertain LTI plant $G(s)$ given by (5.12) is given. There exist an LTI controller K such that the closed loop is stable for all $\Delta \in r\Delta$*
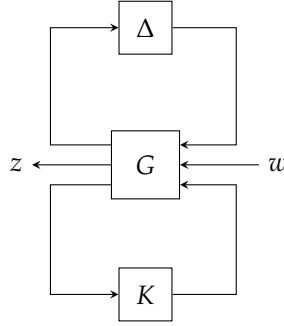
Figure 5.1: The uncertain interconnection

and achieves the performance level characterized by P_p if there exist a set of variables $v = \{X, Y, K, L, M, N\}$ such that the linearized version of the constraint (omitted for brevity)

$$
\begin{pmatrix} I & 0 & 0 \\ \mathbf{A} & \mathbf{B}_p & \mathbf{B}_w \\ 0 & I & 0 \\ \mathbf{C}_q & \mathbf{D}_{pq} & \mathbf{D}_{wq} \\ 0 & 0 & I \\ \mathbf{C}_z & \mathbf{D}_{pz} & \mathbf{D}_{wz} \end{pmatrix}^T
\begin{pmatrix} 0 & I & & & & \\ I & 0 & & & & \\ \hline & & Q & S & & \\ & & S^T & R & & \\ \hline & & & & Q_p & S_p \\ & & & & S_p^T & R_p \end{pmatrix}
\begin{pmatrix} I & 0 & 0 \\ \mathbf{A} & \mathbf{B}_p & \mathbf{B}_w \\ 0 & I & 0 \\ \mathbf{C}_q & \mathbf{D}_{pq} & \mathbf{D}_{wq} \\ 0 & 0 & I \\ \mathbf{C}_z & \mathbf{D}_{pz} & \mathbf{D}_{wz} \end{pmatrix} \prec 0
$$

(5.14)

and $\mathbf{X} \succ 0$ hold.

Proofs of both theorems are given in [173] in detail.

Once again, in this step we optimize over P_p while performing a line search over r. Theoretically, since the analysis result is feasible for some r_a, the controller step should at least give a feasible result for $r = r_a$ and possibly larger values should also return feasible results. However, numerically it is not the case. One might step down a little to actually obtain feasible results. In our cases, we allowed the maximum retreat value to be the $0.99r$ of the previous step. We have also observed that this might actually improve the conditioning of the LMI solution though by no means guaranteed.

Remark 5.7. *Note that same theorem can be formulated for all $\Delta \in \mathbf{\Delta}$ and a closed loop plant $(G(r) \star K)(s)$, in other words we can also modify the plant information to scale the uncertainty by subsuming the r parameter suitably into the plant. To demonstrate the numerical problem, we assume that the uncertainties are of unstructured LTI type and for simplicity assume constant multipliers. For parametric uncertainties, it suffices to scale down the respective uncertainty channels for the scaling as shown in Figure 5.2.*

$$
\begin{pmatrix} r\Delta \\ I \end{pmatrix}^T \begin{pmatrix} Q & S \\ S^T & R \end{pmatrix} \begin{pmatrix} r\Delta \\ I \end{pmatrix} = \begin{pmatrix} \Delta \\ I \end{pmatrix}^T \begin{pmatrix} r^2 Q & rS \\ rS^T & R \end{pmatrix} \begin{pmatrix} \Delta \\ I \end{pmatrix} \succeq 0.
$$
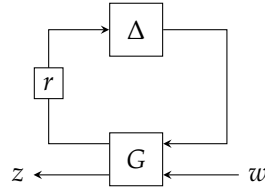
Figure 5.2: Reflecting the uncertainty scaling to the plant

Out of our test experience, we have found out that reflecting the scaling to the plant is better for numerical stability. Seemingly the reason for this is the numerical noise introduced when r is small in the early iteration steps. Notice how the square of r drives the Q block to zero if $0 < r \ll 1$. In case of a feasible multiplier is found, this multiplier should be stripped off from r since it will be again used in the controller step, but due to the numerical inaccuracies wild changes are possible and usually the resulting multiplier information is contaminated. We have found out that we have more freedom in the scaled plant case since one can decrease the bad effect of small numbers via balanced realizations, cleaning up the state-space matrices etc. Moreover, as we show later, in the frequency dependent multiplier case, r variable becomes garbled in the factorizations, minimal realizations etc. Hence, in this work, it is recommended to scale the plant instead of the multipliers.

Hence, we have a theoretically increasing sequence of analysis and synthesis uncertainty sizes

$$r_{si} = 0 < r_{a1} \le r_{s1} \le \ldots \le r_{an} \simeq r_{sn}$$

Similarly, the performance objective gets worse or at least stays constant at after each succesful iteration revealing an increasing sequence of real scalar such as the robust $\mathcal{L}_2$ gain or a similar functional.

The iteration terminates when the last approximate equality is satisfied with desired accuracy or both limits are close enough to 1 together with agreeing performance level P_p. Notice that we don't allow the iteration to terminate even if the r values agree, the performance levels should also agree for numerical consistency. The aforementioned numerical difficulty might exhibit a phenomenon such that both r_a and r_s come very close to 1 but don't quite reach to 1. We have coded an extra condition that if r values come close to 1 within the prescribed accuracy, the code simply assumes $r = 1$, such that the oscillations are removed and the $r = 1$ is tested at each step.

Another numerical difficulty is the factorization of $I - XY = UV^T$. Since the controller construction involves the inverses of U and V, it is imperative that the factorization is well-conditioned with respect to inversion.

5.1.5 *The Multiplier-Controller Iteration with Dynamic Multipliers*

From our analysis results it can be seen that dynamic multipliers provide substantial conservatism reduction. However, the iterative control design procedure given above

can not handle the dynamic multipliers in a straightforward fashion. Although, the mechanism is essentially the same, the only missing step is subsuming the frequency-dependent part of the multipliers into the outer factors. Let us give a conceptual example to demonstrate the obstacle. For notational convenience we partition the closed loop plant into the uncertainty and performance channels

$$H := (G \star K) = \begin{pmatrix} H_q \\ H_z \end{pmatrix}$$

Suppose we are given with a feasible robustness/performance analysis LMI in frequency domain i.e.

$$\begin{pmatrix} I & 0 \\ H_q \\ \hline 0 & I \\ H_z \end{pmatrix}^* \left(\begin{array}{cc|cc} Q(i\omega) & S(i\omega) & & \\ S^*(i\omega) & R(i\omega) & & \\ \hline & & Q_p & S_p \\ & & S_p^T & R_p \end{array} \right) \begin{pmatrix} I & 0 \\ H_q \\ \hline 0 & I \\ H_z \end{pmatrix} \prec 0$$

holds for some $P(i\omega), P_p$ for all $\omega \in \mathbb{R}_e$ and suppose that the frequency-dependent multiplier is parametrized with outer factors, similar to what we have shown in our analysis examples before, as the following;

$$(\star)^* \left(\star \right)^* \left(\begin{array}{cc|cc} M_1 & M_2 & & \\ M_2^T & M_3 & & \\ \hline & & Q_p & S_p \\ & & S_p^T & R_p \end{array} \right) \left(\begin{array}{cc|cc} \Psi_1 & \Psi_2 & & \\ \Psi_3 & \Psi_4 & & \\ \hline & & I & 0 \\ & & 0 & I \end{array} \right) \begin{pmatrix} I & 0 \\ H_q \\ \hline 0 & I \\ H_z \end{pmatrix} \prec 0$$

Now, if we collect the frequency dependent parts together and leave the constant multiplier, we have

$$\left(\star \right)^* \left(\begin{array}{cc|cc} M_1 & M_2 & & \\ M_2^T & M_3 & & \\ \hline & & Q_p & S_p \\ & & S_p^T & R_p \end{array} \right) \left(\begin{array}{c} \Psi_1 + \Psi_2 H_q \\ \Psi_3 + \Psi_4 H_q \\ \hline 0 \quad I \\ H_z \end{array} \right) \prec 0$$

Had it been the case that we have $\begin{pmatrix} I & 0 \end{pmatrix}$ in the top row of the outer factor, we could simply use our previous synthesis technique and we would be done. However, we don't have any solution to cope with such a complication. In other words, the obstacle here is due to how we proceed with the synthesis step. Thus, the problem is exclusive to this synthesis method. We remark this to avoid the confusion that might lead to the conclusion that the robust synthesis problem is difficult because of the complications given above. The difficulty lies with the solution not with the problem. Thus, as it is, we need to find a way to obtain the structure on that block such that we obtain an augmented plant from which we can extract the controller and hence obtain an augmented open loop plant.

Notice that if we had $\Psi_2(i\omega)$ identically zero and Ψ_1 invertable with a stable inverse, we can multiply the inequality with $\begin{pmatrix} \Psi_1^{-1} \\ & I \end{pmatrix}$ and obtain the desired structure

$$\left(\star \right)^* \left(\begin{array}{cc|cc} M_1 & M_2 \\ M_2^T & M_3 \\ \hline & & Q_p & S_p \\ & & S_p^T & R_p \end{array} \right) \left(\begin{array}{cc} I & 0 \\ (\Psi_3 + \Psi_4 H_{q1})\Psi_1^{-1} & \Psi_4 H_{q2} \\ 0 & I \\ H_{z1}\Psi_1^{-1} & H_{z2} \end{array} \right) \prec 0.$$

Then, one can show that the resulting open-loop system becomes

$$G_{aug} = \begin{pmatrix} (\Psi_3 + \Psi_4 G_{pq})\Psi_1^{-1} & \Psi_4 G_{wq} & \Psi_4 G_{uq} \\ G_{pz}\Psi_1^{-1} & G_{wz} & G_{uz} \\ G_{py}\Psi_1^{-1} & G_{wy} & 0 \end{pmatrix} \tag{5.15}$$

thus, the obstacle needs to be avoided via finding a way to obtain an equivalent multiplier of the form

$$P(i\omega) = \begin{pmatrix} \Psi_1(i\omega) & \Psi_2(i\omega) \\ \Psi_3(i\omega) & \Psi_4(i\omega) \end{pmatrix}^* \begin{pmatrix} M_1 & M_2 \\ M_2^T & M_3 \end{pmatrix} \begin{pmatrix} \Psi_1(i\omega) & \Psi_2(i\omega) \\ \Psi_3(i\omega) & \Psi_4(i\omega) \end{pmatrix} \tag{5.16}$$

$$= \begin{pmatrix} \hat{\Psi}_1(i\omega) & 0 \\ \hat{\Psi}_3(i\omega) & \hat{\Psi}_4(i\omega) \end{pmatrix}^* \hat{M} \begin{pmatrix} \hat{\Psi}_1(i\omega) & 0 \\ \hat{\Psi}_3(i\omega) & \hat{\Psi}_4(i\omega) \end{pmatrix} \tag{5.17}$$

$$\tag{5.18}$$

where $\hat{\Psi}_1$ needs to biproper and bistable. This has been proposed in [56, 57] (see also [189] for state-space derivation). Here the essential difficulty is that Ψ_i are often tall basis transfer matrices and are not invertible. Hence we look for square factorizations that are inherently linked to J-spectral factorizations of quadratic forms. We will first take a detour on the structural properties of the multipliers in general before we state the actual multiplier replacement. The style is based on [69].

Definition 5.8 (Inertia)**.** *The triple obtained by the enumeration of the number of the positive, zero and negative eigenvalues is said to be the inertia of a hermitian matrix A and denoted by in $A = \{n_+, n_0, n_-\}$ e.g.*

$$\text{in } I_{2\times 2} = \{2, 0, 0\} \;, \text{in } 0_{n\times n} = \{0, n, 0\} \;, \text{in } \begin{pmatrix} 1 & \\ & -1 & \\ & & -1 \end{pmatrix} = \{1, 0, 2\}$$

Specifically, $\nu(A) = n_-, \pi(A) = n_+, \zeta(A) = n_0$ where we use the abbreviations νegative, πositive, and ζero.

Recall that we have the following two main inequalities that are of interest by the IQC theorem;

$$\int_{-\infty}^{\infty} \begin{pmatrix} \widehat{\Delta(v)}(i\omega) \\ \hat{v}(i\omega) \end{pmatrix}^{*} \Pi(i\omega) \begin{pmatrix} \widehat{\Delta(v)}(i\omega) \\ \hat{v}(i\omega) \end{pmatrix} d\omega \succeq 0 \tag{5.19}$$

$$\begin{pmatrix} I \\ G(i\omega) \end{pmatrix}^{*} \Pi(i\omega) \begin{pmatrix} I \\ G(i\omega) \end{pmatrix} \preceq -\epsilon I \tag{5.20}$$

These inequalities impose constraints on the inertia of the frequency-dependent multiplier. Consider the following simple fact: let a multiplier Π partitioned as

$$\Pi = \begin{pmatrix} \Pi_1 & \Pi_2 \\ \Pi_2^* & \Pi_3 \end{pmatrix} \tag{5.21}$$

Lemma 5.9. *The number of negative eigenvalues of Π is greater than or equal to that of Π_1.*

Proof. Since

$$\begin{pmatrix} I & 0 \\ -\Pi_2^* \Pi_1^{-1} & I \end{pmatrix} \begin{pmatrix} \Pi_1 & \Pi_2 \\ \Pi_2^* & \Pi_3 \end{pmatrix} \begin{pmatrix} I & -\Pi_1^{-1}\Pi_2 \\ 0 & I \end{pmatrix} = \begin{pmatrix} \Pi_1 & 0 \\ 0 & \Pi_3 - \Pi_2^*\Pi_1^{-1}\Pi_2 \end{pmatrix}$$

and since the number can only increase.

Here, we assumed that Π_1^{-1} exists. If not, then, we can make it nonsingular without changing the number of negative eigenvalues by adding a sufficiently small matrix, ϵI. Since we are not interested in the number of zero eigenvalues, this operation causes no problem. □

Next, we show that the inertia is further constrained by the outer factor rank.

Lemma 5.10. *For a hermitian matrix Π, there exists an $X \in \mathbb{R}^{m \times n}$ such that*

$$\begin{pmatrix} I \\ X \end{pmatrix}^{T} \Pi \begin{pmatrix} I \\ X \end{pmatrix} \prec 0 \tag{5.22}$$

if and only if Π has at least n negative eigenvalues.

Proof. ($\Rightarrow$) Complete the outer factors to a square matrix as

$$P = \begin{pmatrix} I & 0 \\ X & I \end{pmatrix}^{T} \Pi \begin{pmatrix} I & 0 \\ X & I \end{pmatrix}$$

and inertia is preserved i.e. in $\Pi = $ in P. Note that $(1,1)$ block of P is (5.22). Hence, from Lemma 5.9, we have, $n = \nu(P_{11}) \leq \nu(P) = \nu(\Pi)$.

($\Leftarrow$) Assume $n + m \geq \nu(\Pi) \geq n$. Let $U = \begin{pmatrix} U_1 \\ U_2 \end{pmatrix} \in \mathbb{R}^{\nu(\Pi) \times n}$ be a matrix spanning the negative eigenspace where U_1 is square. If U_1 is invertible, then, $X = U_2 U_1^{-1}$ is a solution. Or we perturb with ϵI, and use $X = U_2(U_1 + \epsilon I)^{-1}$. □

Thus a quadratic form has to have at least as many negative eigenvalues as the outer factor rank to be negative definite since the quadratic form must be negative definite on the image of outer factor. Using this information makes it easier to state some conclusions about the inertia of a frequency-dependent multiplier. Obviously we need to make sure that the inertia stays the same on the imaginary axis. Hence we can make use of a result regarding the frequency-dependent case by the following (see [126] and references therein):

Theorem 5.11. *Let $\phi(i\omega)$ be a hermitian bounded measurable matrix-valued function. The following statements are equivalent:*

1. *the functional*

$$\sigma(f) = \int_{-\infty}^{\infty} \hat{f}^*(i\omega)\phi(i\omega)\hat{f}(i\omega)d\omega$$

   is nonnegative for all $f \in \mathcal{L}_2^k(0, \infty)$.

2. *$\phi(i\omega) \succeq 0$ almost everywhere for $\omega \in (0, \infty)$.*

Proof.
   $(2) \implies (1)$ is a direct consequence.
   $(1) \implies (2)$ The quadratic form $\sigma(f)$ is time-invariant on $\mathcal{L}_2(-\infty, \infty)$. If $\sigma \geq 0$ on $\mathcal{L}_2(0, \infty)$ then $\sigma \geq 0$ on $\mathcal{L}_2(t_0, \infty)$ for any $t_0 > -\infty$. Moreover,

$$\bigcup_{t > -\infty} \mathcal{L}_2(t, \infty)$$

is dense in $\mathcal{L}_2(-\infty, \infty)$ and σ is continuous on $\mathcal{L}_2(-\infty, \infty)$. Therefore $\sigma \geq 0$ on $\mathcal{L}_2(-\infty, \infty)$ and hence item 2 holds. □

The next result from [57] reveals the IQC multiplier structure for robustness tests.

Theorem 5.12. *If a hermitian, bounded, matrix-valued, and invertible (on $i\mathbb{R}_e$) multiplier H satisfies the IQC and the corresponding FDI (5.19) and (5.20) then there exists a matrix-valued, bounded and invertible (on $i\mathbb{R}_e$) S such that*

$$H(i\omega) = S^*(i\omega) \begin{pmatrix} -I_{n_p} & 0 \\ 0 & I_{m_q} \end{pmatrix} S(i\omega) \quad \forall \omega \in \mathbb{R}_e$$

Proof. From (5.20) and Theorem 5.11 we can conclude that for all $\omega \in \mathbb{R}_e$, $H(i\omega)$ has at least n_p negative eigenvalues. Conversely, from (5.19) and the nominal case we also see that H_{22} is positive semi-definite. Finally, from the invertibility of H on the extended imaginary axis, such a diagonalizing congruence transformation with some S always exists. □

The following is also from [57]:

Theorem 5.13. *Let*

$$H(s) := \begin{pmatrix} H_{11}(s) & H_{12}(s) \\ H_{12}^*(s) & H_{22}(s) \end{pmatrix} \in \mathcal{RL}_\infty$$

be a hermitian, bounded and invertible transfer matrix on the imaginary axis with $H_{22}(s) \succ 0$ on $i\mathbb{R}_e$. Then there exists a factorization of the form

$$H(i\omega) = S^*(i\omega) J_H S(i\omega) \quad \forall \omega \in \mathbb{R}_e$$

where

$$S(s) := \begin{pmatrix} R(s) & 0 \\ Q(s) & P(s) \end{pmatrix}$$

with $P(s), R(s) \in \mathcal{RH}_\infty$ with stable inverses.

Proof. For the sake of brevity, we omit the frequency dependence from the notation of transfer matrices. First, from the assumption $H_{22} \succ 0$ and Lemma 5.9 we have

$$H_{11} - H_{12} H_{22}^{-1} H_{12}^* \prec 0 \tag{5.23}$$

for all $\omega \in \mathbb{R}_e$. We write

$$H = \begin{pmatrix} H_{11} - H_{12} H_{22}^{-1} H_{12}^* & 0 \\ 0 & 0 \end{pmatrix} + \begin{pmatrix} H_{12} \\ I \end{pmatrix} H_{22}^{-1} \begin{pmatrix} H_{12}^* & I \end{pmatrix}$$

Hence both H_{22} and (5.23) can be replaced with biproper, bistable spectral factors which will be defined next. Let $\hat{P}$ denote the spectral factor of $H_{22} = \hat{P}^*\hat{P}$ and R denote similarly that of (5.23). Then we have

$$\begin{aligned} H &= \begin{pmatrix} -R^*R & 0 \\ 0 & 0 \end{pmatrix} + \begin{pmatrix} H_{12}\hat{P}^{-1} \\ \hat{P}^* \end{pmatrix} \begin{pmatrix} \hat{P}^{-*}H_{12} & \hat{P} \end{pmatrix} \\ &=: \begin{pmatrix} -R^*R & 0 \\ 0 & 0 \end{pmatrix} + \begin{pmatrix} Q^* \\ P^* \end{pmatrix} \begin{pmatrix} Q^* \\ P^* \end{pmatrix}^* \\ &= \begin{pmatrix} R(s) & 0 \\ Q(s) & P(s) \end{pmatrix}^* \begin{pmatrix} -I & \\ & I \end{pmatrix} \begin{pmatrix} R(s) & 0 \\ Q(s) & P(s) \end{pmatrix} \end{aligned}$$

$\square$

Notice that the claim is only valid on the imaginary axis. For factorizations with respect to other contours, see [8]. The assumption of $H_{22} \succ 0$ is a mild one since many of the practically relevant multipliers have this property. However, passivity multipliers and some other shifted parameter intervals might have positive semi-definite block. In this case either a different factorization is employed (e.g. [56]) or the uncertainty channel is shifted until the desired property is achieved.

Now we are at a point where we know the inertia properties of the multiplier and also we know that the inertia stays the same on the imaginary axis. Moreover, with

certain inertia of the lower left block, we can turn back to our problem of finding a suitable replacement of the multiplier with a new one involving invertible, biproper, and bistable factors. First let us state a classical and powerful result regarding the transfer matrix factorization (see [203, Thm. 13.19],[47, Thm. 7.3], and [201, Thm. 2]).

Theorem 5.14. *Let A, B, Q, S, R be matrices of compatible dimensions such that $Q = Q^T$ and $R = R^T \succ 0$, with (A, B) stabilizable. Suppose either one of the following assumptions is satisfied*

(A1) A has no eigenvalues on the imaginary axis.

(A2) Q is positive or negative semidefinite and (A, Q) has no unobservable modes on the imaginary axis.

Then,

(I) The following are equivalent;

(a) The hermitian matrix

$$\Phi(s) = \begin{pmatrix} (sI - A)^{-1}B \\ I \end{pmatrix}^* \begin{pmatrix} Q & S \\ S^T & R \end{pmatrix} \begin{pmatrix} (sI - A)^{-1}B \\ I \end{pmatrix}$$

satisfies $\Phi(i\omega) \succ 0$ for all $\omega \in \mathbb{R}_e$.

(b) There exists a unique symmetric X such that the matrix Riccati equation

$$XA + A^T X - (XB + S)R^{-1}(XB + S)^T + Q = 0$$

and $A - BR^{-1}(XB + S)^T$ is Hurwitz.

(c) The Hamiltonian matrix

$$\begin{pmatrix} A - BR^{-1}S^T & -BR^{-1}B^T \\ -(Q - SR^{-1}S^T) & -(A - BR^{-1}S^T)^T \end{pmatrix}$$

has no eigenvalues on the imaginary axis.

(II) The following statements are also equivalent:

(d) $\Phi(i\omega) \succeq 0$ for all $\omega \in \mathbb{R}_e$.

(e) There exists a unique symmetric X such that

$$XA + A^T X - (XB + S)R^{-1}(XB + S)^T + Q = 0$$

and $A - BR^{-1}(XB + S)^T$ has all its eigenvalues in the closed left-half plane.

Every such Φ has a spectral factorization $\Phi = \Phi_s^* \Phi_s$ where $\Phi_s, \Phi_s^{-1} \in \mathcal{RH}_\infty$. A Φ_s is denoted as the spectral factor of Φ.

In particular we are interested in the following corollary;

Corollary 5.15. *Consider a square hermitian transfer matrix $G \in \mathcal{RL}_{\infty}^{\bullet \times \bullet}$ with its inverse $G^{-1} \in \mathcal{RL}_{\infty}^{\bullet \times \bullet}$ and $G(\infty) \succ 0$. Then, G has a spectral factorization G_s such that*

$$G = G_s^* G_s$$

where $G_s, G_s^{-1} \in \mathcal{RH}_{\infty}^{\bullet \times \bullet}$.

Note that the system G need not be obtained from a quadratic form as we will continue considering. However, via separating the stable and the unstable modes with a state transformation and from the hermitian property of G, we can obtain a particular structure without loss of generality. The structure is actually simpler to demonstrate; since the LTI system interconnection $y = G_1 G_2 u$ can be realized as

$$\begin{pmatrix} \dot{x} \\ y \end{pmatrix} = \begin{pmatrix} A_1 & B_1 C_2 & B_1 D_2 \\ 0 & A_2 & B_2 \\ C_1 & D_1 C_2 & D_1 D_2 \end{pmatrix} \begin{pmatrix} \dot{x} \\ u \end{pmatrix}, \tag{5.24}$$

then any factorization $G = G_s^* G_s$ admits a realization of the form

$$G = G_s^* G_s = \left[\begin{array}{cc|c} -A_s^T & 0 & 0 \\ 0 & A_s & B_s \\ \hline -B_s^T & 0 & 0 \end{array} \right] + \left[\begin{array}{c} C_s^T \\ 0 \\ \hline D_s^T \end{array} \right] \left[\begin{array}{cc|c} 0 & C_s & D_s \end{array} \right] \tag{5.25}$$

partitioned accordingly. Also we have $G(\infty) = D_s^T D_s$. For the computation of the spectral factors consider the following multiplier with tall outer factors that satisfies

$$\Phi(i\omega)^* M \Phi(i\omega) \succ 0$$

for all $\omega \in \mathbb{R}_e$ as we had a few examples in Chapter 4. Using the minimal realization for $\Phi(s)$ we also have

$$\begin{pmatrix} B_{\Phi}^T (sI - A_{\Phi})^{-*} & I \end{pmatrix} \begin{pmatrix} C_{\Phi}^T M C_{\Phi} & D_{\Phi}^T M C_{\Phi} \\ C_{\Phi}^T M D_{\Phi} & D_{\Phi}^T M D_{\Phi} \end{pmatrix} \begin{pmatrix} (sI - A_{\Phi})^{-1} B_{\Phi} \\ I \end{pmatrix} \tag{5.26}$$

which is the desired form given in Theorem 5.14. Though we have omitted the proof, the relation with the Riccati equation can be sketched using the LMI version of this constraint. Via KYP Lemma, this is equivalent to the existence of a symmetric matrix X such that

$$\begin{pmatrix} I & 0 \\ A_{\Phi} & B_{\Phi} \\ C_{\Phi} & D_{\Phi} \end{pmatrix}^T \begin{pmatrix} 0 & X & 0 \\ X & 0 & 0 \\ 0 & 0 & M \end{pmatrix} \begin{pmatrix} I & 0 \\ A_{\Phi} & B_{\Phi} \\ C_{\Phi} & D_{\Phi} \end{pmatrix} \succ 0 \tag{5.27}$$

holds. This means the Algebraic Riccati Inequality, which is nothing but straightforward multiplication and a Schur complement thanks to $\Phi(\infty) = D_{\Phi}^T M D_{\Phi} \succ 0$,

also holds:

$$XA_\Phi + A_\Phi^T X - (XB_\Phi + \underbrace{C_\Phi^T M D_\Phi}_{S}) \underbrace{(D_\Phi^T M D_\Phi)^{-1}}_{R^{-1}} (XB_\Phi + C_\Phi^T M D_\Phi)^T + \underbrace{C_\Phi^T M C_\Phi}_{Q} \succ 0$$

(5.28)

Thus the corresponding Riccati Equation

$$XA_\Phi + A_\Phi^T X - (XB_\Phi + C_\Phi^T M D_\Phi)(D_\Phi^T M D_\Phi)^{-1}(XB_\Phi + C_\Phi^T M D_\Phi)^T + C_\Phi^T M C_\Phi = 0$$

(5.29)

has a unique stabilizing solution X and

$$A_\Phi - B_\Phi(D_\Phi^T M D_\Phi)^{-1}(XB_\Phi + C_\Phi^T M D_\Phi)^T$$

is Hurwitz. Since $(D_\Phi^T M D_\Phi) \succ 0$ we can replace this matrix with an arbitrary square factorization (square root, Cholesky etc.) $\hat{D}_\Phi^T \hat{D}_\Phi \succ 0$. Therefore, one possiblity of realization of the spectral factor $\Phi_s(s)$ is given by

$$\Phi_s(s) = \left[\begin{array}{c|c} A_\Phi & B_\Phi \\ \hline \hat{D}_\Phi^{-T}(XB_\Phi + C_\Phi^T M D_\Phi)^T & \hat{D}_\Phi \end{array} \right]$$

such that $\Phi(s), \Phi^{-1}(s) \in \mathcal{RH}_\infty$.

With a slight abuse of the general signature matrix definition, which is a diagonal matrix with all entries on the diagonal are either 1 or -1, we use the following:

Definition 5.16. *Let M be an invertible, hermitian matrix with $\pi(M) = p, \nu(M) = n$. A diagonal matrix of $J = \mathrm{diag}\{-I_n, I_p\}$ is said to be the signature matrix of M.*

When $\nu(M) \neq 0$ the type of factorizations given in Theorem 5.12 is known as "*J-spectral factorization*" and exact solvability conditions are derived which relate the solvability of a certain Riccati equation to the existence of such factorizations (see, e.g.,[159]). However, to the best of our knowledge, there is no simple implementable result that guarantees the solvability of such indefinite Riccati equations. Since we aim for an automated iteration algorithm, we can not utilize these nice algebraic results. Additionally, there are also numerous generalizations, nuances about the assumptions whether (A, B) is just stabilizable or also controllable, whether Q is indefinite in general etc (see [105]) in the previous theorem. However, these are not relevant here as they still do not provide conditions for which the Riccati equation always has a solution. Due to this missing technical step, we make use of particular sign assumptions on the subblocks of the multiplier to perform partial factorizations and then obtain an overall factorization in the suitable form with steps that have solutions guaranteed to exist. For these steps, it suffices to use the standard spectral factorization results well-known from LQ-type problems.

Remark 5.17. *We have to reemphasize that it's the structure that matters and not the method with which we arrive to the desired structure. For a particular custom multiplier,*

one can utilize different properties of the factorization. However, since many multipliers share the property of having $H_{22} \succ 0$ we use it as an assumption. Therefore, there is nothing holistic about the methodolgy. As an example passivity multipliers that we have utilized before can not be factorized using this argument. Hence, one can use the the results of [56].

Now that we have given the basic idea behind the dynamic multiplier factorization, we have enough material to describe the steps of the controller-multiplier iteration.

The Pseudo-Code for Controller-Multiplier Iteration

The actual technical problems are all addressed above and can be found in the literature also cited above. However, for the practitioners who are not interested in the proofs and other derivation related issues we provide a standalone rundown of the controller-iteration steps.

PRELIMINARY STEP.   Before starting the controller design, it is important to check a few often overlooked issues before starting the design iteration.

- The plant G is a generalized plant and, if any, the D_{uy} block of the state-space representation is zeroed. After the control design, the original controller can be recovered under the assumption that $(I - D_K D_{uy})^{-1}$ is nonsingular.

- The performance weights are not too demanding i.e. high-performance nominal control design might have very little robustness properties hence it's better to redesign the performance weights after looking at the robust controller obtained later. By doing so one can see the effect of the weights by plotting the performance channel entries.

- The control channels are weighted, even slightly, to avoid the controller gains blowing up when unconstrained by the LMI solvers. This might not be relevant for the synthesis case however due to the non-convex nature of the iteration it's more likely to get a infeasible analysis certificate even though the synthesis step returns a feasible controller.

- After the interconnection of the weights it is crucial that the state-space data is minimal and balanced. It also helps to cleanup the numerical noise from the state-space matrices i.e. zeroing out the entries that are less than, say, 10^{-6}.

Then we are ready to obtain the first nominal controller that will allow us to start the iteration.

INITIAL STEP.   The initial step is designing *any* controller that stabilizes the system and satisfies some performance specifications that can be described as a quadratic form. For the common transparency case, we can use the $\mathcal{H}_\infty$ norm of the force

error and position error for the remote and local site. Then required conditions to be checked while minimizing γ is given by Theorem 5.3 for

$$P_p = \begin{pmatrix} -\gamma^2 I & \\ & I \end{pmatrix}$$

where γ^2 is inserted into another variable to make the condition affine. Then, using the factorization $I - XY = UV^T$ we obtain U and V. Then using these matrices we backsubstitute the X, Y, K, L, M, N varibles to obtain the controller matrices. Alternatively one can also utilize the results of [52] with a two step approach to solve the LMIs, first eliminating the controller matrices from the LMI and obtain valid Lyapunov matrices then using these, solving the original LMI for the controller matrices. We reemphasize that the method from which we obtain the controller is irrelevant. One can also use the reduced order controller construction algorithm of [68]. It has been demonstrated that the resulting controller is numerically more well-conditioned. Moreover, it has been shown that the unconstrained parts of the problem can be identified which is a major issue in a MIMO setting.

ANALYSIS STEP.   Once we have obtained a nominally stabilizing controller, the nominal part of the uncertain closed loop plant, $(G \star K)$, is obtained. Since this interconnection is for the full uncertainty size, we then parametrize the uncertainty size and reflect it to the system as depicted in Figure 5.3. This allows us to use the same multipliers without scaling with r, hence avoiding multipliying the decision variables with small numbers. Therefore, with the initial balanced and minimal realization of the plant such parameterization is relatively healthier than scaling the unknowns a priori. Another problem is to strip down the r value after a feasible multiplier is found (with spectral factorization in mind). Factorizing a small scalar from a matrix should be avoided.

In summary, we use the parametrization of the dynamic multipliers

$$\Pi(i\omega) = \Psi^*(iw) M \Psi(i\omega)$$

Then, either in frequency domain or via minimal state-space representations, we form the system

$$H_{aug} := \begin{pmatrix} \Psi(i\omega) & \\ & I \end{pmatrix} \begin{pmatrix} I & 0 \\ H_q \\ \hline 0 & I \\ H_z \end{pmatrix}.$$

Hence, we have the familiar FDI

$$H_{aug}^* \begin{pmatrix} M & \\ & P_p \end{pmatrix} H_{aug} \prec 0$$

together with individual multiplier class inequalities e.g. positivity of D-scalings etc. Hence, along the lines of the examples in Chapter 4 and the conditions given above, the FDIs are converted to LMIs and solved for the performance optimization.
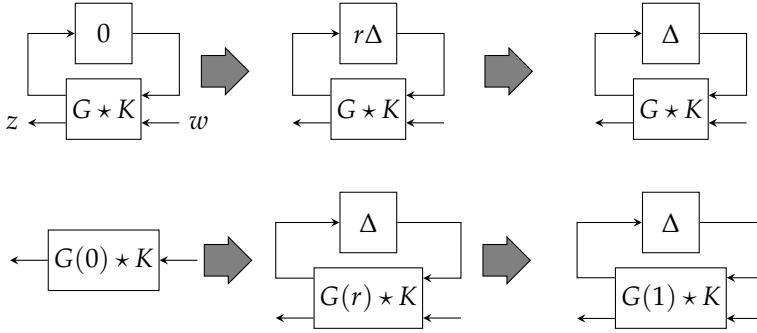
Figure 5.3: Parametrization of the plant with uncertainty size

Remark 5.18. *Once again, it's important to remind that the positivity of the involved Lyapunov certificates in the LMI set are not required in the analysis, since all the systems are stable i.e. the closed loop is stabilized by $K(s)$ and the outer basis matrices live in $\mathcal{RH}_\infty$, there is no need to enforce positivity constraints. Doing so would constrain the set of valid symmetric matrices significantly.*

After the squaring the multipliers, we obtain the new augmented open loop plant by reshaping the augmented closed loop equations given by (5.15). Starting from an arbitrary $r \in [0, 1]$ depending on the success/failure of the feasibility result, r is increased/decreased, say via a bisection algorithm, until a particular r_a^* is achieved.

Synthesis Step.   The multiplier-augmented new plant is subjected to the variable transformation "controller $\to v$". Then via Theorem 5.6 the LMIs are solved. The initial r can be taken as r_a^* and the bisection is reduced to the interval $r \in [0.99r_a^*, 1]$ such that if for some numerical reason r_a^* is not feasible, a little play is introduced to relax the numerical conditioning. 0.99 is based on our numerical experience. However, we have also seen improvement if this play value is a function of the iteration number. In other words, in the early iterations the play value can be relaxed down to 0.95 and then getting stricter as the iteration progresses.

Another important issue after the synthesis is that we have to treat carefully the innocent looking $I - XY = UV^T$. The numerical noise contaminating U, V entries plays a big role in obtaining healthy controller matrix data due to the inverses of U and V. The essential difficulty is the eigenvalues of XY approaching to unity hence rendering the matrix $I - XY$ badly conditioned with respect to inversion. Some optimization-based remedies regarding the LMI problem setup are given in [173] such that the resulting matrix eigenvalues are forced away from unity. However, even when this is established, it's not guaranteed that the resulting matrices U, V would be free of problems. There are many possibilities and in our opinion, a comprehensive code should check as many possibilities as possible. Although, this should be left to numerical analysts, seemingly the easiest method is basing the

matrices on $(I - XY)^{-1} = V^{-T}U^{-1}$ instead of factorization and then inversion. We have implemented a simple two-stage validation scheme. First, we try the regular factorize-invert method and clean up the matrices free from dangling tiny entries. Then closed loop is formed and stability is checked. If the closed loop eigenvalues are sufficiently away from zero and the controller matrix entries are less than some large number then the result is marked as a valid one. Otherwise, the inverse is factorized and same process is repeated with condition number checks etc. After this step the last known previous attempt is also recorded and if the next analysis step can not improve the current controller is discarded and the last known attempt is utilized. Obviously, many other checks should be implemented however it goes beyond the scope of this manuscript.

Remark 5.19. *It should be noted that balancing the plant data between the analysis and the synthesis steps leads to worse numerical margins as one particular feasible result in one step tends to be infeasible in another step. We can speculate that this type of modifications don't work (though theoretically should help) since the LMI solvers indeed push the decision variables to such an extreme that slight changes in the constant part of the LMIs render the solutions infeasible. Combined with the various factorizations, we have decided to not to modify the plant among the iteration steps. However the remark for the initial balancing step is not affected and should be performed regardless of this. It's unfortunately up to the designer to watch for very high-frequency behavior of the plant-controller interaction as this can affect the feasibility of the iteration.*

Remark 5.20. *In the norm minimization cases for performance specification, e.g., $\mathcal{H}_\infty$ norm γ, it's very important to keep the norm constrained from above in a rather stringent fashion. One can see that a single number to drive the whole optimization procedure, often involving hundreds of decision variables, is simply asking for trouble. In practice, it's a good rule of thumb to set the upper bound norm for performance 5-10 times the nominal case performance. Otherwise, unrealistic, nonsensical γ values in the order of $[10^3, 10^4]$ or higher can be obtained resulting with seemingly valid controller matrices. Even if the result is numerically correct, those iterations should be discarded and a smaller γ and/or smaller r values should be sought. Otherwise, either the next iteration or the discretized implementation are likely to suffer from unpredictable side-effects. If the robust performance γ is much larger than the nominal case then it might be a sign of a drastic qualitative change in the system properties and thus it might help to shift the nominal case such that $\tilde{\Delta} = 0$ corresponds to an uncertain plant already closer to the problematic region in order to start with better robustness properties.*

TERMINATION STEP.   After the synthesis and analysis steps, the r value typically gets saturated at some particular r^* or it starts to fluctuate around it. In case of such fluctuations, the algorithm should see whether the performance objective obtained at each step is close to each other. Otherwise it's a sign of a numerically invalid solution. One can either decrease the uncertainty size r or constraint the performance

objective further to force each solution come closer. We have chosen another simple rule for the implementation:

- After the synthesis step, check whether it's the first run of the iteration. If so, no convergence check is necessary.

- Collect r and γ (both of analysis and synthesis steps) of the current iteration and compare it with the previous iteration. (Check if $r \approx 1$. If true, then compare only the performance.) Check if there is any significant progress has been recorded (larger than some predefined value).

- Check also whether analysis and synthesis r and γ values are close to each other.

- If all true terminate, otherwise continue.

Controller Design for the TU/e 1-DoF System

In this chapter, the synthesis conditions of the previous chapter is applied to a control design problem for a rotational 1-DoF experimental setup. Different uncertainty structures are considered and compared.

6.1 THE EXPERIMENTAL SETUP

At the Control Systems Technology department of Eindhoven University of Technology, a 1-Degree-of-Freedom prototype has been realized within the project of constructing a 5-DoF haptics local device for robotically assisted eye surgery([70]). The setup is shown in Figure 6.1. The actuation is provided to a capstan drive via a DC servo motor Maxon RE 35 which is connected to a statically balanced circular strip plate. This piece is also connected to an inner segment via elastic elements and the relative motion of these pieces make it possible to obtain a force measurement. An additional linear piece attached to the inner segment for handling the device. Due to the capstan mechanism, there is a nominal rotational reduction of $i = \frac{1}{10}$. The system consists of four major inertial components; the motor and the encoder, outer strip segment, inner segment and the linear end-effector. The physical values are given in Table 6.1. The system can be approximated by the block diagram depicted
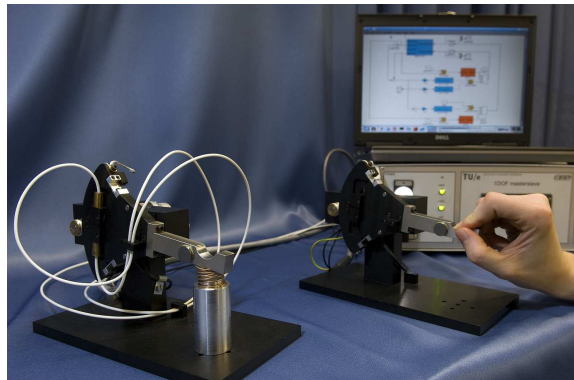
Figure 6.1: TU/e 1-DoF Experimental Setup (Image is taken from [70])

Table 6.1: Physical Values of the Experimental Setup

Inertia kg m^2		Stiffness N m/rad	
$J_{mot+enc}$	7.0×10^{-6}	k_{mot}	1.5×10^2
J_{pulley}	4.6×10^{-7}	k_{wire}	2.9×10^3
J_{outer}	2.7×10^{-4}	k_{ts}	3.5×10^3
$J_{inner+end}$	4.4×10^{-4}	$k_{mot,b}$	7.9×10^3

in Figure 6.2.

If we enumerate all the blocks from left to right, starting from one to four, then the mathematical model of each device is given by:

$$\frac{J_1}{i}\ddot{x}_1 = \frac{u}{i} - \frac{k_1}{i}(x_1 - x_2) \tag{6.1}$$

$$\frac{J_2}{i}\ddot{x}_2 = \frac{k_1}{i}(x_1 - x_2) - k_c(ix_2 - x_3) \tag{6.2}$$

$$J_3\ddot{x}_3 = k_c(ix_2 - x_3) - k_4(x_3 - x_4) \tag{6.3}$$

$$J_4\ddot{x}_4 = k_4(x_3 - x_4) \tag{6.4}$$

where $k_c = (\frac{1}{k_{wire}} + \frac{1}{k_{mot,b}})^{-1}$ and u is the motor input. The theoretical model response is shown in Figure 6.3. The identification and the model verification is also provided in [70]. Based on the frequency response data, we have also added damping to the model artificially both to improve the numerical properties of the model and also match the physical setup. The damping coefficients to each spring element/group is given in Table 6.2. We will use the same model for the remote device in what follows below.

Note that up to the first zero of the system, same behavior can be represented with a second order transfer function

$$\tilde{G}(s) = \frac{1}{0.0015s^2 + 0.00287s + 0.25}.$$

Figure 6.2: Simplified block diagram of the experimental setup (Adapted from [70])

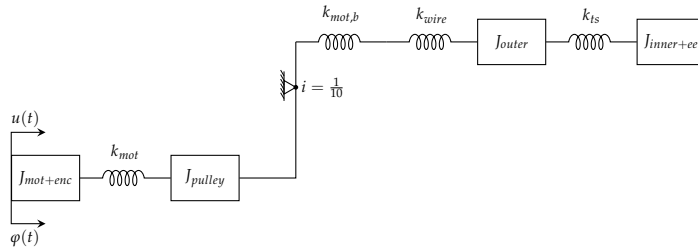| Damping $\frac{\mathrm{N\,m\,s}}{\mathrm{rad}}$	
b_{mot}	1.8×10^{-3}
$b_{wire+mot,b}$	1.0×10^{-5}
b_{ts}	1.0×10^{-3}

Table 6.2: The additional damping coefficients that are included in the model.

A similar simplification is used in [120, 121] and the resulting controllers which are based on this model have been experimentally implemented. Due to the low-frequency nature of the task, this simplification did not cause any problems during the experiments.

We nevertheless present the full model LFT interconnection structure but in the controller design cases only the simplified model is used. This is due to the fact that the system is altered significantly (e.g., the steel cables are replaced by plastic cables and the housing of the shafts are subjected to wear etc.) from its original construction. Hence, we have used a simple model obtained from identification experiments. This also serves as a perfect case where unmodeled dynamics deviates from the theretical model and we have to rely on the approxiamte FRF measurements. Thus, we include the full LFT model to demonstrate that the complexity of the model is not an essential obstacle and still can be used conveniently.

6.1.1 *Incorporating the human dynamics*

To be able to model both cases of "user holding/released the device" and "remote device is in free-air/contact" cases we need to introduce a set of models of the possible human users and environment dynamics. However, those models depend on grasp configuration, task-environment and other parameters. One can start with
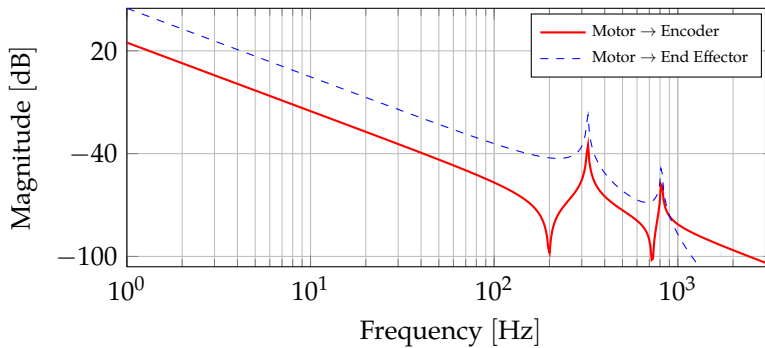

Figure 6.3: The frequency response of the hypothetical models from the motor actuation to the position measurements.
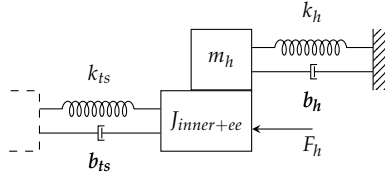
Figure 6.4: Including the uncertain human model in the system shown in Figure 6.2.

Parameter Variation Intervals		
m_h	$[0, 0.53]$	$\mathrm{kg\,m^2/rad}$
b_h	$[0, 8.58]$	$\mathrm{N\,m\,s/rad}$
k_h	$[0, 994.2]$	$\mathrm{N\,m/rad}$
k_e	$[0, 3000]$	$\mathrm{N\,m/rad}$

Table 6.3: Identified Uncertain Human Parameters as Rotational Mechanical Components

a predefined task case, say a MIS or a peg-in-hole assembly and limit the relevant cases that can occur together with some engineering safety tolerance. That would reduce the set of possible physically relevant operators significantly. In the absence of refined human and environment models, we would simply follow the ubiquitous mass-spring-damper modeling paradigm as shown in Figure 6.4. Here, we adopt the usage of an external force model but this does not bring in any complications since we do not invoke any passivity assumptions. Moreover we will assume that the parameters of the human dynamics vary in time. Additionally the human force f_h is low-pass filtered to emphasize the $\approx 10\,\mathrm{Hz}$ bandwidth. Note that by adding another under-damped mass-spring-damper component to the human dynamics one can also model the hand tremor and motor noise if needed with the possibility of selecting the frequency band where these effects become dominant.

The human arm model is identified experimentally by fitting a second order mass-spring-damper model for different grasp configurations (see, e.g., [120]). Then, using these frequency response data, uncertainty intervals in which the parameters of the human arm varies through time are selected. Similarly the environment is assumed to be a pure stiff spring with time-varying stiffness coefficient. The parameter intervals are given in Table 6.3[1].

Next, we obtain the LFT interconnection of the uncertain model. We first write down the equations of motion of the combined inertial element $J_{inner+ee}/m_h$

$$(J_4 + m_h)\ddot{x}_4 = k_3(x_3 - x_4) + b_3(\dot{x}_3 - \dot{x}_4) - k_h x_4 - b_h \dot{x}_4 - f_h$$

---

[1]We keep using m_h notation for convenience however it should be understood as J_h due to the rotational nature of motion.

and hence

$$\ddot{x}_4 = (J_4 + m_h)^{-1} \left(k_3(x_3 - x_4) + b_3(\dot{x}_3 - \dot{x}_4) - k_h x_4 - b_h \dot{x}_4 - f_h \right)$$

$$= \left(\frac{1}{J_4} - \frac{1}{J_4} \frac{m_h}{J_4} \left(1 + \frac{m_h}{J_4} \right)^{-1} \right) \left(k_3(x_3 - x_4) + b_3(\dot{x}_3 - \dot{x}_4) - k_h x_4 - b_h \dot{x}_4 - f_h \right).$$

The first term in the second equality can be shown to be

$$\delta_{m_h} \star \begin{pmatrix} -\frac{m_h}{2J_4} & \frac{m_h}{2J_4} \\ -\frac{1}{J_4} & \frac{1}{J_4} \end{pmatrix}$$

with $\delta_{m_h}(t) \in [0,2]$ for all $t > 0$. Then, labeling the remaining uncertain terms with uncertainty outputs we have

$$\ddot{x}_4 = \frac{1}{J_4} \left(k_3(x_3 - x_4) + b_3(\dot{x}_3 - \dot{x}_4) - \frac{m_h}{2J_4} p_1 - p_2 - p_3 - f_h \right) \tag{6.5}$$

$$p_1 = \delta_{m_h} q_1 \tag{6.6}$$

$$p_2 = \delta_{b_h} q_2 \tag{6.7}$$

$$p_3 = \delta_{k_h} q_3 \tag{6.8}$$

$$q_1 = \left(k_3(x_3 - x_4) + b_3(\dot{x}_3 - \dot{x}_4) - \frac{m_h}{2J_4} p_1 - p_2 - p_3 - f_h \right) \tag{6.9}$$

$$q_2 = \frac{b_h}{2} \dot{x}_4 \tag{6.10}$$

$$q_3 = \frac{k_h}{2} x_4 \tag{6.11}$$

where $\delta_{m_h}, \delta_{b_h}, \delta_{k_h} \in [0,2]$ for all $t > 0$. The resulting state equations are obtained as

$$\hat{E}\dot{x} = \hat{A}x + \hat{B}_p p + \hat{B}_w w + \hat{B}_u u \tag{6.12}$$

$$q = \hat{C}_q x + \hat{D}_{pq} p + \hat{D}_{wq} w + \hat{D}_{uq} u \tag{6.13}$$

where

$$\hat{E} = \begin{pmatrix} I_4 & & & & \\ & J_1 & & & \\ & & \frac{J_2}{i} & & \\ & & & J_3 & \\ & & & & J_4 \end{pmatrix}, \hat{B}_p = \begin{pmatrix} 0 & 0 & 0 \\ 0 & 0 & 0 \\ 0 & 0 & 0 \\ 0 & 0 & 0 \\ 0 & 0 & 0 \\ 0 & 0 & 0 \\ 0 & 0 & 0 \\ -\frac{m_h}{2J_4} & -1 & -1 \end{pmatrix}, \hat{B}_w = \begin{pmatrix} 0 \\ 0 \\ 0 \\ 0 \\ 0 \\ 0 \\ 0 \\ -1 \end{pmatrix}, \hat{B}_u = \begin{pmatrix} 0 \\ 0 \\ 0 \\ 0 \\ 1 \\ 0 \\ 0 \\ 0 \end{pmatrix}$$

$$\tag{6.14}$$

$$\hat{A} = \begin{pmatrix} & & 0_4 & & & & I_4 & \\ -k_1 & k_1 & 0 & 0 & -b_1 & b_1 & 0 & 0 \\ \frac{k_1}{i} & \frac{-k_1}{i} - ik_2 & k_2 & 0 & \frac{b_2}{i} & \frac{-b_2}{i} - ib_2 & b_2 & 0 \\ 0 & ik_2 & -k_2 - k_3 & k_3 & 0 & ib_2 & -b_2 - b_3 & b_3 \\ 0 & 0 & k_3 & -k_3 & 0 & 0 & b_3 & -b_3 \end{pmatrix}$$

(6.15)

$$\hat{C}q = \begin{pmatrix} 0 & 0 & k_3 & -k_3 & 0 & 0 & b_3 & -b_3 \\ 0 & 0 & 0 & 0 & 0 & 0 & 0 & \frac{b_h}{2} \\ 0 & 0 & 0 & \frac{k_h}{2} & 0 & 0 & 0 & 0 \end{pmatrix},$$

$$\hat{D}_{pq} = \begin{pmatrix} \frac{m_h}{2J_4} & -1 & -1 \\ 0 & 0 & 0 \\ 0 & 0 & 0 \end{pmatrix}, \hat{D}_{wq} = \begin{pmatrix} -1 \\ 0 \\ 0 \end{pmatrix}, \hat{D}_{uq} = \begin{pmatrix} 0 \\ 0 \\ 0 \end{pmatrix}, \quad (6.16)$$

The position measurements are done at the motor location with an encoder and the force measurements are based on the relative motion of the $J_{inner+ee}$ and J_{outer} since the elasticity of the coupling is known. This leads to the following measurement channel structure:

$$\hat{C}y = \begin{pmatrix} 1 & 0 & 0 & 0 & 0 & 0 & 0 & 0 \\ 0 & 0 & k_3 & -k_3 & 0 & 0 & 0 & 0 \end{pmatrix},$$

$$\hat{D}_{py} = \begin{pmatrix} 0 & 0 & 0 \\ 0 & 0 & 0 \end{pmatrix}, \hat{D}_{wy} = \begin{pmatrix} 0 \\ 0 \\ 0 \end{pmatrix}, \hat{D}_{uy} = \begin{pmatrix} 0 \\ 0 \\ 0 \end{pmatrix}, \quad (6.17)$$

6.1.2 *Incorporating the environment dynamics*

The remote device is simply another copy of the local device, hence shares the same structure given by (6.12),(6.13). For the remote device, we only consider a spring with time-varying characteristics however it can also be assumed to admit a more detailed structure similar to the human dynamics. It's relatively simpler to obtain the LFT interconnection since we can simply remove the $\delta_{m_e}, \delta_{b_e}$ uncertainty channels such that only the environment stiffness coefficient remains uncertain. We will assume that the environment stiffness can change arbitrarily fast in order to model hard contacts or sudden release from a constraint, say, sliding over an edge. The uncertainty matrices are modified such that

$$q = k_e x_4, p = \delta_{k_e} q.$$

The environment uncertainty is selected as a time-varying parameter $k_e \in [0, 3000]$ N m/rad to model the relatively high stiff contacts.

6.1.3 *The Generalized Plant Model*

Combining the both device models, we can then define the performance channels. For the force tracking we select the error of the force measurements to be minimized. For the position tracking we select the devices' encoder reading difference to be minimized. We also penalize the actuator outouts to make the numerical optimization problem healthier. We will further emphasize the frequency bands of interest with frequency dependent weights defined below. Translating these into the matrix form, we obtain the following plant $G \in \mathcal{RH}_\infty^{(n_q+n_z+n_y)\times(m_p+m_w+m_u)}$

$$G := \left[\begin{array}{c|ccc} A & B_p & B_w & B_u \\ \hline C_q & D_{pq} & D_{wq} & D_{uq} \\ C_z & D_{pz} & D_{wz} & D_{uz} \\ C_y & D_{py} & D_{wy} & 0 \end{array} \right] \tag{6.18}$$

with particular entries are defined as the following; let $e_{\frac{i}{8}}$ denote the ith column of the 8×8 identity matrix,

$$A = I_2 \otimes \hat{A}$$

$$B_p = \begin{pmatrix} \hat{B}_p & 0 \\ 0 & -e_{\frac{8}{8}} \end{pmatrix}, B_w = I_2 \otimes \hat{B}_w, B_u = I_2 \otimes \hat{B}_u$$

$$C_y = I_2 \otimes \hat{C}_y, D_{py} = 0$$

$$D_{wy} = 0$$

$$C_q = \begin{pmatrix} \hat{C}_q & 0 \\ 0 & \frac{k_e}{2}e_{\frac{4}{8}}^T \end{pmatrix}, D_{pq} = \begin{pmatrix} \hat{D}_{pq} & 0 \\ 0 & 0 \end{pmatrix}, D_{wq} = \begin{pmatrix} \hat{D}_{wq} & 0 \\ 0 & 0 \end{pmatrix}, D_{uq} = 0$$

Then, the performance channels are given by

$$z = \begin{pmatrix} x_l - x_r \\ f_l - f_r \\ u_l \\ u_r \end{pmatrix}$$

which can be expressed as

$$C_z = \begin{pmatrix} e_{\frac{1}{8}}^T & -e_{\frac{1}{8}}^T \\ k_3(e_{\frac{3}{8}} - e_{\frac{4}{8}})^T & -k_3(e_{\frac{3}{8}} - e_{\frac{4}{8}})^T \\ 0 & \\ 0 & \end{pmatrix}, D_{pz} = D_{wz} = 0, D_{uz} = \begin{pmatrix} 0_2 \\ I_2 \end{pmatrix}.$$

Figure 6.5: Diagram of (a) operator/master device and (b) environment/slave device.

Thus, we have obtained a plant-uncertainty interconnection $\Delta - G$ where

$$\Delta := \begin{pmatrix} \delta_{m_h} & & & \\ & \delta_{b_h} & & \\ & & \delta_{k_h} & \\ & & & \delta_{k_e} \end{pmatrix} \tag{6.19}$$

6.1.4 *Simplified System Model*

In the previous publications, [120, 121] the simplified model is utilized while capturing the essential complications making the problem substantially simpler. We have followed the same idea by adopting the scheme depicted in Figure 6.5. In this simplified model, the dynamics of the devices are lumped into second-order mass-spring-damper models and the human/environment dynamics are interconnected directly to the corresponding device models.

For the performance objectives, it has been selected to minimize the position error $x_m - x_s$ and the force error $f_h - f_e$, as opposed to minimizing $f_h - f_s$ and $f_e - f_m$ independently. In other words it is the interaction forces we desire to match but not the individual force reference signals at each side. However, this has an inherent well-posedness problem when the user releases the device. As can be seen in Figure 6.5, when the user dynamics are absent there is no control authority left to influence f_h (and f_e too due to the same reasoning). Therefore, the system (control design problem) is analytically uncontrollable (infeasible) for the full uncertainty region. However this can be avoided by allowing for slight tolerances to account for the modeling imperfections and to avoid this analytical pathology.

The reason for this artificial problem is the over-simplification of the model since in the original model the force sensor is not collocated with the human input. The force measurements are in fact obtained via the relative motion of the outer and inner segments as we have modeled above. However, before we discard this modeling approach, we would like to emphasize that the device is not ideally free from any friction and measurement uncertainties. Thus even untouched the model still involves joint and cable frictions and unmodeled inertial asymmetries which
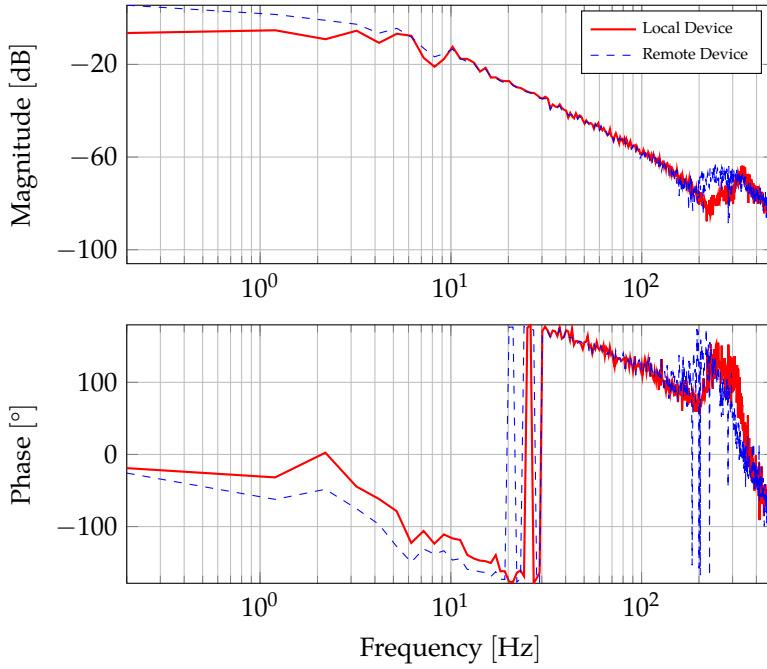
Figure 6.6: The frequency response data from the identification experiments.

can be lumped into the human dynamics. Therefore, all these hard-to-model effects can be reflected to the already uncertain human model. As a practical example, the friction of the device can be attributed to the damping uncertainty of the human model. Hence, one can always assume that a minimal interaction with the human is always present even though this minimal interaction might be due to the angular inertia, friction etc.

6.2   Three Controller Design Cases

6.2.1   *Uncertain Plant with Arbitrarily Fast Time-Varying Stiffness Coefficients*

We start with designing a robust controller for an uncertain plant in which only the stiffness elements of the human and the environment models are taken as arbitrarily fast varying real parametric uncertainties. Hence, the environment is assumed to be a single spring and the human damping and the mass values are assumed to be the halves of the maximum values identified by the experiments while leaving the stiffness coefficient as uncertain. Thus, the involved multipliers with respect to

Analysis		Synthesis	
r_a	γ_a	r_s	γ_s
0.00	0	0.50	1.33
0.52	9.56	0.52	2.42
0.83	10	0.83	4.34
1.00	7.09	0.99	5.33
1.00	5.28	1.00	4.83
1.00	4.82	1.00	4.75
1.00	4.75	1.00	4.72
1.00	4.72	1.00	4.7
1.00	4.7	1.00	4.68
1.00	4.68	1.00	4.68

Figure 6.7 & Table 6.4: The progress report of the *D-K* iteration of the with increasing uncertainty set size and resulting worst case-$\mathcal{L}_2$ gain.

these uncertainties are taken as full block multipliers i.e.

$$
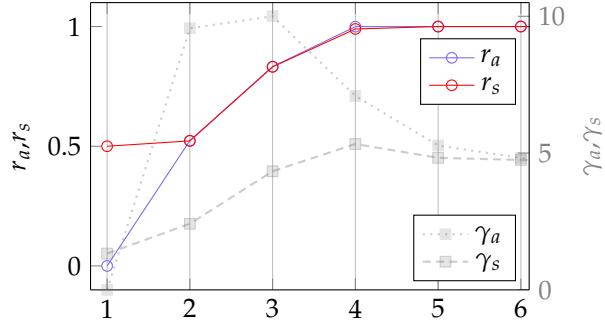\begin{pmatrix} \delta_h & & \\ & \delta_e & \\ 1 & 0 \\ 0 & 1 \end{pmatrix}^T \left(\begin{array}{c|c} Q & S \\ \hline S^T & R \end{array} \right) \begin{pmatrix} \delta_h & & \\ & \delta_e & \\ 1 & 0 \\ 0 & 1 \end{pmatrix} \succeq 0
$$

for all $\delta_h \in [0, \bar{\delta}_h]$N/m and $\delta_e \in [0, \bar{\delta}_e]$N/m. By enforcing the constraint $Q \prec 0$ (and since zero uncertainty enforces $R \succeq 0$) it is sufficient to guarantee the constraint over the whole parameter box by just checking at the corners of the hyperrectangle set $[0, \bar{\delta}_h] \times [0, \bar{\delta}_e]$.

Then using the synthesis results from the previous chapter, we design a controller with the iteration steps given in Figure 6.7. Notice that, even though the iterations lead to full uncertainty case $r = 1$, due to the performance mismatch the iteration is continued until an agreement up to some precision is achieved.

6.2.2   *Uncertain Plant with Time-Varying Stiffness Coefficients with Bounded Rate of Variation*

After achieving robust stability with the first design, we then consider the fact that we are aware of additional bounds on the rate of variations of the model parameters for the human hand. First of all we can safely assume that the human can not exert full grasp force instantaneously though it can happen pretty fast. We have assumed that the human can grasp the handle and fully squeeze in about half a second. Therefore, assuming that the human stiffness coefficient is differentiable, the maximum values for the stiffness coefficient can be achieved in half a second and hence $\max_{t>0} \left| \dot{k}_h(t) \right| \leq 2\bar{k}_h$.

Using the multiplier structure given in Section 4.2.3 for the slowly varying parameter, with basis function

$$\Phi(s) = \begin{pmatrix} 1 \\ \frac{1}{s+1} \end{pmatrix}$$

we have the following multiplier for the control design;

$$\Pi(i\omega) = (\star)^* \left(\begin{array}{cc|cc} -D_1 & & & \\ & -D_2 & & \\ \hline & & Q & S \\ & & D_1 & \\ & & & D_2 \\ \hline & & S & R \end{array} \right) \left(\begin{array}{cc|c|cc} \Phi(i\omega) & \Phi_c(i\omega) & & & \\ 0 & I & & & \\ \hline & & 1 & & \\ \hline & & & \Phi(i\omega) & \\ & & & \Phi_b(i\omega) & \\ \hline & & & & 1 \end{array} \right)$$

where $\Phi^*(i\omega)D_1\Phi(i\omega) > 0$ for all $\omega \in \mathbb{R}_e$, $D_2 \succ 0$, $Q < 0$ and

$$\begin{pmatrix} k_e \\ 1 \end{pmatrix}^T \begin{pmatrix} Q & S \\ S & R \end{pmatrix} \begin{pmatrix} k_e \\ 1 \end{pmatrix} > 0.$$

for all $k_e(t) \in [0, 3000], t \geq 0$.

We have obtained the lower worst-case $\mathcal{L}_2$ gains as shown in the Figure 6.8 with the simplest basis functions of order one. Further, to demonstrate the conservatism reduction via increasing the basis length in the IQC multiplier parametrization, we use the basis length $d = 2$, i.e.,

$$\Phi(s) = \begin{pmatrix} 1 \\ \frac{1}{s+1} \\ \frac{1}{(s+1)^2} \end{pmatrix}$$

and we obtain better results which are given in Figure 6.9. Increasing the length further does not contribute to significant changes hence even with the shortest basis lengths we arrive at significantly improved results.

We validate the improvement through experiments given in the next section since the resulting worst-case $\mathcal{L}_2$ gains tell very little, if any, about the real-time implementation performance[2]. In what follows, the controller denoted by C_2 refers to the design with $d = 2$.

6.2.3 *Uncertain Plant with a More Complicated Human Model*

In this test case, we treat the mass-spring-damper parameters of the human model as slowly varying uncertainties together with arbitrarily fast varying environment

---

[2]In fact, contemporary control literature is obsessed with $\mathcal{L}_2$ gain. We emphasize that even the DC gain of a performance weight affects the feasible γ level and moreover if one has three different designs with $\gamma = 8, 4, 2$ respectively, it doesn't mean that each design is twice as better. Practically, it's a boolean indicator that something has been improved (whether relevant or not).

Analysis		Synthesis	
r_a	γ_a	r_s	γ_s
0.00	0	0.20	1.33
0.20	1.83	0.20	1.56
0.32	1.86	0.31	1.7
0.83	4.24	0.82	2.54
0.98	3.08	0.97	2.71
1.00	2.8	1.00	2.73
1.00	2.74	1.00	2.73
0.99	2.71	0.98	2.69
1.00	2.73	1.00	2.72
1.00	2.72	1.00	2.72

Figure 6.8 & Table 6.5: The progress report of the *D-K* iteration of the with increasing uncertainty set size and resulting worst case-$\mathcal{L}_2$ gain.

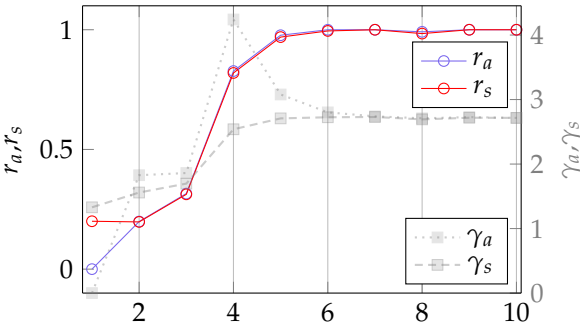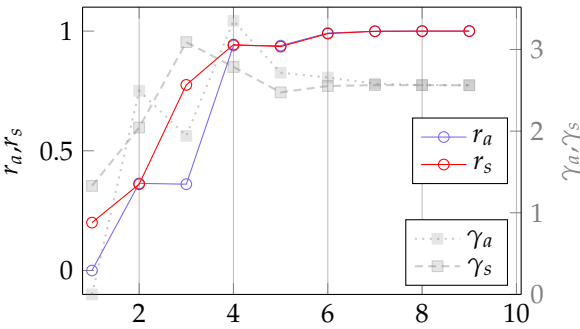| Analysis		Synthesis	
r_a	γ_a	r_s	γ_s
0.00	0	0.20	1.33
0.36	2.5	0.36	2.04
0.36	1.94	0.78	3.09
0.94	3.35	0.94	2.79
0.94	2.72	0.94	2.47
0.99	2.66	0.99	2.55
1.00	2.58	1.00	2.56
1.00	2.56	1.00	2.56
1.00	2.56	1.00	2.56

Figure 6.9 & Table 6.6: The progress report of the *D-K* iteration of the with increasing uncertainty set size and resulting worst case-$\mathcal{L}_2$ gain.

stiffness coefficient uncertainty. Therefore, we use three dynamic multiplier blocks and a static multipliers for the overall design. Consequently, the uncertainty set is significantly larger than the previous cases. The motivation for such complication is to be able to compare whether a reduced mass argument would hold and provide better performance than this more realistic but at the same time significantly more conservative design. Thus the $P - \Delta$ interconnection is modeled as

$$\begin{pmatrix} q \\ z \\ y \end{pmatrix} = P \begin{pmatrix} p \\ w \\ u \end{pmatrix}, p = \Delta q$$

where the uncertainty Δ is given by Equation (6.19).

In this control design problem, we start by assuming the nominal case to be $P_{nom} = P \star 0.5\Delta$. This due to the fact we have mentioned previously that the model loses the observability at the zero uncertainty case. Hence, we assume that the uncertainty blocks assume the mid values of their corresponding intervals and we try to increase the set size by expanding towards both ends simultaneously. Thus, for the uncertainty operator

$$\Delta : \mathbb{R}_+ \to [0, \overline{m_h}] \times [0, \overline{b_h}] \times [0, \overline{k_h}] \times [0, \overline{m_e}]$$

we define the scaled uncertainty operator

$$\Delta_s : \mathbb{R}_+ \to [0, 2] \times [0, 2] \times [0, 2] \times [0, 2]$$

where

$$\Delta(t) = \begin{pmatrix} \delta_{m_h}(t) & & & \\ & \delta_{b_h}(t) & & \\ & & \delta_{k_h}(t) & \\ & & & \delta_{k_e}(t) \end{pmatrix} = \Delta_s(t)T = T\Delta_s(t)$$

for all $t > 0$ with $T = \text{diag}(\frac{\overline{m_h}}{2}, \frac{\overline{b_h}}{2}, \frac{\overline{k_h}}{2}, \frac{\overline{k_e}}{2})$. Then, we simply rewrite

$$\Delta_s = \Delta_{ss} + I_4$$

with $\Delta_{ss} : \mathbb{R}_+ \to [-1, 1] \times [-1, 1] \times [-1, 1] \times [-1, 1]$. Then by absorbing the unity feedback path into the plant we obtain P_{nom}. Due to this centering operation, we obtain the robustness and performance certificates in the original parameter interval

$$\delta_i = \left[\frac{1-r}{2}, \frac{1+r}{2} \right], i \in \{m_h, b_h, k_h, k_e\}$$

for any r that leads to a feasible LMI solution. The resulting evolution of the controller multiplier iteration is given in Figure 6.10. As we have expected, towards the end of the uncertainty ranges, the performance gets worse with each slight increase of r

| Analysis		Synthesis	
r_a	γ_a	r_s	γ_s
0.00	0	0.10	0.88
0.38	17.36	0.68	26.42
0.69	22.22	0.75	25.73
0.75	24.11	0.76	26.4
0.76	26.33	0.76	26.46
0.76	26.41	0.76	25.9
0.77	26.42	0.76	26.24
0.77	26.31	0.76	25.94
0.76	24.62	0.74	20.15
0.78	38.27	0.79	38.14
0.79	37.93	0.79	38.69
0.79	38.61	0.79	38.36
0.79	38.68	0.79	38.66
0.81	59.26	0.82	59.77
0.82	59.43	0.82	59.72
0.82	58.99	0.82	59.41
0.82	79.12	0.83	79.84
0.83	74.06	0.84	78.57
0.84	80.45	0.84	80.47
0.84	80.21	0.84	80.24
0.84	90.9	0.84	90.79
0.84	90.37	0.84	87.5
0.84	90.96	0.84	90.84
0.84	98.66	0.84	99.48
0.84	99.03	0.84	99.07
0.84	98.64	0.84	98.8
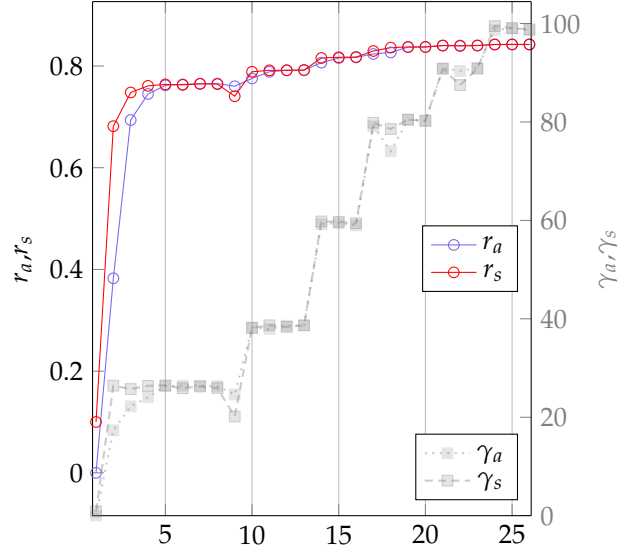
Figure 6.10 & Table 6.7: The progress report of the *D-K* iteration of the with increasing uncertainty set size and resulting worst case-$\mathcal{L}_2$ gain.

scaling. The iteration is terminated manually since the performance indicator γ was around 100 which is a nonsensical value if compared to the previous design cases where it was smaller more than an order of magnitude.

The figure also provides us an opportunity to demonstrate the variable bounding implementation that we have described in the previous chapter. In Figure 6.10, one can see that the γ increase has step-like behavior. This is due to our implementation of testing the progress of previous iterations. If at some point the progress is negligible, the algorithm progressively gives away from performance to increase the admissible uncertainty set size. We can also see that for a minute change in r, we give away a lot of performance. With the resulting $r = 0.84$, we obtain robustness in the face of [8,92] % of the original uncertain parameter intervals.

6.3   Controller Comparison

In this section we will refer to the designed controllers by C_1, C_2, C_3 following the introduction order and the corresponding frequency domain properties are shown in Figure 6.11. Furthermore, to make the time domain responses more meaningful, we first define a few motion profiles.

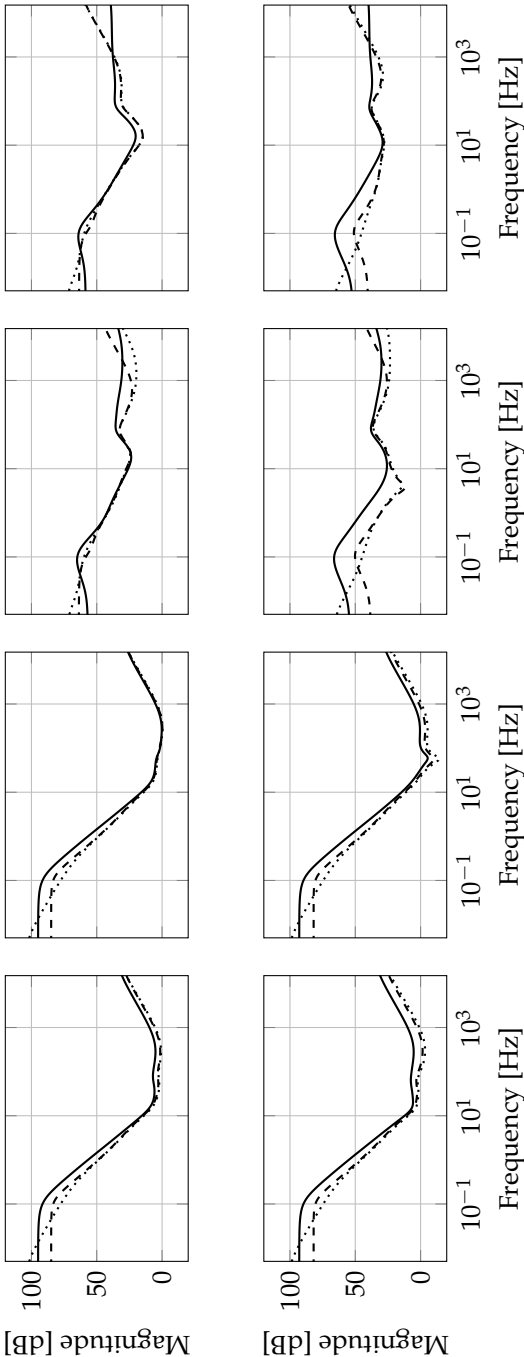**Free air**   This describes the case where the operator holds the local

Figure 6.11: The frequency domain properties of the controllers. C_1: -·-·, C_2: ——, C_3: ·······

	device handle with arbitrary grip tension and moves the local device up and down such that the remote device tracks the motion. The remote device is not in contact with any obstacle throughout the motion.
Soft Spring Contact	This describes the case where the operator holds the handle with a certain grip tension and moves the local device down into the spring such that the remote device squeezes a soft spring.
Hard Spring Contact	This describes the case where the operator holds the handle with a certain grip tension and moves the local device down into the spring such that the remote device squeezes hard spring.
Rigid Contact	This describes the case where the operator tries to push the handle with a certain grip tension down such that the remote device is pressed against a rigid object.
Contact Tapping	This describes the case where the operator taps the handle with the index finger while the remote device comes into contact with an obstacle (spring or rigid) as a result of the tapping to test abrupt changes from free air to contact scenario.
Contact Slide	This describes the case while the operator tries to push down the local device handle during the remote device is in contact with an obstacle (spring or rigid). Thus the operator is being resisted by the local device. Then the obstacle in the remote environment is pulled out manually such that a sudden change in the environment from contact to free air scenario is tested.

The resulting controllers are discretized via the `tustin` function with 2000 Hz sampling frequency and implemented using the xPC Target toolbox of MATLAB. The experiments are performed with the same device with an arbitrary combination of motion profiles listed above. Due to the proximity switches, the workspace is limited to $\approx [-35, 35]°$ where $0°$ denotes the horizontal configuration of the device handle. Hence, the contact slide motion is done rather carefully as we needed to stop before the device trips the switch which in turn stops the data streaming. Moreover, there are also hard-coded rate limiters for safe operation such that if the device handle angular velocity exceeds a threshold the device turns off the drives and disconnects (similarly the data stream is stopped). Hence, the rigid contact motion is carried out with caution. Though the responses are stable throughout the rigid contact, the controllers are aggressive enough to trip the rate-limiters hence cause abrupt data stream in the case of a particular contact tapping. In fact when tapping

approaches *striking with the finger* ($\approx 1.5\,\text{m/s}$ fingertip speed at around $4.7\,\text{Hz}$) the instantaneous rebound speed of the remote device on the obstacle trips the drive. Since our goal is to present the motion at one shot in order to demonstrate the robustness against time-variations, the contact tapping profile is carried out with a predefined force limit in mind.

It should be noted that none of the controllers have been designed to cope with completely rigid objects. In other words, we did not incorporate the unilateral constraint case (rigid contact) into account. Not only we lack the proper framework with adequate flexibility to handle such cases with performance specifications, it is also an unrealistic goal at the outset. As we will show the problem is not essentially a state-constraint problem but rather the inherent stiffness modes of the devices that are excited in the rigid contact case. Nevertheless the controllers exhibit satisfactory robustness properties with surprisingly rigid contact rendering performance contingent upon operator behavior.

6.3.1 *Description of the Experiments*

In each controller test, a right-handed male operator[3] tried out the different scenarios listed above in about $[1,2]$ min. The resulting overall data stream is shown in Figures 6.13 to 6.15. Due to the lower stiffness coefficient, the soft contact cases can be seen around $20°$ with more compression stroke length and hard contact cases take place around $5°$. The rigid contact is designed to meet with the obstacle such that the device position reading is around $0°$. Lastly, in the soft contact cases it is possible to fully compress the soft spring and hit the rigid aliuminum spring holder visible in Figure 6.1.

6.3.2 *Comparison Of Controllers Based On Different Contact Profiles*

Free air

The free air performance of the controllers are given in Figures 6.16 to 6.18. As seen from these plots we obtain good position tracking precision. The zoomed in parts show that as the bandwidth increases (which is provided manually as fast as the operator is able to shake the handle) a slight loss of performance is recorded. The differences between three controllers are quite small, e.g., Design 2 achieves $0.15°$ better tracking in the high bandwidth area then Designs 1 and 3. Therefore we conclude that free-air performance is very good. This simply shows that the nominal stability and nominal performance is not drastically affected by the robustness concerns in the design optimization.

It should be noted that even when the human is applying a nonnegligible force, the controllers are trying to close this force mismatch via applying a torque along the direction human motion at the local device i.e. acting like a friction compensator thus reducing the difference $f_h - f_l$. Similarly in the remote device the difference is

---

[3]More properly, the author himself though still using the third person narrative.

compansated via $f_e - f_r$ via tracking closely the local force vector. These two actions combined leads to the very good position tracking and as a bonus we do not need a precise force tracking unless the positions of the devices are constrained or distorted by soft contact which is presented below.

Soft Contact

The soft contact measurements are given in Figures 6.19 to 6.21. In the C_1 and C_2 cases, we can see that the handle is taken too far and after the full compression we hit the rigid column which the spring is mounted on. Notice that the rigid contact is completely stable for both cases however this is due to the existence of the spring as we will present the rigid contact performance later for C_1. For C_2 this performance is consistent. Regarding the force feeling, the three designed controllers exhibit realistic replication of the remote spring stiffness. An informal survey among a dozen experimenters also confirmed this subjective result.

One can see that the tracking property of C_2 is superior to the other two though the difference is very small. Additionally, due to the increased robustness, C_3 starts exhibiting some loss of performance (see Figure 6.21, starting from 56 secs.)

Hard contact

The hard contact measurements are given in Figures 6.22 to 6.24. Unlike the previous cases, the immediate difference is that C_3 starts to render the hard spring softer hence the increase in displacement around $-6°$ in Figure 6.24. Moreover, to be able to show the reduced conservatism around [70,74] s we have performed some contact tapping and performance is visibly worsened. However, C_1 and C_2 still gives a very good force response and position tracking at the same time.

Rigid contact

The rigid contact measurements are given in Figures 6.25 to 6.27. As none of the controller has a guaranteed robustness properties for this type of interaction, we would like to see to what extent the controllers can push performance without driving the system to instability.

In fact, numerically, there is a mild and indirect robustness constraint imposed. Note that, when we model the uncertainty and include the maximum values of the springs, the numbers are quite high compared to the state space entries of the system. For example if we design a controller in the face of a spring with maximum admissible stiffness coefficient $10 \, \text{kN/m}$ the model is surely dominated with such numbers. Therefore, though it is not guaranteed, the numerical algorithm is somewhat forced to include some robustness around this comparatively huge number. Consequently, after a threshold value, the uncertainty limit $2 \cdot 10^5$ is qualitatively not that different than $1 \cdot 10^6$ in terms of robustness properties since the LMI conditions are very unlikely to be substantially different. Hence, it is not completely true that there is no robustness constraint imposed on the system. However, this does not

entirely rule out the fact that there might exist some systems that has qualitatively different properties after some huge value. In turn, it is unlikely that the current LMI solvers are able to detect and take into account those numerical problems accurately.

This is shown by the rigid contact responses. Again, increased uncertainty set size, forces C_3 both be more robust with less performance and at the same time the robustness margin is comparatively smaller. By the loss of performance, the remote device introduces oscillations during contact and they are not handled successfully if the user has a light grip on the local device handle. As seen around 84 s and at the end of the motion, the device shows temporarily an oscillatory behavior. At the end of the motion, C_3 additionally trips the drive. Another evidence for such robustness increase/performance decrease can be found on the actuator output plots Figures 6.31 to 6.33. Clearly, C_3 is less aggressive than the other controllers and thus has less stabilizing capabilities in the region where robustness is not guaranteed.

It is quite the contrary for C_1 and C_2 since the rigid contact performance is quite satisfactory. We can distinguish the effect of taking the rate-of-variation bound into account as C_2 shows superior performance even with a few contact sliding motion after pressing down the rigid block. Moreover towards the end we can see the contact tapping responses.

Although not visible in the plots, C_1,C_2 suffer from an effect due to the assumptions we have made about the human mass coefficient. It is sometimes possible to find a very light touch pattern during rigid contact such that the controller overreacts and a pseudo-limit cycle is triggered though it is difficult to maintain without letting it decay. This is partially due to the fact that controller gains are tuned for continous contact but the operator touches just enough to register a nonnegligable force on the sensor without actually engaging the hand dynamics with the local device handle. This produces a small kickback since the controller expects some inertial resistance but absence of it causes a rapid overreaction/correction motion.

We should emphasize that this is not an essential limitation of the algorithm and by adjusting the performance weights or using the full model of the system it can be avoided. However, we are under the impression that even with this model the obtained results are very promising.

It is much to our surprise that the contact rendering of C_2 is almost flawless especially, when the user comes down with relatively higher velocity on to the obstacle. This is yet another evidence that with adequate robustness properties of the system, there is no need to utilize sophisticated control design methods just for the sake of a framework to handle unilateral constraints.

We conclude this section by pointing to a rigid contact phenomenon with firm grip case. Since superior to C_1,C_3 designs, we consider the controller C_2 responses. In the rigid contact case, we have experienced an interesting pattern; while the user drives the local device down, the remote device comes into contact with the rigid object almost simultaneously hence we have a very satisfactory immersion level about the rigidity of the contact. However notice that when the remote device comes into contact with the obstacle, the local device stops with some residual rapid decaying oscillations as shown in Figure 6.12. Same experiment is repeated
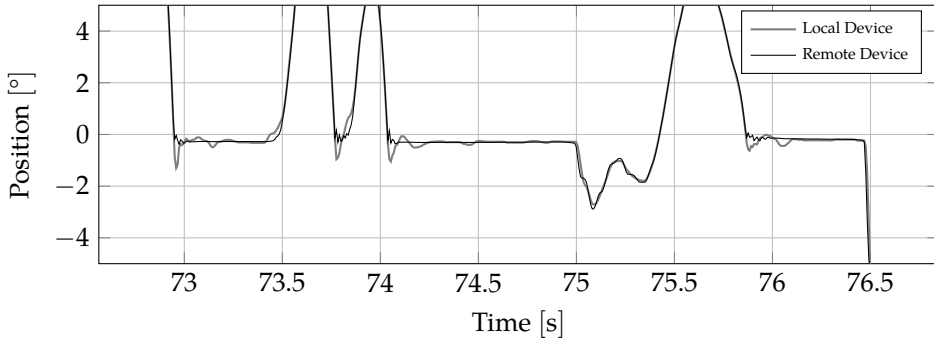
Figure 6.12: Design 2 rigid contact close-up

by grabbing the forearm firmly from a point closer to the elbow with left hand and applying a slight clock-wise twisting torque such that the muscles at the forearm are constrained. Then, the oscillations mentioned above became more pronounced in terms of immersion[4]. Therefore, just by changing the arm configuration and clamping/relasing muscle groups touch sensation can be altered.

Alternatively, by using a headphone playing loud music to cover the contact sound and looking away from the remote device we have repeated the same motion. This experimental technique is common in the literature and additionally in some cases the user is given the opportunity to view the remote device from a computer display to render a distant operation condition. According to our subjective judgement, the resulting immersion difference was insignificant.

---

[4]The reader can verify this by raising the right hand with palm pointing left, making a fist and hitting a rigid surface with holding the forearm firmly with left hand. The absence of the common vibration dissipation through the muscles and tendons makes the touch significantly different. Obviously, the ideal case would be temporarily blocking the sensory mechanisms of the forearm to isolate the information provided by the hand. This issue should be obvious to the relevant medical fields however any relevant literature in those areas so far eluded us
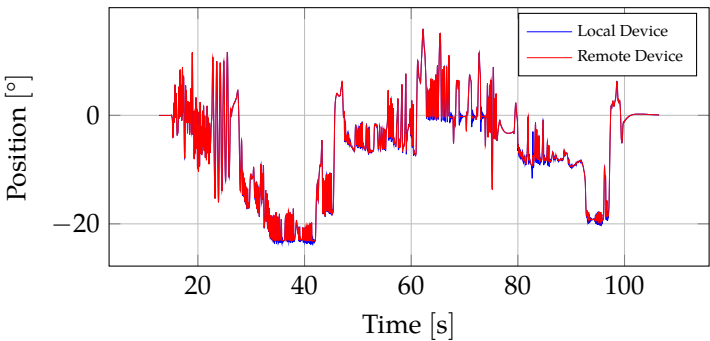
Figure 6.13: Design 1 experiment : real-time encoder reading
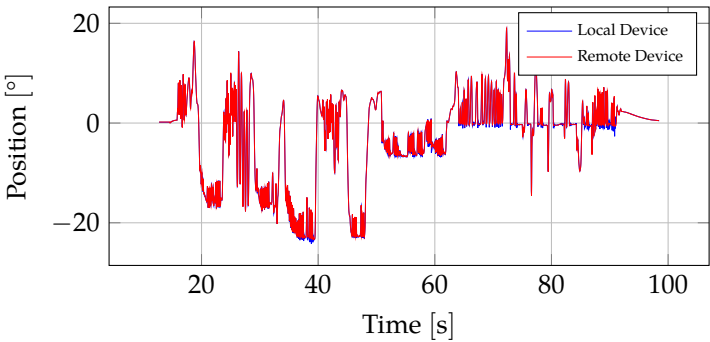
Figure 6.14: Design 2 experiment : real-time encoder reading
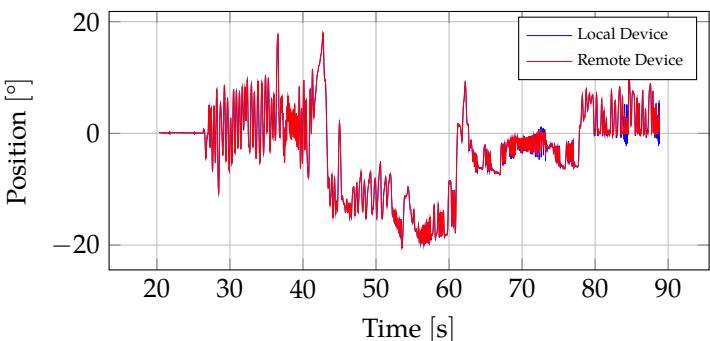
Figure 6.15: Design 3 experiment : real-time encoder reading
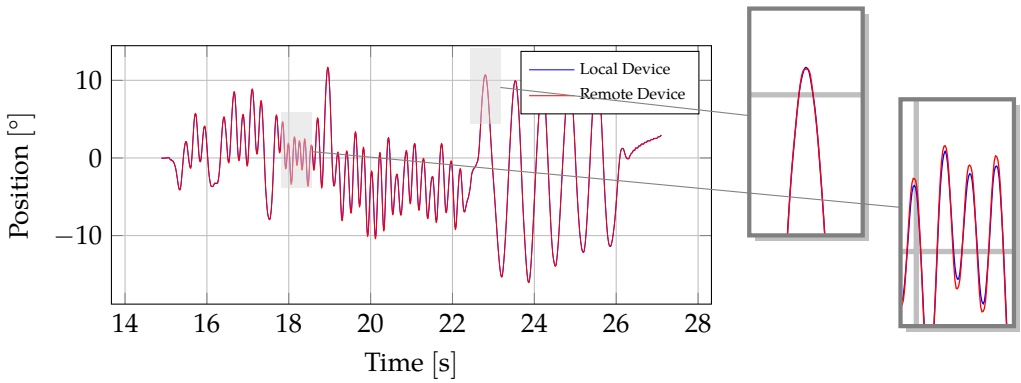
Figure 6.16: Design 1 experiment detail: Free-air section
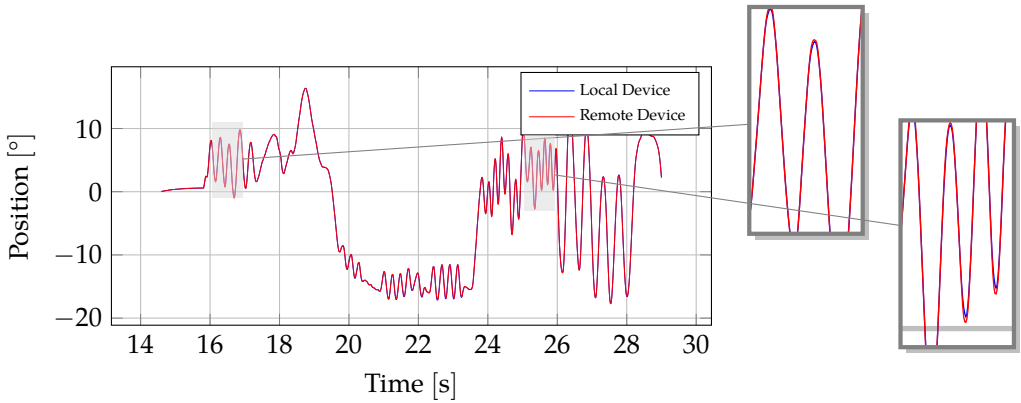
Figure 6.17: Design 2 experiment detail: Free-air section
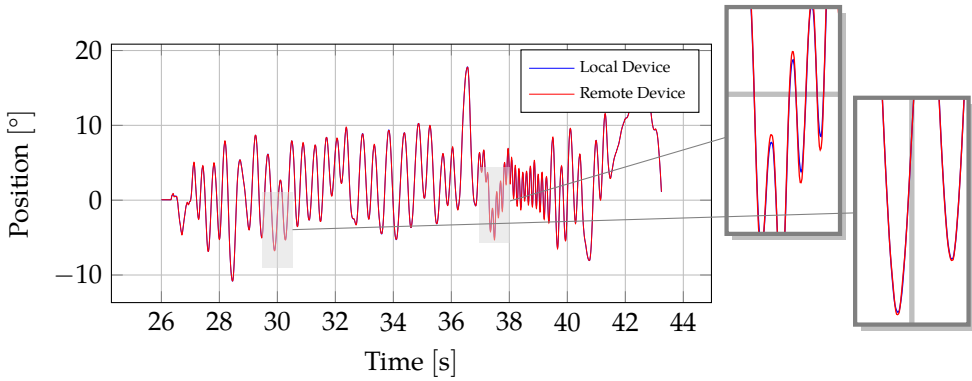
Figure 6.18: Design 3 experiment detail: Free-air section
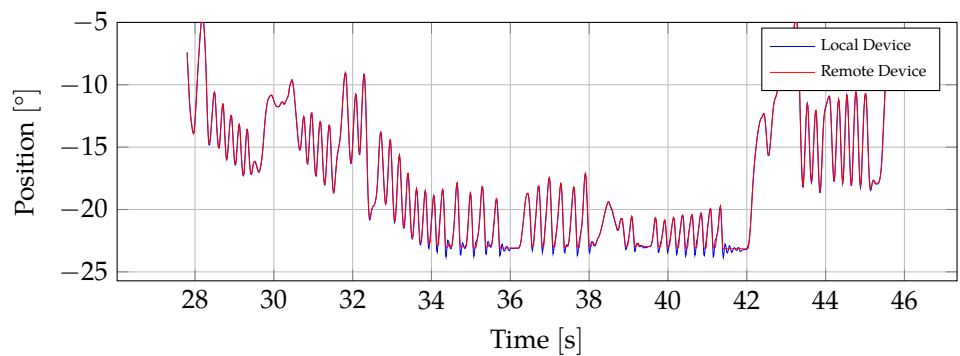
Figure 6.19: Design 1 experiment detail: Soft contact section
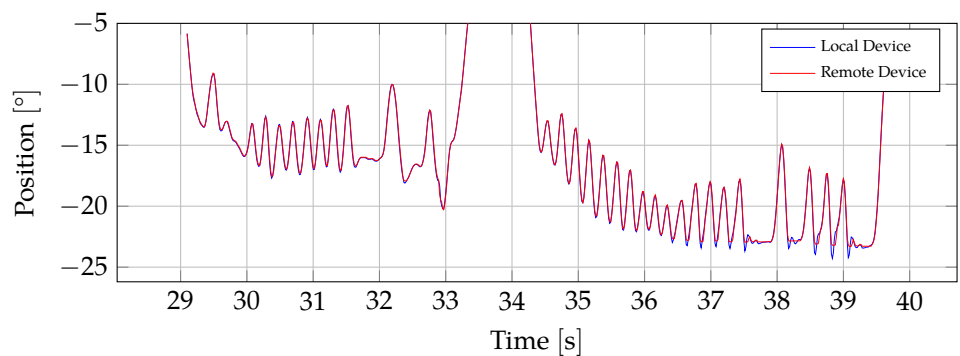
Figure 6.20: Design 2 experiment detail: Soft contact section
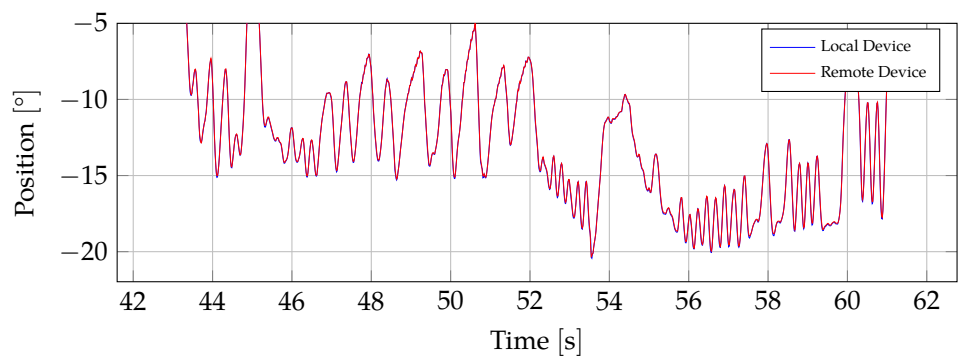
Figure 6.21: Design 3 experiment detail: Soft contact section
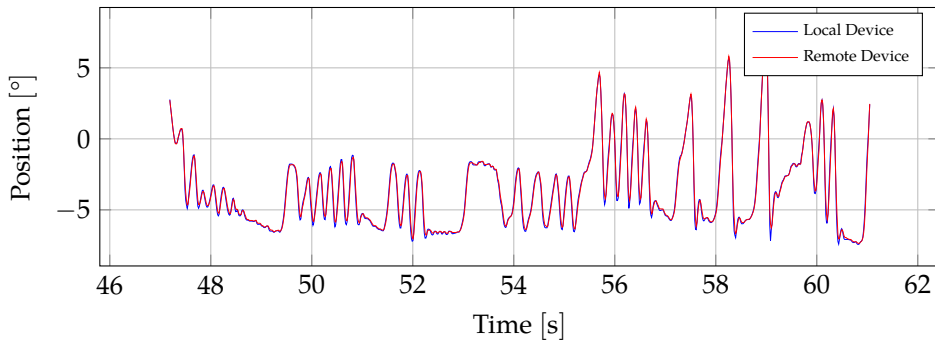
Figure 6.22: Design 1 experiment detail: hard contact section
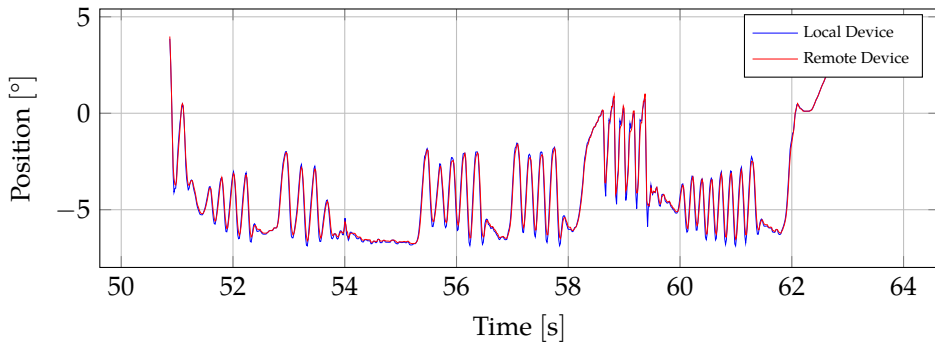
Figure 6.23: Design 2 experiment detail: hard contact section
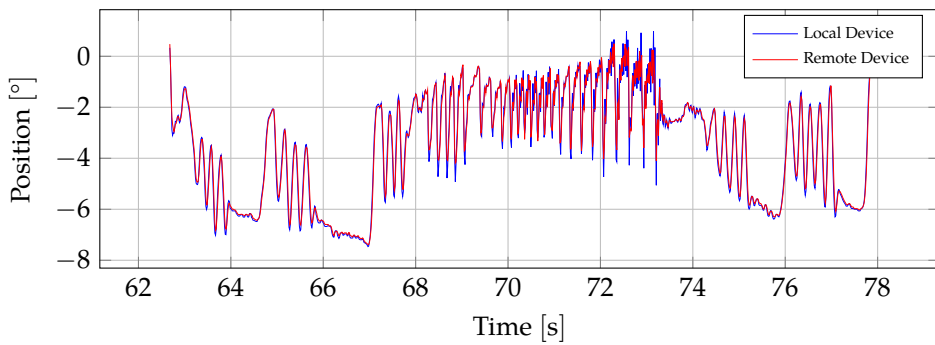
Figure 6.24: Design 3 experiment detail: hard contact section
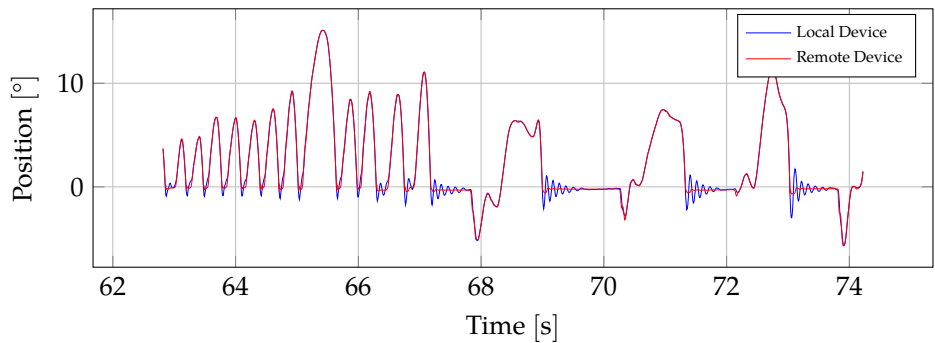
Figure 6.25: Design 1 experiment detail: rigid contact section
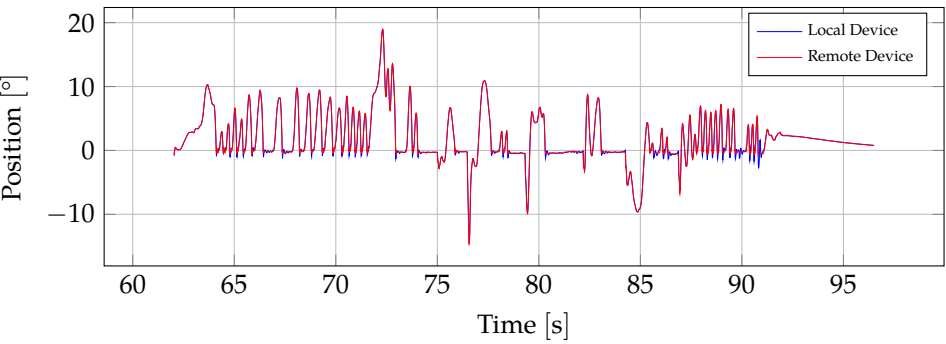
Figure 6.26: Design 2 experiment detail: rigid contact section
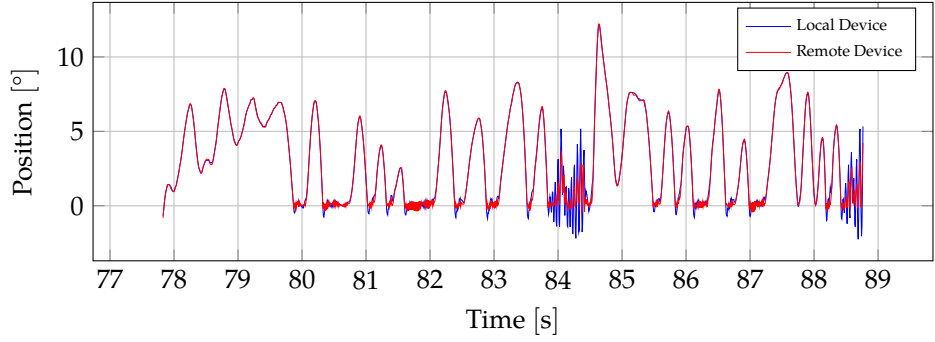
Figure 6.27: Design 3 experiment detail: rigid contact section

Figure 6.28: Design 1 experiment: Measured Human and Environment Forces as Torques at the Actuator Shaft
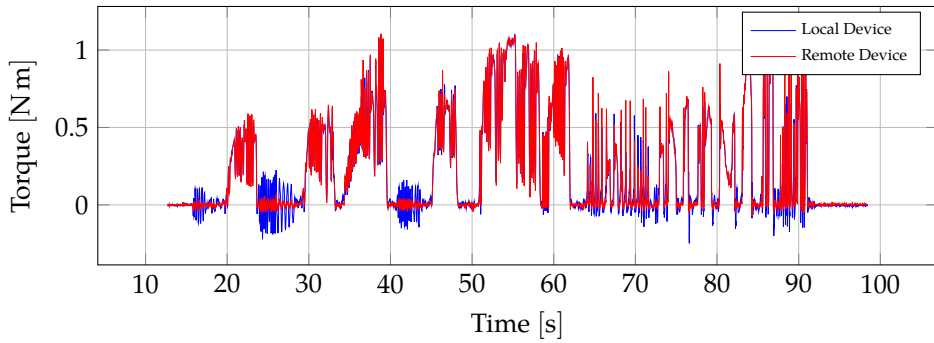
Figure 6.29: Design 2 experiment: Measured Human and Environment Forces as Torques at the Actuator Shaft
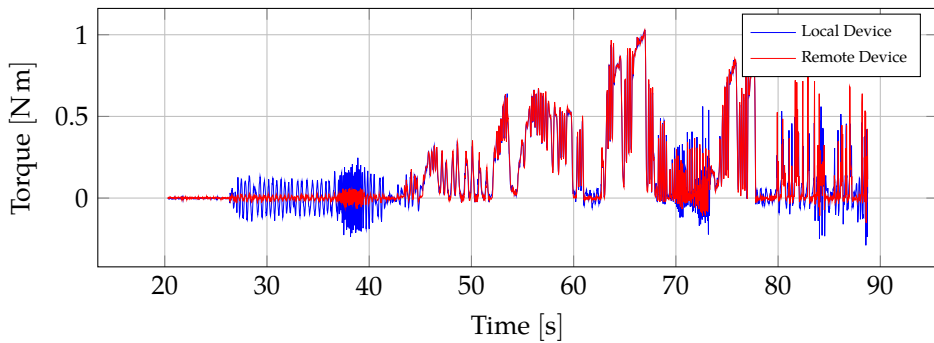
Figure 6.30: Design 3 experiment: Measured Human and Environment Forces as Torques at the Actuator Shaft
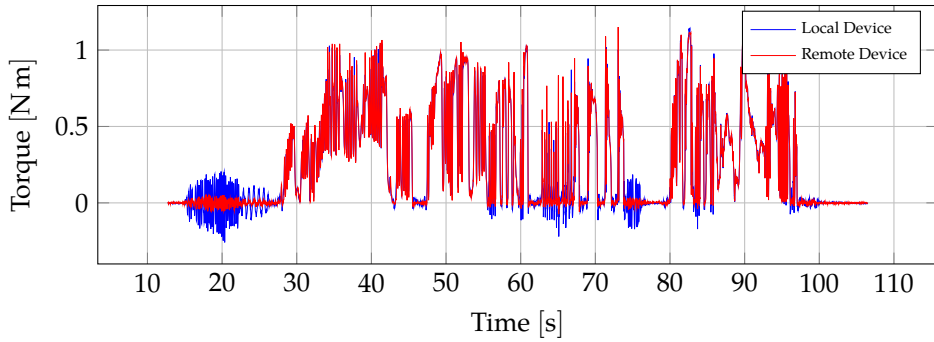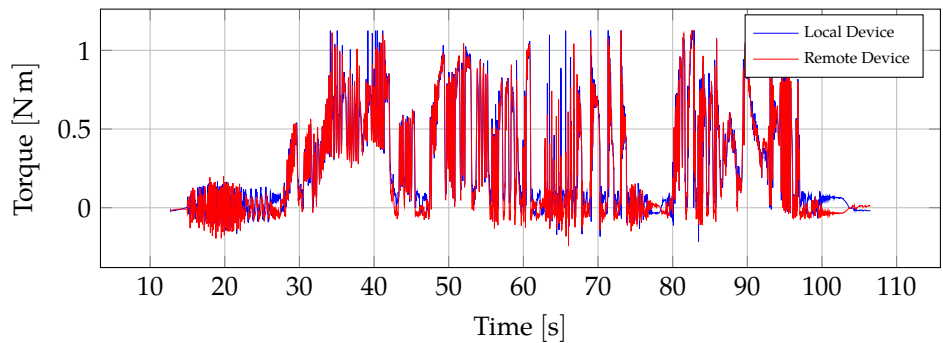
Figure 6.31: Design 1 experiment: Actuator Input Torque
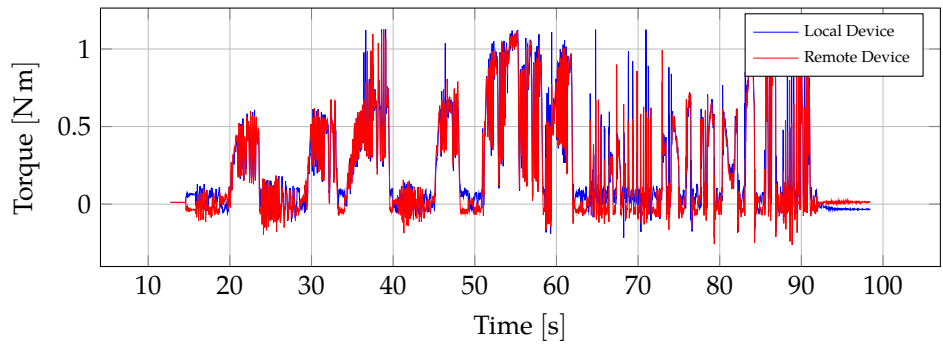
Figure 6.32: Design 2 experiment: Actuator Input Torque
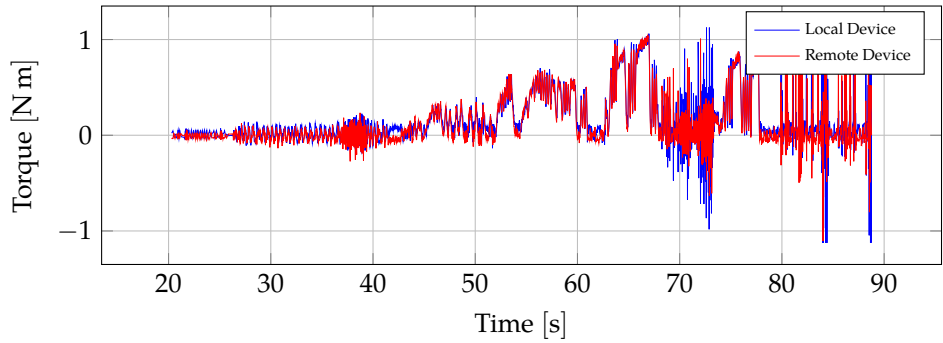
Figure 6.33: Design 3 experiment: Actuator Input Torque

6.4   Closing Remarks

In this chapter, we have shown that a systematic control design for bilateral teleoperation problem is feasible and results have been verified through a basic implementation study. Based on these results we claim that a *transparency*-like objective can be achieved with robust and high-performance controller via a thorough modeling step of the involved systems. Thus, we believe that we have presented a counter-example free from the methodological drawbacks of classical stability-transparency tradeoff while still amenable to the essential stability/performance tradeoff. Moreover, the designed controllers do not show unexpected robustness or performance behaviors and the performance-stability properties worsen as we approach or go beyond the theoretical guarantees.

Still, in accordance with our claims in the Chapter 3, this design, regardless of the appeal or superiority, cannot be accepted as a genuine bilateral teleoperation method, since we use the questionable transparency-like objective as the performance index.

We cannot help but include yet another rant about the control design in the literature for bilateral teleoperation. Instead of mentioning the typical absence of arguments on describing how any PD controller in the loop is tuned or why we should bother to perform endless derivations to tune one or, if we are lucky, a very few more parameters, we limit the discussion to the following.

In majority of the network-based modeling papers, for some unknown reason and as if it is possible, the concept of local controllers are introduced and the controllers that only communicate over the line between local and remote devices are emphasized for further analysis (see Figure 2.12). Quite often, it is assumed that the local controllers achieve "high-precision tracking" locally and derive the conditions to render the interconnection passive. Then delays and other complications are introduced and tedious derivations are presented though the undelayed bilateral teleoperation problem is still open for a satisfying performance definition. The subsequent result is either deriving constraints on PD controller gains without any comment on how we are supposed to tune the "local" controllers[5]. We emphasize that the closed loop stability is guaranteed by all controllers and the locality of the controller does not exclude it from the interconnection stability consideration. Alternatively, some controller entries in Figure 2.12 are assumed to be zero and the number of variables is reduced. In the four-channel case, the methods are exclusively limited to compensated dynamics type, cross-coupling controllers where each entry is specifically equals some part of the cancellation of dynamics to reach to the ideal transparent system.

We openly accept that we fail to understand the rationale behind these arguments.

Thus, if we are to investigate our controllers in this *local* and *interdevice* controller distinction, we see that the position controllers (from inputs 1-2 to outputs 1-2 in Figure 6.11) look like PI controllers though the roll-off is of the double integrator

---

[5]which is far from trivial while respecting passivity and simultaneously achieving precise tracking

type. The force controllers are clearly not PID-like. Moreover, let us check whether transparency optimization rules in terms of the controller entries (see (2.4) and Figure 2.12)

- $K(2,1) = (\text{Dynamics of the environment} + K(2,2))$

- $K(1,4) = -1 + K(2,4)$

- $K(1,3) = 1 + K(2,3)$

- $K(1,2) = -(\text{Dynamics of the user} + K(1,1))$

hold or not. Obviously, since we use position signals for feedback we can't simply use the data given in Figure 2.12 without multiplying the third and fourth columns with $i\omega$. Even then, we can verify that none of the conditions are valid. In some cases, there are more than 20 dB differences for the second and third conditions and also the first and last conditions are not verifiable since they involve time-varying operators as opposed to LTI assumptions in the Lawrence' analysis. Nevertheless, we obtain a a high level of transparency[6] with controllers that do not even remotely resemble conditions of the classical transparency conditions. The apparent mismatch comes from the fact that we do not care whether the resulting closed loop *2-port* hybrid matrix is $\begin{pmatrix} 0 & I \\ I & 0 \end{pmatrix}$ or not. We simply optimize the controller to minimize the induced gain of the performance channels. Moreover, this also shows that the well-known transparency optimized control laws given above can only be taken into account in the passivity-based absolute stability framework.

In the light of the discussion above, we strengthen our claim that how to arrive at complicated structures by manual tuning or cross-coupling controllers is unknown and current literature does not answer this question contrary to the ubiquitous claims. Note that, the matter at hand is a complexity problem but not a matter of engineering experience obtained from loop-shaping practices that implies our position completely opposed to the claims of [32].

Despite the risk of overemphasizing this remark, we need to reiterate that there is no holistic issue about the presented method. If there exists a better MIMO technique or a better structured controller design technique then they immediately qualify as valid ones. However, the essential argument remains unaltered that modeling and defining proper performance objectives are crucial independent of the method to arrive at the controllers.

---

[6]in the informal sense involving human perception if compared to the Lawrence' formal definition.

Conclusions

In the light of all the arguments presented so far, we believe that we have clarified the underlying discrepancy between the actual bilateral teleoperation problem and how academic literature handles it. Moreover, we have provided a competitive alternative method that led to a high degree of realism experimentally. Therefore, we can safely claim that many technical problems reported in the literature are methodological and can be solved efficiently via careful modeling and robust control design phases without invoking questionable assumptions a priori. However, this claim does not reach out to the real solution of the bilateral teleoperation problem. Put better, we only claim that we have provided the solution for the simplified version of the problem. The actual question of *What makes this device good?* or even the harder *How can we improve the device?* are completely open. Unfortunately, we believe that clarifying this fact is a contribution.

Nevertheless, an important property of the method proposed here is that it provides consistent performance over different motion profiles and does not suffer from the artifacts of the method we have utilized. Moreover, we do not alter the hardware specifications by introducing virtual dissipation elements hence the results can be used to create devices that can be used in the investigations of the aforementioned open questions.

Another important problem that we have not touched upon is the delayed bilateral teleoperation synthesis problem that somewhat dominated the literature as if the undelayed case is completely studied. To justify our deliberate choice we distinguish two cases; there is a strong possibility backed by various studies that there exists an upper bound on the delay duration a human operator can cognitively compansate for during a bilateral teleoperation task. Beyond this delay value the human cannot associate the remote motion with the local device motion. Therefore let us denote this upper bound by T whatever it might be other than being very likely to be around 1 s, then we have the following obvious dichotomy,

- The actual transmission delay is higher than T,

- The actual transmission delay is lower than or equal to T.

In the first case, we believe that there is no need to even consider the problem since it is even harder to find the relevant performance objectives of how a human operator can be made to immerse into the task with an excessive time delay. In the second case, if there is significant time delay, one can use the multipliers given Chapter 4 for delay uncertainties and utilize it in the synthesis method given in Chapter 5 directly, with guaranteed improvements over the existing techniques.

Additionally, if the communication delay is of the time-varying nature, one can always buffer the input/output to regularize the delay and use the known upper bound of the buffer period. The reason why this would always give a better performance is simply because the existing time-varying delay robustness analysis and synthesis tools are simply too conservative. Utilizing them surely would lead to stable interconnections but at the cost of unacceptable low performance levels which undermines the motivation the problem. Dealing with a known constant time-delay is, in turn, much easier and sharper results can be obtained. Note that practically every packet-switched network video/audio stream protocol use such buffering schemes unlike the vast majority of the time-delay teleoperation literature. In fact, this is not even a control-theoretical issue and should be left to digital communication experts for the optimal methods which go well-beyond control design knowledge. Moreover, the problem is far more sophisticated than the choice between TCP or UDP protocols.

Following this argument, we have the following conclusions elaborated in this thesis;

1. The bilateral teleoperation is fundamentally an interdisciplinary problem. Current literature underestimates the broadness of the scope of this technology and claims to solve a stability problem that is not inline with the actual bilateral teleroperation. The majority of the proposed problem formulations are of *What if we had sampling, two users, time-varying delay?* nature. Though, these scenarios are certainly worth considering, the proposed solutions only handle the stability issues. Our first conclusion emphasizes this;

   The bilateral teleoperation problem is not a typical control problem in which stabilization is the crucial point and achievable performance is an extra bonus. Without the required performance levels, a stable bilateral teleoperation system is useless.It might even decrease the human task performance.

2. As we have shown in Chapter 6, the 2-port network modeling framework is not general enough to capture the problem in its entirety. Over the last two decades, certain derivations are established as facts for the perfect transparent device however one can still obtain better designs with alternative methods that do not obey the predicted performance conditions which are stated in numerous sources. If the following definition of transparency is adopted

   > Transparency is defined, meaning that the human operator should ideally feel as if directly acting in the remote environment (is not able to feel the technical systems/communication network at all)..
   > ([73])

   which seems to be the case in the literature, then there is a discrepancy between what is being sought after and the corresponding formulation.

   Transparency objective that relates the performance to the operator feel and comfort with the definiton above does not necessarily imply that an ideal

teleoperation system should have a hybrid system representation $\left(\begin{smallmatrix} 0 & I \\ I & 0 \end{smallmatrix}\right)$. This formulation completely ignores the human perception and moreover it is impossible to achieve. Additionally, as a control objective it relies on naive control concepts such as exact dynamics cancellation and plant inversion. In a time-varying system these arguments are invalid.

3. A vast majority of the network-theory based stability conditions can be red-erived by the IQC framework in a lossless fashion. Due to this equivalence there is no added value of using scattering transformations or wave variables over the proposed framework.

   Insisting on the network theoretical treatment of the subject is a matter of preference. IQC framework already covers the classical methods and offers significantly larger set of possibilities to be utilized in stability analysis and controller synthesis. Here the emphasis is on the anachronistic focus of the literature.

4. As we have shown via a simple implementation, high-performance controllers can be designed using a sufficiently accurate model of the system and careful simplifications by the robust control design methodology.

   The D-K iteration with dynamic multipliers leads to significantly less conservative results compared to static multiplier based designs which includes wave-variable- and passivity-based methods. The disadvantege of model based design is obtaining the accurate models and the weight selection. The latter is a significant obstacle in judging the true optimality of the design. Even in the cases where the problem solution is guaranteed to be optimal, the design itself due to the performance weights selection can be non-optimal. However, this difficulty is not in par with the conservative methods. In other words, this difficulty can be overcome with educated guesses in a trial-and-error phase which permits at least some systematic procedure up to an extent. A conservative method does not permit such by-pass steps.

5. It is shown that depending on the uncertainty modeling complexity, the control design problem can be made robust to different uncertain operators of different kind including delays, parameters, particular nonlinearities etc. However, as reassuring and positive it might seem, more robust solutions lead necessarily to lower performance levels. Therefore, it is the highest priority to get a model with reduced uncertainty as much as possible. Even if there does not exist a suitable method to handle the resulting obstacles, this will nevertheless make the problem visible and unambigious.

   Due to the absence of a rigorous objective, we might pursue for the improvements over the method presented here. The immediate improvement that can be relevant is the application of Linear Parameter Varying controller synthesis via scheduling over the forces sensed in remote and local

environments. The synthesis framework is already established however once again, the performance objective is missing therefore we hit the same bottleneck.

6. The teleoperation literature (and partially the control theory literature in general) have the tendency to motivate engineering problems inside a seemingly rigorous mathematica.l framework. However, often there is an implicit transition from the actual problem to the watered down, oversimplified version of the same problem that disconnects the solution from the physical motivation. Alternatively, unrealistic reasons are used to justify certain assumptions. A typical example is the claim that force sensors are expensive to implement and force sensorless possibilities are explored. That statement is only true relatively if the remote and/or local device cost is significantly low. If we can succeed providing the operator a realistic touch sensation, the sensors would compensate the investment costs in a very short amount time[1]. We certainly refrain from declaring what is worth of focus or not however motivating a mathematical problem with questionable engineering scenarios is false and unfortunately very common. Same problems can be investigated without any engineering motivation for the sake of the problem alone.

There are more important open problems than the rather specialized delayed teleoperation problem or force-sensorless teleoperation. The delay robustness problem is studied in the last two decades extensively outside the teleoperation context. As a result of this effort we already have a variety of methods IQCs, Lyapunov-Krasovskii functionals etc. The importance of the delay instability is due to the unrealistic ambitious objective of physics equalization. Similarly force-sensorless teleoperation or multi-user teleoperation etc. are problems with invalid motivation from a technological point of view since the bilateral teleoperation system is an human oriented technology not a network controlled system. The problem is finding the tool for designing the controller but not modifying the problem for the control design tool.

---

[1]A surgical robotic system price is in the order of million USD with very high maintenance costs. The typical force sensor cost is negligible

Network Theory Primer

In this appendix, we provide a collection of basic network theory concepts for the convenience of the nonexperts of the field, to be used as a quick reference while we discuss the tools used in the bilateral teleoperation studies. Our focus would be on interconnections and stability of these interconnections hence circuit theory preliminaries and physics of the components are omitted.

A.1 TERMINOLOGY

We start with ideal circuits for which the external influences such as the magnetic interference, temperature gradient as well as internal characteristics such the conductor element length and resistance etc. are negligible. Hence a signal traveling through a conducting medium between location A and B distorted i.e., if an arbitrary property of the signal at any point between and including A and B is measured, we obtain the same results. This allows us to use the simplifications in block diagrams and calculations that point A and B have the same measurable characteristics through time. This is typically shown with a path connecting A and B. The interpretation is that A and B and also every other point on that path share the same variables of interest on that line. Therefore, A and B are said to be interconnected terminals connected by a "wire". Clearly creating terminals are as simple as cutting the connection arbitrarily on this path. Often, we define hypothetical terminals as if there were distinct points on the circuit and we have connected them artificially.

Following Jan C. Willems' formulation for a systematic definition of terminals and ports in [196]; an electrical circuit is a device, a black box, with wires so-called terminals through which the circuit can interact with its surroundings. In electrical circuits, the interaction takes place via the electrical voltage drop across the terminals and the electrical current that flows through the black box. Therefore each terminal admits two real variables attached to it, the potential and the current. Conventionally, the current is denoted with a positive number when it flows into the circuit. Thus, an interconnection is connecting a wire from terminal A of the black box (x) to B of (y) enforcing the following to hold

$$V_A = V_B \quad \text{and} \quad I_A = -I_B$$

Then, we can look at the resulting interconnected system (z) as (x) and (y) combined and exhibiting the same phenomenon at their terminals A and B.

The collection of physically attainable phenomena are abstracted with the notion of the behavior set ([152]): Consider a circuit with N terminals. Let $\mathcal{B} \subseteq (\mathbb{R}^N \times \mathbb{R}^N)^{\mathbb{R}}$

denote the behavior set that is defined as the set of all admissible potential and current trajectories compatible with the network architecture at each terminal. Here $(\mathbb{R}^N \times \mathbb{R}^N)^{\mathbb{R}}$ denotes the set of all maps $f : \mathbb{R} \to \mathbb{R}^N \times \mathbb{R}^N$ e.g. each terminal voltage and current evolution through time and $\mathcal{B}$ is the restriction to the maps that are compatible with the network structure. Roughly speaking, behavior set excludes all the trajectories that are physically impossible to attain by the black box. Thus, when it is said that a particular trajectory is in the behaviour set i.e.,

$$(V_1, \ldots, V_N, I_1, \ldots, I_N) := (V, I) \in \mathcal{B}$$

it implies that there exists an initial condition $(V(0), I(0))$ such that (V, I) is a an admissible trajectory through time (with a particular external excitation sequence if present).

Assuming a conservative magnetic field, a circuit can be modeled via the well-known Kirchhoff voltage and current laws compactly described as

$$(V, I) \in \mathcal{B} \implies (V + \alpha \mathbb{1}, I) \in \mathcal{B} \quad \forall \alpha \in \mathbb{R}^{\mathbb{R}} \tag{KVL}$$

$$(V, I) \in \mathcal{B} \implies \sum_{k=1}^{N} I_k = \mathbb{1}^T I = 0 \tag{KCL}$$

where $\mathbb{1}$ denotes a vector with all entries are equal to 1 whose size is clear from the context.

Let, $P \subseteq \{1, \ldots, N\}$ denote an m-tuple selection of indices out of N terminals of a circuit. Then, terminals P_i for all $i \in P$ are said to form a port if

$$(V, I) \in \mathcal{B} \implies p^T I = 0 \tag{Port KCL}$$

where p is a vector with kth entry being 1 if $k \in P$ and 0 otherwise. This is nothing but a reformulation of the well-known port condition from circuit theory. Thus, we can also define a port as the set of terminals that satisfy port KCL. Given a port with n-terminals with V, I denoting the through and across variables, the instantaneous power is given by

$$P = \sum_{k=1}^{n} V_k(t) I_k(t)$$

and the energy transfered in the time interval is given by the total power delivered to/from that port in the time interval $[t_1, t_2]$:

$$E = \int_{t_1}^{t_2} \sum_{k=1}^{n} V_k(t) I_k(t) dt$$

These formulas hold only if the terminals form a port and a port can have arbitrary number of terminals e.g., op-amps, transistors, $Y - \Delta$ resistance networks are examples for three terminal ports.

Using a mechanical-electrical analogy, the mechanical teleoperation devices are converted to a network of ports. In network theory applications to bilateral teleoperation, the "system" refers to the network model that is hypothetically disconnected (thus admitting virtual terminals) from its "surroundings" such as the "load" and the "source" of a circuit. This system is allowed to interact with its surroundings via "ports". In our context, load refers to the environment that is to be explored and the source is the human exploring the environment from a distance via the teleoperation system.

Remark A.1. *We have to note that, in this formulation, a single mass can not be modeled as a 1-port; mass does not satisfy the port KCL unless it is thought to be applying an opposite force to a fixed inertial frame at a distance. This is why the electrical analog of a mass (in the force-current context) is required to be a* grounded *capacitor. The interested reader is referred to [179] for the interesting story of the development of an exact mechanical analogue of a capacitor,* the inerter *which is succesfully implemented by McLaren Mercedes and Renault F1 teams and being used since 2005[1]. We also refer to [196] for a comprehensive analysis together with the common pitfalls and nonintuitive power/energy results. Though, the inappropriateness of view of input/output formalism which is adopted also in this thesis is brought to attention in numerous studies by Jan C. Willems and his colleagues, we are obliged to use the input/output formulation as we have no results regarding the behavioral approach to bilateral teleoperation systems (yet). However, the potential of a behavioral modeling of teleoperation systems is unavoidable if the engineer insists on "physics matching" as the performance objective covered in Chapter 3.*

Since every two-terminal port can be characterized by two variables ("through" and "across" quantities), it is possible to characterize the interconnected n-port networks as if one quantity is due to the other. This is done by imposing an artificial causality scheme; two of these time-dependent trajectories can be selected as free variables and the remaining ones become dependent variables ([152]). This is the simplest kind of input/output view of physical systems via treating one port variable as the *cause* and the other one as the *effect* of this cause e.g. the current is due to the voltage drop across the terminals or vice versa.

Depending on the choice of the free variables, the system can be expressed in terms of impedance, admittance and hybrid parameters for two-port networks and their combinations for general n-port network interconnections. In the cases where the two-port is LTI, with a slight abuse of notation, we will use the term "immitance" matrix to refer to any of these representations. Suppose that a two-port immitance matrix is partitioned as

$$\begin{pmatrix} q \\ y \end{pmatrix} = \begin{pmatrix} G_1 & G_2 \\ G_3 & G_4 \end{pmatrix} \begin{pmatrix} p \\ u \end{pmatrix}$$

where q, y, p, u represent the flow (current, velocity etc.) and the effort (potential difference, force etc.) signals. Then, obtaining one representation from another is

---
[1] According to the official statements.

possible by a combination of the following elementary "permutation" and "partial inversion" operations:

$$\begin{pmatrix} q \\ y \end{pmatrix} = \begin{pmatrix} G_2 & G_1 \\ G_4 & G_3 \end{pmatrix} \begin{pmatrix} u \\ p \end{pmatrix}, \qquad \text{(Permutation)}$$

$$\begin{pmatrix} p \\ y \end{pmatrix} = \begin{pmatrix} G_1^{-1} & -G_1^{-1}G_2 \\ G_3 G_1^{-1} & G_4 - G_3 G_1^{-1} G_2 \end{pmatrix} \begin{pmatrix} q \\ u \end{pmatrix}. \qquad \text{(Partial Inversion)}$$

In the latter operation it is assumed that the inverse exists. The existence of inverses are limiting the realizability of networks as impedance or admittance matrices. Moreover, in [2], it has been shown that a hybrid matrix realization is always possible regardless. This is yet another artifact of input/output formulation. However, since we are interested in the asymptotical stability of the complete interconnection including the nominal stability, such problematic cases are not within the scope of the practical interest.

For our purposes, we consider only the immitance matrices that describe G as an input-output mapping (as opposed to transmission or ABCD parameters) as follows:

$$\begin{pmatrix} q \\ y \end{pmatrix} = \begin{pmatrix} G_1 & G_2 \\ G_3 & G_4 \end{pmatrix} \begin{pmatrix} p \\ u \end{pmatrix} , \quad \begin{pmatrix} p \\ u \end{pmatrix} = \begin{pmatrix} \Delta_s & 0 \\ 0 & \Delta_l \end{pmatrix} \begin{pmatrix} q \\ y \end{pmatrix}. \tag{A.1}$$

Therefore, the overall interconnection can be depicted by the block diagram given in Figure 2.2a. In relation to teleoperation, the blocks Δ_s and Δ_l refer to the human and the unknown environment.

A.2   Passivity Theorem

In this section passivity related important concepts are defined in a compact fashion. Nevertheless, the material given here is well-known and can be found in many classical sources such as [36, 71, 168]. We chose to follow [36] closely for the presentation style.

Let V be a linear space equipped with a scalar product, $\mathcal{T}$ be the index set of time and F be a class of functions $x : \mathcal{T} \to V$.

Definition A.2. *A linear truncation operator P_T is defined on F as*

$$P_T(x)(t) = \begin{cases} x(t) & \text{for } t \leq T \\ 0 & \text{for } t > T \end{cases} \tag{A.2}$$

In most of the cases, $\mathcal{T}$ is the closed positive real line and $V = \mathbb{R}^n$, hence the scalar product becomes the inner product defined on $\mathbb{R}^n$. The subscript $\cdot_T$ will be used as a shorthand notation for $P_T(\cdot)$. We also define $\mathcal{H}$ and its extension $\mathcal{H}_e$ as

$$\mathcal{H} := \left\{ x \in F \mid \|x\|^2 = \langle x_T, x_T \rangle < \infty \right\}$$
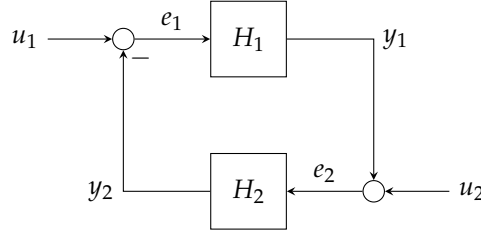
Figure A.1: Negative feedback interconnection

and

$$\mathcal{H}_e := \left\{ x \in F \mid \forall T \in \mathcal{T}, \|x_t\|^2 = \langle x_T, x_T \rangle < \infty \right\}$$

Definition A.3. *Let $H : \mathcal{H}_e \to \mathcal{H}_e$. H is said to be passive if and only if there exists a constant β such that*

$$\langle Hx, x \rangle_T \geq \beta \quad \forall x \in \mathcal{H}_e, \forall t \in \mathcal{T}$$

If moreover, there exists positive real number δ such that

$$\langle Hx, x \rangle_T \geq \delta \|x_T\|^2 + \beta \quad \forall x \in \mathcal{H}_e, \forall t \in \mathcal{T}$$

H is said to be strictly passive.

The scalar β is used to model the initial offset for nonlinear systems and will be taken as zero since we would be focusing on linear systems exclusively.

Definition A.4. *For an LTI operator H, passivity is equivalent to the corresponding transfer function $H(s)$ being positive real:*

$$\text{Re}\{H(i\omega)\} \geq 0 \Longleftrightarrow \hat{u}^*(i\omega)\,\text{Re}\{H(i\omega)\}\,\hat{u}(i\omega) \geq 0$$
$$\Longleftrightarrow \int_{-\infty}^{\infty} \hat{u}^*(i\omega)\,\text{Re}\{H(i\omega)\}\,\hat{u}(i\omega)d\omega \geq 0$$
$$\Longleftrightarrow \int_{-\infty}^{\infty} [H(i\omega)\hat{u}(i\omega)]^*\hat{u}(i\omega)d\omega \geq 0$$

for all $\omega \in \mathbb{R}_e$ and for all $u \in \mathcal{L}_2^n$. Furthermore, if the condition

$$\int_0^{\infty} H(u)(\tau)^T u(\tau)d\tau \geq \delta \|u\|_2^2 + \epsilon \|H(u)\|_2^2$$

is satisfied with $\delta > 0$, $\epsilon = 0$ (or $\delta = 0$, $\epsilon > 0$) then the operator is said to be Strictly Input (Output) Passive with level δ (or level ϵ) respectively.

Suppose we are given with two dynamical systems $H_1, H_2 : \mathcal{H}_e \to \mathcal{H}_e$ for which the system structure is given in time-domain with

$$\dot{x} = f(x, e) \tag{A.3}$$
$$y = h(x, e) \tag{A.4}$$

for both systems where $f : \mathbb{R}^n \times \mathbb{R}^m \mapsto \mathbb{R}^n$ is locally Lipschitz and $h : \mathbb{R}^n \times \mathbb{R}^m \mapsto \mathbb{R}^p$ is a continous function satisfying $f(0,0) = 0, h(0,0) = 0$.

Definition A.5 (Well-posedness). *Consider the system interconnection given in Figure A.1. The interconnection is said to be well-posed if there exist unique solutions e_1, e_2 to the equations*

$$e_1 = u_1 - h_2(x_2, e_2) \tag{A.5}$$
$$e_2 = u_2 + h_1(x_1, e_1) \tag{A.6}$$

for all admissible (x_1, x_2, u_1, u_2). In the LTI case, assume that the respective transfer functions $H_1, H_2 \in \mathcal{RH}_\infty$. Then the interconnection is well posed if $(I - H_1 H_2)^{-1}$ is a proper transfer matrix.

Note that, in our context u_1, u_2 model the voluntary part of the human/environment force input as mentioned in Chapter 2.

Theorem A.6. *Consider the well-posed feedback interconnection shown in Figure A.1 and described by Equations (A.5) and (A.6). Assume that there exist constants $\gamma_1, \beta_1, \delta_1, \beta_1', \epsilon_2, \beta_2'$ such that the following conditions hold*

$$\|H_1 x\|_T \le \gamma_1 \|x_T\| + \beta_1 \tag{A.7}$$
$$\langle x, H_1 x \rangle_T \ge \delta_1 \|x_T\|^2 + \beta_1' \tag{A.8}$$
$$\langle H_2 x, x \rangle_T \ge \epsilon_2 \|H_2 x_T\|^2 + \beta_2' \tag{A.9}$$

for all $x \in \mathcal{H}_e$ and for all $T \in \mathcal{T}$. If

$$\delta_1 + \epsilon_2 > 0 \tag{A.10}$$

then, $u_1, u_2 \in \mathcal{H}$ imply that $e_1, e_2, y_1, y_2 \in \mathcal{H}$

A well-known absolute stability analysis result for the LTI network is due to Llewellyn [116]. An explicit indication of the frequency dependence is omitted for notational convenience.

Theorem A.7 (Llewellyn's Criteria). *A two-port network N, described by its transfer matrix*

$$N(i\omega) = \begin{pmatrix} N_{11}(i\omega) & N_{12}(i\omega) \\ N_{21}(i\omega) & N_{22}(i\omega) \end{pmatrix}$$

and interconnected to passive LTI termination immitances as in Figure 2.2a, is stable if and only if

$$R_{11} > 0 \text{ or } R_{22} > 0, \tag{A.11}$$

and

$$4 \left(R_{11} R_{22} + X_{12} X_{21} \right) \left(R_{11} R_{22} - R_{12} R_{21} \right) - \left(R_{12} X_{21} - R_{21} X_{12} \right)^2 > 0 \tag{A.12}$$

or

$$2R_{11}R_{22} - |N_{12}N_{21}| - \text{Re}\{N_{12}N_{21}\} > 0 \qquad (\text{A.12}')$$

for all $\omega \in \mathbb{R}_e$, where R_{ij} and X_{ij} denote the real and imaginary parts of N_{ij} respectively.

As is the case for Llewellyn's stability conditions, it is straightforward to derive unconditional stability tests if the network is represented by scattering parameters. In what follows, we denote transformed passive LTI uncertainties with $\tilde{\Delta}_s, \tilde{\Delta}_l$ which are unity gain bounded. The corresponding interconnection is supposed to be given by the loop equations $q = Sp$, $p = \tilde{\Delta}q$ i.e.

$$\underbrace{\begin{pmatrix} q_1 \\ q_2 \end{pmatrix}}_{q} = \underbrace{\begin{pmatrix} S_{11} & S_{12} \\ S_{21} & S_{22} \end{pmatrix}}_{S} \underbrace{\begin{pmatrix} p_1 \\ p_2 \end{pmatrix}}_{p}, \ \begin{pmatrix} p_1 \\ p_2 \end{pmatrix} = \underbrace{\begin{pmatrix} \tilde{\Delta}_s & 0 \\ 0 & \tilde{\Delta}_l \end{pmatrix}}_{\tilde{\Delta}} \begin{pmatrix} q_1 \\ q_2 \end{pmatrix}. \qquad (\text{A.13})$$

Rollett's conditions ([108, 162, 182]) for stability are then formulated as follows:

Theorem A.8. *Consider the same network given in Llewellyn's criteria which is represented in scattering parameters. The interconnection is stable if and only if the inequality*

$$K = \frac{1 + |\nabla|^2 - |S_{11}|^2 - |S_{22}|^2}{2 |S_{12}S_{21}|} > 1 \qquad (\text{A.14})$$

holds for all frequencies together with an auxiliary condition in terms of $\nabla = S_{11}S_{22} - S_{12}S_{21}$. This extra condition can be stated in at least five different ways, such as

$$1 - |S_{11}|^2 > |S_{12}S_{21}| \ \ or \ (1 - |S_{22}|^2) > |S_{12}S_{21}|.$$

(See [41] for further details).

In [41], Edwards and Sinsky reduced Rollet's conditions to a single quantity denoted as μ to be checked for being greater than unity for all $\omega \in \mathbb{R}_e$.

Theorem A.9. *Verifying Rollet's conditions is equivalent to verifying the single condition*

$$\mu := \frac{1 - |S_{11}|^2}{|S_{22} - S_{11}^*\nabla| + |S_{12}S_{21}|} > 1 \qquad \forall \omega \in \mathbb{R}_e.$$

A Terminological Classification

In this chapter, we give the general outline how we have classified the touch technologies to isolate bilateral teleoperation which is our main focus. Moreover, we give some specific details about the human body for a quick reference.

B.1 THE ADOPTED TERMINOLOGY

The somatosensory system involves complicated chemical and mechanical components and there are different layers of sensory mechanisms that contribute to the overall perception. Hence, it is not always directly possible to use a reduction argument that simplifies the involved processes. In fact, depending on the type of sensation, different layers of these mechanisms are excited.

The main two branches of technology relating to the touch perception are the tactile and kinesthetic feedback (as we define below). The terminology is yet to reach a steady-state standard, however, what follows below seems plausible considering the variations and nuances found in the literature. Since there is no fixed definition for such perception we would use a rough classification based on the magnitude-frequency content of the motion[1]. We have to emphasize that this classification is completely conceptual and only serves to exclude the parts that are not studied in this thesis. Therefore, we refer the reader to the authoritative resources of the involved physiology, e.g., [90]. We start with a somewhat detailed sensory classification to support our choice of amplitude-frequency based grouping.

Typically, the touch perception is also classified into these two groups; tactile feedback and kinesthetic (proprioceptive) feedback, hence the naming of the involved technologies. For practical purposes, one can use the analogy of parallel connected high-pass and low-pass filters to indicate the frequency band of interest respectively. For our control-oriented context, let us define a few key concepts with an engineering point of view.

In physiology, the sensors on the skin which take different physical measurements are called *receptors* and prefixed with their area of specialization such as *thermoreceptors*, *mechanoreceptors*, *nocioreceptors* (pain) etc. The signals that trigger an action on these receptors are denoted as the *stimuli*. In case of a stimulus, these receptors, through some chemical processes, exhibit a series of *action potentials* or electrical discharge pulses i.e. a *spike train*. In the engineering terminology, this can be modeled as a nonuniform Dirac comb with varying frequency as a function of the stimuli intensity or a digital frequency modulation (FM) signal. The frequency

---

[1]In the Fourier analysis sense

increases with the stimulus intensity. Furthermore, at the input side of this sensor there is a dead-zone nonlinearity hence the stimuli should exceed a particular threshold to trigger a receptor firing.

There is also another process, called *neural* or *sensorial adaptation* which quantifies the frequency decay of firing under constant stimulus. We can see the tangible effect of this process frequently e.g., our nose looses the sensitivity to a powerful smell if exposed to it for some time or we stop noticing the touch of glasses on the face or the ring on the finger. Some sensors have a slow decay rate whereas others decay in a matter of seconds. The slow sensors often called the *slowly adapting (SA)* and others are called *fast adapting (FA)* or *rapidly adapting* type [17].

As shown in Table B.1, and also surveyed in [101], there are four main types of mechanisms that are utilized for the force and texture sensing with varying operating conditions and spatial authority. Although all contribute to the high frequency stimulus perception with varying levels, slowly adapting receptors are mainly tuned to detect the low frequency information range (up to 30 Hz). The fast adapting Meissner(FAI) and Pacinian(FAII) Corpuscles can be excited in the frequency range of $[10,60]$ Hz and $[60,1000]$ Hz respectively. Thus, small-area receptors (Type I) are excited with the rate of skin deformation whereas relatively large-area receptors (Type II) are with the acceleration of the skin. Moreover, FAI units are located closer to the skin surface, have high unit density with small surface area forming a grid of sensors. On the other hand, FAII units are located in the subcutaneous tissue and work as a single load cell with relatively large surface area. This allows experts to assume that FAI units are mainly responsible for spatial information about the skin deformation and FAII units are responsible for the high frequency information with response delays in the range of $[50,500]$ ms [202]. Another interesting note in [101] is that due to their single unit nature FAII units offers the possibility to provide high frequency information with a single vibration display, while for FAI units it is more appropriate to supply an array of haptic displays for lower frequency range.

The SAI disk receptor has a small, localized receptive surface area as opposed to the SAII with a large field with a decaying sensitivity from center to the edges. Individual Ruffini endings are excited by stretch of the skin in specific directions. The majority of hand receptors consists of FAI units ($> 40\%$), then SAI units cover almost a quarter which followed by SAII covering 19% and FAII 13%.

B.1.1   *Weber ratio and Just-Noticeable-Difference(JND)*

The Weber ratio is defined as the ratio between the minimal stimulus intensity change in any physical quantity that triggers a change perception and the intensity of the stimulus. In case of a constant or static stimulus, the ratio is denoted with Just-Noticeable- Difference (JND). For engineering purposes, this derived unit can be beneficial to design the frequency behavior of the haptic systems which exhibit a particular sensitivity pattern.

Feature	Meissner Corpuscles (FAI)	Pacinian Corpuscles (FAII)	Merkel's Disks (SAI)	Ruffini Endings (SAII)
Rate of adaptation	Rapid	Rapid	Slow	Slow
Location	Superficial dermis	Dermis and subcutaneous	Basal epidermis	Dermis and subcutaneous
Mean receptive area	$13\,mm^2$	$101\,mm^2$	$11\,mm^2$	$59\,mm^2$
Spatial resolution	Poor	Very poor	Good	Fair
Sensory units	43%	13%	25%	19%
Response frequency range	$[10,200]$ Hz	$[70,1000]$ Hz	$[0.4,100]$ Hz	$[0.4,100]$ Hz
Min. threshold frequency	40 Hz	$[200,250]$ Hz	50 Hz	50 Hz
Sensitive to temperature	No	Yes	Yes	At > 100 Hz
Spatial summation	Yes	No	No	Unknown
Temporal summation	Yes	No	No	Yes
Physical parameter sensed	Skin curvature, velocity, local shape,flutter, slip	Vibration, slip, acceleration	Skin curvature, local shape, pressure	Skin stretch, local force

Table B.1: Functional Features of Cutanous Mechanoreceptors (Adapted from [202])

B.1.2 *Tactile Feedback*

Tactile feedback, in general, is utilized to distinguish fine details such as shape, curvature, vibration, acceleration, and texture perception. Hence, the high-frequency content of the touch information is indispensable to transmit such information. Since the amplitude of the motion at these frequencies are quite small, the palm and finger tissues act as a low-pass filter and avoid such information to penetrate into the skin. Thus, only a limited part of the sensors have access to this information.

A striking example to the mind-boggling quality of feedback is the Braille system used by visually impaired or disabled individuals (Figure B.1). The average reading speed with Braille system is about 125-150 words per minute ([1]) in contrast with 200-250 words per minute by eyesight.

Most of today's technological devices utilize this modality to send and receive information. Many mobile phone applications and a few gaming consoles such as Nintendo Wii™, Sony Playstation ™ etc., utilize short vibrational patterns to alert the user that some action has been performed e.g. the user hovers over a hot spot on the screen or some moving object hits an obstacle etc.

The tactile technology is, thus, concerned with the vibrational pattern and high-frequency sweep of stimuli. Communication via small vibrational or textural subtleties allows the tactile technology to focus on the low-stroke, high-bandwidth haptic displays. The required low-stroke action is often generated by a small and agile electrical motor with a load eccentricity with respect to the rotor shaft axis. The angular velocity of the motor then defines the frequency of the vibration. Since the involved mechanisms on the human limbs and hands are rapidly adapting, the bus speed in this modality can be very high compared to the kinesthetic feedback in which the human should track and pick out patterns from relatively slow and large-amplitude motion profiles via measuring muscle stretch amount and various other quantities.
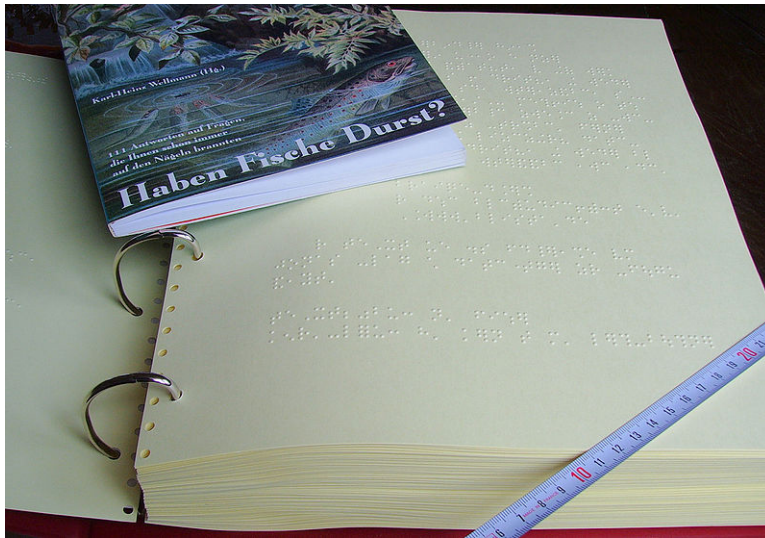
Figure B.1: A comparative case for the spatial resolution: The volume of the same content in the form of Braille and regular text (Karl-Heinz Wellmann, **[Wikipedia:Brailleschrift]**)

B.1.3 *Kinesthetic (Proprioceptive) Feedback*

Proprioception[2] (*Proprius+perceptio* : the act of gathering/perceiving of own) is the ability to sense the limb configurations and motion without using a visual aid (cf. vestibular feedback which is to used to sense the balance and the spatial body orientation). Kinesthetic feedback, together with limited force sensing abilities of muscles and tendons and relatively small interference of tactile feedback system, is "vital" to have control of our own body. It's a futile attempt to describe the importance of this often overlooked perception (or hidden sense) other than referring to the 1998 BBC *Horizon* documentary "*The man who lost his body*" and the paper [123] about Ian Waterman. He is the only person known to date who can cope with the loss of proprioceptive feedback while still being able to stand up, walk, maintain posture etc. without any artificial support. Unfortunately, he is completely dependent on his visual feedback as he tirelessly computes trajectories of his body parts on-the-fly to compensate for the loss of kinesthetic feedback even when gesturing with hands.

Thus, whether we are aware of it or not, proprioception is indispensable for us to survey the environment. The force on our limbs, our body configuration at that instance, and our body motion are sensed via sensors in the joints, muscle tendons and muscles themselves. Unlike the tactile feedback characteristics given previously, the compliance, the distribution of pressure and and the shape information is measured in a relatively coarse fashion. Hence, when combined with tactile feedback

---

[2]We will not go into the nuances between kinesthetic and proprioceptive feedback

and the brain's internal comparison database, we use an unparalleled sophistication to actually perceive the environment without using any visual feedback, even if the object is foreign to us. In [11], a convenient summary of the properties is presented. Distilling even further for a general picture about the proprioception, we provide the following quick facts.

The compression or stretch of the receptors covered previously changes the amplitude of the impulse of the action potential which, in turn, used as the position information. Similarly the frequency of these firings are interpreted as the velocity information. For the limb position and motion, the bandwidth of the kinesthetic sensing is around [20,30] Hz with varying accuracy in terms of JND around [0.8,2.5]°. Moreover, the control bandwidth is reported to be task-dependent: [1,2] Hz for unexpected signals; [2,5] Hz for periodic signals, < 5 Hz for generated or learned trajectories and finally about 10 Hz for reflex actions.

Regarding the force sensing, it has been experimentally demostrated that pressure JND decreases as the pressure area increases; e.g., the overall average JND drops to 3.7% with a contact area of 20.27 cm^2 from 15.6% with a contact area of 1.27 cm^2.

The kinesthetic technology can be used in conjunction with tactile technology to provide a full manipulative immersion. Moreover, in the case of *exoskeletons*, it can be the essential ingredient to protocol between the environment and the human body. Especially, rehabilitation patients can benefit from such technologies via combining the visual and the kinesthetic feedback to amplify the disabled or impaired control action of the problematic limb. Thus, kinesthetic technology is mainly involved as low-frequency based manipulative or explorative motion tasks. Considering the current hardware limitations, many tasks depend primarily and rather primitively on kinesthetic cues for bilateral teleoperation and virtual reality applications.

B.1.4 *Teleoperation*

Teleoperation is the general name for providing human actions to a different media that is not accessible (or only in a costly way) to direct contact in a precise fashion. Microcomponent assembly, minimal invasive surgery (MIS), space station maintenance and construction, underwater exploration and construction are all typical application examples that the human either can not be present or physically interact with comfortably. The *da Vinci*™ surgery robot from Intuitive Surgical Inc. is a well-known example of *unilateral* human manipulation to achieve high precision tracking with surgical tools inside very tight incisions.

However, as often motivated by the *bilateral* teleoperation studies, the human operators, expecially the experienced ones, often lack the ability to employ their precise tactile and kinesthetic abilities to take decisions or to monitor their progress since they rely on vision feedback from the cameras exclusively. In some particular practices, surgeons might resort to inserting their fingers inside the incision to feel the relevant tissue stiffness difference to get a better spatial understanding when the view is contaminated with blood or other bodily fluids. In the case of an obstruction

during an insertion of an instrument into the body, they might tend to correct the instrument based on their force feel at hand. Hence, the realism is diminished as opposed to the increased precision by the teleoperation methods.

B.1.5   *(Computer) Haptics*

In general, haptics technology encompasses all the items that have been covered up to this point. However, it is also often used as a placeholder for the concept of creating artificial or virtual object perception with a force-feedback capable device. Computer haptics also have additional challenges such as rendering deformations in case of a soft object or realistic graphical presentation of object interaction in terms of collisions etc. In other words, not only the forces are important but the consequences of these force interactions need to be handled in a precise fashion. Conversely, computer haptics is free from the hardware limitations or the noisy measurements, as the objects and the physical laws that they should obey are computer generated.

B.1.6   *Virtual Reality*

This term refers to a set of artificially generated immersion techniques that can rely on either a single or multiple modalities at once. The common applications consist of special googles that cover the human vision. By tracking the head movements and adjusting the scene that is projected onto the special headset, the user can immerse into the artificial environment. Combined with headphones and if possible with haptics, the experience can be substantially improved. Especially haptics can increase the immersion level much more compared to only visual+audio supplements since otherwise the realism can be destroyed quickly if the user tries to touch any object or surface while actually waving his hand. The persuasiveness of the scene depicted on the headset needs to be backed up with at least a slight kinesthetic feedback, if not tactile, since the loss of tactile feedback is relatively less important in an exploration task.

References

[1] American Council of the Blind. *A Brief Description of Braille*. 06/2012 (cit. on p. 161).
     URL: `http://acb.org/node/67`.

[2] B. D. O. Anderson, R. Newcomb, and J. Zuidweg. "On the Existence of *H* Matrices".
     In: *IEEE Transactions on Circuit Theory* 13.1 (1966), pp. 109–110 (cit. on p. 154).
     DOI: `10.1109/TCT.1966.1082537`.

[3] R. Anderson and M. Spong. "Bilateral control of teleoperators with time delay". In:
     IEEE Transactions on Automatic Control 34.5 (1989), pp. 494–501 (cit. on pp. 18, 28, 34,
     36, 41, 42, 72, 79).
     DOI: `10.1109/9.24201`.

[4] C. Andriot and R. Fournier. "Bilateral control of teleoperators with flexible joints by
     the H_∞ approach". In: *Telemanipulator Technology*. Ed. by H. Das. Vol. 1833. 1. Boston,
     MA, USA: SPIE, 1993, pp. 80–91 (cit. on p. 29).
     DOI: `10.1117/12.142099`.

[5] P. Arcara and C. Melchiorri. "Control schemes for teleoperation with time delay: A
     comparative study". In: *Robotics and Autonomous Systems* 38.1 (2002), pp. 49–64 (cit. on
     p. 72).
     DOI: `10.1016/S0921-8890(01)00164-6`.

[6] J. Atkinson. "The Recording Angel". In: *Stereophile* 33.2 (2010), p. 3 (cit. on p. 56).
     URL: `http://www.stereophile.com/content/recording-angel`.

[7] A. Aziminejad, M. Tavakoli, R. V. Patel, and M. Moallem. "Transparent Time-Delayed
     Bilateral Teleoperation Using Wave Variables". In: *IEEE Transactions on Control Systems
     Technology* 16.3 (2008), pp. 548–555 (cit. on p. 72).
     DOI: `10.1109/TCST.2007.908222`.

[8] H. Bart, I. Gohberg, M. A. Kaashoek, and A. C. M. Ran. *A State Space Approach to
     Canonical Factorization with Applications*. Vol. 200. Operator Theory: Advances and
     Applications. Springer-Verlag, 2010, p. 432 (cit. on p. 108).
     DOI: `10.1007/978-3-7643-8753-2`.

[9] L. Basañez and R. Suárez. "Teleoperation". In: *Springer Handbook of Automation*. Ed. by
     S. Y. Nof. Springer Berlin Heidelberg, 2009, pp. 449–468 (cit. on p. 18).
     DOI: `10.1007/978-3-540-78831-7_27`.

[10] A. Bemporad. "Predictive control of teleoperated constrained systems with unbounded
     communication delays". In: *Proceedings of 37th IEEE Conference on Decision and Control*.
     Vol. 2. 1998, pp. 2133–2138 (cit. on p. 44).
     DOI: `10.1109/CDC.1998.758651`.

[11] S. J. Biggs and M. A. Srinivasan. "Haptic Interfaces". In: ed. by K. M. Stanney. Vol. 39. Handbook of virtual environments: Design, implementation, and applications.Human factors and ergonomics. Lawrence Erlbaum Associates, 2002. Chap. 5, pp. 93–116 (cit. on p. 163).

[12] H. Boessenkool, D. A. Abbink., C. J. Heemskerk, and F. C. van der Helm. "Haptic shared control improves tele-operated task performance towards performance in direct control". In: *Proceedings of IEEE World Haptics Conference, (WHC)*. 2011, pp. 433–438 (cit. on p. 52).
DOI: `10.1109/WHC.2011.5945525`.

[13] E. F. Bolinder. "Survey of Some Properties of Linear Networks". In: *IRE Transactions on Circuit Theory* 4.3 (1957), pp. 70–78 (cit. on p. 32).
DOI: `10.1109/TCT.1957.1086385`.

[14] S. Boyd, L. E. Ghaoui, E. Feron, and V. Balakrishnan. *Linear Matrix Inequalities in System and Control Theory*. Vol. 15. Studies in Applied Mathematics. Society for Industrial and Applied Mathematics (SIAM), 1994 (cit. on p. 82).

[15] S. P. Buerger and N. Hogan. "Complementary Stability and Loop Shaping for Improved Human–Robot Interaction". In: *IEEE Transactions on Robotics* 23.2 (2007), pp. 232–244 (cit. on pp. 28, 29, 90).
DOI: `10.1109/TRO.2007.892229`.

[16] S. P. Buerger, H. Krebs, and N. Hogan. "Characterization and control of a screw-driven robot for neurorehabilitation". In: *Control Applications, 2001. (CCA '01). Proceedings of the 2001 IEEE International Conference on*. 2001, pp. 388–394 (cit. on p. 28).
DOI: `10.1109/CCA.2001.973896`.

[17] G. Burdea. *Force and touch feedback for Virtual Reality*. New York: Wiley, 1996 (cit. on pp. 18, 160).

[18] P. Buttolo, P. Braathen, and B. Hannaford. "Sliding control of force reflecting teleoperation - Preliminary studies". In: *Presence* 3.2 (1994), pp. 158–172 (cit. on p. 44).

[19] M. C. Çavuşoğlu, A. Sherman, and F. Tendick. "Design of bilateral teleoperation controllers for haptic exploration and telemanipulation of soft environments". In: *IEEE Transactions on Robotics and Automation* 18.4 (2002), pp. 641–647 (cit. on pp. 53–55).
DOI: `10.1109/TRA.2002.802199`.

[20] W.-K. Chen. *Active network analysis*. Singapore Teaneck, N.J: World Scientific, 1991 (cit. on pp. 30, 32).

[21] H. C. Cho and J. H. Park. "Impedance Control with Variable Damping for Bilateral Teleoperation under Time Delay". In: *JSME International Journal Series C Mechanical Systems, Machine Elements and Manufacturing* 48.4 (2005), pp. 695–703 (cit. on p. 75).

[22] N. Chopra, P. Berestesky, and M. W. Spong. "Bilateral Teleoperation Over Unreliable Communication Networks". In: *IEEE Transactions on Control Systems Technology* 16.2 (2008), pp. 304–313 (cit. on p. 43).
DOI: `10.1109/TCST.2007.903397`.

[23] N. Chopra, M. W. Spong, R. Ortega, and N. E. Barabanov. "On tracking performance in bilateral teleoperation". In: *IEEE Transactions on Robotics* 22.4 (2006), pp. 861–866 (cit. on p. 42).

DOI: `10.1109/TRO.2006.878942`.

[24]   G. A. V. Christiansson. "Wave Variables and the 4 Channel Architecture for Haptic Teleoperation". In: *Haptics: Perception, Devices and Scenarios*. Vol. 5024. Lecture Notes in Computer Science. Springer Berlin / Heidelberg, 2008, pp. 169–174 (cit. on p. 42). DOI: `10.1007/978-3-540-69057-3_20`.

[25]   G. A. Christiansson. "Hard Master Soft Slave Haptic Teleoperation". PhD thesis. Delft University of Technology, 2007 (cit. on p. 53). URL: `http://repository.tudelft.nl/assets/uuid:9c06083b-1140-4acb-a788-01d28ca97e70/3me_christiansson_20071012.pdf`.

[26]   E. J. Colgate. "The control of dynamically interacting systems". PhD thesis. Massachusetts Institute of Technology, 1988 (cit. on p. 30). DOI: `1721.1/14380`.

[27]   E. J. Colgate and N. Hogan. "Robust control of dynamically interacting systems". In: *International Journal of Control* 48.1 (1988), pp. 65–88 (cit. on pp. 22, 27, 30). DOI: `10.1080/00207178808906161`.

[28]   J. E. Colgate. "Coordinate Transformations and Logical Operations for Minimizing Conservativeness in Coupled Stability Criteria". In: *Journal of Dynamic Systems, Measurement, and Control* 116.4 (1994), pp. 643–649 (cit. on pp. 34, 35, 78, 79). DOI: `10.1115/1.2899263`.

[29]   J. Colgate. "Robust impedance shaping telemanipulation". In: *IEEE Transactions on Robotics and Automation* 9.4 (1993), pp. 374–384 (cit. on pp. 29, 78). DOI: `10.1109/70.246049`.

[30]   J. Colgate and J. Brown. "Factors affecting the Z-Width of a haptic display". In: *IEEE International Conference on Robotics and Automation*. Vol. 4. 1994, pp. 3205–3210 (cit. on pp. 52, 53). DOI: `10.1109/ROBOT.1994.351077`.

[31]   J. Colgate and G. Schenkel. "Passivity of a class of sampled-data systems: Application to haptic interfaces". In: *Journal of Robotic Systems* 14.1 (1997), pp. 37–47 (cit. on pp. 78, 79). DOI: `10.1002/(SICI)1097-4563(199701)14:1<37::AID-ROB4>3.0.CO;2-V`.

[32]   R. Daniel and P. McAree. "Fundamental Limits of Performance for Force Reflecting Teleoperation". In: *The International Journal of Robotics Research* 17.8 (1998), pp. 811–830 (cit. on pp. 47, 48, 85, 145). DOI: `10.1177/027836499801700801`.

[33]   E. Delgado, M. Diaz-Cacho, D. Bustelo, and A. Barreiro. "Generic Approach to Stability Under Time-Varying Delay in Teleoperation: Application to the Position-Error Control of a Gantry Crane". In: *IEEE/ASME Transactions on Mechatronics* PP.99 (2012), pp. 1–11 (cit. on p. 72). DOI: `10.1109/TMECH.2012.2208758`.

[34]   E. Delgado, A. Barreiro, and M. Díaz-Cacho. "Delay and its time-derivative dependent Stability of teleoperation systems". In: *IEEE International Symposium on Industrial Electronics (ISIE)*. 2010, pp. 137–142 (cit. on p. 72). DOI: `10.1109/ISIE.2010.5637613`.

[35]   E. Delgado, M. Díaz-Cacho, and A. Barreiro. "Stability of Teleoperation Systems for Time-Varying Delays by Neutral LMI Techniques". In: *Mathematical Problems in Engineering* 2012 (2012), pp. 1–17 (cit. on p. 72).
DOI: 10.1155/2012/467629.

[36]   C. A. Desoer and M. Vidyasagar. *Feedback Systems: Input-Output Properties*. Electrical Science Series. Academic Press, New York, 1975, p. 280 (cit. on pp. 33, 67, 154).

[37]   N. Dhruv and F. Tendick. "Frequency Dependence of Compliance Contrast Detection". In: *Proceedings of the ASME Dynamic Systems and Control Division*. Vol. 69. 2000, pp. 1087–1093 (cit. on p. 54).

[38]   J. Dudragne, C. Andriot, R. Fournier, and J. Vuillemey. "A Generalized Bilateral Control Applied to Master-Slave Manipulators". In: *Proceedings of the 20th international symposium on industrial robots*. 1989, pp. 435–442 (cit. on pp. 27, 49).

[39]   G. E. Dullerud and F. Paganini. *A Course in Robust Control Theory: A Convex Approach (Texts in Applied Mathematics)*. 2nd ed. Vol. 36. Texts in Applied Mathematics. Springer, 2005, p. 444 (cit. on p. 55).

[40]   M. Dyck, A. Jazayeri, and M. Tavakoli. "Is the human operator in a teleoperation system passive?" In: *World Haptics Conference (WHC), 2013*. 2013, pp. 683–688 (cit. on p. 23).
DOI: 10.1109/WHC.2013.6548491.

[41]   M. Edwards and J. Sinsky. "A new criterion for linear 2-port stability using a single geometrically derived parameter". In: *IEEE Transactions on Microwave Theory and Techniques* 40.12 (1992), pp. 2303–2311 (cit. on pp. 35, 77, 78, 80, 81, 157).
DOI: 10.1109/22.179894.

[42]   E. Eisenberg. *The Recording Angel: Explorations in Phonography*. Mcgraw-Hill, 1986 (cit. on p. 57).

[43]   S. E.Salcudean, M. Zhu, W.-H. Zhu, and K. Hashtrudi-Zaad. "Transparent Bilateral Teleoperation under Position and Rate Control". In: *The International Journal of Robotics Research* 19.12 (2000), pp. 1185–1202 (cit. on p. 38).
DOI: 10.1177/02783640022068020.

[44]   L. Eusebi and C. Melchiorri. "Force reflecting telemanipulators with time-delay: stability analysis and control design". In: *IEEE Transactions on Robotics and Automation* 14.4 (1998), pp. 635–640 (cit. on p. 72).
DOI: 10.1109/70.704237.

[45]   J. F. F. Sturm. "Using SeDuMi 1.02, a Matlab Toolbox for Optimization Over Symmetric Cones," in: *Optimization Methods and Software* 11.12 (1999), pp. 625–653 (cit. on p. 85).

[46]   M. Fan, A. Tits, and J. Doyle. "Robustness in the presence of mixed parametric uncertainty and unmodeled dynamics". In: *IEEE Transactions on Automatic Control* 36.1 (1991), pp. 25–38 (cit. on pp. 70, 82).
DOI: 10.1109/9.62265.

[47]   B. A. Francis. *A Course on $\mathcal{H}_\infty$ Control Theory*. Vol. 88. Lecture Notes in Control and Information Sciences. Springer Berlin / Heidelberg, 1987 (cit. on pp. 83, 109).
DOI: 10.1007/BFb0007371.

[48] M. Fu, H. Li, and S. Niculescu. "Robust stability and stabilization of time-delay systems via integral quadratic constraint approach". In: *Stability and Control of Time-delay Systems*. Ed. by L. Dugard and E. Verriest. Vol. 228. Lecture Notes in Control and Information Sciences. Springer Berlin / Heidelberg, 1998, pp. 101–116 (cit. on p. 72).
DOI: `10.1007/BFb0027482`.

[49] M. J. Fu and M. C. Çavuşoğlu. "Three-dimensional human arm and hand dynamics and variability model for a stylus-based haptic interface". In: *IEEE International Conference on Robotics and Automation (ICRA)*. 2010, pp. 1339–1346 (cit. on p. 29).
DOI: `10.1109/ROBOT.2010.5509927`.

[50] K. Furuta, K. Kosuge, Y. Shiote, and H. Hatano. "Master-slave manipulator based on virtual internal model following control concept". In: *Proc. IEEE Int. Conf. Robotics and Automation*. Vol. 4. 1987, pp. 567–572 (cit. on p. 18).
DOI: `10.1109/ROBOT.1987.1088064`.

[51] P. Gahinet. "Explicit controller formulas for LMI-based H_∞ synthesis". In: *Automatica* 32.7 (1996), pp. 1007–1014 (cit. on p. 97).
DOI: `10.1016/0005-1098(96)00033-7`.

[52] P. Gahinet and P. Apkarian. "A linear matrix inequality approach to H_∞ control". In: *International Journal of Robust and Nonlinear Control* 4.4 (1994), pp. 421–448 (cit. on pp. 97, 113).
DOI: `10.1002/rnc.4590040403`.

[53] P. J. Gawthrop and G. P. Bevan. "Bond-graph modeling". In: *IEEE Control Systems Magazine* 27.2 (2007), pp. 24–45 (cit. on p. 21).

[54] M. A. Geeves and K. C. Holmes. "Structural mechanism of muscle contraction." In: *Annual Review of Biochemistry* 68 (1999), pp. 687–728 (cit. on pp. 23, 24).
DOI: `10.1146/annurev.biochem.68.1.687`.

[55] R. C. Goertz and W. M. Thompson. "Elecrtonically Controlled Manipulator". In: *Nucleonics* 12.12 (1954), pp. 46–47 (cit. on p. 18).

[56] K.-C. Goh. "Canonical factorization for generalized positive real transfer functions". In: *Proc. 35th IEEE Conf. Decision and Control (CDC)*. Vol. 3. 1996, pp. 2848–2853 (cit. on pp. 91, 105, 108, 112).
DOI: `10.1109/CDC.1996.573550`.

[57] K.-C. Goh. "Structure and factorization of quadratic constraints for robustness analysis". In: *Proc. 35th IEEE Conf. Decision and Control (CDC)*. Vol. 4. 1996, pp. 4649–4654 (cit. on pp. 91, 105, 107).
DOI: `10.1109/CDC.1996.577607`.

[58] A. Haddadi and K. Hashtrudi-Zaad. "Bounded-Impedance Absolute Stability of Bilateral Teleoperation Control Systems". In: *IEEE Transactions on Haptics* 3 (2009), pp. 15–27 (cit. on pp. 68, 75, 78, 81).
DOI: `10.1109/TOH.2009.48`.

[59] B. Hannaford. "A design framework for teleoperators with kinesthetic feedback". In: *IEEE Transactions on Robotics and Automation* 5.4 (1989), pp. 426–434 (cit. on pp. 18, 19, 28, 49).
DOI: `10.1109/70.88057`.

[60]   B. Hannaford and J.-H. Ryu. "Time-domain passivity control of haptic interfaces". In: *IEEE Transactions on Robotics and Automation* 18.1 (2002), pp. 1–10 (cit. on pp. 20, 43).
        DOI: 10.1109/70.988969.

[61]   K. Hashtrudi-Zaad and S. Salcudean. "Transparency in time-delayed systems and the effect of local force feedback for transparent teleoperation". In: *IEEE Transactions on Robotics and Automation* 18.1 (2002), pp. 108–114 (cit. on p. 38).
        DOI: 10.1109/70.988981.

[62]   K. Hashtrudi-Zaad and S. E. Salcudean. "Analysis of Control Architectures for Tele-operation Systems with Impedance/Admittance Master and Slave Manipulators". In: *The International Journal of Robotics Research* 20.6 (2001), pp. 419–445 (cit. on p. 75).
        DOI: 10.1177/02783640122067471.

[63]   K. Hashtrudi-Zaad and S. E. Salcudean. "On the use of local force feedback for transparent teleoperation". In: *Proc. IEEE International Conference on Robotics and Automation*. Vol. 3. 1999, pp. 1863–1869 (cit. on pp. 38, 39).
        DOI: 10.1109/ROBOT.1999.770380.

[64]   K. Hashtrudi-Zaad and S. E. Salcudean. "Transparency in time-delayed systems and the effect of local force feedback for transparent teleoperation". In: *IEEE Transactions on Robotics and Automation* 18.1 (2002), pp. 108–114 (cit. on p. 40).
        DOI: 10.1109/70.988981.

[65]   S. S. Haykin. *Active Network Theory*. Addison-Wesley Series in Electrical Engineering. Addison-Wesley, 1970 (cit. on pp. 30, 81).

[66]   M. V. Headrick. "Origin and evolution of the anchor clock escapement". In: *IEEE Control Systems Magazine* 22.2 (2002), pp. 41–52 (cit. on p. 24).
        DOI: 10.1109/37.993314.

[67]   A. Helmersson. "An IQC-based Stability Criterion for Systems with Slowly Varying Parameters". In: *14th World Congress of IFAC*. Vol. F. IFAC. Beijing, China, 1999, pp. 525–530 (cit. on p. 71).

[68]   A. Helmersson. "Employing Kronecker Canonical Form for LMI-Based H_∞ Synthesis Problems". In: *IEEE Transactions on Automatic Control* 57.8 (2012), pp. 2062–2067 (cit. on p. 113).
        DOI: 10.1109/TAC.2011.2179846.

[69]   A. Helmersson. "IQC Synthesis based on Inertia Constraints". In: *14th World Congress of IFAC*. Beijing,China, 1999, pp. 163–168 (cit. on p. 105).

[70]   R. Hendrix. "Robotically assisted eye surgery: A haptic master console". PhD thesis. Technische Universiteit Eindhoven, 2010 (cit. on pp. 117, 118).
        URL: http://alexandria.tue.nl/extra2/696904.pdf.

[71]   D. Hill and P. Moylan. "Stability results for nonlinear feedback systems". In: *Automatica* 13.4 (1977), pp. 377–382 (cit. on p. 154).
        DOI: 10.1016/0005-1098(77)90020-6.

[72]   S. Hirche and M. Buss. "Human-Oriented Control for Haptic Teleoperation". In: *Proceedings of the IEEE* 100.3 (2012), pp. 623–647 (cit. on pp. 42, 81).
        DOI: 10.1109/JPROC.2011.2175150.

[73] S. Hirche, M. Ferre, J. Barrio, C. Melchiorri, and M. Buss. "Bilateral Control Archi-
      tectures for Telerobotics". In: *Advances in Telerobotics*. Ed. by M. Ferre, M. Buss, R.
      Aracil, C. Melchiorri, and C. Balaguer. Vol. 31. Springer Tracts in Advanced Robotics.
      Springer Berlin Heidelberg, 2007, pp. 163–176 (cit. on pp. 49, 148).
      DOI: 10.1007/978-3-540-71364-7_11.

[74] Histoire de la Television. *Paul Nipkow*. 04/2013 (cit. on p. 10).
      URL: http://histv2.free.fr/nipkow/nipkow1884a.htm.

[75] N. Hogan. "Controlling impedance at the man/machine interface". In: *IEEE Interna-
      tional Conference on Robotics and Automation (ICRA)*. Vol. 3. 1989, pp. 1626–1631 (cit. on
      pp. 22, 23, 28).
      DOI: 10.1109/ROBOT.1989.100210.

[76] N. Hogan. "Impedance Control: An Approach to Manipulation: Part I — Theory".
      In: *Journal of Dynamic Systems, Measurement, and Control* 107.1 (1985), pp. 1–7 (cit. on
      p. 21).
      DOI: 10.1115/1.3140702.

[77] N. Hogan. "Impedance Control: An Approach to Manipulation: Part II — Implemen-
      tation". In: *Journal of Dynamic Systems, Measurement, and Control* 107.1 (1985), pp. 8–16
      (cit. on p. 21).
      DOI: 10.1115/1.3140713.

[78] N. Hogan. "Impedance Control: An Approach to Manipulation: Part III — Applica-
      tions". In: *Journal of Dynamic Systems, Measurement, and Control* 107.1 (1985), pp. 17–24
      (cit. on p. 21).
      DOI: 10.1115/1.3140701.

[79] P. F. Hokayem and M. W. Spong. "Bilateral teleoperation: An historical survey". In:
      Automatica 42.12 (2006), pp. 2035–2057 (cit. on pp. 18, 44, 56, 72).
      DOI: 10.1016/j.automatica.2006.06.027.

[80] R. Horowits and R. J. Podolsky. "The positional stability of thick filaments in activated
      skeletal muscle depends on sarcomere length: evidence for the role of titin filaments."
      In: *The Journal of Cell Biology* 105.5 (1987), pp. 2217–2223 (cit. on p. 23).
      DOI: 10.1083/jcb.105.5.2217.

[81] J. C. Houk and Z. W. Rymer. "Neural Control of Muscle Length and Tension". In:
      Comprehensive Physiology. Vol. II. John Wiley & Sons, Inc., 2011. Chap. 8, pp. 257–323
      (cit. on p. 26).
      DOI: 10.1002/cphy.cp010208.

[82] Z. Hu, S. Salcudean, and P. Loewen. "Robust controller design for teleoperation
      systems". In: *IEEE International Conference on Systems, Man and Cybernetics*. Vol. 3.
      1995, pp. 2127–2132 (cit. on p. 29).
      DOI: 10.1109/ICSMC.1995.538094.

[83] W. Iida and K. Ohnishi. "Reproducibility and operationality in bilateral teleoperation".
      In: *Proceedings of 8th IEEE International Workshop on Advanced Motion Control (AMC)*.
      2004, pp. 217–222 (cit. on p. 56).
      DOI: 10.1109/AMC.2004.1297669.

[84]   T. Iwasaki and S. Hara. "Generalized KYP lemma: unified frequency domain inequalities with design applications". In: *IEEE Transactions on Automatic Control* 50.1 (2005), pp. 41–59 (cit. on p. 67).
DOI: 10.1109/TAC.2004.840475(410)50.

[85]   T. Iwasaki and S. Hara. "Well-posedness of feedback systems: insights into exact robustness analysis and approximate computations". In: *IEEE Transactions on Automatic Control* 43.5 (1998), pp. 619–630 (cit. on p. 63).
DOI: 10.1109/9.668829.

[86]   A. Jazayeri and M. Tavakoli. "Revisiting Llewellyn's absolute stability criterion for bilateral teleoperation systems under non-passive operator or environment". In: *IEEE/RSJ International Conference on Intelligent Robots and Systems (IROS)*. 2012, pp. 70–75 (cit. on pp. 79–81).
DOI: 10.1109/IROS.2012.6385949.

[87]   U. Jönsson and A. Rantzer. "Systems with Uncertain Parameters – Time-Variations with Bounded Derivatives". In: *International Journal of Robust and Nonlinear Control* 6.9/10 (1996), pp. 969–982 (cit. on p. 71).

[88]   M. Jun and M. Safonov. "Rational multiplier IQCs for uncertain time-delays and LMI stability conditions". In: *IEEE Transactions on Automatic Control* 47.11 (2002), pp. 1871–1875 (cit. on p. 72).
DOI: 10.1109/TAC.2002.804477.

[89]   P. Kammermeier, A. Kron, J. Hoogen, and G. Schmidt. "Display of Holistic Haptic Sensations by Combined Tactile and Kinesthetic Feedback". In: *Presence: Teleoperators and Virtual Environments* 13.1 (2004), pp. 1–15 (cit. on p. 59).
DOI: 10.1162/105474604774048199.

[90]   E. Kandel, J. Schwartz, T. Jessell, S. Siegelbaum, and A. Hudspeth, eds. *Principles of Neural Science*. 5th ed. McGraw-Hill, 2000, p. 1760 (cit. on p. 159).

[91]   C.-Y. Kao and A. Rantzer. "Stability analysis of systems with uncertain time-varying delays". In: *Automatica* 43.6 (2007), pp. 959–970 (cit. on p. 72).
DOI: 10.1016/j.automatica.2006.12.006.

[92]   S. Katsura, W. Iida, and K. Ohnishi. "Medical mechatronics – An application to haptic forceps". In: *Annual Reviews in Control* 29.2 (2005), pp. 237–245 (cit. on p. 56).
DOI: 10.1016/j.arcontrol.2005.05.003.

[93]   H. Kazerooni, T.-I. Tsay, and K. Hollerbach. "A controller design framework for telerobotic systems". In: *IEEE Transactions on Control Systems Technology* 1.1 (1993), pp. 50–62 (cit. on pp. 26, 28, 29).
DOI: 10.1109/87.221351.

[94]   B. Khademian and K. Hashtrudi-Zaad. "Unconditional stability analysis of dual-user teleoperation systems". In: *Proceedings of IEEE Haptics Symposium*. 2010, pp. 161–166 (cit. on pp. 75, 76).
DOI: 10.1109/HAPTIC.2010.5444660.

[95]   H. K. Khalil. *Nonlinear Systems*. 3rd ed. Prentice Hall, 2002 (cit. on pp. 30, 81).

[96]   R. Kilchenman and M. Goldfarb. "Force saturation, system bandwidth, information transfer, and surface quality in haptic interfaces". In: *Proc. ICRA Robotics and Automation IEEE Int. Conf.* Vol. 2. 2001, pp. 1382–1387 (cit. on p. 52).

DOI: `10.1109/ROBOT.2001.932803`.

[97]   J.-P. Kim and J. Ryu. "Robustly Stable Haptic Interaction Control using an Energy-bounding Algorithm". In: *The International Journal of Robotics Research* 29.6 (2010), pp. 666–679 (cit. on p. 44).
DOI: `10.1177/0278364909338770`.

[98]   K. Kim, E. J. Colgate., J. Santos-Munne, A. Makhlin, and M. Peshkin. "On the Design of Miniature Haptic Devices for Upper Extremity Prosthetics". In: *IEEE/ASME Transactions on Mechatronics* 15.1 (2010), pp. 27–39 (cit. on p. 59).
DOI: `10.1109/TMECH.2009.2013944`.

[99]   Y. S. Kim and B. Hannaford. "Some practical issues in time domain passivity control of haptic interfaces". In: *Proc. IEEE/RSJ Int Intelligent Robots and Systems Conference*. Vol. 3. 2001, pp. 1744–1750 (cit. on p. 43).

[100]   F. M. Klomp. "Haptic Control for Dummies: An introduction and analysis". MSc Thesis. Technische Universiteit Eindhoven (TU/e), Control Systems Technology Group, 2006 (cit. on pp. 44, 56).
URL: `http://alexandria.tue.nl/repository/books/633244.pdf`.

[101]   D. A. Kontarinis and R. D. Howe. "Tactile Display of Vibratory Information in Teleoperation and Virtual Environments". In: *Presence* 4.4 (1995), pp. 387–402 (cit. on p. 160).

[102]   H. Köroğlu and C. W. Scherer. "Robust Performance Analysis for Structured Linear Time-Varying Perturbations With Bounded Rates-of-Variation". In: *IEEE Transactions on Automatic Control* 52.2 (2007), pp. 197–211 (cit. on p. 71).
DOI: `10.1109/TAC.2006.890482`.

[103]   K. Kosuge, Y. Fujisawa, and T. Fukuda. "Control Of Mechanical System With Man-machine Interaction". In: *Proceedings of the lEEE/RSJ International Conference on Intelligent Robots and Systems (IROS)*. Vol. 1. 1992, pp. 87–92 (cit. on p. 29).
DOI: `10.1109/IROS.1992.587304`.

[104]   K. Krishnaswamy. "Passive teleoperation of hydraulic systems". PhD thesis. University of Minnesota, 2004 (cit. on p. 21).

[105]   V. Kučera. "A review of the matrix Riccati equation". In: *Kybernetika* 9.1 (1973), pp. 42–61 (cit. on p. 111).
URL: `http://dml.cz/dmlcz/124651`.

[106]   K. J. Kuchenbecker, J. Fiene, and G. Niemeyer. "Improving Contact Realism through Event-Based Haptic Feedback". In: *IEEE Transactions on Visualization and Computer Graphics* 12.2 (2006), pp. 219–230 (cit. on p. 60).
DOI: `10.1109/TVCG.2006.32`.

[107]   R.-F. Kuo and T.-H. Chu. "Unconditional Stability Boundaries of a Three-Port Network". In: *IEEE Transactions on Microwave Theory and Techniques* 58.2 (2010), pp. 363–371 (cit. on p. 76).
DOI: `10.1109/TMTT.2009.2038660`.

[108]   K. Kurokawa. "Power Waves and Scattering Matrix". In: *IEEE Transactions on Microwave Theory and Techniques* 13.3 (1965), pp. 194–202 (cit. on p. 157).
DOI: `10.1109/TMTT.1965.1125964`.

[109]   K.-U. Kyung, D.-S. Kwon, and G.-H. Yang. "A Novel Interactive Mouse System for Holistic Haptic Display in a Human-Computer Interface". In: *International Journal of Human-Computer Interaction* 20.3 (2006), pp. 247–270 (cit. on p. 59).
DOI: `10.1207/s15327590ijhc2003_5`.

[110]   E. Laroche, L. Barbé and, B. Bayle, and M. de Mathelin. "A methodology for identification of uncertain LFR model of the human operator for telemanipulation with force-feedback". In: *49th IEEE Conference on Decision and Control (CDC)*. 2010, pp. 2005–2010 (cit. on p. 29).
DOI: `10.1109/CDC.2010.5717433`.

[111]   Lateral Science. *Mechanical Television*. 04/2013 (cit. on p. 10).
URL: `http://www.lateralscience.co.uk/television/mechTV.html`.

[112]   D. Lawrence. "Stability and transparency in bilateral teleoperation". In: *IEEE Transactions on Robotics and Automation* 9.5 (1992), pp. 625–637 (cit. on pp. 30, 38, 49–51, 53).
DOI: `10.1109/70.258054`.

[113]   D. Lee and M. W. Spong. "Passive Bilateral Teleoperation With Constant Time Delay". In: *Robotics, IEEE Transactions on* 22.2 (2006), pp. 269–281 (cit. on p. 72).
DOI: `10.1109/TRO.2005.862037`.

[114]   S. Lee and H. S. Lee. "Modeling, design, and evaluation of advanced teleoperator control systems with short time delay". In: *IEEE Transactions on Robotics and Automation* 9.5 (1993), pp. 607–623 (cit. on pp. 28, 30).
DOI: `10.1109/70.258053`.

[115]   G. Leung, B. Francis, and J. Apkarian. "Bilateral controller for teleoperators with time delay via μ-synthesis". In: *IEEE Transactions on Robotics and Automation* 11.1 (1995), pp. 105–116 (cit. on pp. 29, 37, 42, 72).
DOI: `10.1109/70.345941`.

[116]   F. B. Llewellyn. "Some fundamental properties of transmission systems". In: *Proceedings of the IRE* 40.3 (1952), pp. 271–283 (cit. on pp. 32, 156).
DOI: `10.1109/JRPROC.1952.273783`.

[117]   J. Löfberg. " YALMIP : A Toolbox for Modeling and Optimization in MATLAB". In: *Proceedings of the CACSD Conference*. Taipei, Taiwan, 2004 (cit. on pp. 82, 85).
URL: `http://users.isy.liu.se/johanl/yalmip`.

[118]   G. Lombardi and B. Neri. "Criteria for the evaluation of unconditional stability of microwave linear two-ports: a critical review and new proof". In: *IEEE Transactions on Microwave Theory and Techniques* 47.6 (1999), pp. 746–751 (cit. on pp. 77, 81).
DOI: `10.1109/22.769346`.

[119]   R. Lozano, N. Chopra, and M. Spong. "Passivation Of Force Reflecting Bilateral Teleoperators With Time Varying Delay". In: *Proceedings of the 8. Mechatronics Forum*. 2002, pp. 24–26 (cit. on p. 72).

[120]   C. A. L. Martínez, R. van de Molengraft, and M. Steinbuch. "High Performance and Stable Teleoperation under Bounded Operator and Environment Dynamics". In: *10th IFAC Symposium on Robot Control (SYROCO)*. Vol. 10.1. 2012, pp. 373–379 (cit. on pp. 119, 120, 124).
DOI: `10.3182/20120905-3-HR-2030.00067`.

[121] C. A. L. Martínez, R. van de Molengraft, and M. Steinbuch. "Robust performance control design for bilateral teleoperation under time-varying bounded operator and environment dynamics". In: *Proceedings of the American Control Conference (ACC)*. 2012, pp. 3465–3470 (cit. on pp. 119, 124).

[122] I. Masubuchi, A. Ohara, and N. Suda. "LMI-based controller synthesis: A unified formulation and solution". In: *International Journal of Robust and Nonlinear Control* 8.8 (1998), pp. 669–686 (cit. on p. 97).
DOI: 10.1002/(SICI)1099-1239(19980715)8:8<669::AID-RNC337>3.0.CO;2-W.

[123] D. McNeill, L. Quaeghebeur, and S. Duncan. "IW - The Man Who Lost His Body". In: *Handbook of Phenomenology and Cognitive Science*. Ed. by D. Schmicking and S. Gallagher. Springer Netherlands, 2010, pp. 519–543 (cit. on p. 162).
DOI: 10.1007/978-90-481-2646-0_27.

[124] D. T. Mcruer. *Pilot-Induced Oscillations and Dynamic Human Behavior*. NASA Contractor Report 4683. National Aeronautics and Space Administration (NASA), 1995 (cit. on p. 23).

[125] A. Megretski and A. Rantzer. "System analysis via integral quadratic constraints". In: *IEEE Transactions on Automatic Control* 42.6 (1997), pp. 819–830 (cit. on pp. 63–65, 84).
DOI: 10.1109/9.587335.

[126] A. Megretski and S. Treil. "Power Distribution Inequalities in Optimization and Robustness of Uncertain Systems". In: *Journal of Mathematical Systems, Estimation, and Control* 3.3 (1993), pp. 301–317 (cit. on p. 107).

[127] G. Meinsma, Y. Shrivastava, and M. Fu. "A dual formulation of mixed μ and on the losslessness of (D, G) scaling". In: *IEEE Transactions on Automatic Control* 42.7 (1997), pp. 1032–1036 (cit. on p. 70).
DOI: 10.1109/9.599990.

[128] L. Meli. "A novel approach for two fingers grasping devices with cutaneous and kinesthetic force feedback". MA thesis. University of Siena, 2012, p. 52 (cit. on p. 59).

[129] B. M. Millman. "The Filament Lattice of Striated Muscle". In: *Physiological Reviews* 78.2 (1998), pp. 359–391 (cit. on p. 23).

[130] P. Mitra and G. Niemeyer. "Model-mediated Telemanipulation". In: *The International Journal of Robotics Research* 27.2 (2008), pp. 253–262 (cit. on p. 61).
DOI: 10.1177/0278364907084590.

[131] S. K. Mitra. *Analysis and synthesis of linear active networks*. New York: J. Wiley, 1969 (cit. on p. 30).

[132] F. Miyazaki, S. Matsubayashi, T. Yoshimi, and S. Arimoto. "A new control methodology toward advanced teleoperation of master-slave robot systems". In: *Proc. IEEE International Conference on Robotics and Automation (ICRA)*. Vol. 3. 1986, pp. 997–1002 (cit. on p. 18).
DOI: 10.1109/ROBOT.1986.1087546.

[133] S. Munir and W. J. Book. "Internet-based teleoperation using wave variables with prediction". In: *IEEE/ASME Transactions on Mechatronics* 7.2 (2002), pp. 124–133 (cit. on p. 43).
DOI: 10.1109/TMECH.2002.1011249.

[134]   F. Mussa-Ivaldi, N. Hogan, and E. Bizzi. "Neural, mechanical, and geometric fac-
         tors subserving arm posture in humans". In: *The Journal of Neuroscience* 5.10 (1985),
         pp. 2732–2743 (cit. on pp. 23, 25).
         URL: http://www.jneurosci.org/content/5/10/2732.

[135]   E. Naerum and B. Hannaford. "Global transparency analysis of the Lawrence tele-
         operator architecture". In: *Proc. IEEE Int. Conf. Robotics and Automation (ICRA)*. 2009,
         pp. 4344–4349 (cit. on p. 38).
         DOI: 10.1109/ROBOT.2009.5152791.

[136]   G. Niemeyer and J.-J. E. Slotine. "Designing force reflecting teleoperators with large
         time delays to appear as virtual tools". In: *Proc. IEEE International Conference on Robotics
         and Automation*. Vol. 3. 1997, pp. 2212–2218 (cit. on p. 43).
         DOI: 10.1109/ROBOT.1997.619290.

[137]   G. Niemeyer and J.-J. E. Slotine. "Stable adaptive teleoperation". In: *IEEE Journal of
         Oceanic Engineering* 16.1 (1991), pp. 152–162 (cit. on pp. 18, 28, 34, 36, 41, 72, 79).
         DOI: 10.1109/48.64895.

[138]   G. Niemeyer and J.-J. E. Slotine. "Telemanipulation with Time Delays". In: *The In-
         ternational Journal of Robotics Research* 23.9 (2004), pp. 873–890 (cit. on pp. 41, 72,
         79).
         DOI: 10.1177/0278364904045563.

[139]   G. Offer and K. Ranatunga. "Crossbridge and filament compliance in muscle: impli-
         cations for tension generation and lever arm swing". In: *Journal of Muscle Research and
         Cell Motility* 31 (4 2010), pp. 245–265 (cit. on p. 23).
         DOI: 10.1007/s10974-010-9232-7.

[140]   C. Ottenheijm, L. Heunks, and R. Dekhuijzen. "Diaphragm adaptations in patients
         with COPD". In: *Respiratory Research* 9.1 (2008), p. 12 (cit. on p. 25).
         DOI: 10.1186/1465-9921-9-12.

[141]   C. Pacchierotti, F. Chinello, and D. Prattichizzo. "Cutaneous device for teleoperated
         needle insertion". In: *Proceedings of 4th IEEE RAS & EMBS Int Biomedical Robotics and
         Biomechatronics Conference (BIOROB)*. 2012, pp. 32–37 (cit. on p. 59).
         DOI: 10.1109/BioRob.2012.6290853.

[142]   A. Packard and J. Doyle. "The complex structured singular value". In: *Automatica* 29.1
         (1993), pp. 71–109 (cit. on pp. 22, 66, 82).
         DOI: 10.1016/0005-1098(93)90175-S.

[143]   A. Packard and J. Teng. "Robust Stability with Time Varying Perturbations". In:
         Proceedings of 28th Allerton Conference. 1990 (cit. on p. 71).

[144]   J. H. Park and H. C. Cho. "Sliding-mode controller for bilateral teleoperation with
         varying time delay". In: *IEEE/ASME International Conference on Advanced Intelligent
         Mechatronics*, 1999, pp. 311–316 (cit. on pp. 44, 72).
         DOI: 10.1109/AIM.1999.803184.

[145]   C. Passenberg, A. Peer, and M. Buss. "A survey of environment-, operator-, and task-
         adapted controllers for teleoperation systems". In: *Mechatronics* 20.7 (2010). Special
         Issue on Design and Control Methodologies in Telerobotics, pp. 787–801 (cit. on
         pp. 44, 53, 56).
         DOI: 10.1016/j.mechatronics.2010.04.005.

[146]   A. Pinkus. *N-widths in Approximation Theory, , 1980*. Springer Verlag, New York, 1980 (cit. on p. 83).

[147]   M. Pirola and G. Ghione. "Immittance and *S*-Parameter-Based Criteria for the Unconditional Stability of Linear Two-Ports: Relations and Invariance Properties". In: *IEEE Transactions on Microwave Theory and Techniques* 57.3 (2009), pp. 519–523 (cit. on p. 77). DOI: 10.1109/TMTT.2009.2013310.

[148]   İ. Polat. "A Note on Passivity Based Stability Conditions for Bilateral Teleoperation". In: *Proceedings of 18th IFAC World Congress, Milano*. 2011 (cit. on p. 63). DOI: 10.3182/20110828-6-IT-1002.00665.

[149]   İ. Polat. "An IQC formulation of stability analysis for bilateral teleoperation systems with time delays". In: *Proceedings of IEEE World Haptics Conference, (WHC)*. 2011, pp. 505–509 (cit. on p. 63). DOI: 10.1109/WHC.2011.5945537.

[150]   İ. Polat. "Stability analysis of bilateral teleoperation systems with time-varying environments". In: *American Control Conference (ACC), 2011*. 2011, pp. 1139–1144 (cit. on p. 63).

[151]   İ. Polat and C. W. Scherer. "Stability Analysis for Bilateral Teleoperation: An IQC Formulation". In: *IEEE Transactions on Robotics* 28.6 (2012), pp. 1294–1308 (cit. on pp. 63, 92). DOI: 10.1109/TRO.2012.2209230.

[152]   J. W. Polderman and J. C. Willems. *Introduction to Mathematical Systems Theory: A behavioral approach*. Vol. 26. Texts In Applied Mathematics. Springer New York, 1998 (cit. on pp. 151, 153).

[153]   E. B. V. Poorten, Y. Yokokohji, and T. Yoshikawa. "Stability analysis and robust control for fixed-scale teleoperation". In: *Advanced Robotics* 20.6 (2006), pp. 681–706 (cit. on pp. 32, 33). DOI: 10.1163/156855306777361640.

[154]   P. Prekopiou, S. Tzafestas, and W. Harwin. "Towards variable-time-delays-robust telemanipulation through master state prediction". In: *Proceedings of 1999 IEEE/ASME International Conference on Advanced Intelligent Mechatronics*. IEEE. 1999, pp. 305–310 (cit. on p. 30). DOI: 10.1109/AIM.1999.803183.

[155]   D. V. Raaij. *Notes on the Control of Teleoperation Systems*. Technical Report 2010.050. Eindhoven University of Technology, Dept. of Mech. Eng., Control Systems Technology Group, 2010 (cit. on p. 56).

[156]   G. Raisbeck. "A Definition of Passive Linear Networks in Terms of Time and Energy". In: *Journal of Applied Physics* 25.12 (1954), pp. 1510–1514 (cit. on p. 75). DOI: 10.1063/1.1702374.

[157]   G. J. Raju. "Operator adjustable impedance in bilateral remote manipulation". PhD thesis. Massachusetts Institute of Technology, 1989 (cit. on p. 28). DOI: 1721.1/14445.

[158]   G. J. Raju, G. C. Verghese, and T. B. Sheridan. "Design issues in 2-port network models of bilateral remote manipulation". In: *IEEE International Conference on Robotics and Automation (ICRA)*. 1989, pp. 1316–1321 (cit. on pp. 40, 49).

DOI: 10.1109/ROBOT.1989.100162.

[159]   A. Ran. "Necessary and sufficient conditions for existence of *J*-spectral factorization for para-Hermitian rational matrix functions". In: *Automatica* 39.11 (2003), pp. 1935–1939 (cit. on p. 111).
DOI: 10.1016/S0005-1098(03)00201-2.

[160]   A. Rantzer. "On the Kalman–Yakubovich–Popov Lemma". In: *Systems & Control Letters* 28.1 (1996), pp. 7–10 (cit. on pp. 67, 83).
DOI: DOI:10.1016/0167-6911(95)00063-1.

[161]   J.-P. Richard. "Time-delay systems: An overview of some recent advances and open problems". In: *Automatica* 39.10 (2003), pp. 1667–1694 (cit. on p. 72).
DOI: DOI:10.1016/S0005-1098(03)00167-5.

[162]   J. Rollett. "Stability and Power-Gain Invariants of Linear Twoports". In: *IRE Transactions on Circuit Theory* 9.1 (1962), pp. 29–32 (cit. on pp. 32, 74, 157).
DOI: 10.1109/TCT.1962.1086854.

[163]   L. B. Rosenberg and B. D. Adelstein. "Perceptual decomposition of virtual haptic surfaces". In: *Proceedings of IEEE Symposium on Research Frontiers in Virtual Reality*. 1993, pp. 46–53 (cit. on p. 52).
DOI: 10.1109/VRAIS.1993.378264.

[164]   J.-H. Ryu, J. Artigas, and C. Preusche. "A passive bilateral control scheme for a teleoperator with time-varying communication delay". In: *Mechatronics* 20.7 (2010). Special Issue on Design and Control Methodologies in Telerobotics, pp. 812–823 (cit. on p. 43).
DOI: 10.1016/j.mechatronics.2010.07.006.

[165]   J.-H. Ryu, D.-S. Kwon, and B. Hannaford. "Stability guaranteed control: time domain passivity approach". In: *IEEE Transactions on Control Systems Technology* 12.6 (2004), pp. 860–868 (cit. on p. 43).
DOI: 10.1109/TCST.2004.833648.

[166]   J.-H. Ryu, D.-S. Kwon, and B. Hannaford. "Stable teleoperation with time-domain passivity control". In: *IEEE Transactions on Robotics and Automation* 20.2 (2004), pp. 365–373 (cit. on p. 43).
DOI: 10.1109/TRA.2004.824689.

[167]   M. G. Safonov. *Stability and Robustness of Multivariable Feedback Systems*. MIT Press, Cambridge, MA, 1980 (cit. on pp. 63, 64).

[168]   A. van der Schaft. L_2-*Gain and Passivity Techniques in Nonlinear Control*. Ed. by M. Thoma. Vol. 218. Lecture Notes in Control and Information Sciences. Springer Berlin / Heidelberg, 1996 (cit. on p. 154).
DOI: 10.1007/3-540-76074-1.

[169]   C. W. Scherer. "LPV Control and Full Block Multipliers". In: *Automatica* 37.3 (2001), pp. 361–375 (cit. on p. 63).
DOI: DOI:10.1016/S0005-1098(00)00176-X.

[170]   C. W. Scherer. "Relaxations for Robust Linear Matrix Inequality Problems with Verifications for Exactness". In: *SIAM Journal on Matrix Analysis and Applications* 27.2 (2005), pp. 365–395 (cit. on p. 82).
DOI: 10.1137/S0895479803430953.

[171] C. W. Scherer. "Robust Controller Synthesis is Convex for Systems without Control Channel Uncertainties". In: *Model-Based Control : Bridging Rigorous Theory and Advanced Technology*. Springer US, 2009, pp. 13–30 (cit. on pp. 91, 95).
DOI: `10.1007/978-1-4419-0895-7_2`.

[172] C. W. Scherer., P. Gahinet, and M. Chilali. "Multiobjective output-feedback control via LMI optimization". In: *IEEE Transactions on Automatic Control* 42.7 (1997), pp. 896–911 (cit. on pp. 91, 97).
DOI: `10.1109/9.599969`.

[173] C. W. Scherer and S. Weiland. *Linear Matrix Inequalities in Control*. Unpublished Lecture Notes, Online Available, 1999 (cit. on pp. 97, 102, 114).
URL: `http://www.dcsc.tudelft.nl/~cscherer/lmi/notes99.pdf`.

[174] G. Scorletti. "Robustness analysis with time-delays". In: *Proceedings of the 36th IEEE Conference on Decision and Control*. Vol. 4. 1997, pp. 3824–3829 (cit. on p. 72).
DOI: `10.1109/CDC.1997.652457`.

[175] C. Seo, J. Kim, J.-P. Kim, J. H. Yoon, and J. Ryu. "Stable bilateral teleoperation using the energy-bounding algorithm: Basic idea and feasibility tests". In: *IEEE/ASME International Conference on Advanced Intelligent Mechatronics (AIM)*. 2008, pp. 335–340 (cit. on p. 44).
DOI: `10.1109/AIM.2008.4601683`.

[176] J. Sheng and M. W. Spong. "Model predictive control for bilateral teleoperation systems with time delays". In: *Proc. Canadian Conf. Electrical and Computer Engineering*. Vol. 4. 2004, pp. 1877–1880 (cit. on p. 44).
DOI: `10.1109/CCECE.2004.1347575`.

[177] T. B. Sheridan and W. R. Ferrell. "Remote Manipulative Control with Transmission Delay". In: *IEEE Transactions on Human Factors in Electronics* HFE-4.1 (1963), pp. 25–29 (cit. on p. 34).
DOI: `10.1109/THFE.1963.231283`.

[178] T. Sheridan. "Telerobotics". In: *Automatica* 25.4 (1989), pp. 487–507 (cit. on p. 18).
DOI: `10.1016/0005-1098(89)90093-9`.

[179] M. C. Smith. "Synthesis of mechanical networks: the inerter". In: *IEEE Transactions on Automatic Control* 47.10 (2002), pp. 1648–1662 (cit. on p. 153).
DOI: `10.1109/TAC.2002.803532`.

[180] J. E. Speich, L. Shao, and M. Goldfarb. "Modeling the human hand as it interacts with a telemanipulation system". In: *Mechatronics* 15.9 (2005), pp. 1127–1142 (cit. on p. 29).
DOI: `10.1016/j.mechatronics.2005.06.001`.

[181] J. A. Spudich. "The myosin swinging cross-bridge model." In: *Nature Reviews. Molecular Cell Biology* 2.5 (2001), pp. 387–392 (cit. on p. 23).
DOI: `10.1038/35073086`.

[182] A. P. Stern. "Stability and Power Gain of Tuned Transistor Amplifiers". In: *Proceedings of the IRE* 45.3 (1957), pp. 335–343 (cit. on p. 157).
DOI: `10.1109/JRPROC.1957.278369`.

[183] S. Stramigioli, A. van der Schaft, B. Maschke, and C. Melchiorri. "Geometric scattering in robotic telemanipulation". In: *IEEE Transactions on Robotics and Automation* 18.4 (2002), pp. 588–596 (cit. on p. 43).

DOI: `10.1109/TRA.2002.802200`.

[184]   E. L. Tan. "Simplified graphical analysis of linear three-port stability". In: *IEE Proceedings Microwaves, Antennas and Propagation* 152.4 (2005), pp. 209–213 (cit. on p. 76).
DOI: `10.1049/ip-map:20045035`.

[185]   T. Tsuji, K. Goto, M. Moritani, M. Kaneko, and P. Morasso. "Spatial characteristics of human hand impedance in multi-joint arm movements". In: *Proceedings of the IEEE/RSJ/GI International Conference on Intelligent Robots and Systems (IROS)*. Vol. 1. 1994, 423–430 vol.1 (cit. on p. 29).
DOI: `10.1109/IROS.1994.407441`.

[186]   T. Tsuji, P. Morasso, K. Goto, and K. Ito. "Human hand impedance characteristics during maintained posture". In: *Biological Cybernetics* 72 (6 1995), pp. 475–485 (cit. on p. 28).
DOI: `10.1007/BF00199890`.

[187]   R. H. Tütüncü, K. C. Toh, and M. J. Todd. "Solving semidefinite-quadratic-linear programs using SDPT3". In: *Mathematical Programming* 95.2 (2003), pp. 189–217 (cit. on p. 85).
DOI: `10.1007/s10107-002-0347-5`.

[188]   J. Ueda and T. Yoshikawa. "Force-reflecting bilateral teleoperation with time delay by signal filtering". In: *IEEE Transactions on Robotics and Automation* 20.3 (2004), pp. 613–619 (cit. on p. 43).
DOI: `10.1109/TRA.2004.825516`.

[189]   J. Veenman and C. W. Scherer. "IQC-Synthesis with General Dynamic Multipliers". In: *Proceedings of 18th IFAC World Congress, Milano*. 2011, pp. 4600–4605 (cit. on pp. 91, 105).
DOI: `10.3182/20110828-6-IT-1002.00776`.

[190]   J. Vertut and P. Coiffet. *Teleoperation and robotics*. London Englewood Cliffs, N.J: Prentice-Hall, 1986 (cit. on p. 18).

[191]   A. Villaverde, A. Blas, J. Carrasco, and A. Torrico. "Reset Control for Passive Bilateral Teleoperation". In: *IEEE Transactions on Industrial Electronics* 58.7 (2011), pp. 3037–3045 (cit. on p. 44).
DOI: `10.1109/TIE.2010.2077610`.

[192]   D. W. Weir, E. J. Colgate, and M. A. Peshkin. "Measuring and Increasing Z-Width with Active Electrical Damping". In: *Proc. symposium Haptic interfaces for virtual environment and teleoperator systems haptics 2008*. 2008, pp. 169–175 (cit. on p. 53).
DOI: `10.1109/HAPTICS.2008.4479938`.

[193]   J. Wildenbeest, D. A. Abbink., C. J. Heemskerk, F. C. van der Helm, and H. Boessenkool. "The Impact of Haptic Feedback Quality on the Performance of Teleoperated Assembly Tasks". In: *IEEE Transactions on Haptics* PP.99 (2012), p. 1 (cit. on p. 52).
DOI: `10.1109/TOH.2012.19`.

[194]   B. Willaert, B. Corteville, D. Reynaerts, H. Van Brussel, and E. Vander Poorten. "Bounded Environment Passivity of the Classical Position-Force Teleoperation Controller". In: *IEEE/RSJ International Conference on Intelligent Robots and Systems (IROS)*. 2009, pp. 4622–4628 (cit. on pp. 82, 85, 86).
DOI: `10.1109/IROS.2009.5354510`.

[195]   B. Willaert, B. Corteville, D. Reynaerts, H. Van Brussel, and E. B. Vander Poorten. "A
        Mechatronic Analysis of the Classical Position-Force Controller Based on Bounded
        Environment Passivity". In: *The International Journal of Robotics Research* 30.4 (2010),
        pp. 444–462 (cit. on pp. 75, 82).
        DOI: `10.1177/0278364910378334`.

[196]   J. C. Willems. "The Behavioral Approach to Open and Interconnected Systems". In:
        IEEE Control Systems Magazine 27.6 (2007), pp. 46–99 (cit. on pp. 151, 153).
        DOI: `10.1109/MCS.2007.906923`.

[197]   D. Woods. "Reappraisal of the unconditional stability criteria for active 2-port net-
        works in terms of S parameters". In: *IEEE Transactions on Circuits and Systems* 23.2
        (1976), pp. 73–81 (cit. on p. 77).
        DOI: `10.1109/TCS.1976.1084179`.

[198]   A. Yıldız, J. N. Forkey, et al. "Myosin V Walks Hand-Over-Hand: Single Fluorophore
        Imaging with 1.5 nm Localization". In: *Science* 300.5628 (2003), pp. 2061–2065 (cit. on
        p. 23).
        DOI: `10.1126/science.1084398`.

[199]   Y. Yokokohji, T. Imaida, and T. Yoshikawa. "Bilateral teleoperation under time-varying
        communication delay". In: *IEEE/RSJ International Conference on Intelligent Robots and
        Systems,(IROS)*. Vol. 3. 1999, pp. 1854–1859 (cit. on pp. 42, 43, 72).
        DOI: `10.1109/IROS.1999.811748`.

[200]   Y. Yokokohji and T. Yoshikawa. "Bilateral control of master-slave manipulators for
        ideal kinesthetic coupling-formulation and experiment". In: *IEEE Transactions on
        Robotics and Automation* 10.5 (1994), pp. 605–620 (cit. on pp. 27, 28, 49, 50, 56).
        DOI: `10.1109/70.326566`.

[201]   D. C. Youla. "On the factorization of rational matrices". In: *IRE Transactions on Infor-
        mation Theory* 7.3 (1961), pp. 172–189 (cit. on p. 109).
        DOI: `10.1109/TIT.1961.1057636`.

[202]   C. Youngblut, R. Johnston, S. H. Nash, R. A. Wienclaw, and C. A. Will. *Review of
        Virtual Environment Interface Technology*. Tech. rep. ADA314134. Institute for Defense
        Analyses, 1996 (cit. on pp. 160, 161).

[203]   K. Zhou, J. C. Doyle, and K. Glover. *Robust and Optimal Control*. Prentice-Hall, Upper
        Saddle River, 1996 (cit. on pp. 92, 109).

Acknowledgements

This thesis would never have been possible without the support and assistance of numerous people. In fact it wasn't even planned to be finished at all. Strictly speaking, Maarten Steinbuch persuaded me with his irresistible negotiation skills in about fifteen minutes for finishing the thesis during a casual chat in some colloquium or something along those lines (for the record, there were drinks involved too). I owe him more than this manuscript for his support and pragmatic approach to idealism (and making it look like not a contradiction). There are not many of his kind in the academic circles who can tell the difference between a proof and a solution.

I would like to thank also to my thesis committee members especially for daring to get to the bottom of this unconventional text.

This thesis was supposed to be finished and published under Delft Center for Systems and Control (DCSC), TUDelft affiliation. But it did not quite happen that way. Nevertheless I would like to thank Carsten W. Scherer for admitting me to this PhD program and giving me the chance to work in this project and his guidance during his time in DCSC.

A special thanks goes to Cesar Lopez for teaching me how to tame the experimental setup used in this thesis and for our technical discussions.

Now the difficult part; I don't know how to sum up the list of people whom I have become friends with, enjoyed their company and benefited from their support. After scratching many versions, because I suck big time, this is what I decided to do, so here we go; the people in DCSC, I wish the best for all of you (if you know what I mean), the people in CST (TU/e) for your spirit and comfortable environment, the best secretariat in the world ever! Kitty, Esther, Saskia, Ellen in DCSC and Geertje and Petra in CST, the Delft Haptics Lab people for the fun, dudes of the "pimientos" gang for the beer watch nights (often, judging by its residents, in the most unfortunately named place, "Tango"), Rotterdam tayfası, Delft tayfası, my awesome band Bike2Rome, my inmates from that house in Koornmarkt for all the occasions that, for some reason, I cannot remember much, Ronald from TMC, Joris and Sinar from ASML for the smooth transition to real life, all the nice people in TEX-SX.

Most importantly, I am thankful to mom and dad for being who they are. I am still amazed by how they can contain their patience and understanding no matter how crazy stuff I come up with; "*Hocam, sizin oğlan neden böyle?*"

Finally, all that is worth of something in this is due to Nazlı who always managed to find a way to make me do things right with her love and unparalleled optimism towards life. Gratitude my lady, gratitude…